

**STUDIES ON SOME SUPPORTED TRANSITION
METAL COMPLEX AND METAL OXIDE CATALYSTS
FOR OXIDATION REACTIONS**

**THESIS SUBMITTED TO THE
COCHIN UNIVERSITY OF SCIENCE AND TECHNOLOGY
IN PARTIAL FULFILMENT OF THE
REQUIREMENTS FOR THE DEGREE OF**

**DOCTOR OF PHILOSOPHY
IN
CHEMISTRY
IN THE FACULTY OF SCIENCE**

By

K. O. XAVIER

**DEPARTMENT OF CHEMICAL OCEANOGRAPHY
COCHIN UNIVERSITY OF SCIENCE AND TECHNOLOGY
KOCHI - 682 016, KERALA**

JUNE 2000

dedicated to my loving parents

" When you know a thing, to hold that you know it, and when you don't know a thing, to allow that you don't know it, this is the true knowledge. "

Confucius, 551-479 BC

12th June, 2000

CERTIFICATE

This is to certify that this thesis is an authentic record of research work carried out by Mr. K. O. Xavier under our supervision, in partial fulfillment of the requirements for the degree of Doctor of Philosophy of Cochin University of Science and Technology, and further that no part thereof has been presented before for any other degree.


Prof. Jacob Chacko,
Department of Chemical Oceanography
Cochin University of Science
and Technology
Kochi-16


Prof. K. K. Mohammed Yusuff
Department of Applied Chemistry
Cochin University of Science
and Technology
Kochi-22

DECLARATION

I hereby declare that the work presented in this thesis entitled " Studies on some supported transition metal complex and metal oxide catalysts for oxidation reactions " is entirely original and was carried out by me independently under the supervision of Prof. Jacob Chacko, Department of Chemical Oceanography and Prof.K.K. Mohammed Yusuff, Department of Applied Chemistry, Cochin University of Science and Technology, and has not been included in any other thesis submitted previously for the award of any degree.



K. O. Xavier

Kochi-16

12th June, 2000

My sincere thanks to

Prof. Jacob Chacko, Supervising^g guide: for making this work possible through his willingness to guide my research in Catalysis and for his continued advice, support and constant encouragement throughout the course of this investigation

Prof. K.K. Mohammed Yusuff, Supervising guide: for giving his time and expertise for the smooth completion of the work; the stimulating discussions with him were a source of enthusiasm for proceeding in the work

Prof. Madhavan Pillai, Dean, Faculty of Science: for granting permission to use the facilities in the Department of Applied Chemistry for a part of this work, his keen interest in my work and constant encouragement

Dr. Chandramohanakumar, Head, Department of Chemical Oceanography: for the support and his words of encouragement

Ms. A. A. Lalljee & Mr. I. A. Lalljee, Directors, Sud-Chemie India Ltd.(SCIL): for their interest, encouragement and active support, especially for the permission to use the facilities at SCIL, Cochin

Mr. B. Sen, Senior General Manager, R&D, SCIL, Baroda: for being an unfailing source of optimism, positive outlook and sincere words

Mr. K. T. Govindankutty, former General Manager, R&D, SCIL, Cochin: for granting me permission to do research and for his continued interest in my work

Dr. K. K. Abdul Rashid, Chief Manager, R&D, SCIL, Cochin: for being a source of inspiration and help, for leading me in the direction of research; being instrumental in getting me permission to use the facilities at SCIL, and for giving valuable advice and support during the early part of the work

Mr. K. T. Jose, Manager, R&D, SCIL, Cochin: for instilling motivation in me, for his constant support and reassurance

Prof. S. Sugunan & Dr. Muraleedharan Nair: for their active support and encouragement

Members of the Faculty, Department of Applied Chemistry: for the help and motivation they provided

All my colleagues in R&D, SCIL: *for the interest they have shown in my work*

Dr. P. A. Unnikrishnan: *for the timely help and advice on several occasions*

The non teaching staff (COD & A₃C): *for their cooperation and assistance*

My lab mates: *for cordial and pleasant working atmosphere; special thanks to Rani, Preetha and Suja for helping to ensure continuity in experiments and Ms. Jyothi and Ms. Jalaja for their help in preparing the thesis and also for critical reading of the draft*

Friends: *for their pleasing company which has given momentous experiences. I particularly thank Munga, Joseph, Unnikrishnan, Krishnakumar, Babu and Lisen in COD and Binoy, Rohid, Renu, Veneetha, Anas, Suja Haridas and Jean for their valuable help in many ways; Josy Cabral and Joshy C. Palatty for the companionship*

Dr. Varghese John & Jithin: *for the immense love and support*

My parents: *who gave their prayers and a vision for the future and who patiently bore much to see me through this research*

My brothers, sister and their families: *for sharing my responsibilities to spare me for research*

K. O. Xavier

PREFACE

The application of catalytic science envisages the production of materials and development of processes which address the critical needs of society through economic growth and environmentally sustainable progress. Though homogeneous catalysts have the potential to achieve these targets through efficient, selective chemical transformations at milder conditions, it has grown only at a slower rate due to economic and technical limitations. Heterogenization of homogeneous catalysts has emerged as a welcome alternative. However, efforts are still required to refine the conventional heterogeneous systems like metal oxide catalysts to maximize the yield of desired product at commercially more acceptable conditions.

Zeolite encapsulated transition metal complexes have received wide attention as an effective heterogenized system that combines the tremendous activity of the metal complexes and the attractive features of the zeolite structure. Zeolite encapsulated complexes offer a bright future for attempts to replace homogeneous systems retaining its catalytic activity and minimizing the technical problems, especially for the partial oxidation of organic compounds. Studies on some zeolite encapsulated transition metal complexes are presented in this thesis. The ligands selected are technically important in a bio-mimetic or structural perspective. Attempts have been made in this study to investigate the composition, structure and stability of encapsulated complexes using available techniques. The catalytic activity of encapsulated complexes was evaluated for the oxidation of some organic compounds. The recycling ability of the catalyst as a result of the encapsulation was also studied.

Our studies on Cu-Cr/Al₂O₃, a typical metal oxide catalyst, illustrate the use of design techniques to modify the properties of such conventional catalysts. The catalytic activity of this catalyst for the oxidation of carbon monoxide was measured. The effect of additives like CeO₂ or TiO₂ on the activity and stability of this system was also investigated. The additive is potent to improve the activity and stability of the catalyst so as to be more effective in commercial usage.

The thesis is structured into eight chapters. Chapter I gives a comprehensive account of the attractive features of zeolite encapsulated complexes. The experimental techniques used in the present study are described in Chapter II. The chapters III to VI deal with the synthesis and characterization of zeolite encapsulated complexes. The catalytic activity studies of the zeolite encapsulated complexes are discussed in Chapter VII. Chapter VIII gives the details regarding the catalytic studies on the metal oxide catalyst. A gist of the conclusions arrived at on the basis of our investigation is provided at the end of the thesis.

CONTENTS

CHAPTER I	GENERAL INTRODUCTION	
1. 1	Introduction	2
1. 2	Recent Trends in Catalysis	2
1. 3	Catalysts in Industry	3
1. 3. 1	Homogeneous Catalysts	4
1. 3. 2	Metal oxide Catalysts	6
1. 3. 3	Noble metal catalysts	8
1. 3. 4	Zeolite and Zeolite based catalysts	9
1. 4	Towards Heterogenizing Homogeneous Catalysts	10
1. 4. 1	Heterogeneous molecular Catalysts	11
1. 4. 2	Supported homogeneous catalysts	11
1. 5	Emerging Frontiers in Heterogenization- Zeolite encapsulation	14
1. 5. 1	Milestones	14
1. 5. 2	Structural considerations	16
1. 5. 3	Merits and Demerits	18
1. 5. 4	Enzymes and Enzyme mimics	19
1. 6	Zeolite encapsulation methods	23
1. 6. 1	Flexible ligand method	23
1. 6. 2	Ship-in-a-Bottle	24
1. 6. 3	Zeolite synthesis method	25
1. 7	Characterisation of zeolite complexes	26
1. 7. 1	Molecular modelling and simulation	27
1. 7. 2	Entrapment Identification	27
1. 7. 3	Physico-chemical methods	28
1. 7. 4	Oxygen adsorption	32
1. 7. 5	Thermal analysis	33
1. 7. 6	Electrochemical methods	33
1. 8	Host-Guest Interactions in Zeolite complexes	34
1. 9	Catalysis by Zeolite encapsulated complexes	35
1. 10	Future outlook	41
1. 11	Scope of the present study	43
	REFERENCES	46
CHAPTER II	MATERIALS AND METHODS	
2. 1	Introduction	56
2. 2	Reagents	56
2. 3	Synthesis of ligands	56
2. 4	Synthesis of Y zeolite supported metal complexes	58
2. 4. 1	Modification of Y zeolite	58
2. 4. 2	Encapsulation of metal complexes in Y zeolite	58
2. 5	Preparation of metal oxide catalysts	59

2. 6	Physico-chemical methods	59
2. 6. 1	Chemical analysis	59
2. 6. 2	CHN analysis	61
2. 6. 3	Atomic absorption spectrophotometer	61
2. 6. 4	Surface area analysis	61
2. 6. 5	Pore volume analysis	62
2. 6. 6	X-ray diffraction	62
2. 6. 7	Scanning electron microscopy	63
2. 6. 8	Magnetic moment measurement	63
2. 6. 9	Diffuse reflectance spectra	63
2. 6. 10	Infrared spectra	64
2. 6. 11	EPR spectra	64
2. 6. 12	TG analysis	65
2. 7	Catalytic studies	65
	REFERENCES	66

CHAPTER III STUDIES ON Y ZEOLITE ENCAPSULATED TRANSITION METAL COMPLEXES OF DIMETHYLGLYOXIME

3. 1	Introduction	68
3.2	Experimental	69
3. 2. 1	Materials	69
3. 2. 2	Synthesis of zeolite encapsulated complexes	69
3. 2. 3	Analytical methods	70
3. 3	Results and Discussion	70
3. 3. 1	Metal exchanged zeolites	70
3. 3. 1. 1	Chemical analysis	70
3. 3. 1. 2	X-ray diffraction pattern	72
3. 3. 1. 3	Surface area and pore volume	73
3. 3. 1. 4	Infrared spectra	74
3. 3. 2	Zeolite encapsulated complexes	76
3. 3. 2. 1	Chemical analysis	76
3. 3. 2. 2	SEM analysis	78
3. 3. 2. 3	X-ray diffraction pattern	82
3. 3. 2. 4	Surface area and pore volume	82
3. 3. 2. 5	Magnetic moment	85
3. 3. 2. 6	Electronic spectra	87
3. 3. 2. 7	Infrared spectra	91
3. 3. 2. 8	EPR spectra	94
3. 3. 2. 9	TG analysis	96
3. 4	Summary and Conclusion	100
	REFERENCES	102

CHAPTER IV STUDIES ON Y ZEOLITE ENCAPSULATED TRANSITION METAL COMPLEXES OF 3-FORMYLSALICYLIC ACID

4. 1	Introduction	105
------	--------------	-----

4.2	Experimental	106
4.2.1	Materials	106
4.2.2	Synthesis of zeolite encapsulated complexes	106
4.2.3	Analytical methods	107
4.3	Results and Discussion	107
4.3.1	Chemical analysis	107
4.3.2	X-ray diffraction pattern	108
4.3.3	Surface area and pore volume	109
4.3.4	Magnetic moment	110
4.3.5	Electronic spectra	111
4.3.6	Infrared spectra	114
4.3.7	EPR spectra	117
4.3.8	TG analysis	119
4.4	Summary and Conclusion	122
	REFERENCES	123

CHAPTER V STUDIES ON Y ZEOLITE ENCAPSULATED TRANSITION METAL COMPLEXES OF N,N'-ETHYLENEBIS(7-METHYLSALICYLIDENEAMINE)

5.1	Introduction	125
5.2	Experimental	126
5.2.1	Materials	126
5.2.2	Synthesis of zeolite encapsulated complexes	126
5.2.3	Analytical methods	126
5.3	Results and Discussion	126
5.3.1	Chemical analysis	126
5.3.2	X-ray diffraction pattern	127
5.3.3	Surface area and pore volume	128
5.3.4	Magnetic moment	130
5.3.5	Electronic spectra	131
5.3.6	Infrared spectra	133
5.3.7	EPR spectra	136
5.3.8	TG analysis	137
5.4	Summary and Conclusion	141
	REFERENCES	142

CHAPTER VI STUDIES ON Y ZEOLITE ENCAPSULATED TRANSITION METAL COMPLEXES OF N,N'-ETHYLENEBIS(5,6-BENZOSALICYLIDENEAMINE)

6.1	Introduction	144
6.2	Experimental	145
6.2.1	Materials	145
6.2.2	Synthesis of zeolite encapsulated complexes	145
6.2.3	Analytical methods	145

CHAPTER I

GENERAL INTRODUCTION

1. 1 INTRODUCTION

Civilization has traversed a path of astonishing progress and has made rapid strides of development in the twentieth century. In order to achieve this development, it was necessary to invent a number of new materials and to evolve ways and means for their fast and cheap production in large quantities. The development of the science and practice of catalysis has opened up new vistas for the fast and selective production of desired chemical molecules. This scientific revolution has triggered the advent of molecular design techniques which have unlimited scope and potential to provide for the most basic of all human needs— health, food, energy and materials. The dictum that underlines all catalyst research is the development of cost effective methods that have an inherent commitment to environmental sustainability. Catalyst technology has become all pervasive in our society and includes in its domain enzymes (biocatalysts), pharmaceuticals, petrochemicals, energy, plastics and fibers and what not.

1. 2 RECENT TRENDS IN CATALYSIS

Catalysis is directly or indirectly involved in almost all processes in modern industries. In early days, the preparation of heterogeneous catalysts and their operation were considered to be more an art than a science. Later, with the advent of modern sophisticated surface science techniques, catalysts and catalyst based technologies have undergone tremendous changes. A catalyst is a surface active material i.e. catalysis occurs at the surface of the catalyst and hence the activity of the catalyst depends very much on the nature of its surface. The performance of industrial catalytic processes is determined not only by the activity of the catalyst but also the process parameters like nature of feed and operating conditions such as temperature, pressure, space velocity, etc. All these factors ultimately determine the exact nature of chemical species and their relative concentration on the catalyst surface under actual process conditions. Recognizing the exact nature of these surface species and fine tuning them for still better catalytic performance are the main objectives of catalyst-research.

The rapid growth of human population and high standard of living of modern society necessitate considerable enhancement in the production of materials. Increased production results in an increase of undesirable by-products and therefore in elevated levels of environmental pollution. Therefore, chemical technology focuses on developing novel environment-friendly catalysts that can provide high selectivity leading to minimum toxic effluents, without sacrificing on yield and energy requirements. The development of a three-way catalytic converter for controlling auto exhaust emissions^{1, 2}, application of molecular sieves for better selectivity³ and alternative chemical routes via catalytic oxidation, hydroxylation, etc. for fine chemical^{4, 5} are some of the achievements of these efforts.

Progress in the science of catalysis and its industrial applications is highly essential to cater to the demands of modern society. In order to achieve this it is necessary to replace present technologies with new, energy-efficient, environment-friendly catalytic processes of high selectivity. This quest has triggered a renewed interest in metal complexes which are known to exhibit remarkable catalytic properties. Furthermore, the heterogenization of homogeneous catalysts has also received considerable importance as it avoids the technical problems in using homogeneous catalysis, but preserves the catalytic performance.

1.3 CATALYSTS IN INDUSTRY

Traditionally, industrial catalysts have been classified as homogeneous and heterogeneous. Metal complexes and organometallic compounds are the important homogeneous catalysts. These catalysts are soluble in the reaction medium and are used in the production of high purity, high value chemicals. Usually, homogeneous catalytic reactions are very complex and proceed as a closed cycle of linked chemical reactions which involve different intermediate species. However, they exhibit high efficiency and selectivity and operate at milder conditions of temperature and pressure. Moreover, homogeneous catalysts of definite stoichiometry and structure can be easily made with more reproducibility. In contrast to homogeneous catalysts, heterogeneous catalysts are

usually solid surfaces or species attached to solid surface. They are mainly used for the production of large scale commodity chemicals such as methanol and ammonia and in the production of gasoline from petroleum.

Both homogeneous^{6, 7} and heterogeneous⁸⁻¹⁰ catalysts were extensively used in industry since the beginning of the twentieth century. But, heterogeneous catalysis has grown at a faster rate than homogeneous catalysis in industry. The main technical problem in the use of homogeneous systems is the separation of catalysts from reactants and products, which is practically very easy in the case of heterogeneous catalysts. The deactivation of homogeneous catalysts by the self aggregation of the active sites may also restrict its application in industrial processes, whereas heterogeneous catalysts are relatively more stable. The above mentioned facts may be the reason for the tardy growth of homogeneous catalyst systems in industry. However, the ability of homogeneous systems to catalyse a variety of specifically designed chemical transformations promises lot of scope for future developments.

1. 3. 1 Homogeneous catalysts

One of the first industrially applied homogeneous processes is Oxo process¹¹ discovered by Otto Roelen in 1938. In this process, the hydroformylation of olefins occurs in presence of carbon monoxide and hydrogen at 140-180 °C and a pressure of 200-300 atm over cobalt hydride carbonyl complexes. Later, this catalyst was modified with trialkyl phosphine to lower the reaction pressures and to obtain higher selectivity. The technical importance of this process is because the primary reaction product, the aldehyde, can be easily converted to industrially important secondary products like alcohols, acids, diols, amines or esters¹².

Another interesting achievement in this field was the use of Reppe reactions for the commercial production of various chemicals⁶. This reaction involves the addition of a base to olefinic or acetylenic C-C bond with simultaneous insertion of CO. The synthesis of acrylic acid from acetylene, CO and water with activated nickel carbonyl catalyst.

$\text{HNi(CO)}_3\text{X}$, is one of such reactions. Reppe carbonylations also include reactions such as propionic acid from ethylene and water, and acetic acid from methanol.

Catalysis by protons using acids (H_2SO_4 , BF_3 , H_3PO_4) was employed to a large extent in alkylation reactions, for example, in the production of alkylated gasoline from isobutylene and in the production of cumene, xylene and styrene from benzene⁶. A similar acid catalysed reaction is Koch synthesis⁶ in which olefins and other compounds readily react with CO and water or alcohol to produce carboxylic acid or corresponding ester respectively. The carboxylic acids formed from isobutylene, diisobutylene and from mixture of olefins in the range $\text{C}_6\text{-C}_{10}$ are used as starting materials for resins, lacquers and synthetic lubricating oils.

Another significant discovery in the field of homogeneous catalysis was the development of Wacker process for the production of acetaldehyde from ethylene¹³. Soluble metal complex salts like palladium(II) chloride were used as catalysts for this process. This catalyst operates at 10.5 atm and 125-130 °C to obtain a yield of 95%. Wacker process is widely accepted in industry as it replaced expensive acetylene with cheap ethylene for the manufacture of acetaldehyde.

Rh complexes have been found to be more efficient catalysts than that based on cheaper and abundant metals. One of these complexes, $\text{RhCl(PPh}_3)_3$, widely known as Wilkinson's catalyst, can be used for the hydrogenation of olefins¹⁴. Also, the complexes such as RhH(CO)PPh_3 catalyse hydroformylation of propene to n-butraldehyde at 10-20 atm and give a yield of > 90% for the linear product, whereas $\text{Co}_2(\text{CO})_8$ catalyst performs this reaction only at high pressures (~200 atm) and produces a lower yield of 70%¹⁵. Monsanto's rhodium catalysed carbonylation of methanol to acetic acid is also very attractive as it replaces conventional high pressure processes with low pressure ones and shows a high selectivity¹⁶. A similar example is the use of rhodium complexes for oxo-process in presence of triphenylphosphine as co-catalyst⁶. The advantages of this rhodium based oxo-process are lower operating pressure and better selectivity for straight chain product.

Olefins and dienes can be oligomerised by means of homogeneous catalysts under mild conditions. The Esso process with alkyl aluminium chloride and titanium tetrachloride ^{6, 7}, the shell process with nickel-phosphine catalysts ^{6, 17} and the Ethyl process with the classical Ziegler trialkylaluminium catalyst ^{7, 13} are some of the industrially important homogeneous processes for ethylene oligomerisation. Homogeneous oxidation catalysis ⁶ is also known, for example, cyclohexane to adipic acid, butane to vinegar, propylene to propylene oxide and p-xylene to terephthalic acid. Furthermore, the direct addition of hydrocyanic acid to butadiene can be performed over nickel(0) phosphine or phosphite complexes at atmospheric pressure and 30-150 °C ¹⁸.

Besides above established homogeneous processes, some relatively new catalytic processes were developed and commercialized. The application of Wilkinson's metal complex to selectively hydrogenate biologically active substrates like steroids is an excellent example for such achievements ⁶. In addition, Monsanto has introduced a process ¹⁵ using Wilkinson's catalyst for producing L-dopa (3,4-dihydroxyphenylalanine), an effective drug against Parkinson's disease. The introduction of this process was highly significant as it was a classic example for the application of homogeneous catalysts in the synthesis of fine chemicals and also it is one of the most selective catalytic reactions known ¹⁹. Some of the recent studies have focused on the use of homogeneous catalysts for regioselective and enantioselective reactions ^{20, 21}. Since homogeneous catalysts are generally active at low temperatures, more new developments can be expected in this area. There is scope for new catalysts and new reactions in wake of energy and raw material considerations that will determine the direction of worldwide developments in chemical technology.

1. 3. 2 Metal oxide catalysts

Heterogeneous transition metal oxide catalysts are extensively used for various industrial applications where working conditions are more economical. A number of such systems like mixed metal oxide, perovskites, spinels ²²⁻²⁴, etc. were reported to be active for several reactions. Also, there is a pronounced interest for replacing highly

expensive noble metal catalysts with metal oxide alternatives. Main attraction of metal oxide systems is the low cost and easier methods of preparation as compared to that of other catalytic materials.

Many of the recent studies show that the performance of an industrial catalyst with respect to activity and selectivity depends greatly on the nature of the active sites formed on the catalyst surface during pretreatment or as a consequence of the catalytic reaction on it. The newly developed sophisticated surface science techniques provide valuable informations on the nature of active sites and their influence on catalytic activity. The application of such techniques was reviewed by several authors^{25, 26}. Furthermore, the physical properties like thermal and mechanical stability, surface area, porosity, shape, dimension, etc. are to be optimised for the successful operation of catalytic processes in industry.

Iron catalyst for ammonia synthesis is one of the classic industrial catalysts^{27, 28}. A quite large number of studies have been conducted using a combination of surface techniques to characterize this catalyst. The catalytic synthesis of methanol has gained considerable importance in the wake of energy crisis as it can be used as a starting material for the synthesis of various chemicals. A catalyst consisting of CuO and ZnO on alumina support is presently used for the manufacture of methanol²⁹. CuO-ZnO/Al₂O₃ catalyst is also used for water gas shift reaction in fertilizer plants³⁰. Supported nickel oxide catalyst is used for the steam reforming of hydrocarbon feedstocks like naphtha, LPG and natural gas into methane for its further conversion to hydrogen, ammonia, ammonia based fertilizers and methanol³¹.

γ -Al₂O₃ supported oxides of Mo or W, promoted with oxides of Co or Ni are used for the hydrotreating of petroleum fractions³². The bulk preparation of styrene, one of the most important monomers in modern petrochemical industry, is based on the dehydrogenation of ethylbenzene over potassium promoted iron catalyst³³. Some of the other catalytic processes in this class are ammoxidation of propylene to acrylonitrile over silica supported bismuth-molybdate catalyst³⁴, oxidation of methanol to

formaldehyde over iron molybdate ³⁵, hydrolysis of acrylonitrile to acrylamide and hydrogenation of nitrobenzene to aniline over Cu based catalysts ¹⁰, oxidative coupling of methane by Li doped MgO ³⁶, Fischer-Tropsch synthesis over CuO-ZnO/Al₂O₃ catalysts ³⁷, Claus process by alumina catalysts ¹⁰, V₂O₅/TiO₂ catalysed oxidation of o-xylene to phthalic anhydride ¹⁰ and selective catalytic reduction of NO_x over V₂O₅/TiO₂/SiO₂ catalyst ³⁸.

1.3.3 Noble metal catalysts

Supported noble metal catalysts have found numerous applications in industries because of the advantages such as high specific activity and mild reaction conditions compared to metal oxide systems. Another attractive feature of noble metal catalysts is the ability to enhance the productivity in industrial processes. However, there are some disadvantages in the use of noble metal catalysts. They are relatively scarce and therefore expensive, and sensitive to impurities due to low amounts of metal present in the catalyst. High volatility and ease of oxidation of noble metals are the other problems encountered in their commercial use. In spite of these disadvantages, noble metal catalysts are the best choice for a number of applications where transition metal oxides have failed to remain efficient in hostile environment like high temperature, numerous poisons and fluctuating gas compositions.

Automobile exhaust catalysts comprise a complex formulation composed of precious metals like Pt, Pd & Rh, additives like CeO₂ and alumina stabilized with La₂O₃ ^{39, 40}. The support and active components are dispersed on a monolith structure for the effective control of emissions from automobiles ^{1, 2}. Catalysts containing Pt or Pd were used for the high temperature combustion of flue gases ^{41, 42}. In 1991, British Petroleum and Kellogg announced the development of a new process for ammonia synthesis using ruthenium supported on a high surface area graphite carrier as catalyst ⁴³. Bimetallic Pt-Re catalyst is used for the reforming naphtha or other petroleum fractions with low octane number to gasoline fractions with higher octane number or to aromatic feedstocks for petrochemical industry ⁴⁴. Selective hydrogenation of acetylenes to

corresponding olefins in C₂, C₃ and C₄ petrochemical streams is generally carried out on different types of supported Pd catalysts⁴⁵.

Supported Pt catalyst is used for the dehydrogenation of paraffins to olefins¹⁰. The use alumina supported Ru catalyst for the effective conversion of glucose to sorbitol was reported⁴⁶. A Pt-Rh alloy catalyst is used for the oxidation of ammonia to NO/NO₂ in the manufacture of nitric acid^{47, 48}. Another important applications of noble metal catalysts are industrial gas purifications such as deoxo process^{49, 50}, oxidation of CO to CO₂^{51, 52}, etc. CO oxidation over noble metal catalysts is generally identified as structure sensitive reaction and the reported structure sensitivity is higher for Pd which shows higher activity than Pt⁵³.

1.3.4 Zeolites & Zeolite based catalysts

Catalysis by zeolites has been extensively studied for a broad range of reactions in the past few decades^{3, 54-57}. The characteristic features that make them attractive as heterogeneous catalysts are well defined crystalline structure, uniformly arranged pores with one or more discrete sizes, high internal surface area, good thermal stability, highly acidic sites when ion exchanged with protons, well dispersed metal sites on ion exchanging with metal cations and reproducibility of various forms. In general, zeolite catalysis involves both acid catalysed reactions and other chemical transformations. The former is due to the confinement of acid sites in zeolite pores, whereas the latter is the result of presence of ion exchanged metal sites along with the acidic sites. The major achievement in the field of zeolite catalysis was their introduction as cracking catalysts by Mobil in 1959⁵⁸.

The advantage of molecular sieve catalysts over amorphous silica-alumina is size/shape selectivity. This remarkable feature of zeolites has been exploited to perform many large scale selective reactions in the field of petroleum refining, petrochemical manufacture, synfuels production, NO_x abatement and fine chemical industry⁵⁸. Generally, zeolites show four types of selectivities. They are: (1) reactant selectivity

when pore size limits the entrance of reacting molecules⁵⁹, (2) product selectivity when some of the product formed within the pores are too bulky to diffuse out⁵⁹, (3) restricted transition state selectivity when certain reactions are prevented due to the non-availability of required space for corresponding transition state⁶⁰ and (4) molecular traffic control in zeolites with more than one type of pore system. Reactant molecules enter the zeolite through one type of pore system while products diffuse out through the other type of pore⁶¹.

The invention of new zeolite materials has enabled the development of improved technologies for the successful production of various chemicals. For instance, extra large pore molecular sieve catalysts were developed to perform shape selective catalysis on reactants too large to enter the pores of large molecular sieves. This idea was illustrated in some liquid phase and vapour phase reactions⁶²⁻⁶⁴. Furthermore, the catalysts produced by modifying nonacidic molecular sieves with acidic guest materials were found industrial applications for shape selective base catalysis⁶⁵. This material has also been used for the industrial production of some chemicals in environmentally friendly manner as compared to conventional catalytic processes which involve several hazardous intermediates⁶⁶.

Metal exchanged zeolites are known to catalyse a variety of oxidation reactions. Among them, titanium containing zeolite is a unique material that can catalyse a broad range of oxidation reactions⁶⁷. Another interesting system is vanadium exchanged zeolites which was found to be effective for high temperature oxidation, oxyfunctionalisation, oxidation of NO with oxygen⁶⁸, etc. In addition, the recent importance of enantioselective synthesis has led to the development of zeolites that can perform shape selective, asymmetric, heterogeneous catalysis⁶⁹.

1. 4 TOWARDS HETEROGENIZING HOMOGENEOUS CATALYSTS

Although, homogeneous catalysts show excellent catalytic properties, their applications are limited as they are difficult to separate from the reaction medium.

Attempts have been made to combine the high activity and selectivity of homogeneous catalysts with operational benefits of heterogeneous catalysts by heterogenizing known homogeneous catalysts⁷⁰. Several approaches have been considered for this purpose, which can be classified into two. They are:

- 1) *Heterogeneous molecular catalysts*- prepared by methods which induce rearrangement of ligands around the metal center.
- 2) *Supported homogeneous catalysts*- prepared by methods which preserve the structure of metal complex as much as possible.

1. 4. 1 Heterogeneous molecular catalysts

Heterogeneous molecular catalysts are prepared by anchoring the organometallic complex through a direct bond between the metal center and a surface atom. This direct linkage leads to changes in the coordination environment around the metal center. The structure of supported complex can be very different from the precursor complex to obtain entirely new heterogeneous organometallic catalyst. Metal carbonyl clusters anchored on silica support are good example for this class of catalysts⁷¹⁻⁷⁴. Although, the reactivity of this system is promising, it has only limited scope for industrial applications since they are very unstable towards degradation under reaction conditions. Heterogeneous molecular catalysts of Re were synthesized by supporting its complexes on inorganic carriers like alumina, alumina-silica and niobia and were studied for the metathesis of olefins⁷⁵. Even though, these complexes have shown catalytic activity, the presence of variety of surface species restrict them to be well defined⁷⁶.

1. 4. 2 Supported homogeneous catalysts

In supported homogeneous catalysts, the structure of the metal complex is almost identical to that of the precursor homogeneous catalyst. For this kind of heterogenization, many different approaches have been considered which belong to three classes. They are:

- 1) Catalysts anchored on functionalised solids
- 2) Supported liquid phase catalysts
- 3) Encapsulated, intercalated or entrapped catalysts

}

(1). Catalysts anchored on functionalised solids

Homogeneous catalysts are anchored to an inorganic oxide or an organic polymer by bonding the solid with one (more) ligand(s) at a position away from the atom coordinated to the metal center. These systems can be synthesized in two ways. The first method consists in functionalising the support by reacting its surface with a bifunctional ligand and then the metal complex is supported by a ligand exchange reaction with surface groups. For example, the anchoring of phosphine complexes to polymers is done by chloromethylating phenyl rings of the polymer by chloromethyl ethers, then functionalising by reacting with LiPPh_2 and exchanging with homogeneous catalyst¹⁴. In the second approach, a metal complex containing desired amount of functionalised ligand reacts with the solid surface to form the supported complex. $\text{Ni}(\text{CO})_4$, as an example, was anchored by reacting it with phosphinated silica at optimum experimental conditions⁷⁰. Supported homogeneous catalysts were tested for a number of industrially important reactions. Although the catalytic activity of these catalysts is as good as their homogeneous counterparts, the disadvantages including leaching of metal complex in liquid phase reactions and aggregation to form binuclear species restrict its usage in industry⁷⁷.

(2). Supported liquid phase catalysts

Catalysis in biphasic media is one of the efficient methods to solve the problem of catalysts separation from reaction medium and therefore this technique has found a number of applications⁷⁸⁻⁸². However, this method is not effective when the solubility of reactants in catalyst phase is too low and hence activity is too low as a result of lower interfacial surface. In such cases, supporting the catalyst in a thin film of nonvolatile liquid deposited on a solid of high specific surface area improves significantly the

activity⁸³⁻⁸⁶. The isomerisation of pentene-1 catalysed by RhCl_3 supported in a thin film of ethylene glycol and hydroformylation of propene catalysed by $(\text{Ph}_3\text{P})_2\text{Rh}(\text{CO})\text{Cl}$ in benzylbutylphthalate film are some the examples of supported liquid phase catalysts⁸⁷⁻⁸⁸. Supported aqueous phase catalysts were developed by supporting water/organic solvent biphasic catalysts⁸⁹. However, a complete evaluation of the catalytic properties of supported liquid phase systems, such as kinetic analysis, recycling tests, metal leaching, etc. has to be performed to scale up this class of catalysts to industrial applications.

(3). *Encapsulated, intercalated or entrapped catalysts*

Transition metal complexes can be immobilized in the voids of a porous inorganic or organic solid by encapsulation, intercalation or entrapment. A variety of compounds have been encapsulated in the porous network of preformed solids mostly in large zeolites. In contrast to those supported on nonporous inorganic oxides, zeolite encapsulated complexes are stable under reaction conditions due to reduced dimerisation or aggregation. Additionally more selectivity is also induced via steric effects of the zeolite framework

Intercalated catalysts are prepared by introducing cationic complexes as such between the silicate layers of swelling clays, such as smectites by ion exchanging⁹⁰⁻⁹². The increase of interlayer spacing provides evidence for intercalation. The enhanced selectivity of intercalated catalysts in reactions indicates the presence of steric effects⁹². The special feature of this system is the possibility to adjust the size of interlayers by incorporating complexes of different sizes⁹³, whereas zeolite pores are rigid.

In the case of entrapped catalysts, metal complex is introduced directly in the mixture of reactants used for the synthesis of the solid support. A number of entrapped complexes were prepared and successfully tested for reactions such as hydrogenation, isomerisation and hydroformylation. It is possible to obtain good activity, selectivity and stability for such systems by the simultaneous choice of the metal complex and support in such a way that it allows the diffusion of reactants and products.

supported in Y zeolite modified with Li was reported to be particularly active for hydrogenation reactions⁹⁹. The intrazeolite chemistry of iron carbonyls also received much attention. $\text{Fe}(\text{CO})_5$, $\text{Fe}_2(\text{CO})_9$ and $\text{Fe}_3(\text{CO})_{12}$ were adsorbed in Y-zeolite without any change in the structure¹⁰⁰. Zeolite X or Y supported dicobalt octacarbonyls were prepared by either direct sublimation¹⁰¹ or adsorption from pentane solution¹⁰². Nickel tetracarbonyl in zeolite support was also studied¹⁰³.

Zeolites, X and Y allow the entrapment of certain organometallics like bis (dithiophosphato)nickel which cannot be supported on carrier like silica gel¹⁰⁴. $\text{Tris}(\pi\text{-allyl})\text{rhodium}$ was a well studied system to illustrate the synthesis of organometallic compounds in zeolite cavities¹⁰⁵. Metallocenes can be easily exchanged into zeolites and its interactions with zeolite lattice can be studied using various spectroscopic techniques. Goder and Ozin exchanged ferrocene and found its homogeneous distribution in zeolite¹⁰⁶. Zeolites were also used to preferentially support redox active species, both internally and externally. It is interesting that such systems allow rapid electron transfer between the surface species and intrazeolite species¹⁰⁷.

Many coordination complexes were prepared in zeolites not only with a view to derive active and selective catalysts but also to investigate the interactions between the zeolite framework and the complexes. The early work was confined to some systems that are not very stable and can be destroyed by evacuation or gentle heating¹⁰⁸⁻¹¹⁰. Intrazeolite hexamethylisocyanide complex of Co was one of such well characterized complex¹¹¹. Later, several workers focused on the encapsulation of complexes of monodentate ligands. These studies were first reviewed by Lungford^{111, 112} and later on by Mortier and Schoonheydt¹¹³ and Ozin and Gil¹¹⁴. A few complexes with bi- and polydentate ligands were synthesized in zeolites and characterized. Among them, metal complexes of ethylenediamine, pyridine, salen, phthalocyanine and porphyrin have received much attraction as effective catalysts for various reactions¹¹⁵⁻¹¹⁸.

1.5.2 Structural considerations

Zeolites are microporous, crystalline, three dimensional aluminosilicates composed of SiO_4 and AlO_4^- tetrahedra joined through shared oxygen bridges. These tetrahedra are arranged in such a way that two Al atoms never come in the adjoining tetrahedra but are separated by at least one silicon tetrahedron. The basic building block of A, X and Y zeolite is a sodalite unit which is a cubo-octahedron formed from 24 tetrahedra of SiO_4 and AlO_4^- and consists of six 4-membered cube faces and eight 6-membered octahedron faces. When the sodalite units are connected each other at their square faces, the resulting structure is called A-zeolite and if they are joined at the hexagonal faces, X and Y structures are formed. The large cavities in these zeolite structures are called super cage or α -cage while smaller cavities are called sodalite cage or β -cage. The structure of Y zeolite is shown in Figure I. 1. The unit cell formulae and other characteristics of A, X and Y zeolites⁵⁶ are given in Table I. 1.

Table I. 1

Properties of zeolites A, X and Y

Zeolite	Unit cell formula	Mol. ratio $\text{SiO}_2/$ Al_2O_3	α -cage diameter	α -cage aperture
A	$\text{Na}_{12}(\text{AlO}_2)_{12}(\text{SiO}_2)_{12} n\text{H}_2\text{O}$	2 : 1	11 Å	4 Å
X	$\text{Na}_{86}(\text{AlO}_2)_{86}(\text{SiO}_2)_{106} n\text{H}_2\text{O}$	2.5 : 1	13 Å	8 Å
Y	$\text{Na}_{56}(\text{AlO}_2)_{56}(\text{SiO}_2)_{136} n\text{H}_2\text{O}$	5 : 1	13 Å	8 Å

Silicon tetrahedron maintains electrical neutrality whereas a trivalent Al atom when bound to four oxygen atoms, the resultant Al tetrahedron will have a net negative charge. In synthetic zeolites, the net negative charge on the lattice is counter balanced by protons. It is also possible to introduce transition metal ions into the zeolite lattice in place of protons by ion exchanging Na^+ form of the zeolite with desired transition metal ion. The existence of exchangeable cations in the zeolite lattice provides the possibility of inclusion of metals and chemically interesting metal complexes.

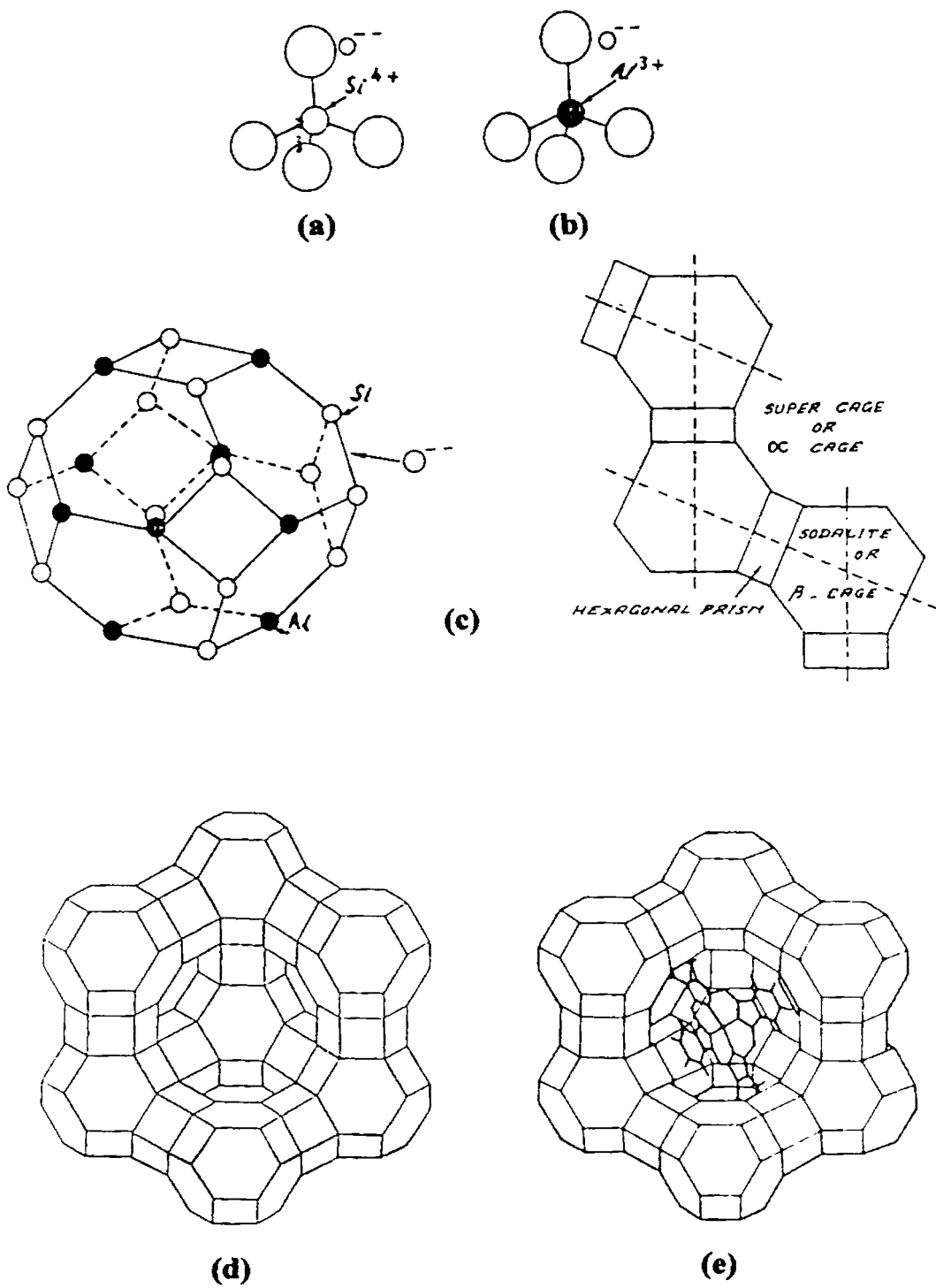


Figure I. 1

(a). SiO_4 tetrahedra, (b). AlO_4^- tetrahedral, (c). Sodalite unit
 (d). Y Zeolite and (e). Y Zeolite encapsulated iron phthalocyanine

Metal complexes of about 10 to 13 Å in diameter can be synthesized inside the α -cage of zeolites X and Y. As the openings of the cages are small, the complexes once formed inside the cages cannot move out through the openings, but remain trapped. Zeolite can be considered as a solid solvent and the entrapped molecule as a solute which is not mobile. During catalysis, zeolite cage acts as a molecular scale microreactor containing metal complex catalyst. The reactants can enter through openings, undergo reaction at metal site and exit as products. In this special microreactor, the framework atoms (reactor walls) also influence the catalytic activity through its electronic and steric effects on the encapsulated complexes. Additionally, the well known sieving and orienting properties of zeolite network structure could be explored in catalytic reactions which require high selectivity.

1.5.3 Merits and Demerits

Synthesis of metal complexes in the super cage of zeolites offers several advantages over their homogeneous counterparts so as to conveniently use them as catalysts for many reactions^{114, 119}. It is generally stated that the activity of metal complex in solution phase is retained or improved on encapsulating in zeolite cavities. In addition, the encapsulated complexes are able to work at milder temperature and pressure as compared to that of conventional heterogeneous catalysts. The most attractive advantage of such heterogenized systems is the ease of separation of catalysts from reactants and products. In fact, zeolite encapsulated metal complexes combine the merits of both homogeneous and heterogeneous catalytic systems, but at the same time, minimise the demerits of both.

Zeolites are attractive hosts for catalytic species due to their high thermal stability, well defined structure, large internal surface area, etc.¹²⁰. Enhanced size and shape selectivity due to zeolite framework besides that due to the constraints in guest molecule is an important feature of encapsulated catalysts. The interaction of metal complex with zeolite may alter its electronic structure and thereby its catalytic performance. In short,

besides the tremendous activity of guest compounds, the encapsulated catalysts show the attractive features of zeolites.

The stability of metal complexes in actual reaction conditions is expected to be improved on encapsulating in zeolite pores¹²¹. This effect may be explained in terms of the following aspects: (1) the complexes are immobilized inside the cavity, (2) dimerisation processes of the complexes are retarded resulting longer life and (3) zeolite imparts additional stability to the complex by acting as ligands. The high stability of the catalysts provides the ability to work at elevated temperatures which in turn tend to overcome diffusional restrictions, promote reactions with high activation energy and to withstand severe conditions of regeneration process.

Like any other catalytic material zeolite encapsulated metal complexes also have some limitations¹¹⁴. The various problems associated with zeolite catalysts including pore plugging, poisoning, migration, leaching and structural defects of zeolite matrix are also applicable in the case of catalysts immobilized in them. The catalytic activity may be severely affected by clogging of pores by products. Such situations make necessary frequent catalyst regeneration by high temperature operation that is difficult when encapsulated complex is thermally unstable. Less mobility of molecules in zeolite cavity due to the entrapped complexes restricts its use for catalysing reactions of bigger molecules. However, the main issue in encapsulation is the preparation of homogeneously distributed metal complexes in zeolite framework. The goal of achieving well defined intrazeolite catalysts is possible only by strictly optimising the preparation conditions.

1.5.4 Enzymes and Enzyme mimics

Enzymes are one of the most efficient catalysts known which exhibit extreme selectivities in chemical transformations. Enzymes catalyse reactions at ambient temperatures, that are possible on heterogeneous systems only at high temperatures and pressures. It is also interesting to mention that they are environment friendly catalysts

working without producing any hazardous by-products. A large number of drugs, pharmaceuticals and specialty chemicals are manufactured by biochemical methods using enzymes¹²²⁻¹²⁴. In spite of the remarkable achievements in biocatalysis, enzyme technology has limited to the low volume, high value chemicals due to raw material wastage in cell growth, difficulties in product separation, non-continuous operation and low stability of biochemical catalysts.

Enzymes are composed of a metal complex as active site embedded in a large protein structure. The functions of protein molecule are: (1) protecting active sites from self destructing reactions like dimerisation; (2) inducing substrate selectivity due to protein channels; and (3) providing stereochemical environment at the active centre for the specific chemical transformation to take place¹²⁵. The desire to understand and exploit the chemistry of enzymes has prompted an extensive research on synthetic porphyrin, phthalocyanine and Schiff base models of enzyme active sites¹²⁶⁻¹²⁸ and later on superstructured mimics¹²⁹ with a controlled steric environment for better selectivity. The comparative evaluation of activity, selectivity and stability of both synthetic models and natural enzymes has given very promising results in the case of biomimetic oxidation of hydrocarbons¹³⁰⁻¹³².

It was known that inorganic materials like zeolite could provide the best arrangement for the catalytically active sites in their cavities and direct substrates towards it. Furthermore, the channels and cages in zeolite framework are very similar to those created by the protein structure of enzyme. Hence, new catalysts can be designed by replacing the protein portion of natural enzymes by the zeolite framework. These hybrid catalysts combine the attractive features of zeolites and tremendous activity and selectivity of enzymes. Therefore, zeolite encapsulated metal complexes, referred to as 'Zeozymes', have been described as model compounds for mimicking enzymes^{117, 125, 133}.

Several zeolite complexes were designed and successfully developed to act as zeozymes with respect to activity and stability in catalytic reactions. Nature performs

selective oxidation of organic materials to usable hydrophilic compounds by means of the monooxygenase enzymes of the cytochrome P450 family ¹²⁶. The desire to mimic cytochrome P450 has led to the development of new zeolite based Fe/Pd oxidation catalysts ¹³³⁻¹³⁵. Models of cytochrome P450 consisting of organometallic complexes encapsulated in zeolites were also designed ^{116, 117}. These systems control selectivity and inhibit autoxidation, but do not show any mechanistic analogy with enzymatic processes and exhibit only low oxidation rate as compared to that of enzymes.

Recently, an efficient mimic for cytochrome P450 was reported and its catalytic activity was found to be promising for industrial applications ^{135, 136}. This catalyst comprises iron phthalocyanine (FePc) complexes encapsulated in Y zeolite which are in turn embedded in a polydimethylsiloxane (PDMS) membrane as represented in Figure I. 2. The role of polymer is to act as an interface between two immiscible phases as phospholipid membrane in which cytochrome P450 resides. This system oxidises alkanes at room temperature at rates comparable to those of the enzyme. Furthermore, the oxidation activity of zeolite encapsulated iron phthalocyanine complex has enhanced to 300 times higher on supporting in the membrane. Intrazeolite complex preferentially sorbs polar compounds, whereas membrane embedded system sorbs cyclohexane and creates a barrier against polar compounds. Moreover, the polymer allows high sorption and fast diffusion of reagents together with the homogeneous distribution of catalyst particles.

Zeolite encapsulated cobalt(I) salen was also suggested as a synthetic mimic for studying the oxygen binding properties of hemoglobin ^{125, 137}. A cross sectional representation of this system is shown in Figure I. 3. This system is superior to other reported models with respect to the stability against deteriorious processes of autoxidation and dimerisation. However, in contrary to the behaviour of hemoglobin, the rate of oxygen binding decreases after the initial adsorption. This may be due to the fact that the binding becomes increasingly difficult as the molecule moves from the exterior to interior of zeolite crystallite ¹²⁵.

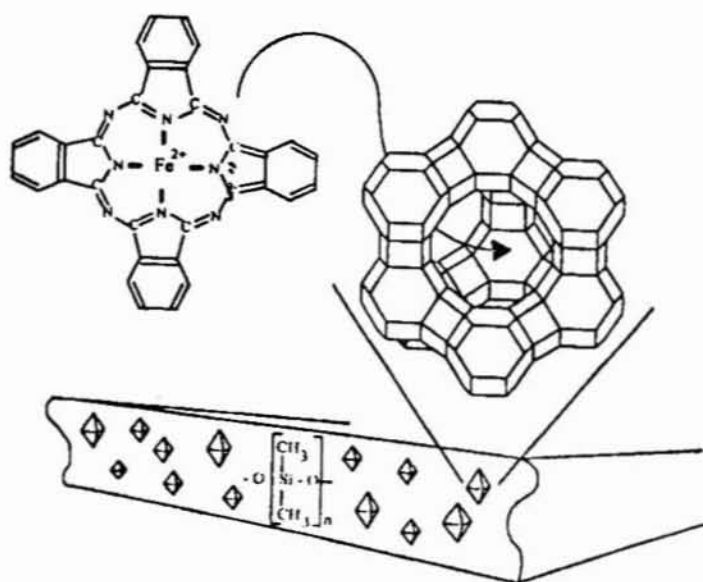


Figure I. 2
Schematic representation of encapsulation of FePc and subsequent incorporation in PDMS-membrane

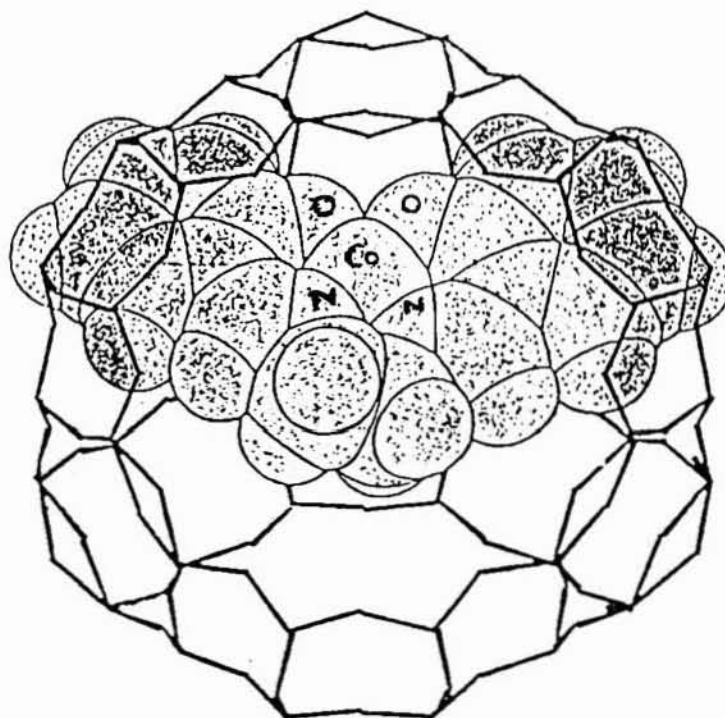


Figure I. 3
Cross sectional representation of Cobalt(I) salen

1. 6 ZEOLITE ENCAPSULATION METHODS

Three methods, currently used for encapsulating metal complexes in zeolites are:

- 1) **Flexible ligand method**- involves diffusion of ligand molecules through the zeolite pores followed by reaction with transition metal ions previously introduced into the lattice
- 2) **Ship-in-the bottle method**- metal complex is synthesized inside the zeolite cavity from smaller components or assembling the ligand from smaller species around the transition metal ions inside the zeolite cavities
- 3) **Zeolite synthesis method**- involves the synthesis of zeolite structure around the pre-formed transition metal complex

These three approaches are discussed below:

1. 6. 1 Flexible ligand method

In this approach the ligand molecule must be flexible enough to diffuse through the zeolite pores. Once the ligand has entered the zeolite cage and reacted with previously exchanged transition metal ions, the complex formed is too large and rigid, and therefore it cannot escape from the cages.

This concept was first experimented by Herron¹³⁷ to prepare Co-salen complexes in the supercages of faujacite. The salen ligand offers a high desired flexibility to pass through the zeolite channels due to the possible free rotation around the C-C σ -bond connecting the two salicylidene moieties. This has led to the synthesis of salen complexes with cobalt¹³⁷, manganese¹¹⁹, iron¹³⁸, rhodium¹³⁹ and palladium¹⁴⁰ ions within Y-zeolite cages. This method was used for preparing complexes of several simple ligands like bipyridine. Highly selective complexation of these ligands to form bis- or tris- coordinated complex in zeolite cavities was achieved by adjusting the ligand to metal ion ratio and the temperature of synthesis^{141, 142}. Later on, transition metal complexes of several other Schiff base ligands were encapsulated^{119, 143}.

1. 6. 2 Ship-in-a-Bottle method

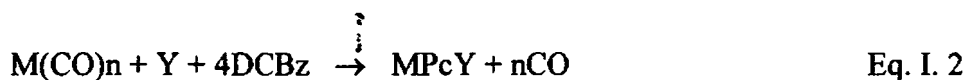
Ship-in-a Bottle method was first used by Romanovsky and co-workers^{144, 145}. Later phthalocyanine complexes of cobalt¹⁴⁶, copper¹⁴⁷, iron¹⁴⁸, manganese¹⁴⁹, nickel¹⁴⁵, osmium¹⁴⁵, rhodium¹⁵⁰ and ruthenium¹⁴⁵ were synthesized. This method involves the diffusion of dicyanobenzenes into the zeolite matrix where it undergoes cyclisation around a previously introduced metal ion to form a tetradentate macrocycle which is too large to exit. After mixing the ion exchanged zeolite and 1,2-dicyanobenzenes, tetramerisation is induced by heating in vacuum at temperatures between 250 °C and 350 °C¹⁵¹. The complexation temperature determined by differential scanning calorimetry^{146, 147} varies with the type of transition metal ion and the structure of the zeolite. The reaction takes place according to Eq. I. 1.



Zeolite encapsulated substituted phthalocyanines were synthesized by using substituted dicyanobenzenes as starting reagent. For example, the synthesis of intrazeolite tetra-t-butyl-substituted iron-phthalocyanine¹⁵², perfluorophthalocyanines of iron¹⁵³, cobalt^{154, 155}, copper^{154, 155} and manganese¹⁵⁴ and iron-tetranitrophthalocyanine¹⁵⁶ was reported. However, in the case of tetranitrophthalocyanines, it was doubtful that the complexes are located mostly on the external surface.

Another approach of Ship-in-a-Bottle synthesis involves the introduction of the transition metal by adsorption of corresponding carbonyl complex or metallocene in zeolite, followed by the synthesis of phthalocyanine ligand around the transition metal. This method was mainly used for preparing intrazeolite iron-phthalocyanine from the adsorbed iron pentacarbonyls or ferrocene^{145, 157-159}. Intrazeolite iron pentacarbonyls are decomposed thermally leading to metal clusters in the supercages which react with dicyanobenzene to give metal phthalocyanine. Alternatively, metal carbonyls can also be introduced by direct ligand exchange of CO by 1,2-dicyanobenzene at lower temperatures. As indicated in Eq. I. 2, no protons and hence no acid sites are produced

during complex formation via carbonyl route. However, in both cases the major disadvantage is the formation of large amount of excess metal clusters in zeolite since only one phthalocyanine complex can be formed per super cage.



The use of adsorbed ferrocene as a source for iron was also successfully described by Parton *et al*¹⁵⁸. This reaction is represented in Eq. I. 3.



This method has the advantage that the encapsulated complex is free from uncomplexed metal species. However, large amount of free phthalocyanine was observed inside the zeolite after complexation reaction¹⁵⁹. The entrapped free ligands may create diffusional restrictions in pores for reactants and products in various catalytic reactions.

Ship-in-a-Bottle technique was also applied for encapsulating complexes in molecular sieves without cation exchange capacity, such as VPI-5¹⁵⁸ and for the synthesis of porphyrin type ligands in the super cages of Y-zeolite. The encapsulation of iron and manganese-tetramethylporphyrin in the super cages of Y-zeolite was reported by Nakamura *et al*¹⁶⁰. Chan and Wilson¹⁶¹ claimed the formation of intrazeolite tetraphenylporphyrins on treating metal exchanged zeolite with pyrrol and benzaldehyde¹⁶¹. However, more experimental evidences yet to be presented for ensuring true complex encapsulation.

1. 6. 3 Zeolite synthesis method

Zeolite synthesis method is a recent innovation in which metal complexes are encapsulated by forming zeolite structure around the preformed complexes¹⁶²⁻¹⁶⁵. The complex is added as a template during the crystallisation of zeolites. This method can be applied only if the complex is stable enough to withstand the zeolite synthesis

conditions (i.e., pH, temperature and hydrothermal condition) and has sufficient solubility to get a random distribution of the complex in the synthesis medium to form well defined homogeneous product. This method offers several advantages including mild preparation conditions and well defined intrazeolite metal complexes.

Rankel and Valyocsik ¹⁶² attempted the synthesis of intrazeolite complexes of bipyridine, phenanthroline and phthalocyanine by this method. It was claimed that the homogeneous encapsulation of metal complexes is possible in zeolite X and, AlPO₄-5 and AlPO₄-11 by preventing the aggregation of the complexes in aqueous synthesis medium. If organic templates are used for zeolite synthesis, they are removed by calcining the final product. The intrazeolite complex might be destroyed during this calcination step. Hence, zeolite synthesis method appears to be effective only in the cases where the synthesis of zeolite matrix is possible without the use of any further organic templates.

1. 7 CHARACTERISATION OF ZEOLITE COMPLEXES

Encapsulation of metal complexes in porous solids like zeolite helps to combine the characteristics of both zeolite and metal complex to obtain new hybrid catalysts. A complete characterization of such composite materials is necessary to ensure encapsulation and provide fruitful informations on the real state of complex and zeolite support. In general, zeolite encapsulated complexes are characterized to address the following aspects:

1. internal versus external confinement and the distribution of guest compounds in zeolite host
2. nature of the complex formed in zeolite cavity compared to that in solution phase
3. the degree of complexation
4. the effect of host-guest interactions on the structure of complex.
5. whether zeolite framework is preserved on encapsulation

6. the stability in comparison to free metal complexes
7. the ability to provide vacant coordination sites for catalytic reaction.

Several approaches ^{114, 166-168} have been reported for investigating above aspects and their influence on catalytic performance. These approaches include molecular modelling, entrapment identification, physico-chemical properties of the zeolite complexes, adsorption studies, stability studies and electrochemical studies. A brief account of various characterization methods is given below:

1. 7. 1 Molecular modelling and simulation

The use of computerised molecular graphics analysis ¹⁶⁹ has provided a better understanding of the properties of zeolite encapsulated complexes and the science behind their catalysis. The structure of Y zeolite encapsulated iron phthalocyanine (FePc) has been studied using molecular modelling method ¹⁷⁰. It was shown that the FePc was located at the center of the supercage with the bridging N atoms pointing towards the four rings of the cubo-octahedra. The planarity of the complex is disturbed to accommodate bigger phthalocyanine ligand in the supercage ^{170, 171}.

Molecular graphics techniques are also useful for modelling and simulating catalysis in zeolite cavities ^{172, 173}, particularly for studying the selectivity of zeolite based catalysts ¹⁶⁹. The computer simulation can be achieved either by energy minimization method or by molecular dynamics method ¹⁶⁹. In the first approach, the system moves towards a potential energy minimum through a low energy pathway, whereas the latter approach allows the simulation of a complete chemical system at a finite temperature and pressure in which properties are evolved as a function of time.

1. 7. 2 Entrapment identification

The main issue in the synthesis of zeolite encapsulated complexes is to recognize appropriate conditions at which well defined distribution of guest compounds occur in the zeolite cage, instead of being concentrated on the external surface. The distribution

of guest compounds in zeolite host can be ascertained by several chemical methods. One of such methods is size-dependent chemical reaction as illustrated by reactions between phosphines and encapsulated metal carbonyls ⁷². With smaller phosphines, all the supported carbonyls react to form anionic species in zeolite lattice, but no reaction is observed with phosphines too large to penetrate the pore openings of the zeolite.

The internal entrapment can also be confirmed by studying size/shape selectivity which is imparted by the molecular discriminating nature of the zeolite lattice. For example, Mo(CO)₆ in alkali metal exchanged Y zeolite has showed high activity and selectivity in the hydrogenation of 1,3-butadiene whereas nonzeolitic supports exhibited nonselective hydrogenation properties ⁹⁹. Similarly, zeolite encapsulated Rh(allyl)₂ exhibits high selectivity in olefin hydrogenation as compared to silica supported analogue ¹⁷⁴. To establish the internal confinement of this species, catalytic self poisoning reactions have also been carried out with phosphines of varying sizes ¹⁰⁵. Only smaller phosphines which can penetrate zeolite pores are able to reduce the catalytic activity by coordinating with the entrapped complexes.

In another method, zeolite framework is destroyed by treating with Con. H₂SO₄ and the resulting solution is analysed by UV-Vis. spectroscopy for directly detecting metal complex previously encapsulated in the framework ¹⁷⁵. However, this method can be used only if the complex is stable in Con H₂SO₄.

Besides such chemical methods, modern physical techniques are also used to ensure the presence of guest molecules in zeolite cavities. Some of these techniques are discussed in next section.

1. 7. 3 Physico-chemical methods

(a). Chemical analysis

Chemical analysis is used to find the composition of zeolite complexes. The degree of ion exchange in zeolite and the unit cell formula are derived from the analytical

data¹⁶⁶. The Si/Al ratio of the zeolite complexes is compared with that of pure zeolite to make sure that zeolite framework is preserved on encapsulating complexes.

(b). CHN analysis

CHN analysis is performed to quantify organic ligands complexed to the metal ions. These analytical data also provide informations on the extent of complexation and help to identify the presence of uncomplexed metal ions which are not removed on ion exchanging at the final stage of synthesis.

(c). Surface area analysis

Surface area measurement is the easiest probe to detect encapsulation of guest molecules in zeolite cavities. A lower surface area of intrazeolite complex as compared to metal exchanged zeolite indicates the filling of zeolite pores with complexes. Usually, BET surface area is measured by nitrogen adsorption at liquid nitrogen temperature.

(d). X-ray diffraction spectroscopy

X-ray diffraction is used to study the diffraction pattern of the zeolite. The evaluation of the spectra of host zeolite and zeolite complex is carried out to ensure that zeolite crystallinity is not affected by the encapsulation of metal complex¹⁶⁶.

(e). Electronic spectroscopy

The ultraviolet and visible light absorption spectroscopy gives information about the d orbital splitting of metal ions and ligand-metal interactions through the ligand to metal charge transfer transitions. The nature of coordination can be studied by comparing the spectra with those of known complexes. For example, diffuse reflectance spectroscopy has been applied to tris(ethylenediamine) complex of Co(II) in zeolite Y. The appearance of a band at 20650 cm^{-1} , characteristic d-d transition of an octahedral complex, indicates chelate formation¹⁷⁶. This complex is stable upto $200\text{ }^{\circ}\text{C}$, but it

decomposes at higher temperatures to monoligand complex which arises charge transfer bands in the UV region.

Interestingly, the process of formation of dimethylglyoximato-Co(II) complex during the uptake of dimethylglyoxime in Co-X zeolite has been monitored by in situ UV/Vis microscope spectrophotometry¹⁷⁷. In the case of zeolite entrapped cobalt phthalocyanine complexes, UV-Vis spectra¹⁷⁸ exhibit a splitting of the Q band, which is expected for a lowering of symmetry from D_{4h} to D_{2h} ¹⁷⁹. The protons formed during the complex formation cause partial protonation of the encapsulated metal phthalocyanine and hence symmetry is lowered to D_{2h} ¹⁸⁰. Furthermore, luminescence spectra in UV-Vis region provide informations about the distribution of complexes in the zeolite lattice¹⁴¹.

(f). Fourier Transform Infrared spectroscopy

FTIR spectroscopy provides valuable evidences for the formation of metal complexes in zeolite pores. The ligand molecules are coordinated to transition metal cations if different spectral patterns appear in the free and chelated state or if characteristic bands exhibit shift in frequency upon coordination.

(g). EPR spectroscopy

EPR spectroscopy is a powerful probe to study the bonding of metal complexes in zeolite cavity. For example, it was used to investigate the square planar complexes of Co(II) with low spin ($S=1/2$) doublet ground state in which $3d_z^2$ orbital occupies the unpaired electron. The spin Hamiltonian parameters of such ground states undergo changes during axial ligation which provides means to study the processes of complexation. The complexation process in tetrakis(pyridine)copper(II) was studied much clearly by evaluating the intensity changes in EPR spectra¹⁸¹. Tris(bipyridine) complexes of Co(II), Fe(III) and Ru(III)^{141, 142, 182} in Y zeolite are stable in low spin state upto -196°C , above which the formation of a high spin octahedral state is identified by EPR spectra. EPR spectra are also useful to distinguish monomeric and dimeric complexes from the multiplicity of the hyperfine structure. Zeolite entrapped

Co(II)-Schiff base complexes were analysed for EPR spectra with a view to study the influences of zeolite host on the geometry of the complex. In zeolite encapsulated cobalt phthalocyanines, the protons released during complexation interact with the nitrogen atoms of the complex, resulting non-equivalency of nitrogen atoms which could also be identified by EPR spectra.

(h). Conventional Transmission Electron Microscopy

The size and shape of solid particles, higher than 100 nm can be measured by conventional transmission electron microscopy.

(i). High Resolution Electron Microscopy

The measurement particle size below the nanoscale of individual unit cells is performed by high resolution electron microscopy. This technique is useful to study the formation of extra material on or inside the zeolites and to detect any change in the zeolite framework on encapsulating metal complexes.

(j). X-ray Photoelectron Spectroscopy

X-ray photoelectron spectroscopy can be applied to determine the chemical composition of external parts of the solid in a few nanometers in depth as well as to study the chemical state of surface atoms. The XPS data of encapsulated complexes provide following informations:

1. the distribution of encapsulated complexes in zeolite lattice i.e. either homogeneously distributed throughout the lattice or enriched in a shell close to the zeolite surface.
2. the degree of complexation
3. the structure of complex
4. the interaction with the framework¹⁸³⁻¹⁸⁵

From the detailed analysis of surface elements, it is possible to detect preferential location of metal complex by comparing M:Si, M:Na and L:Si (L is a ligand element) with those expected for bulk composition. A deviation of these values to higher side indicates enrichment of species at or close to the external surface of zeolite lattice. In the case of nickel phthalocyanine encapsulated in Y zeolite, for example, the extent of binding of metal ions to phthalocyanine ligand can be determined via N:Ni ratio¹⁸⁶. The degree of complexation increases as this ratio approaches the maximum value of 8. The reduction of binding energy of the metal from 855.8 for NiY to 854.9 for NiPcY is also an interesting proof for high degree complex formation. The structure of zeolite encapsulated metal phthalocyanine can strongly deviate from that of the free complex. This is indicated by a change of XPS spectra as in the case of NiPcY¹⁸⁶ which gives a doublet instead of a singlet for free complex.

(k). NMR spectroscopy

High resolution magic angle spinning nuclear magnetic resonance spectroscopy (HR MAS NMR) is used to study the interaction of phthalocyanines with the zeolite framework. This study has shown the existence of strong interaction between Al atoms in the pore walls and hydrogen atoms of the phthalocyanine molecule. As a result of these interactions, zeolite framework undergoes local deformations which are indicated by the loss of resolution in the spectrum.

1. 7. 4 Oxygen adsorption

Oxygen adsorption is used to determine the fraction of complexed metal ions in the zeolite lattice which are capable to bind oxygen molecules. The oxygen pulse technique has been applied to measure this fraction of Co(II) metal ions in [Co(II)(bipyridine)(terpyridine)]²⁺-LiY zeolite¹⁸⁷. By this technique, it would be possible to identify the metal complexes which are able to take up oxygen reversibly or irreversibly. For example, cobalt complex of bis(salicylidine)ethylenediamine in zeolite Y does not allow the reversible uptake of oxygen, but it is possible with cobalt complexes

of bis(salicylaldehyde)-methyldipropyltriamine in zeolite NaY¹⁸⁸. The adsorption of oxygen on the metal sites is controlled by the diffusion process.

1.7.5 Thermal analysis

The thermal stability of zeolite encapsulated complexes can be studied by thermogravimetric analysis. Thermal analysis of intrazeolite metal phthalocyanines has been performed in air¹⁸⁹, oxygen, hydrogen and helium¹⁸⁶. The complexes are stable upto 873 K in helium, but decompose at faster rate in air and hydrogen at 700K and even below at < 500 K in oxygen. The poor stability of the encapsulated complex in oxygen atmosphere has been reflected in both gas phase¹⁸⁹ and liquid phase¹⁹⁰ oxidation reactions with molecular oxygen. However, zeolite complexes are not significantly affected in oxyfunctionalisation reactions of alkanes or alkenes at room temperature using t-butylhydroperoxide or iodosobenzene^{191,192}. Also, in the case of metal-porphyrin compounds, photostability has been enhanced upon encapsulating in zeolites¹⁹³.

1.7.6 Electrochemical methods

Increased interest in the encapsulation of metal complexes in supercages of zeolites has prompted several workers to study the electrochemical behavior of various zeolite entrapped complexes and thereby assess the possibility of using them in electrocatalysis¹⁹⁴⁻¹⁹⁶. It is known that electrochemical technique such as cyclic voltametry provides information on the oxidation state and redox chemistry of the active metal atom¹⁹⁷. This technique also gives means to recognize the location of guest compounds i.e at the external surface or encapsulated in zeolite pores¹⁹⁸. The mechanism of electron transfer was suggested by Shaw et al¹⁹⁹ for electroactive ion exchanged zeolite and zeolite encapsulated complexes. In the former case, electron transfer takes place after the electroactive species is exchanged out of the zeolite by electrolyte cations whereas the latter undergo electron transfer within the zeolite cavities.

The electrochemistry of zeolite encapsulated phthalocyanine complexes was extensively studied²⁰⁰⁻²⁰². Encapsulated perhalogenated phthalocyanines also show well

defined redox behavior which is difficult to observe in solution phase^{203, 204}. Ni(bpy) encapsulated in Y zeolite was used for the electroassisted catalytic reduction of organic halides like benzyl chloride, but large molecule like triphenylmethyl bromide is unreactive²⁰⁵. It is expected that this electrochemical behavior reflects the activity and selectivity of intrazeolite complexes. The electroactivity of encapsulated Mn(III)-salen and Ru(III)-salen is very similar to that of dissolved complexes in solution. In the case of encapsulated Co(II)-salen and Fe(III)-salen, the existence of two redox processes indicates the existence of two metal-salen structures in zeolite cavity^{206, 207}. These structures are identified as planar or nonplanar tetradentate structure and bidentate structures. These results indicate that zeolite may be involved in the coordination of the metal ions

1. 8 HOST-GUEST INTERACTIONS IN ZEOLITE COMPLEXES

A better understanding of the influence of zeolite architecture on the structure and reactivity of encapsulated guest complexes is expected to facilitate the design of active catalysts for various chemical reactions. A combination of various spectral techniques is used to study the host-guest interactions in zeolite encapsulated complexes. Herron *et al*²⁰⁸ reported the changes in the properties of tetracarbonyl nickel as a result of encapsulation in zeolite X. It appears that zeolite allows the formation of highly reactive, moderately long lived, coordinatively unsaturated Ni(CO)₃ species in the cavities, whereas no such reactive species can exist in solution phase.

The electrostatic interaction between the zeolite framework and the metal complex is considerably important for understanding the role of zeolite support in the catalysis by encapsulated complexes. For example, copper-ammine complex, an intermediate in the catalytic oxidation of ammonia, was encapsulated and studied by Raman spectroscopy. Pronounced electrostatic interactions have been seen in the absence of water in the zeolite lattice²⁰⁹.

Tris(bipyridine)ruthenium(II) in zeolite Y²¹⁰⁻²¹² was prepared for investigating the host-guest interactions as they are highly probable in such systems to the close proximity of the periphery of the bipyridine ligand to the anionic zeolite framework. The excited state properties of Ru(bpy)₃²⁺ are influenced by zeolite framework upon dehydration, whereas ground state structure is not perturbed. However, this complex in hydrated zeolite resembles its aqueous solution. Tiwary and Vasudevan²¹³ have also reported the effect of zeolite topology on the geometry of this encapsulated complex. Comparative spectroscopic, magnetic and molecular graphics investigations of free and encapsulated complex indicated that encapsulation partially reduces the trigonal distortion observed in unencapsulated complex to restore octahedral geometry. Zeolite encapsulated tris(2,2'- bipyridine)iron was also investigated for the interactions of zeolite framework which induce unusual chemical and physical behaviour for the encapsulated complex²¹⁴⁻²¹⁶.

The difference in the behaviour of Schiff base complexes of Co(II) formed in solution and that in a zeolite cage was studied by changing the polydentate Schiff base ligands²¹⁷. With tetradentate ligand such as salen, four coordinate low spin Co(II) complexes are formed only in low yield in zeolite Y. But in solutions, Schiff base usually readily reacts with the metal to form complexes. However, pentadentate ligands are more effective in reacting with Co(II) ions in zeolite to form complexes in the pores. These observations also reflect the influence of zeolite matrix on complex formation.

1. 9 CATALYSIS BY ZEOLITE ENCAPSULATED COMPLEXES

Zeolite encapsulated metal complexes provide reaction centres for binding and catalysis of molecules those are mobile in zeolite pores^{218, 111}. The steric constraints in zeolite may distort the encapsulated molecules to induce different stability and reactivity for them. The presence of ligand molecules coordinated to the metal enhances the selectivity of metal exchanged zeolites in catalytic reactions. Thus, zeolite encapsulated complexes have catalytic properties which are different from those of cation exchanged zeolite and virgin metal complex. Interestingly, the activity, selectivity and stability of

zeolite complexes are found to be very promising to be exploited as catalysts in various industrially important reactions.

Early investigations on the catalysis by intrazeolite species include the use of zeolite X or Y entrapped metal carbonyls for water gas shift reaction, carbonylation of methanol and aromatic compounds and hydroformylation²¹⁹⁻²²². For example, $\text{Mo}(\text{CO})_6/\text{M}^+\text{Y}$ ($\text{M} = \text{Li}, \text{Na}, \text{K}, \text{Cs}$) was reported to be highly active and selective in the hydrogenation of 1,3-butadiene to cis-2-butene⁹⁹. Zeolite encapsulated monovalent carbonyl species, $\text{M}-(\text{CO})_2^+$, of iridium and rhodium are active catalysts for carbonylation of methanol in the presence of methyl iodide²²³ and the water gas shift reaction²²⁴. However, $[\text{Rh}(\text{CO})_2\text{Cl}]_2$ in Na-Y appears to be inferior to that supported on alumina with respect to the activity for water gas shift reaction⁷². $[\text{Pt}_{15}(\text{CO})_{30}]^{2-}$ was synthesized in FSM-16 (folded-sheet mesoporous material) and was found to be very effective for water gas shift reaction²²⁵. The high activity of this system might be due to the high diffusibility of reactant gases in the honeycomb structure with ordered enormous channels of 20-100 Å diameters. $\text{Fe}_3(\text{CO})_{12}$ in zeolite was also attracted attention as an excellent catalyst for the conversion of syngas²²⁶.

The catalytic properties of zeolite encapsulated metal complexes have been extensively explored in various oxidation reactions. They include the oxidation of carbon monoxide²²⁷, oxidative coupling of methane to methanol over ruthenium-, cobalt-, or manganese-phthalocyanines²²⁸ or tetraphenylporphyrins, oxidation of linear^{229, 230} and cyclic^{187, 230} alkanes, oxidation of hydroquinone to benzoquinone^{187, 229, 230}, oxidation of ethylbenzene^{231, 232}, oxidation of mercaptanes to disulfides^{231, 233, 234}, etc. Many different oxidising agents were used in homogeneously catalysed oxidation reactions¹¹⁷. However, in the case of zeolite complexes only a few of the oxidants can be used due to one or more of the following disadvantages¹¹⁹.

1. oxidants like aromatic peracids are too large to diffuse through the zeolite pores.

2. oxidants like NaClO require a phase transfer catalyst which is too bulky to enter the pores.
3. they are highly expensive.
4. they are not acceptable under environmental aspects.

Generally oxidants like iodosobenzene, organic peroxides, hydrogen peroxide and molecular oxygen are used for oxidation reactions on zeolite complexes. Iodosobenzene (PhIO) was particularly attractive in homogeneous catalysis as oxygen atom donor since it does not form radicals¹¹⁷. Also, PhIO can be easily separated from the reaction products as it is insoluble in solvents like acetonitrile¹⁹⁶. In addition, direct measurement of oxygen transferred to reactants is possible by quantitatively analysing the PhI formed during the reaction. But it has certain disadvantages in oxidation reactions over zeolite catalysts. The two main demerits are reduced reaction rates due to its relatively low mobility in the zeolite pores^{130, 196, 235} and the formation of iodoxybenzene by disproportionation of iodosobenzene^{235, 236}. The former causes iodosobenzene molecules to be trapped in the pores leading to deactivation of the catalyst by pore blocking^{235, 236}. Organic peroxides like t-butylhydrogen peroxide are better oxidising agents than iodosobenzene for zeolite catalysts. However, the amount of uncomplexed metal ions in the zeolite should be minimized to avoid the decomposition of peroxides¹⁵⁸.

The catalytic properties of encapsulated copper phthalocyanines for the oxidation of methane, phenol and aliphatic and aromatic hydrocarbons have been described²³⁷. Cobalt phthalocyanine in faujasite X is able to oxidise propene with high selectivity and resistant to rapid deactivation²³⁸. Zeolite X or Y encapsulated iron phthalocyanine complex catalyses the oxidation of alkanes to alcohols and ketones under ambient conditions with iodosobenzene^{196, 235} or t-butylhydrogen peroxide¹⁵⁸. The catalytic activity of Y zeolite encapsulated iron phthalocyanine complex for the oxidation of a series of homologous n-alkanes was compared with that of free iron phthalocyanine. It was observed that zeolite complex is much superior to free iron phthalocyanine with respect to oxidation efficiency. Moreover, whereas the free complex was completely deactivated during reaction, zeolite complex was found to be unaffected.

The sieving and orienting effect of zeolite framework to obtain high selectivity was also illustrated using phthalocyanine catalyst for the oxidation of alkanes. Zeolite entrapped iron phthalocyanine catalysts showed substrate selectivity, a preference for the smaller cyclohexane molecules in the oxidation of a cyclohexane/cyclododecane mixture with iodosobenzene²³⁵. In contrast to this, the bulkier reactant, cyclododecane was oxidised three times faster than cyclohexane over free iron phthalocyanine. The preferential oxidation of smaller substrates on zeolite complexes can be enhanced by exchanging the zeolites with cations of increased size so as to reduce the effective pore width²³⁵.

Regioselectivity was exemplified using this system. The oxidation of n-octane over free iron phthalocyanine occurs with equal selectivity at 2-, 3-, and 4- positions²³⁷. Encapsulation of the complex in Y or in the molecular sieve VPI-5 results preferential oxidation at 2-position. This is attributed to the orienting effect of zeolite structure on reactant with respect to active sites so that oxidation at the end of chain is preferred^{235, 158}. This effect is more pronounced in the case of Y-zeolite with smaller window size as compared to the VPI-5 structure with larger openings.

Herron²³⁵ reported stereoselective oxidations of methylcyclohexane and norbornane over zeolite encapsulated iron phthalocyanine complex. In the case of oxidation of methylcyclohexane to 4-methylcyclohexanol, the ratio of trans to cis isomers increases from 1.1 over free complex to 2, on encapsulation. In the oxidation of norbornane to norbornenol, encapsulation decreases the exo:endo ratio from 9.2 to 5.5. Stereoselectivity was also reported in the epoxidation of stilbene. Trans-stilbene is preferentially epoxidised over zeolite based iron phthalocyanine and t-butylphthalocyanine complex catalysts¹⁵², whereas corresponding homogeneous complexes catalyse epoxidation of cis-stilbene more easily.

Zeolite encapsulated salen complex also received much attraction as efficient catalysts for the oxidation of organic compounds. Bowers and Dutta¹¹⁹ investigated the oxidation of cyclohexene, styrene and trans- and cis- stilbene over zeolite entrapped

manganese(III) salen complex. The rate of reaction is slower on the zeolite system as compared to that on corresponding homogeneous system. This may be due to the diffusional restrictions imposed by zeolite pores to prevent the substrate molecules from reaching the active sites located inside the supercage of zeolites. However, zeolite complex provides substrate selectivity based on size of the olefins and their mobility in zeolite pores.

Manganese (III) complexes of chloro- or bromo- substituted salen in Y zeolite are also known to catalyse aerobic oxidation of styrene²³⁸. Improved product selectivity, catalyst life and catalyst recovery were observed in the case of zeolite encapsulated complexes than the corresponding homogeneous catalyst. Similarly, VO(salen)/Y was found to be active in the oxidation of toluene²³⁹. Cu(II) salen/Y allows the oxidation of cyclohexanol to cyclohexanone at a temperature of 80 °C, whereas the commercial Cu based catalyst operates at 300 °C²⁴⁰. Zeolite X or Y encapsulated halo- or nitro-substituted salen was evaluated for catalytic activity in the selective oxidation of some organic substrates²⁴¹. Encapsulated substituted salen complexes also exhibit promising performance in selective oxidation reaction and behave quite differently from both free complexes and Cu(II) exchanged zeolites.

Zeolite encapsulated Mn(II)-bipyridyl complexes are known to catalyse oxidation of various alkenes at room temperature²⁴². This supported complex avoids the problems like self oxidation encountered by their homogeneous counterparts and remains effective even after several cycles for cyclohexene oxidation with H₂O₂. Also, this system allows repeated regenerations without the loss of catalytic activity and spectroscopic properties of the complex. Another attractive catalyst is Cu(II)-pyrazole complex in zeolite X which is used for the oxidation of ascorbic acid²⁴³.

Besides oxidation reactions, zeolite encapsulated complexes can also catalyse various hydrogenation reactions^{244, 245, 246, 247, 248}. The palladium(II)-salen complex catalyses the hydrogenation of alkene with poor substrate selectivity²⁴⁹. In an attempt to improve the selectivity, Pd(II)-salen complex was encapsulated in zeolite X and Y²⁴⁴.

The selectivity of this system was evaluated in the hydrogenation of equimolar mixture of hexene-1 and cyclohexene. The linear alkene is preferentially hydrogenated over the encapsulated catalyst, whereas both reactants are hydrogenated in the homogeneous hydrogenation using free Pd-salen. Also, the zeolite system offers advantages including no leaching of Pd as its complexes are trapped in zeolite cavity and hence reactions associated with the reduction of Pd(II) ion are not observed. Similar selectivity was also reported for Ni-salen entrapped in Y zeolite for the hydrogenation of hexene-1 in presence of cyclohexene²⁴⁵. Kimura *et al*¹⁴⁸ synthesized an electron donor-acceptor complex $(\text{Na}^+)_4(\text{FePc})^{4-}$ in NaY by reacting FePcY with sodium naphthalene, $\text{Na}^+(\text{C}_{10}\text{H}_8)^-$. This complex showed an unusual selectivity to obtain high trans:cis ratio of butene-2 in the hydrogenation of butadiene.

Several industrially applied reactions have been studied on zeolite encapsulated transition metal complex catalysts. Direct synthesis of adipic acid from cyclohexane or cyclohexene, an industrially important process, can be catalysed by intrazeolite metal complexes. Zeolite Y supported iron-phthalocyanine²⁴⁶ and cis-manganese(II) bis-2,2'-bipyridyl²⁵⁰ are the two known zeolite complex catalysts for this application. The catalytic oxidation of cyclohexene with aqueous hydrogen peroxide gives cyclohexene oxime as the primary product which is converted to 1,2-cyclohexanediol by hydration. The latter is oxidised to 1,2-cyclohexanedione and adipic acid. The selectivity for adipic acid could be increased to 80% by optimising the catalyst and reaction conditions²⁵⁰. However, the reaction rate is too low to replace existing commercial catalysts.

The reactions of carbon monoxide and nitrogen oxides have great technical importance in the field of exhaust gas purification for the control of their emissions. Zeolite encapsulated ruthenium complexes catalyse the reaction between nitric oxide and ammonia to form nitrogen while water gas shift and Fischer-Tropsch reactions are reported for carbon monoxide²⁵¹. Cobalt phthalocyanine in NaY was found to be more efficient for the oxidation of carbon monoxide by oxygen than free cobalt phthalocyanine complex²⁵².

In literature, both homogeneous²⁵¹ and heterogeneous²⁵² catalyst systems were reported for oxyhalogenation of aromatics. The former poses environmental problems in disposing used catalysts whereas the latter is inconvenient as it is a two stage process operating at elevated temperatures. More recently, oxyhalogenation of aromatics over chloro- or nitro-substituted phthalocyanines of Cu, Fe and Co encapsulated in zeolites X, Y and L under near ambient conditions has been reported²⁵³. A tremendous increase in the turnover frequency for substrate conversion has been claimed when the complexes are encapsulated in the zeolite cavities.

Most of the catalytic reactions over zeolite encapsulated complexes are redox reactions. A few other types of reactions are also known to occur on zeolite complexes. Shape selective catalysis of certain nickel complexes in the oligomerisation of ethane was described by Keim²⁵⁴. The length of the oligomers could be restricted to C₂₀ over zeolite supported complexes, whereas higher carbon numbers are observed over homogeneous systems in solution or supported on amorphous solids. Zeolite encapsulated complexes have also been used in acid-base catalysis²⁵⁵.

1. 10 FUTURE OUTLOOK

The industrial preference of homogeneous catalysts is due to their high activity at low temperatures. Such processes have received much attention also in the wake of high demand for fine chemicals, desire to use new feedstocks and high selectivity for environmental protection. But, nowadays, there is little incentive to develop homogeneously catalysed industrial processes, mainly because of economic factors and operational difficulties. However, the excellent catalytic properties of homogeneous catalysts promise an optimistic prognosis.

The immobilization of homogeneous catalysts has been one of the major areas of investigation in scientific and industrial research for developing improved technologies which are cost effective and convenient for operation. Zeolite encapsulated metal complexes have been the main focus in the search for effective heterogenized systems.

Furthermore, their structural similarities with natural metalloenzymes have simulated a special interest. These systems are named as ' Zeozymes '.

Further development in this biomimetic catalysis by zeolite complexes could possibly focus on the following:

1. Variation of central metal atom of the encapsulated complex
2. Encapsulation of complexes with new ligands
3. Use of molecular sieves of extra large pores
4. Application in new chemical reactions
5. Scale up for commercial use in chemical industries

It is known that certain transition metals are particularly suitable for specific reactions. Furthermore, the electronic and stereochemical properties and hence the catalytic activity of metal complexes are dependent on the nature of the metal. Hence the role of metal ions in the encapsulated complex has to be investigated for optimising the catalytic activity. The nature of ligand also influences the electronic and steric structure of the encapsulated complex. Therefore, the modification of the ligand structure may lead to the development of a stereoselective intrazeolite complex catalyst. The interaction of zeolite matrix on encapsulated complexes has also to be considered while designing such catalysts.

Zeolite support plays an effective role in inducing selectivity in catalytic reactions over intrazeolite complexes. Zeolites like NaY, NaX, ZSM-5 and ALPO-5 have been used by previous workers for supporting metal complexes. The microporous cavities (6-13 Å) of these zeolite hosts limit the size of guest molecules to be encapsulated. Mesoporous sieves such as MCM-41 and FSM-16 consisting of honeycomb structures with numerous channels of 20-100 Å diameter are attractive for encapsulating bulky molecules. Such zeolite complexes are accessible to larger substrates and hence can catalyse reactions involving them.

Zeolite encapsulated complexes exhibit catalytic activity comparable to their homogeneous counterparts. These systems would be suitable for highly selective chemical transformations which are difficult on other types of catalysts. The reactivity of zeolite complexes obtained by the combination of the activity of encapsulated complex and the selectivity due to the complex and the zeolite framework, and operational benefits of these heterogenized systems can be exploited in the vast area of fine chemical and organic synthesis.

In addition to the requirements which are fundamental for catalytic performance, an industrial catalyst must have properties which ensure successful implementation in chemical processes. The shape, dimension and mechanical stability are some of such properties to be optimised by trial-and-error experiments. The scale up of zeolite encapsulated complexes for commercial utility would be a new milestone in the history of catalysis.

1. 11 SCOPE OF THE PRESENT STUDY

The challenge of developing new technologies for fulfilling the demands of modern society can be addressed by the science and technology of catalysis as it plays a key role in modern industrial processes. Success depends on the development of novel, active, selective and stable catalysts which can perform uniquely at milder conditions. The environmental and economic pressures have also emphasized the need for efficient catalysts with improved characteristics. The thrust on the development of powerful catalysts and the desire to comprehend the science behind their catalysis are reflected in the recent spurt of research publications. Two areas which have received wide attention for innovative research are: (i) heterogenization of homogeneous transition metal complex catalysts and (ii) modification of conventional metal oxide catalysts to tailor them to effectively catalyse specific reactions. The present investigation has been confined to these two areas.

Among the heterogenized metal complex catalysts, studies on zeolite encapsulated complexes appear to be more challenging and interesting as they provide ways to explore the shape selectivity of zeolite support and inhibit the deactivation processes of metal complexes. These systems are also attractive in a biomimetic perspective due to their structural resemblance to natural metalloenzymes. Therefore, our studies are limited to the synthesis, characterization and evaluation of catalytic activity of some zeolite encapsulated complexes. Characterization of zeolite encapsulated complexes are often very difficult. In most cases, characterization has been based on the structures of the simple complexes. We have thus chosen, ligand systems, whose simple complexes have already been studied. The following are the ligands selected for the present study:

1. Dimethylglyoxime
2. 3-formylsalicylic acid
3. N,N'-ethylenebis(7-methylsalicylideneamine)
4. N,N'-ethylenebis(5,6-benzosalicylideneamine)

A search through literature has clearly revealed that zeolite encapsulated complexes of these ligands have not yet been studied. The following have been the objectives of the present investigation:

- 1 To synthesize and characterize zeolite encapsulated transition metal complexes.
- 2 To examine the effect of zeolite framework on the structure and geometry of the complexes.
- 3 To study the thermal stability of zeolite complexes.
- 4 To evaluate the catalytic activity of zeolite complexes for the decomposition of hydrogen peroxide and for the oxidation of benzyl alcohol, ethylbenzene and 4-methoxybenzaldehyde

We have also attempted the modification of a supported metal oxide catalyst. Metal oxide catalysts have found numerous industrial applications in a variety of chemical processes. The studies on the nature of active sites and fine tuning them for better performance of the catalyst are the main tasks in the catalyst development. Modification of active sites can be achieved by incorporating small amounts of suitable additives which can impart the desired characteristics for a particular reaction. Cu-Cr/Al₂O₃ is widely studied as a metal oxide catalyst for CO oxidation. This catalyst is attractive as a model system to illustrate the above mentioned approach for improving metal oxide catalysts. The additives, CeO₂ and TiO₂ have been used in the present study for modifying Cu-Cr/Al₂O₃ catalyst. The investigations on the metal oxide catalyst have focused on the following:

1. To ascertain the role of Cu and Cr in the carbon monoxide oxidation and the effect of Cr on the stability of the catalyst to withstand severe thermal and hydrothermal conditions
2. To examine the effect of additives, TiO₂ and CeO₂, on oxidation activity and stability.
3. To identify different crystal phases and evaluate their influence on catalytic performance
4. To investigate the influence of active metal dispersion on oxidation efficiency

There is a growing interest to design and produce metal oxide catalysts for replacing highly expensive noble metal catalysts for applications such as gas purification via CO oxidation. Modified Cu-Cr catalysts are expected to provide a welcome replacement of noble metal catalysts.

REFERENCES

1. G. Kim, *Ind. Eng. Chem. Prod. Res. Dev.*, 21 (1982) 267
2. W. B. Williamson, J. C. Summers and J. F. Skowron, " *Catalyst Technologies for Future Automotive Emission systems* ", SAE Transactions Paper 880103, 97 (1988) 341
3. S. M. Csicsery, *Zeolites*, 4 (1984) 202
4. S. Sivasanker and P. Ratnasamy, *US Patent*, 5453553 (1997)
5. S. Sivasanker and P. Ratnasamy, *US Patent*, 5493061 (1997)
6. J. Falbe and H. Bahrmann, *J. Chem. Edu.*, 61, 11 (1984) 961
7. G. W. Parshall and R. E. Putscher, *J. Chem. Edu.*, 63, 3 (1986) 189
8. J. Haber, *Pure & Appl. Chem.*, 66, 8 (1994) 1597
9. H. Heinemann, *Stud. Surf. Sci. and Catal.*, 101 (1997) 69
10. P. G. Menon, *Chem. Rev.*, 94 (1994) 1021
11. D. Antolovic and E. R. Davidson, *J. Am. Chem. Soc.*, 109 (1987) 5828
12. C. D. Wood and P. E. Garrou, *Organometallics*, 3 (1984) 170
13. J. Smidt, W. Hafner, R. Jira, J. Sedlmeier, R. Sieber, R. Ruttinger and H. Kojer, *Angew.Chem.*, 71 (1959) 176
14. F. A. Cotton and G. Wilkinson, " *Advanced Inorganic Chemistry* ", 5th Edition, Wiley-Interscience, New York, (1988) 1224
15. G. W. Parshall, " *Homogeneous Catalysis* ", Wiley-Interscience, New York, 1980
16. J. F. Roth, J. H. Graddock, A. Hershman and F. E. Paullk, *Chem. Tech.*, 1 (1971) 600
17. R. L. Pruett, *Ann. N. Y. Acad. Sci.*, 295 (1977) 239
18. W. C. Seidel and C. A. Tolman, *Ann. N. Y. Acad. Sci.*, 415 (1983) 201
19. W. S. Knowles, *Acc. Chem. Res.*, 16 (1983) 106
20. J. P. Collman, X. Zhang, V. J. Lee, E. S. Uffelman and J. I. Brauman, *Science*, 261 (1993) 1404
21. M. J. Gunter and P. Turner, *Coord. Chem. Rev.*, 108 (1991) 115
22. J. Haber, " *Perspectives in Catalysis* ", Blackwell Scientific Publications, 1992, 3711
23. A. Bielanski and J. Haber, " *Oxidation in Catalysis* ", Marcel Dekker, New York, 1991
24. A. Bielanski and J. Haber, *Catal. Rev.*, 19 (1979) 1
25. P. G. Menon, " *Hydrogen Effects in Catalysis- Fundamental and Practical Applications* "; Z.Paal , P.G. Menon, (Eds.), Marcel Dekker: New York, (.1988) 117
26. S. A. Bradley, M. J. Gattuso and R. J. Bertolacini, (Eds.); " *Characterisation and Catalyst Development: An Interactive Approach* ", ACS Symposium Series 411, American Chemical Society, Washington, DC, 1989.
27. M. V. Twigg (Ed.), " *Catalyst Handbook* ", Wolfe Publishing, London, 1989
28. J. R. Jennings, (Ed.), " *Catalytic Ammonia Synthesis- Fundamentals and Practice* ", Plenum Press, New York, 1991.
29. G. W. Bridger and M. S. Spencer, (Eds.), " *Catalyst Handbook* ", Wolfe Publishing: London, (1989.) 441
30. M. S. Chhabra and D. K. Mukherjee, *Bull. Catal. Soc. India*, 6, 3 (1996) 2
31. J. R. Rostrub-Nielsen, " *Steam Reforming Catalysts*", Teknisk Forlag, Copenhagen, 1975

32. M. Jian and R. Prins, *Stud. Surf. Sci. and Catal.*, 113 (1998) 111
33. G. F. Froment, " *Proceedings of the 6th International Congress on Catalysis* ", London; Chemical Society: London (1976) 10
34. T. S. R. Prasada Rao and P. G. Menon, *J. Catal.*, 51 (1978) 64
35. B. Delmon, *React. Kinet. Catal. Lett.*, 13 (1980) 203
36. M. D. Phillips and A. D. Eastman, *Catal. Lett.*, 13 (1992) 157
37. M. E. Dry, *Catal. Today*, 6 (1990) 183
38. J. J. Spivey and J. B. Butt, *Catal. Today*, 11 (1992) 465
39. L. L. Hegedus, J. C. Summers, J. C. Schletter and K. Baron, *J. Catal.*, 56 (1979) 321
40. B. Harrison, A. F. Diwell and C. Hallet, *Platinum Metals Rev.*, 32, 2 (1988) 73
41. M. F. M. Zwinkels, S. G. Jaras and P. G. Menon, *Catal. Rev.- Sci. & Eng.*, 35,3 (1993) 319
42. K. Sekizawa, M. Machida, K. Eguchi and H. Arai, *J. Catal.*, 142 (1992) 655
43. S. Knez, S. Shires and S. Tennison, " *Proceedings of the 8th International Symposium on Large Chemical Plants* ", Antwerp, Oct. 12 (1992) 129
44. G. M. Bickle, J. N. Beltramini and D. D. Do, *Ind. Eng. Chem. Res.*, 29 (1990) 1801
45. M. M. Bhasin, *J. Catal.*, 38 (1975) 218
46. B. J. Arena, *Appl. Catal. A Gen.*, 87 (1992) 219
47. B. T. Horner, *Platinum Metals Rev.*, 37 (1993) 76
48. H. Bosch and F. Janssen, *Catal. Today*, 2 (1987) 369
49. M. G. Jones and T. G. Nevell, *J. Catal.*, 122 (1990) 219
50. E. C. Su, W. L. H. Watkins and H. S. Gandhi, *Appl. Catal.*, 12 (1984) 59
51. J. Sarkany and R. D. Gonzalez, *Appl. Catal.*, 5 (1983) 85
52. E. C. Su, C. N. Montreuil and W. G. Rothschild, *Appl. Catal.*, 17 (1985) 75
53. P. Briot and M. Primet, *Appl. Catal.*, 68 (1991) 301
54. E. M. Flanigen, *Pure & Appl. Chem.*, 52 (1980) 2191
55. C. Naccache and Y. B. Taarit, *Pure & Appl. Chem.*, 52, (1980) 2175
56. P. G. Menon, " *Lectures on Catalysis* ", 41st Ann. Meeting, Ind. Acad. Sci., S. Ramasheshan (Ed.), 1975
57. M. E. Davis, *Acc. Chem. Res.*, 2 (1993) 111
58. D. W. Breck, *J. Chem. Edu.*, 41 (1964) 678
59. P. B. Weisz, V. J. Frilette, R. W. Maatman and E. B. Mower, *J. Catal.*, 1 (1962) 307
60. S. M. Csicsery, *J. Catal.*, 19 (1970) 394
61. E. G. Derouane and Z. Gabelica, *J. Catal.*, 65 (1980) 486
62. M. E. Davis, C. Montes, P. E. Hathaway, J. P. Arhancet, D. L. Hasha and J. M. Garces, *J. Am. Chem. Soc.*, 111 (1989) 3919
63. S. B. Hong, E. Mielczarski and M. E. Davis, *J. Catal.*, 134 (1992) 349
64. J. A. Martens, H. Geerts, L. Leplat, G. Vanbutsele, P. J. Grobet and P. A. Jacobs, *Catal. Lett.*, 12 (1992) 367
65. P. E. Hathaway and M. E. Davis, *J. Catal.*, 116 (1988) 279

66. F. P. Gortsema, B. Beshty, J. J. Friedman, D. Matsumoto, J. J. Sharkey, G. Wildman, T. J. Blacklock and S. H. Pan, " *Proceedings of the 14th Conference on the Catalysis of Organic Reactions* ", Albuquerque, NM, April 27-28, 1992
67. D. R. C. Huybrechts, P. L. Buskens and P. A. Jacobs, *J. Mol. Catal.*, 71 (1992) 129
68. P. R. H. P. Rao and A. V. J. Ramaswamy, *J. Chem. Soc., Chem. Commun.*, (1992) 1245
69. A. Corma, M. Iglesias, C. del Pina and F. Sanchez, *J. Chem. Soc., Chem. Commun.*, (1991) 1253
70. A. Choplin and F. Quignard, *Coord. Chem. Rev.*, 178-180 (1998) 1679
71. H. H. Lamp and B. C. Gates, *J. Am. Chem. Soc.*, 108 (1986) 81
72. J. M. Basset, A. Theolier, D. Commereuc and Y. Chauvin, *J. Organomet. Chem.*, 279 (1985) 147
73. B. Besson, A. Choplin, L. D'Ornelas and J. M. Basset, *J. Chem. Soc., Chem. Commun.*, (1982) 843
74. T. R. Krause, M. E. Davies, J. Lieto and B. C. Gates, *J. Catal.*, 94 (1985) 195
75. R. Buffon, A. Auroux, F. Lefebvre, A. Choplin and J. M. Basset, *J. Mol. Catal.*, 76 (1992) 287
76. R. Buffon, A. Choplin, M. Leconte, J. M. Basset, R. Touroude and W. A. Herrmann, *J. Mol. Catal.*, 72 (1992) L7
77. F. R. Hartley, " *Supported Metal Complexes* ", Reidel D, Dordrecht, 1985
78. E. G. Kuntz, *Chem. Tech.*, 17 (1987) 570
79. P. Kalck and F. Monteil, *Adv. Organometal. Chem.*, 32 (1992) 219
80. W. A. Herrmann and C. W. Kohlpaintner, *Angew. Chem. Int. Ed. Engl.*, 32 (1993) 1524
81. F. Joo and A. Katho, *J. Mol. Catal. A: Chem.*, 116 (1997) 3
82. B. Cornils and E. G. Kuntz, *J. Organometal. Chem.*, 502 (1995) 177
83. R. Z. Moravee, W. T. Schelling and C. F. Oldershaw, *Brit. Patent*, 511 (1939) 556
84. G. J. K. Acres, G. C. Bond, B. J. Cooper and J. A. Dawson, *J. Catal.*, 6 (1966) 139
85. P. R. Rony, *Chem. Eng. Sci.*, 23 (1969) 1021
86. P. R. Rony, *J. Catal.*, 14 (1969) 142
87. L. A. Gerritsen, J. M. Herman and J. J. F. Scholten, *J. Mol. Catal.*, 9 (1980) 241
88. T. Uematsu, T. Kawakami, F. Saitho, M. Miura and Hashimoto, *J. Mol. Catal.*, 12 (1981) 11
89. J. P. Arhancet, M. E. Davis, J. S. Merola and B. E. Hanson, *Nature*, 339 (1989) 454
90. T. J. Pinnavaia, R. Raythatha, J. Guo-Shuh, L. J. Halloran and J. F. Hoffman, *J. Am. Chem. Soc.*, 101 (1979) 6831
91. R. Raythatha and T. J. Pinnavaia, *J. Catal.*, 80 (1983) 47
92. J. Blum, A. Rosenfeld, N. Polak, Israelson, H. Schumann and D. J. Avnir, *J. Mol. Catal. A: Chem.*, 107 (1996) 217
93. B. M. Choudary, K. Ravi Kumar and M. Lakshmi Kantam, *J. Catal.*, 130 (1991) 41
94. P. Gallezot, *Catal. Rev.-Sci. Eng.*, 20 (1979) 121
95. D. Ballivet-Tkatchenko, I. Tkatchenko and N. Duc Chau, *Stud. Surf. Sci. Catal.*, 12 (1982) 123

96. G. A. Ozin, J. P. Godber, F. Hugues and L. F. Nazar, *J. Mol. Catal.*, 21 (1983) 313
97. M. Che, M. Richard and D. Olivier, *J. Chem. Soc., Faraday Trans.*, 1, 76 (1980) 1526
98. P. Gallezot, M. Primet and I. Imelik, " *Molecular Sieves II* ", ACS Symp. Ser., 40 (1977) 144
99. Y. Okamoto, A. Maezawa, H. Kane and T. Imanaka, *J. Chem. Soc., Chem. Commun.*, (1988) 380
100. D. Ballivet-Tkatchenko and G. Coudurier, *Inorg. Chem.*, 18 (1979) 558
101. R. L. Schneider, R. F. Howe and K. L. Watters, *Inorg. Chem.*, 23 (1984) 4600
102. M. C. Connaway and B. E. Hanson, *Inorg. Chem.*, 25 (1986) 1445
103. D. Olivier, M. Richard and M. Che, *Chem. Phys. Lett.*, 60 (1978) 77
104. G. H. Woltermann and V. A. Durante, *Inorg. Chem.*, 22 (1983) 1954
105. T. Huang and J. Schwartz, *J. Am. Chem. Soc.*, 104 (1982) 5244
106. G. A. Ozin and J. Godber, *J. Phys. Chem.*, 93 (1989) 878
107. Z. Li and T. E. Mallouk, *J. Phys. Chem.*, 91 (1987) 643
108. P. Pichat, *J. Phys. Chem.*, 79 (1975) 2127
109. Y. Huang, *J. Catal.*, 61 (1980) 461
110. J. Michalik, M. Narayana and L. Kevan, *J. Phys. Chem.*, 88 (1984) 5237
111. J. H. Lungford, *Catal. Rev.-Sci. Eng.*, 12 (1975) 137
112. J. H. Lungford, " *Molecular Sieves II* "; Katzer J R (Ed.); ACS Symp. Ser. (1977) 473
113. W. J. Mortier and R. A. Schoonheydt, *Progr. Solid State Chem.*, 16 (1985) 1
114. G. A. Ozin and C. Gil, *Chem. Rev.*, 89 (1989) 1749
115. J. H. Lunsford, *Rev. Inorg. Chem.*, 9 (1987) 1
116. R. Parton, E. De Vos and P. A. Jacobs, " *Zeolite Microporous Solids: Synthesis, Structure and Reactivity* ", E. G. Derouane, F. Lemos, C. Naccache and F. Ramoa Ribeiro (Eds.), Kluwer Academic Publishers, Dordrecht, The Netherlands (1992) 555
117. D. E. De Vos, F. Thibault-Starzyk, P. P. Knops-Gerrits, R. F. Parton and P. A. Jacobs, *Macromol. Symp.*, 80 (1994) 157
118. R. V. Ramanovsky, *Macromol. Symp.*, 80 (1994) 185
119. C. Bowers and P. K. Dutta, *J. Catal.*, 122 (1990) 271
120. D. W. Break, " *Zeolite Molecular Sieves* "; Wiley, New York 1974
121. C. J. Winscom and W. Lubitz, *Stud. Surf. Sci. and Catal.*, 12 (1982) 15
122. R. L. Hinman, *Chemtech*, June (1994) 45
123. J. E. Gavagan, *J. Org. Chem.*, 60 (1995) 3957
124. A. Kiener, *Chemtech*, Sept. (1995) 31
125. N. Herron, *Chemtech*, Sept. (1995) 542
126. R. E. White and M. J. Coon, *Ann. Rev. Biochem.*, 49 (1980) 315
127. I. C. Gunsalus and S. C. Sligar, *Adv. Enzymol.*, 47 (1978) 1
128. D. Mansuy and P. Battioni, " *Bioinorganic Catalysis* ", J. Reedijk (Ed.), Marcel Dekker, New York (1993) 395
129. J. P. Collman, X. Zhang, V. J. Lee, U. S. Uffelman and J. I. Brauman, *Science*, 261 (1993) 1404
130. A. E. Shilov, *J. Mol. Catal.*, 47 (1988) 351

131. B. R. Cook, T. J. Reinert and K. S. Suslick, *J. Am. Chem. Soc.*, 108 (1986) 7281
132. K. Suslik, B. Cook and M. Fox, *J. Chem. Soc., Chem. Commun.*, (1980) 580
133. N. Herron, *New J. Chem.*, 13 (1989) 761
134. N. Herron and C. A. Tolman, *J. Am. Chem. Soc.*, 109 (1987) 2837
135. R. F. Parton, Ivo F. J. Vankelecom, J. A. C. Mark, C. P. Bezoukhanova, J. B. Uytterhoeven and P. A. Jacobs, *Nature*, 370 (1994) 541
136. Ivo F. J. Vankelecom, R. F. Parton, J. A. C. Mark, J. B. Uytterhoeven and P. A. Jacobs, *J. Catal.*, 163 (1996) 457
137. N. Herron, *Inorg. Chem.*, 25 (1986) 4714
138. L. Gaillon, N. Sajot, F. Bedioui, J. Devynck and Jr. K. J. Balkus, *J. Electroanal. Chem.*, 345 (1993) 157
139. Jr. K. J. Balkus, A. A. Welch and B. E. Gnade, *Zeolites*, 10 (1990) 722
140. S. Kowalak, R. C. Weiss and Jr. K. J. Balkus, *J. Chem. Soc., Chem. Commun.*, (1991) 57
141. W. H. Quale, G. Peeters, G. L. De Roy, E. F. Vansant and J. H. Lunsford, *Inorg. Chem.*, 21 (1982) 2226
142. W. De Wilde, G. Peeters and J. H. Lunsford, *J. Phys. Chem.*, 84 (1980) 2306
143. F. Bedioui, L. Roue, J. Devynck and Jr. K. J. Balkus, *Stud. Surf. Sci. Catal.*, 84B (1994) 917
144. B. V. Romanovsky, " *Proc. 8th Int. Congr. Catal.* ", Verlag Chemie, Weinheim (1984) 657
145. B. V. Romanovsky and A. G. Gabrielov, *J. Mol. Catal.*, 74 (1992) 293
146. Jr. K. J. Balkus and J. P. Ferraris, *J. Phys. Chem.*, 94 (1990) 8019
147. J. P. Ferraris, Jr. K. J. Balkus and A. Schade, *J. Incl. Phenom.*, 14 (1992) 163
148. T. Kimura, A. Fukuoka and M. Ichikawa, *Catal. Lett.*, 4 (1990) 279
149. CA 118 : 212554p
150. Jr. K. J. Balkus, A. A. Welch and B. E. Gnade, *J. Incl. Phenom.*, 10 (1991) 141
151. G. Meyer, D. Wohrle, M. Mohl and G. Schulz-Ekloff, *Zeolites*, 4 (1984) 30
152. M. Ichikawa, T. Kimura and A. Fukuoka, *Stud. Surf. Sci. Catal.*, 60 (1991) 335
153. A. G. Gabrielov, Jr. K. J. Balkus, S. L. Bell, F. Bedioui and J. Devynck, *Microporous Materials*, 2 (1994) 119
154. F. Bedioui, L. Roue, L. Gaillon, J. Devynck, S. L. Bell and Jr. K. J. Balkus, " *Preprints, Div. Of Petroleum Chemistry* ", ACS, 38, 3 (1993) 529
155. Jr. K. J. Balkus, A. G. Gabrielov, S. L. Bell, F. Bedioui, L. Roue, J. Devynck, *Inorg. Chem.*, 33 (1994) 67
156. R. F. Parton, C. P. Bezoukhanova, J. Grobet J, P. J. Grobet and P. A. Jacobs, *Stud. Surf. Sci. Catal.*, 83 (1994) 371
157. A. N. Zakharov and B. V. Romanosky, *J. Inclus. Phenom.*, 3 (1985) 389
158. R. F. Parton, L. Uytterhoeven and P. A. Jacobs, *Stud. Surf. Sci. Catal.*, 59 (1991) 395
159. R. F. Parton, D. R. C. Huybrechts, P. Buskens and P. A. Jacobs, *Stud. Surf. Sci. Catal.*, 65 (1991) 110
160. M. Nakamura, T. Tatsumi and H. Tominaga, *Bull. Chem. Soc. Jpn.*, 63 (1990) 3334

161. Y. W. Chan and R. B. Wilson, " *Preprints. Div. Of Petroleum Chemistry* ", ACS, 33, 3 (1988) 453
162. I. A. Rankel and E. W. Valyocsik, *US Patent*, 4500 503, 1985
163. Jr. K. J. Balkus, S. Kowalak, K. T. Ly and D. C. Hargis, *Stud. Surf. Sci. Catal.*, 69 (1991) 93
164. S. Kowalak and Jr. K. J. Balkus and C. Czech., *Chem. Commun.*, 57 (1992) 774
165. Jr. K. J. Balkus and S. Kowalak, *PCT Intern. Appl.*, WO 92/09527, 1992
166. E. Paez-Mozo, N. Gabriunas, F. Lucaccioni, D. D. Acosta, P. Patrono, A. La Ginestra, P. Ruiz and B. Delmon, *J. Phys. Chem.*, 97 (1993) 12819
167. F. Bedioui, *Coord. Chem. Rev.*, 144 (1995) 39
168. S. Schulz-Ekloff and S. Ernst, " *Handbook of Heterogeneous Catalysis* ", G. Ertl, H. Knozinger and J. Weitkamp (Eds.), Wiley-VCH (1997) 374
169. P. C. H. Mitchell, *Chem. Ind.*, (1991) 308 and references cited therein
170. R. F. Parton, L. Utterhoeven and P. A. Jacobs, *Stud. Surf. Sci. Catal.*, 59 (1991) 395
171. A. G. Gabrielov, Jr. K. J. Balkus, S. L. Bell, F. Bedioui, L. Roue and J. Devynck, *Microp. Mater.*, 2 (1994) 119
172. J. M. Newsam, *J. Phys. Chem.*, 93 (1989) 7689
173. M. Koichi, S. Imamura, J. H. Lunsford , *Inorg. Chem.*, 23 (1984) 3510
174. G. A. Ozin & J. P. Godber, " *Intrazeolite Organometallics: Spectroscopic Probes of Internal Versus External Confinement of Metal Guests. Excited states and Reactive Intermediates: Photochemistry, Photophysics and Electrochemistry* ", A. P. B. Lever (Ed.); ACS Symp. Ser., 307; ACS; Washington, DC, 1986
175. W. DeWilde and J. H. Lunsford, *Inorg. Chim. Acta.*, 34 (1979) L229
176. R. A. Schoonheydt and J. Pelgrims, *J. Chem. Soc., Dalton* (1981) 914
177. H. Diegruber and P. J. Plath, *Stud. Surf. Sci. Catal.*, 12 (1982) 23
178. H. Diegruber and P. J. Plath, *Z. Phys. Chem. (Leipzig)*, 266 (1985) 641
179. L. Edwards and M. Gouterman, *J. Molec. Spectr.*, 33 (1970) 292
180. U. Ahrens and H. Kuhn, *Z. Phys. Chem. (Frankfurt)*, 37 (1963) 1
181. P. S. E. Dai and J. H. Lunsford, *Inorg. Chem.*, 19 (1980) 262
182. K. Mizuno and J. H. Lungford, *Inorg. Chem.*, 22 (1983) 3483
183. S. V. Gudkov, B. V. Romanovsky, E. S. Shpiro, G. V. Antoshin and Kh. M. Minachev, *USSR. Ser. Khim.*, (1980) 2448
184. Kh. M. Minachev and E. S. Shpiro, " *Catalyst surface: Physical Methods of Studying* ", C¹²C Press, Boca raton, (1990) 201
185. J. Strutz, H. Diegruber, N. I. Jaeger and R. Moseler, *Zeolites*, 3 (1983) 102
186. E. S. Shpiro, G. V. Antoshin, O. P. Thachenko, S. V. Gudcov, B. V. Romanovsky and Kh. M. Minachev, *Stud. Surf. Sci. Catal.*, 18 (1984) 31
187. S. Imamura and J. H. Lunsford, *Langmuir*, (1985) 326
188. D. E. De Vos, F. Thibault-Starzyk and P. A. Jacobs, *Angew. Chem. Int. Ed. Engl.*, 33 (1994) 432
189. H. Diegruber, P. J. Plath, G. Schulz-Ekloff, M. Mohl, *J. Mol.. Catal.*, 24 (1984) 115

190. G. Schulz-Ekloff, D. Wohrle, V. Iliev, E. Ignatzek and A. Andreev, *Stud. Surf. Sci. Catal.*, 46 (1989) 315
191. N. Herron, G. D. Stucky and C. A. Tolman, *J. Chem. Soc., Chem. Commun.*, (1986) 1521
192. R. F. Parton, Uytterhoeven and P. A. Jacobs, *Stud. Surf. Sci. Catal.*, 59 (1991) 395
193. D. Wohrle and G. Schulz-Ekloff, *Adv. Mater.*, 4 (1994) 875
194. D. R. Rolisson, *Chem. Rev.*, 90 (1990) 867
195. A. J. Bard and T. E. Mallouk, " *Molecular Design of Electrode Surfaces* ", R. W. Murray (Ed.), Wiley, New York, (1992) 271
196. G. A. Ozin, A. Kuperman and A. Stein, *Angew. Chem. Int. Ed. Engl.*, 28 (1989) 359
197. F. Bedioui, L. Roue, E. Briot, J. Devynck and Jr. K. J. Balkus, *Stud. Surf. Sci. Catal.*, 84 (1994) 917
198. F. Bedioui, L. Roue, E. Briot, J. Devynck, S. L. Bell and Jr. K. J. Balkus, *J. Electroanal. Chem.*, 373 (1994) 19
199. B. R. Shaw, K. E. Creasy, C. J. Lanczycki, J. A. Sargeant and M. Tirhado, *J. Electrochem. Soc.*, 135 (1988) 869
200. F. Bedioui, L. Roue, L. Gaillon, J. Devynck, S. L. Bell and Jr. K. J. Balkus, *Petrol. Preprints, ACS, Div. Petrol Chem.*, 38 (1993) 529
201. A. G. Gabrielov, Jr. K. J. Balkus, S. L. Bell, F. Bedioui and J. Devynck, *Microp. Mater.*, 2 (1994) 119
202. J. S. Krueger and T. E. Mallouk, " *Kinetics and catalysis in Microheterogeneous Systems*", M. Gratzel & Kalyanasundaram (Eds.); Dekker, New York, (1991) 461
203. Jr. K. J. Balkus, A. G. Gabrielov, S. L. Bell, F. Bedioui, L. Roue L and J. Devynck, *Inorg. Chem.*, 33 (1994) 67
204. F. Bedioui, L. Roue, E. Briot, J. Devynck, S. L. Bell and Jr. K. J. Balkus, *J. Electroanal. Chem.*, 337 (1994) 19
205. K. Mesfar, B. Carre, F. Bedioui and J. Devynck, *J. Mater. Chem.*, 3 (1993) 873
206. L. Gaillon, N. Sajot, F. Bedioui, J. Devynck and Jr. K. J. Balkus, *J. Electroanal. Chem.*, 345 (1993) 157
207. F. Bedioui, E. De Boysson, J. Devynck and Jr. K. J. Balkus, *J. Chem. Soc., Faraday Trans.*, 87 (1991) 3831
208. N. Herron, G. D. Stucky and C. A. Tolman, *Inorg. Chim. Acta.*, 100 (1985) 135
209. P. K. Dutta and R. E. Zaykoski, *Inorg. Chem.*, 24 (1985) 3490
210. W. De Wilde, G. Peeters and J. H. Lunsford, *J. Phys. Chem.*, 84 (1980) 2306
211. J. A. Incavo and P. K. Dutta, *J. Phys. Chem.*, 94 (1990) 3075
212. K. Maruszewski, D. P. Strommen and J. R. Kincald, *J. Am. Chem. Soc.*, 115 (1993) 8345
213. S. K. Tiwary and S. Vasudevan, *Inorg. Chem.*, 37 (1998) 5239
214. W. H. Quayle, G. Peeters, G. L. De Roy, E. F. Vasant and J. H. Lunsford, *Inorg. Chem.*, 21, 6 (1982) 2226
215. Y. Umemura, Y. Minai and T. Tominaga, *J. Chem. Soc., Chem. Commun.*, (1993) 1822

216. G. Vanko, Z. Homonnay, S. Nagy and A. Vertes, G. Pal-Borbely and H. K. Beyer, *J. Chem. Soc., Chem. Commun.*, (1996) 785
217. D. E. De Vos, E. J. P. Feijen, R. A. Schoonheydt and P. A. Jacobs, *J. Am. Chem. Soc.*, 116 (1994) 4746
218. B. V. Romanovsky, V. Yu Zakharov and T. G. Borisova, *Moscow Univ. Publ.*, (1982) 170
219. P. A. Jacobs, R. Chantillon, P. DeLaet, J. Verdonck and M. Tielem, *ACS Symp. Ser.*, 218 (1983) 439
220. A. Auroux, V. Bolis, P. Wierzchowski, P. Gravelle and J. Vedrine, *J. Chem. Soc., Faraday Trans.*, 2, 75 (1979) 2544
221. M. Iwamoto, H. Kusano and S. Kagawa, *Inorg. Chem.*, 22 (1983) 3366
222. E. Mantovani, N. Palladino and A. Zarrobbi, *J. Mol. Catal.*, 3 (1977) 285
223. P. Gelin, Y.B. Taarit and C. Naccache, *Stud. Surf. Sci and Catal.*, 7 (1981) 898
224. B. E. Hanson, M. E. Davis, D. Taylor and E. Rode, *Inorg. Chem.*, 23 (1984) 52
225. T. Yamamoto, T. Shido, S. Inagaki, Y. Fukushima and M. Ichikawa, *J. Am. Chem. Soc.*, 118 (1996) 5810
226. D. Ballivet-Tkatchenko and I. Tkatchenko, *J. Mol. Catal.*, 13 (1981) 1
227. B. V. Romanovsky and A. G. Gabrielov, *Mendeleev Commun.*, (1991) 14
228. A. Zsigmond, F. Notheisz, M. Bartok and J. E. Backvall, *Stud. Surf. Sci. and Catal.*, 78 (1993) 417
229. E. Paez-Mozo, N. Gabriunas, R. Maggi, D. Acosta, P. Ruiz and B. Delmon, *J. Mol. Catal.*, 91 (1994) 251
230. R. F. Parton, C. P. Bezoukhanova, E. Thibault-Starzyk, R. A. Reynders, P. J. Grobet and P. A. Jacobs, *Stud. Surf. Sci. and Catal.*, 84 B (1994) 813
231. S. Ernest, Y. Traa and O. Deeg, *Stud. Surf. Sci. and Catal.*, 84 B (1994) 925
232. U. Hundorf, A. Andreev, V. Petrov, I. Iliev, M. Vassileva, V. Ivanova, A. Elias, I. Prahov, D. Wohrle and D. Shopov, " *Proc. 6th Intern. Symp. Heterog. Catal.*", D. Shopov et al (Eds.), Publishing House of the Bulgarian Academy of Sciences, Sofia, 2 (1987) 73
233. G. Schulz-Ekloff, D. Wohrle and A. Andreev, *Wiss. Z Technische Hochschule Leuna-Merseburg*, 32 (1990) 649
234. B. Meunier, *Chem. Rev.*, 92 (1992) 1411
235. N. Herron, *J. Coord. Chem.*, 19 (1988) 25
236. K. H. Bergk, F. Wolf and B. Walter, *J. Prakt. Chem.*, 321 (1979) 529
237. R. Raja and P. Ratnasamy, *Stud. Surf. Sci. Catal.*, 103B (1997) 1037 and references therein.
238. S. P. Varkey and C. R. Jacob, *Ind. J. Chem.*, 37A (1998) 407
239. N. Ulagappan, " *Proceedings of The 31st annual convention of chemists* ", Varanasi, (1994) F1
240. R. Chandra, M. Anupa and P. Subhash, *Ind. J. Chem.*, 35A (1996) 1
241. J. M. Thomas and C. R. A. Catlow, *Progr. Inorg. Chem.*, 35 (1988) 1

242. Peter-Paul Knops-Gerrits, D. De Vos, F. Thibault-Starzyk and P. A. Jacobs, *Nature*, 369, (1994) 543
243. K. K. Mohammed Yusuff and Jose Mathew, *Ind. J. Chem.*, 36A (1997) 303.
244. S. Kowalak, R. C. Weiss and Jr. K. J. Balkus, *J. Chem. Soc., Chem. Commun.*, (1991) 57
245. D. Chatterjee, H. C. Bajai, A. Das and K. Bhatt, *J. Mol. Catal.*, 92 (1994) L235
246. F. Thibault-Starzyk, R. F. Parton and P. A. Jacobs, *Stud. Surf. Sci. and Catal.*, 84B (1994) 1419
247. D. E. De Vos and P. A. Jacobs, " *Proceedings from the Ninth International Zeolite Conference* ", R. Von Ballmoos, J. B. Higgins and M. M. J. Treacy (Eds.), Butterworth-Heinemann, Boston, 2 (1993) 615
248. A. N. Zakharov, *Mendeleev Commun.*, (1991) 80
249. G. Henrici-Olive and S. Olive, *J. Mol. Catal.*, 76, 1 (1975) 121
250. P. P. Knops-Gerrits, F. Thibault-Starzyk and P. A. Jacobs, *Stud. Surf. Sci. and Catal.*, 84B (1994) 1411
251. R. I. de la Rosa, M. J. Clague and A. Butler, *J. Am. Chem. Soc.*, 114 (1992) 760
252. R. Westervelt, *Chem. Week*, 26, Aug. 14 (1996)
253. R. Raja and P. Ratnasamy, *J. Catal.*, 170 (1997) 244
254. W. Keim, " *Homogeneous and Heterogeneous Catalysis* ", Yu. Yermakov and V. Likholobov (Eds.), VNU Science Press, Utrecht, The Netherlands, (1986) 499
255. B. V. Romanovsky, " *Homogeneous and Heterogeneous Catalysis* ", Y. Yermakov and V. Likholobov (Eds.), VNU Science Press Utrecht, The Netherlands, (1986) 343

CHAPTER II

MATERIALS AND METHODS

2. 1 INTRODUCTION

This chapter provides details of the general reagents and other materials used in the present study. A brief account of the methods used for the synthesis of ligands, zeolite supported metal complexes and metal oxide catalysts is given. Procedures of various physico-chemical techniques employed for the characterization studies are also discussed.

2. 2 REAGENTS

The following metal salts were used: $\text{MnCl}_2 \cdot 4\text{H}_2\text{O}$ (E. Merck, GR); FeCl_3 (Qualigens); $\text{CoCl}_2 \cdot 6\text{H}_2\text{O}$ (E. Merck, GR); $\text{NiCl}_2 \cdot 6\text{H}_2\text{O}$ (E. Merck, GR); $\text{CuCl}_2 \cdot 2\text{H}_2\text{O}$ (E. Merck, GR); $\text{Cu}(\text{NO}_3)_2 \cdot \text{H}_2\text{O}$ (NICE, GR); $\text{Cr}(\text{NO}_3)_3 \cdot \text{H}_2\text{O}$ (NICE, GR); $\text{Ce}(\text{NO}_3)_3$ (IRE, Udyogamandal); Ammonium titanyloxalate (TTP, Thiruvananthapuram)

The supports, Y-Zeolite (in powder form) and $\gamma\text{-Al}_2\text{O}_3$ (extrusions of 3 mm dia. and 10 mm length) for preparing the catalyst samples were obtained from Sud-Chemie India Ltd., Binanipuram, Cochin. Dimethylglyoxime, Salicylic acid, Hexamine, 2-hydroxy-acetophenone, 2-hydroxy-1-naphthaldehyde and ethylenediamine obtained from E. Merck were used for the synthesis of ligands.

Hydrogen peroxide (30% w/v), benzyl alcohol, ethylbenzene and 4-methoxybenzaldehyde (E. Merck) were used for the catalytic studies on supported metal complexes. Gas cylinders for carbon monoxide (Air Products, UK), Oxygen, Nitrogen and Hydrogen (Sterling Gases, Cochin) and Helium (Speciality Gases, Bangalore) were used for catalytic studies of metal oxide catalysts.

2. 3 SYNTHESIS OF LIGANDS

2. 3. 1 Dimethylglyoxime (dmg)

Dimethylglyoxime was purified by recrystallisation from methanol and dried in vacuum over anhydrous calcium chloride.

2.3.2 3-Formylsalicylic acid (fsal)

3-Formylsalicylic acid was synthesized by adopting the procedure reported by Duff and Bills ¹. Salicylic acid (40.0 g), hexamethylenetetramine (27.0 g) were mixed together in water (300 ml) and then boiled under reflux for 16 hours. The solution was cooled and acidified with 4 N HCl (300 ml) to obtain a yellow precipitate. This precipitate was filtered, dried and soxhlet extracted with benzene for 8 hours. The benzene solution was evaporated and the residue was dissolved in 3 N NH₃ solution (200 ml). Subsequently, 10% BaCl₂ (100 ml) and 2 N NaOH (50 ml) solutions were added to form the precipitate of barium 3-formylsalicylic acid which was then converted to 3-formylsalicylic acid by acidifying with dil. HCl. The compound separated was collected, purified by recrystallisation from boiling water and dried in vacuum over anhydrous calcium chloride.

2.3.3 N,N'-Ethylenebis(7-methylsalicylideneamine) (Mesalen)

Mesalen ligand was synthesized as per the method reported in the literature ². 2-Hydroxyacetophenone (4.1 g, 3×10^{-2} mol.) in 50 ml methanol was mixed with ethylenediamine (0.9 g, 1.5×10^{-2} mol.). The Schiff base was formed as a yellow precipitate. It was filtered, purified by recrystallisation from methanol and then dried in vacuum over anhydrous calcium chloride.

2.3.4 N,N'-Ethylenebis(5,6-benzosalicylideneamine) (Benzosalen)

The procedure employed for the synthesis of this ligand was reported in the literature ³. 2-hydroxy-1-naphthaldehyde (5.2 g, 3×10^{-2} mol.) and ethylenediamine (0.9 g, 1.5×10^{-2} mol.) were mixed together in 50 ml methanol. The Schiff base was separated out as a yellow powder. It was filtered, washed with methanol and was finally dried in vacuum over anhydrous calcium chloride.

2. 4. SYNTHESIS OF Y ZEOLITE SUPPORTED METAL COMPLEXES

2. 4. 1 Modification of Y Zeolite

Metal exchanged Y zeolite support was prepared as per the following procedure:

(a). Preparation of Na exchanged zeolite (NaY)

The parent zeolite, HY (5.0 g) was ion exchanged with NaCl solution (1 M, 500 ml) under stirring for 24 hours at room temperature. It was then filtered and washed with deionised water till the filtrate was free of chloride ions. The NaY formed was dried at 120 °C for 12 hours.

(a). Preparation of metal exchanged zeolite (MY)

Zeolite, NaY (5.0 g) was stirred with metal chloride solution (0.007 M, 500 ml) of pH 4.0-4.5 at 90 °C for 8 hours. Such low concentration of metal salt solutions of pH 4.0-4.5 was used as dealumination occurs at higher concentrations and $\text{pH} < 4.0^4$. Ferric chloride solution of still lower concentration, 0.001 M, was used, as this destruction is more probable in the case of ion exchange with Fe^{3+} . The slurry was filtered and washed with deionised water to remove chloride ions. It was then dried at 120 °C for 2 hours and finally dehydrated at 450 °C for 4 hours.

2. 4. 2 Encapsulation of metal complexes in Y zeolite

The flexible ligand method was used for encapsulating metal complexes in Y zeolite⁵. In this method, ligand molecules are diffused through the zeolite channels and are allowed to react with the metal ions previously introduced into the supercage to form complexes in it. General procedure for this kind of encapsulation is as follows:

Metal exchanged zeolite, MY (3.0 g) was mixed thoroughly with excess of ligand (ligand to metal mole ratio ~ 2 - 4) and introduced into a glass ampule. It was then sealed and heated. The heating temperature has to be optimised so as to effect the complexation reaction. After this, the resulting material was purified from surface

complexes formed and unreacted ligand by soxhlet extraction with one or more solvents. The soxhlet extraction was continued further for 16 hours after the extracting solvent becomes colourless to ensure the complete removal of surface species. The uncomplexed metal ions in the zeolite and ionisable protons of the ligand, if any, transferred to zeolite framework were removed by ion exchange with NaCl solution (0.1 M, 250 ml) for 24 hours. It was then filtered, washed free off chloride ions and finally dried at 100 °C for 2 hours.

2. 5 PREPARATION OF METAL OXIDE CATALYSTS

Alumina supported Cu or Cu-Cr based metal oxide catalysts were prepared by using the impregnation technique ⁶. This technique is particularly useful to make small crystallites of catalytically active components dispersed on a porous support. It mainly consists of three steps: (i) dipping the support in the impregnating solution containing active components, (ii) drying and (iii) activate by calcination. In the first step, the solution is sucked into the support by capillary action followed by diffusional transport of the solute to the carrier. During the drying step, the metal salt is precipitated and deposited on the surface of pores. The drying and calcination steps determine final distribution of the active components on the support. In incipient wetness impregnation method, the volume of impregnating solution is adjusted so as to get the solution fully absorbed by the support. This method is very effective for precisely controlling the concentration of active ingredients in the catalyst.

2. 6 PHYSICO-CHEMICAL PROPERTIES

2. 6. 1 Chemical analysis

(a). Determination of Si, Al, Na and transition metal ion in zeolite samples

Chemical analyses of zeolites and zeolite encapsulated complexes were done according to the following procedure: The sample was dried at 120 °C for one hour and

was then kept in a desiccator. A known weight (w_1) of the sample was taken in a beaker and the zeolite framework was destroyed by heating with concentrated sulfuric acid (40 ml, 98%) until SO_3 fumes were evolved. It was then cooled, diluted with water and filtered using ashless filter paper. The filtrate was collected in a standard flask. The residue was taken in a platinum crucible with lid and incinerated at 1000 °C for one hour, cooled and then weighed (w_2). Hydrofluoric acid (10 ml, 40%) was added to dissolve the residue and the resulting solution was evaporated on a hot plate to remove silicon in the form of H_2SiF_6 . It was again incinerated at 1000 °C, cooled and weighed (w_3). From the loss in weight, the amount of silica present in the sample can be estimated using Eq. II. 1.

$$\% \text{SiO}_2 = (w_3 - w_2) \times 100 / w_1 \quad \text{Eq. II. 1}$$

The residue in the crucible was fused with potassium persulfate, dissolved in water and was added to the filtrate collected in the standard flask. The solution was then made up to a known volume. This solution was analysed for Al, Na and metal contents using atomic absorption spectrophotometry.

(b). Determination of CeO_2 in Al_2O_3 - CeO_2 support

A known weight of the support, Al_2O_3 - CeO_2 (~ 0.5 g), was fused with potassium hydrogen sulfate (~ 10 g) at 700 °C for one hour. The melt was cooled and then dissolved in hot water. This solution was analysed for CeO_2 by atomic absorption spectrophotometry.

(c). Determination of TiO_2 in Al_2O_3 - TiO_2 support

A known weight of the support, Al_2O_3 - TiO_2 (~ 0.5 g), was fused with KOH (~10g) at 500 °C for one hour. The melt was cooled and extracted with hot water in a polyethylene beaker. This solution was acidified with Con. HCl and used for determining TiO_2 content by atomic absorption spectrophotometry.

(d). Determination of Cu and Cr in metal oxide catalysts

A known weight of the catalyst sample (~ 0.5 g) was fused with potassium hydrogen sulfate (~10 g) at 700 °C for one hour. The fused melt was dissolved in hot water after cooling. This solution was analysed by atomic absorption spectrophotometry for estimating the amount of metals present in the catalyst.

2. 6. 2 CHN analysis

The results of microanalyses for C, H and N in zeolite encapsulated complexes were provided by Central Drug Research Institute, Lucknow.

2. 6. 3 Atomic absorption spectrophotometry

Atomic absorption spectrophotometry (Perkin Elmer 3110) was used for analysing various ingredients in zeolites and metal oxide samples.

2. 6. 4 Surface area analysis

Surface area was determined by BET method ⁸ of nitrogen adsorption at liquid nitrogen temperature in Micromeritics Gemini 2360. The volume of gas adsorbed by the sample was monitored at different relative pressures in the range 0.1-0.9.

Surface area was calculated using the following BET equation (Eq. II. 2):

$$1/V_{\text{ads}} (P_0 - P) = 1/V_m C + [(C-1)/V_m C] P/P_0 \quad \text{Eq. II. 2}$$

where

V_{ads} = volume of gas adsorbed at relative pressure P/P_0

P_0 = saturated vapour pressure

V_m = volume of gas adsorbed for monolayer coverage

C = BET constant

By plotting left side of the Eq. II. 2 against P/P_0 (upto 0.3), a straight line is obtained with a slope of $(C-1)/V_m C$ and an intercept $1/V_m C$. From these values, V_m and hence the number of moles of N_2 adsorbed, X_m , can be calculated.

BET surface area is calculated using Eq. II. 3.

$$S_{\text{BET}} = X_m N A_m 10^{-20} \quad \text{Eq. II. 3}$$

where

N = Avogadro's number

A_m = cross-sectional area of the adsorbate molecule in \AA^2

Total pore volume of the sample at $P/P_0 \sim 0.9$ is computed by converting the volume of N_2 adsorbed at $P/P_0 \sim 0.9$ to volume of liquid equivalent to it using Eq. II. 4.

$$V_{\text{tot}} = V_{\text{ads}} D \quad \text{Eq. II. 4.}$$

where

V_{tot} = total pore volume at $P/P_0 \sim 0.9$

V_{ads} = volume of gas adsorbed at relative pressure ~ 0.9

D = density conversion factor

2. 6. 5 Pore volume analysis

Mercury penetration method was used to measure the pore volume of metal oxide catalysts (Micromeritics Pore sizer 9320). Mercury porosimetry is based on the capillary law governing liquid penetration into small pores. This law, in the case of non-wetting liquid like mercury, is expressed by the Washburn equation, assuming pores are cylindrical.

$$D = \sqrt{\frac{4\gamma \cos\theta}{P}} \quad \text{Eq. II. 5}$$

where

D = Pore diameter

P = Applied pressure

γ = Surface tension (485 dynes/cm for Hg)

θ = Contact angle (usually 130°)

2. 6. 6 X-ray diffraction spectroscopy

Zeolite complexes and Cu-Cr catalysts were analysed for powder X-ray diffraction using ' Rigaka D-Max C ' X-ray diffractometer. The analysis was carried out with a

stationary X-ray source, Ni filtered CuK α radiation ($\lambda=1.5404$) and a movable detector which measures the intensity of diffracted radiation as a function of the angle 2θ between the incident and diffracted beams.

2. 6. 7 Scanning electron microscopy

Scanning electron microscopy analysis of a representative zeolite complex before and after soxhlet extraction was performed at Sree Chitra Institute of Medical Science and Technology, Thiruvananthapuram

2. 6. 8 Magnetic moment measurement

The magnetic susceptibility measurements were carried out at room temperature on a simple Gouy type magnetic balance. The Gouy tube was standardised using Co [Hg(SCN)₄] as suggested by Figgis and Nyholm⁹.

The effective magnetic moment was calculated using Eq. II. 6

$$\mu_{\text{eff}} = 2.84 (X'_m T)^{1/2} \text{ BM} \quad \text{Eq. II. 6}$$

where

T = absolute temperature

X'_m = molar susceptibility corrected for diamagnetism of all atoms present in the complex using pascals constant and that of zeolite frame work per unit metal.

2. 6. 9 Diffuse reflectance spectra

The diffuse reflectance spectra were recorded at room temperature between 200-2000 nm against MgO as standard on a Cary Win spectrophotometer at Regional Sophisticated Instrumentation centre, Indian Institute of Technology, Chennai. The spectra were computer processed and plotted as percentage reflectance versus wavelength. A Kubelka- Munk analysis^{10, 11} was performed on the reflectance data. The Kubelka-Munk factor, F(R), is given by Eq. II. 7

$$F(R) = (1-R)^2 / 2R = k/s \quad \text{Eq. II. 7}$$

where

$F(R)$ = Kubelka-Munk factor

R = the diffuse reflectance of the sample as compared to MgO

k = the molar absorption coefficient

s = the scattering coefficient of the sample.

2. 6. 10 Infrared spectra

Infrared spectra of the ligand and supported complexes in the region 4600 cm^{-1} -400 cm^{-1} were taken in KBr pellets using Shimadzu 8000 Fourier Transform Infrared Spectrophotometer.

2. 6. 11 EPR spectra

The X-band EPR spectra of zeolite supported Cu complexes were recorded at liquid nitrogen temperature using a Varian E-109 X/Q bands spectrophotometer. The g values were estimated relative to tetracyanoethylene (TCNE, $g = 2.0027$). Magnetic moment was determined¹² from the EPR data using Eq. II. 8.

$$\mu_{\text{eff}}^2 = g_{\parallel}^2/4 + g_{\perp}^2/4 + 3kT/\lambda_0 (g-2) \quad \text{Eq. II. 8}$$

where λ_0 is the spin orbit coupling constant for the free metal ion

The density of unpaired electrons at the central metal atom was computed¹³ using Eq. II. 9.

$$\alpha^2_{\text{Cu}} = (A_{\parallel}/P) + (g_{\parallel}-2) + 3/7(g_{\perp}-2) + 0.04 \quad \text{Eq. II. 9}$$

where $1-\alpha^2$ measures the covalency associated with the bonding of metal ion to the ligand and $P=0.036 \text{ cm}^{-1}$.

2. 6. 12 TG analysis

Thermogravimetric analysis was performed on a Shimadzu TGA-50 in the temperature range 30-550 °C at a heating rate of 10 °C/minute in air. About 20 mg sample was taken for each analysis in a platinum crucible hanged from one arm of balance in the instrument. The TG data were computer processed and plotted the % weight against temperature at 5 °C intervals.

2. 7 CATALYTIC STUDIES

Catalytic studies over zeolite complexes and metal oxide catalysts are detailed in Chapter VII and VIII respectively. The following instruments were used for conducting catalytic experiments:

2. 7. 1 Gas chromatographs

Gas Chromatograph Chemito 8510 was used for analysing the reactants and products of the catalytic reactions over zeolite complexes. A SE-30 column was used for separating various components in the reaction mixture.

The analysis of CO in inlet and outlet gas streams was carried out using a Chemito 3865 gas chromatograph for determining CO oxidation activity of various catalysts. A Poropak Q column was used for separating CO₂ formed from unreacted CO in the product stream. The outlet of the column was passed through a methanator for converting CO and CO₂ to methane, which is then sensed by the FID detector.

2. 7. 2 Microcatalytic reactor

Chemisorption studies were carried out in a microcatalytic reactor assembly in which the reactor is heated using a temperature programmer (Century Systems CS-7533). A Chemito 8510 GC was connected on line to the reactor for the gas analysis.

REFERENCES

1. J. C. Duff and E. J. Bills, *J. Chem. Soc.*, (1932) 1987
2. Y. Fujii, T. Isago, M. Sano, N. Yanagibashi, S. Hirasawa and S. Takahashi, *Bull. Chem. Soc. Jpn.*, 49 (1976) 3509
3. Y. Fujii, Y. Kuwana, S. Takahashi, K. Shimizu and K. Hiroi, *Bull. Chem. Soc. Jpn.*, 55 (1982) 2598
4. P. G. Menon, " *Lectures on Catalysis* ", 41st Ann. Meeting, Ind. Acad. Sci.; S. Ramaseshan (Ed.); 1975
5. N. Herron, *Inorg. Chem.*, 25 (1986) 4714
6. F. Severino, J. Brito, O. Carias and J. Laine, *J. Catal.*, 102 (1986) 172
7. A. I. Vogel, " *A Text Book of Quantitative Inorganic Analysis* ", Longmans-Green, London, 1978
8. S. Brunauer, P. H. Emmett and E. J. Teller, *Am. Chem. Soc.*, 60 (1938) 309
9. B. N. Figgis and R. S. Nyholm, *J. Chem. Soc.*, (1958) 4190
10. H. G. Hecht, " *Modern Aspects of Reflectance Spectroscopy* " ; Wendlandt, W. W. Ed.; Plenum Press: New York, 1968
11. S. K. Tiwary and S. Vasudevan, *Inorg. Chem.*, 37 (1998) 5239
12. B. V. Agarwala, *Inorg. Chim. Acta.*, 36 (1979) 209
13. D. Kivelson and R. Neiman, *J. Chem. Phys.*, 35 (1961) 149

CHAPTER III

STUDIES ON Y ZEOLITE ENCAPSULATED TRANSITION METAL COMPLEXES OF DIMETHYLGLYOXIME

Abstract

Y Zeolite encapsulated Mn(II), Fe(III), Co(II), Ni(II) and Cu(II) complexes of dimethylglyoxime have been synthesized and characterized. The compositions of metal exchanged zeolites and zeolite complexes have been deduced from the analytical data. XRD patterns of zeolites or zeolite complexes, and surface area, pore volume and IR spectra of zeolites indicate the retention of crystalline structure on ion exchange or synthesis of complexes. SEM analysis shows that the zeolite complex is free from surface species. The surface area and pore volume data suggest encapsulation of complexes. Magnetic moments, electronic spectra and EPR of Cu(II) complex tentatively assign geometries to the encapsulated complexes. IR spectra explain the coordination of metal ions with dimethylglyoxime. A qualitative idea of the thermal stability of complexes has been given by TG analysis

3. 1 INTRODUCTION

Transition metal complexes of dimethylglyoxime have been studied in the past ¹. Among them, bis(dimethylglyoximato)cobalt(II), also known as cobaloxime(II), is used as a reagent in synthetic organic chemistry and as a protecting chemical in the synthesis of amino acids ². Cobaloxime has received special attention with respect to investigations on the bonding and activation of molecular oxygen in biological systems. For example, cobaloxime simulates closely the reactions of Vitamin B₁₂ and therefore, it is considered as an attractive model compound for studying the oxygen carrying properties of the vitamin ³. Most significantly, cobaloxime can act as a homogeneous catalyst in hydrogenation and dehydrogenation reactions ^{4,5}. The formation of reactive intermediate complexes involving molecular hydrogen, oxygen or olefins has been identified in these reactions.

There is a growing interest to encapsulate metal complexes in zeolites for spectral and catalytic studies. Zeolite encapsulated complexes of nitrogen chelating ligands have been studied using EPR, IR and optical reflectance spectroscopy ⁶⁻⁸. Later on, cobaloxime has also been encapsulated in zeolite for such spectral studies ^{9,10}. Attempts have been made in these studies to propose a reaction scheme for complexation by recognizing the intermediate species formed in the zeolite cavities.

The ability of simple cobalt complexes to chemisorb oxygen and hence to catalyse oxidation reactions has been sustained on encapsulating in the zeolite matrix ^{6-8, 11}. However, not much interest has been evinced in the study of catalysis of encapsulated cobaloxime complexes ¹². The ability of cobaloxime complex to activate molecular oxygen in homogeneous reactions ³ is expected to favour the oxidation reactions over its zeolite encapsulated system also. In light of this, it is worthwhile to evaluate the oxidation activity of zeolite complexes of dimethylglyoxime for exploiting their catalytic potential in chemical reactions.

In this study, Y zeolite encapsulated complexes of Mn(II), Fe(III), Co(II), Ni(II) and Cu(II) with dimethylglyoxime (dmg) were synthesized and characterized. Attempts were made to provide some evidences for the encapsulation and explain the composition and structure of encapsulated complexes. The thermal stability of zeolite complexes was also studied. The results of these studies are presented in this chapter.

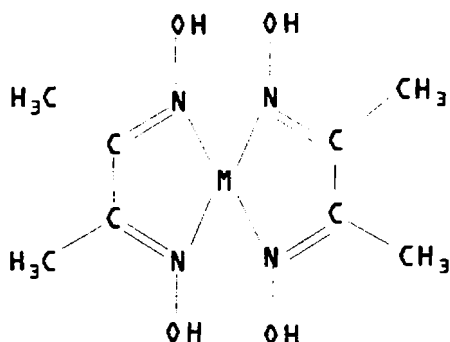


Figure III. 1

Structure of simple dmg complex

3. 2 EXPERIMENTAL

3. 2. 1 Materials

Details regarding the purification of dmg ligand obtained from Merck ER are given in Chapter II. The procedure for the preparation of metal exchanged zeolite is also described in Chapter II. These metal exchanged zeolites were used for synthesizing dmg complexes in the cavities.

3. 2. 2 Synthesis of zeolite encapsulated dmg complexes

The general method used for the synthesis of zeolite encapsulated complexes is described in Chapter II. Metal exchanged zeolite (3.0 g) was thoroughly mixed with the required amount of dmg for keeping the ligand to metal mole ratio at ~ 4. The amount of ligand to be taken for the synthesis was estimated on the basis of the metal content in zeolite supports and found to be as follows: 0.87 g for YMn, 0.39 g for YFe,

0.86 g for YCo, 0.88 g for YNi and 0.85 g for YCu. This mixture was taken in a glass tube, then sealed and heated for 16 hours to effect complexation. The temperature maintained during complexation was 110 °C for YMn-dmg, 100 °C for YFe-dmg and YCo-dmg and 90 °C for YNi-dmg and YCu-dmg. The resultant mass, except in the case of YNi-dmg, was soxhlet extracted with methanol until the extracting solvent becomes completely colourless. The soxhlet extraction with methanol was further continued for another 16 hours to ensure the complete removal of the surface complexes and the free ligand. As Ni-dmg is slightly soluble in methanol, chloroform was used in the case of YNi-dmg as the extracting solvent in the first stage and then methanol was used in the second stage for removing the free ligand. The purified zeolite complex was again ion exchanged with sodium chloride solution (250 ml, 0.1 M, 24 hours) to remove any uncomplexed metal ions. Zeolite complex obtained was filtered, washed to remove chloride ions, dried at 100 °C for 2 hours and stored in vacuum over anhydrous calcium chloride.

3. 2. 3 Analytical methods

The analytical methods and other characterization techniques used are described in Chapter II

3. 3 RESULTS AND DISCUSSION

3. 3. 1 METAL EXCHANGED ZEOLITE SUPPORTS

3. 3. 1. 1 Chemical analysis

The analytical data of NaY and various metal exchanged zeolites are presented in Table III. 1. The data reveal a Si/Al ratio of 2.43 for NaY which corresponds to a unit cell formula $\text{Na}_{56} [(\text{AlO}_2)_{56} (\text{SiO}_2)_{136}]^{13}$. The Si/Al ratio remains the same in all metal exchanged zeolites indicating that no destruction of zeolite framework has occurred by the process of dealumination during ion exchange. In order to avoid dealumination, metal chloride solutions of very low concentration (0.007 M) and pH ~ 4.0-4.5 were

used for ion exchange. Ferric chloride solution of still lower concentration (0.001 M) was used for preparing FeY as dealumination is more probable in this case. Zeolite framework was reported to be preserved while ion exchanging with very dilute metal salt solutions¹⁴. The metal loading in zeolites was found to be more than 3 % except in the case of FeY for which the metal content is 1.55 %.

Table III. 1

Analytical data of metal exchanged zeolites

Sample	% Si	% Al	% Na	% metal
NaY	21.76	8.60	7.50	
MnY	21.62	8.56	3.41	3.44
FeY	21.75	8.59	5.29	1.55
CoY	21.53	8.52	3.35	3.64
NiY	21.79	8.62	3.28	3.72
CuY	21.48	8.48	3.12	3.86

Table III. 2

Composition of metal exchanged zeolites

Sample	Degree of ion exchange (%)	Unit cell formula
NaY		$\text{Na}_{56} [(\text{AlO}_2)_{56}(\text{SiO}_2)_{136}] n\text{H}_2\text{O}$
MnY	39.51	$\text{Na}_{33.8}\text{Mn}_{11.1} [(\text{AlO}_2)_{56}(\text{SiO}_2)_{136}] n\text{H}_2\text{O}$
FeY	26.23	$\text{Na}_{41.4}\text{Fe}_{7.3} [(\text{AlO}_2)_{56}(\text{SiO}_2)_{136}] n\text{H}_2\text{O}$
CoY	39.12	$\text{Na}_{34}\text{Co}_{11} [(\text{AlO}_2)_{56}(\text{SiO}_2)_{136}] n\text{H}_2\text{O}$
NiY	39.65	$\text{Na}_{33.8}\text{Ni}_{11.1} [(\text{AlO}_2)_{56}(\text{SiO}_2)_{136}] n\text{H}_2\text{O}$
CuY	38.64	$\text{Na}_{34.4}\text{Cu}_{10.8} [(\text{AlO}_2)_{56}(\text{SiO}_2)_{136}] n\text{H}_2\text{O}$

The degree of ion exchange and unit cell formulae of the metal exchanged zeolites were derived from the analytical data and are given in Table III. 2. The degree of ion exchange is represented as the percentage of Na^+ ions replaced by metal ions from the total amount of Na equivalent to Al content of the zeolite. The unit cell formula represents the composition of a unit cell in the metal exchanged zeolites. The degree of ion exchange in various metal exchanged zeolites used in the present study are comparable to that reported in the literature^{15,16}.

3.3.1.2 X-ray diffraction pattern

X-ray diffraction patterns of the zeolite samples HY, NaY, FeY and CoY are given in Figure III. 2.

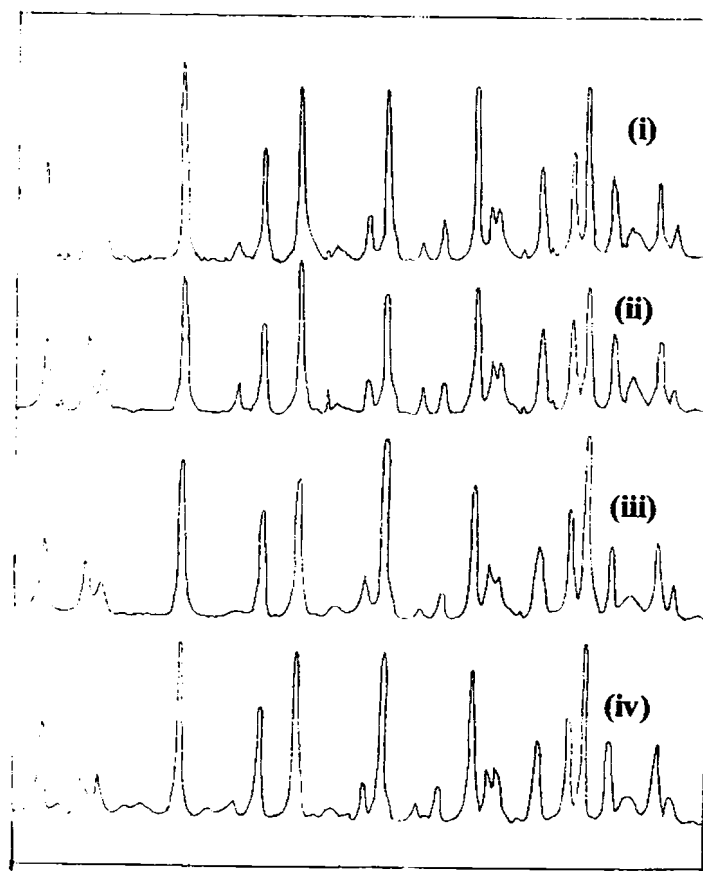


Figure III. 2

XRD patterns of (i) HY, (ii) NaY, (iii) FeY and (iv) CoY

The XRD patterns of metal exchanged zeolites are very similar to that of the parent HY zeolite. Furthermore, these XRD patterns are similar to those reported in the literature¹⁷. Crystalline structure was almost preserved in the metal exchanged zeolites. The crystalline nature of Y zeolite was reported to be affected by metal exchange using metal salt solutions of concentration > 0.02 M and $\text{pH} < 4$ ¹⁴. XRD data in the present case reveal that the collapse of zeolite framework by dealumination could be avoided by using very dilute metal chloride solutions of pH in the range 4.0-4.5 (vide page 58). Furthermore, crystalline phases of metal ions were not detected in any of the patterns. This implies that metal ions are finely dispersed at the cation sites of the zeolite rendering them non-detectable by XRD.

3. 3. 1. 3 Surface area and pore volume

Surface area and pore volume of parent HY zeolite and metal exchanged zeolites measured by low temperature nitrogen adsorption at relative pressure (P/P_0) in the range 0.1-0.9 are given in Table III. 3. The nitrogen adsorption isotherms of the zeolites NaY, MnY, FeY and CuY are given in Figure III. 3.

Table III. 3

Surface area and pore volume data of metal exchanged zeolites

Sample	Surface area (m^2/g)	Pore volume (ml/g)
HY	546	0.3045
NaY	545	0.3045
MnY	531	0.2961
FeY	540	0.3011
CoY	532	0.2966
NiY	528	0.2944
CuY	534	0.2978

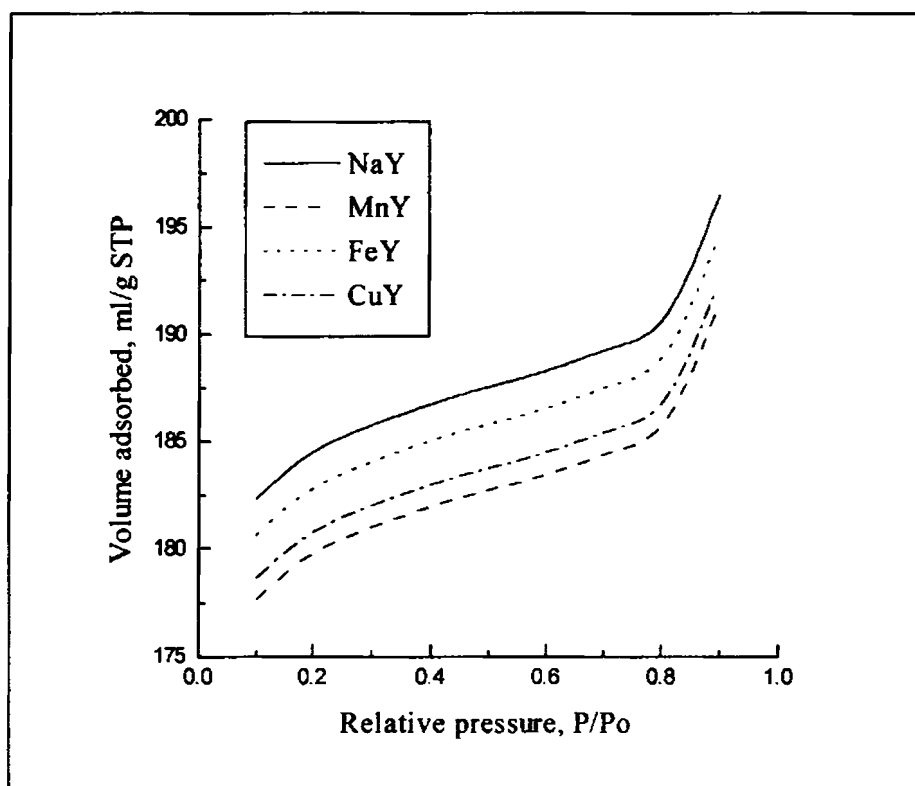


Figure III. 3

Nitrogen adsorption isotherms of metal exchanged zeolites

Surface area of NaY is $545 \text{ m}^2/\text{g}$ whereas that of metal exchanged zeolites varies in the range $528\text{-}540 \text{ m}^2/\text{g}$. These values indicate that surface area is only marginally reduced on introducing metal ions into the zeolite lattice by ion exchange. This observation further rejects the possibility of the destruction of zeolite matrix on ion exchange since a drastic drop in surface area of NaY zeolite is likely if the structure is collapsed. Surface area of zeolite used in the present study is comparable to that of zeolite used for encapsulating metal complexes in earlier studies¹⁸. Pore volume of zeolites at the relative pressure ~ 0.9 is in the range $0.2940\text{-}0.3050 \text{ ml/g}$.

3. 3. 1. 4 FTIR spectra

FTIR spectra of HY, NaY and CoY zeolites are shown in Figure III. 4. The IR bands are listed in Table III. 4. The IR bands of zeolite can be attributed to the

vibrations of $(\text{Si/Al})\text{O}_4$ groups designated as TO_4 i.e. internal vibrations of SiO_4 and AlO_4 and external vibrations between the tetrahedra ¹⁹. The frequencies of these vibrations are sensitive to Si/Al ratio and framework structure.

In the present case, the bands were found to appear almost at the same position in the spectra of the parent zeolite and all the metal exchanged zeolites. Furthermore, these bands are in agreement with the reported IR data of Y zeolite ¹⁹. This observation further reveals that the zeolite framework remains unaffected on ion exchanging using metal chloride solution of low concentration.

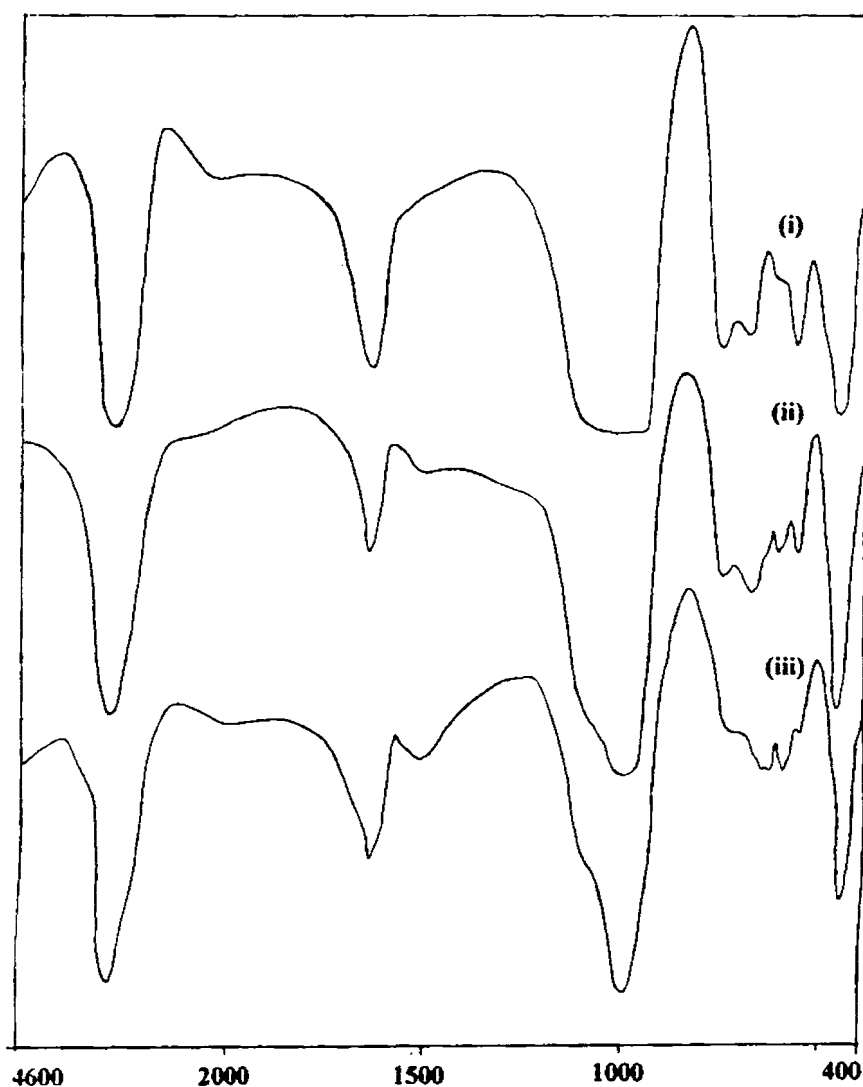


Figure III. 4

IR spectra of (i) HY, (ii) NaY and (iii) CoY

Table III. 4

IR spectral data of metal exchanged zeolites

HY	NaY	CoY	Tentative Assignments
465	461	459	$\gamma_{\text{symmetric}}$
565	569	572	$\gamma_{\text{symmetric}}$ (external)
683	682	679	
750	754	752	$\gamma_{\text{asymmetric}}$ (internal)
1000	998	1000	$\gamma_{\text{asymmetric}}$ (external)
1647	1640	1654	$\delta_{\text{H-O-H}}$
3453	3599	3453	$\gamma_{\text{O-H}}$

The very broad band at $\sim 1000 \text{ cm}^{-1}$ is attributed to external asymmetric stretching vibration of TO_4 units whereas internal asymmetric stretching vibration is responsible for the band at $\sim 750 \text{ cm}^{-1}$. The symmetric stretching vibrations give rise to bands at $\sim 570 \text{ cm}^{-1}$ and $\sim 460 \text{ cm}^{-1}$. The stretching and bending vibrations of water molecules present in the zeolite lattice could be seen at $\sim 3500 \text{ cm}^{-1}$ and $\sim 1650 \text{ cm}^{-1}$ respectively.

3.3.2 ZEOLITE ENCAPSULATED DMG COMPLEXES

Zeolite encapsulated dmg complexes of Mn(II), Fe(III), Co(II), Ni(II) and Cu(II) ions were synthesized using the flexible ligand method. The complexes were characterized using chemical analysis, SEM, XRD, surface area, pore volume, magnetic moment and electronic, FTIR and EPR spectroscopy. Thermal behaviour of the zeolite complexes was studied using TG analysis.

3.3.2.1 Chemical analysis

The analytical data of the zeolite complexes are given in Table III. 5. The data show that the Si/Al ratio of the zeolite complexes is 2.43 as in the case of the metal exchanged zeolites. This indicates that zeolite framework structure was retained without any

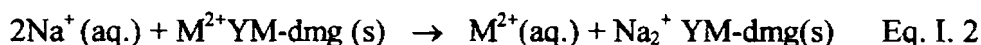
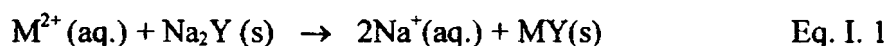
change on encapsulation. Such retention of zeolite framework on encapsulation of metal complexes via flexible ligand method was reported by earlier workers also^{20, 21}.

Table III. 5

Analytical data of encapsulated complexes

Sample	% Metal	% Si	% Al	% Na	% C	% H	% N
YMn-dmg	2.64	19.24	7.61	5.11	4.30	0.72	2.50
YFe-dmg	0.97	20.08	7.89	6.46	1.57	0.26	0.91
YCo-dmg	1.78	19.45	7.71	6.56	2.77	0.46	1.62
YNi-dmg	1.63	19.48	7.70	6.15	2.59	0.43	1.50
YCu-dmg	1.58	19.44	7.68	6.30	2.30	0.38	1.33

The metal content in zeolite complexes and metal exchanged zeolites indicates that only a portion of the metal initially present has undergone complexation and the remaining portion was found to be back exchanged with Na⁺ ions. The process of metal ion exchange in zeolite to form MY and the back exchange of uncomplexed metal ions from the lattice after complexation are represented by Eq. I. 1 and Eq. I. 2 respectively.



About 40 - 80 % of the metal initially present in the metal exchanged zeolite was found to remain in the lattice after complexation and subsequent ion exchange with sodium chloride solution. This metal is expected to have undergone complexation with dmg in the pores of Y zeolite. The charge neutralisation of encapsulated dmg complexes might have occurred by the interaction of negatively charged oxide ions of zeolite matrix.

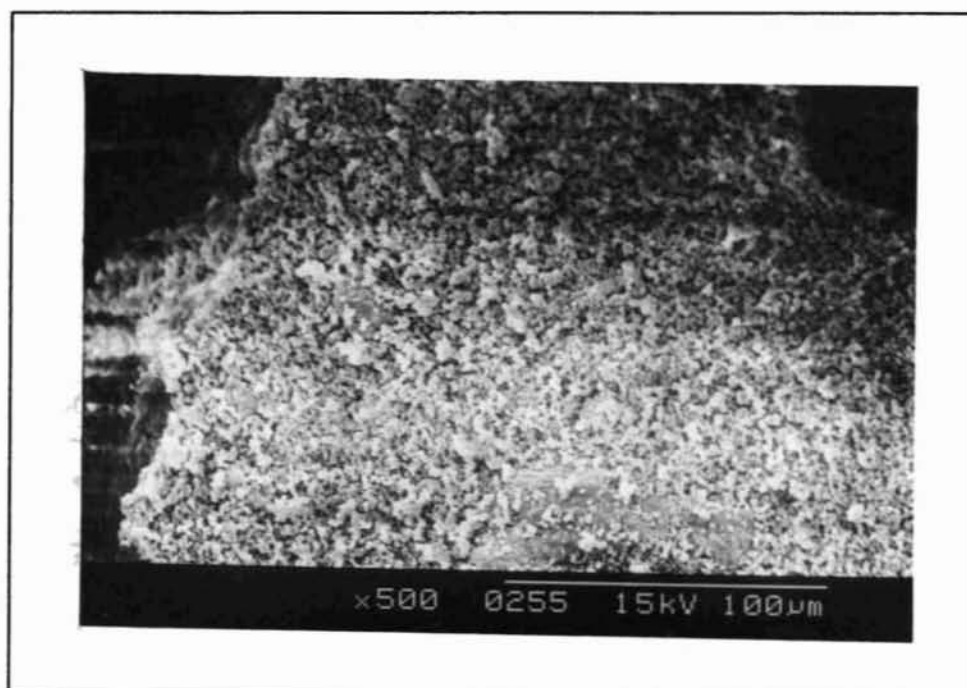
From the analytical data (Table III. 5), the empirical formulae of encapsulated dmg complexes were derived as MnL_{1.86}, FeL_{1.88}, CoL_{1.91}, NiL_{1.94} and CuL_{1.92} in YMn-dmg, YFe-dmg, YCo-dmg, YNi-dmg and YCu-dmg respectively. In the case of free dmg

complexes a ligand to metal mole ratio of 2 has been reported, but the mole ratio is slightly less than two in zeolite complexes. This lower value may be due to the presence of minute traces of free metal ions in the lattice that could not be removed in the final ion exchanging with NaCl solution. The encapsulated complexes might have shielded these metal ions from ion exchanging with Na⁺ ions. The traces of uncomplexed metal ions are unlikely to cause any serious interference in the behaviour of the encapsulated complexes. Similar observation has been made in the case of other zeolite encapsulated complexes by earlier workers also²².

3.3.2.2 SEM analysis

Scanning electron micrographs of YCo-dmg before and after soxhlet extraction are shown at different magnifications in Figure III. 5, III. 6 and III. 7. In the SEM taken before the extraction, the surface atoms of zeolite lattice are not clearly visible. But, in the SEM taken after the extraction, the particle boundaries on zeolite surface are more clear and therefore it can be assumed that surface species formed during complexation reaction were completely removed by soxhlet extraction. The SEM of such clear zeolite surface has been observed for zeolite encapsulated phthalocyanine and salen complexes and has been given as the evidence for the complete removal of surface complexes^{23, 24}. In fact the soxhlet extraction of YCo-dmg with methanol for 16 hours (after the solvent becomes colourless) has led to the complete removal of surface complexes. Therefore, in all the preparations of zeolite complexes similar procedure for the removal of surface complexes was employed.

(i)



(ii)

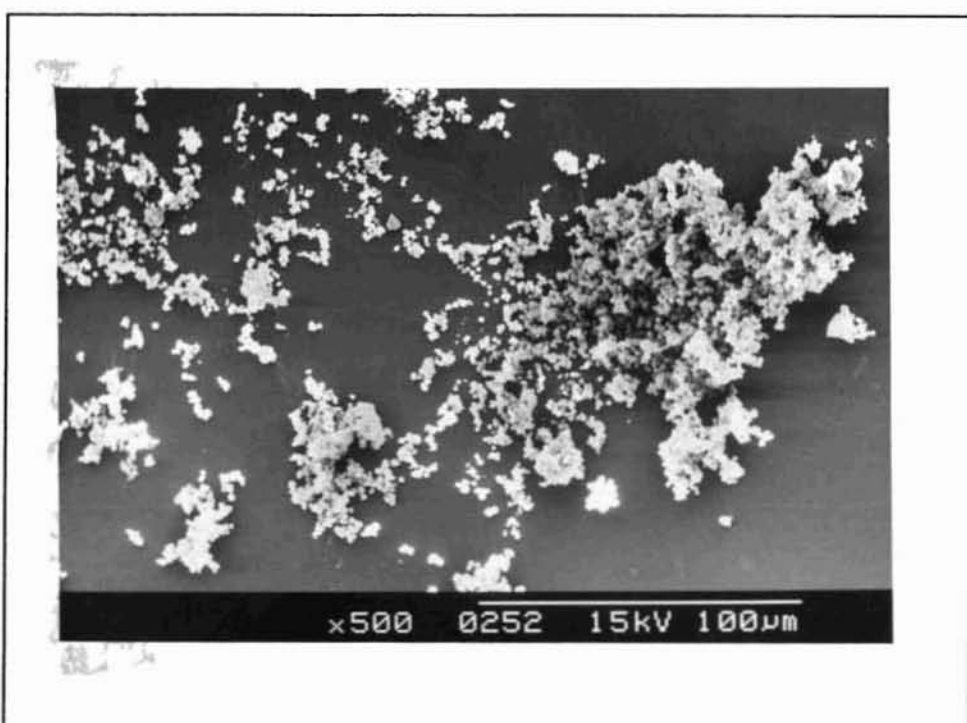
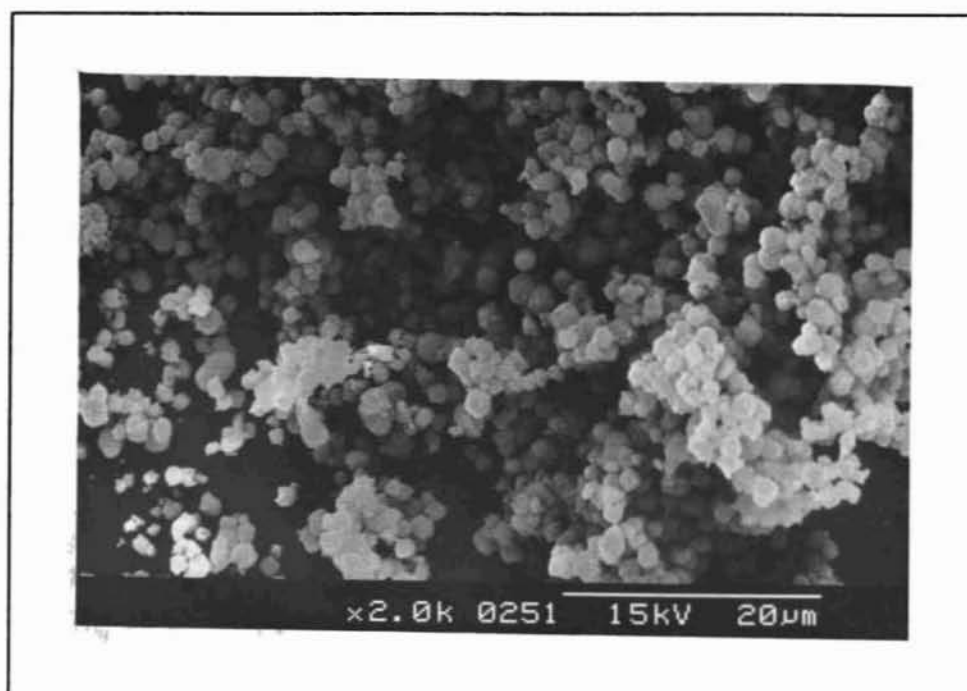


Figure III. 5

SE micrographs of YCo-dmg (x 0.5 k) (i). before and (ii). after soxhlet extraction

(i)



(ii)

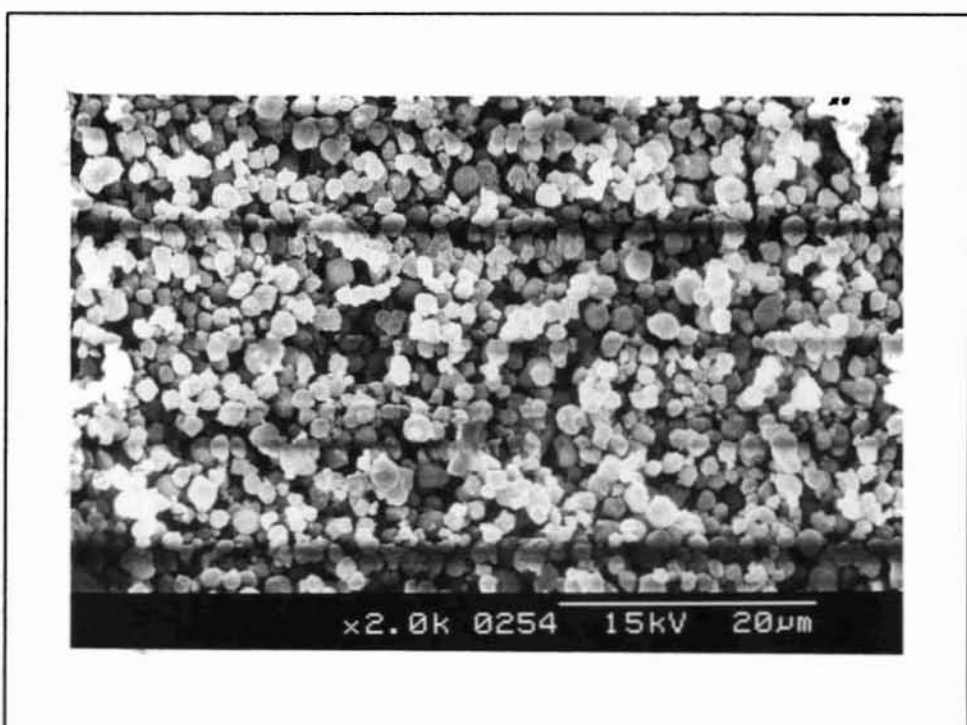
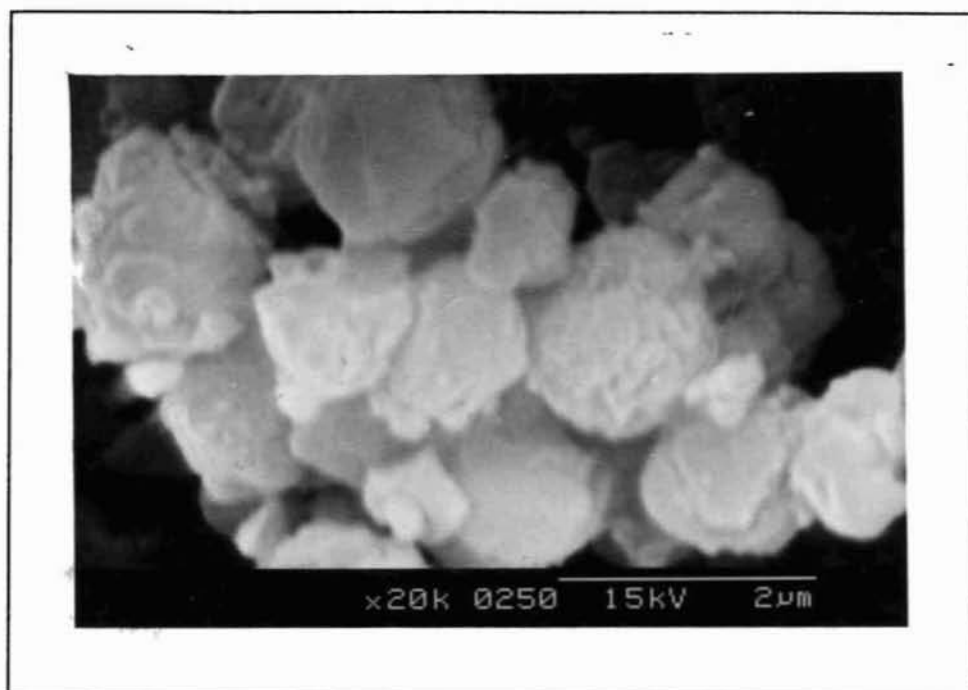


Figure III. 6

SE micrographs of YCo-dmg (x 2 k) (i). before and (ii). after soxhlet extraction

(i)



(ii)

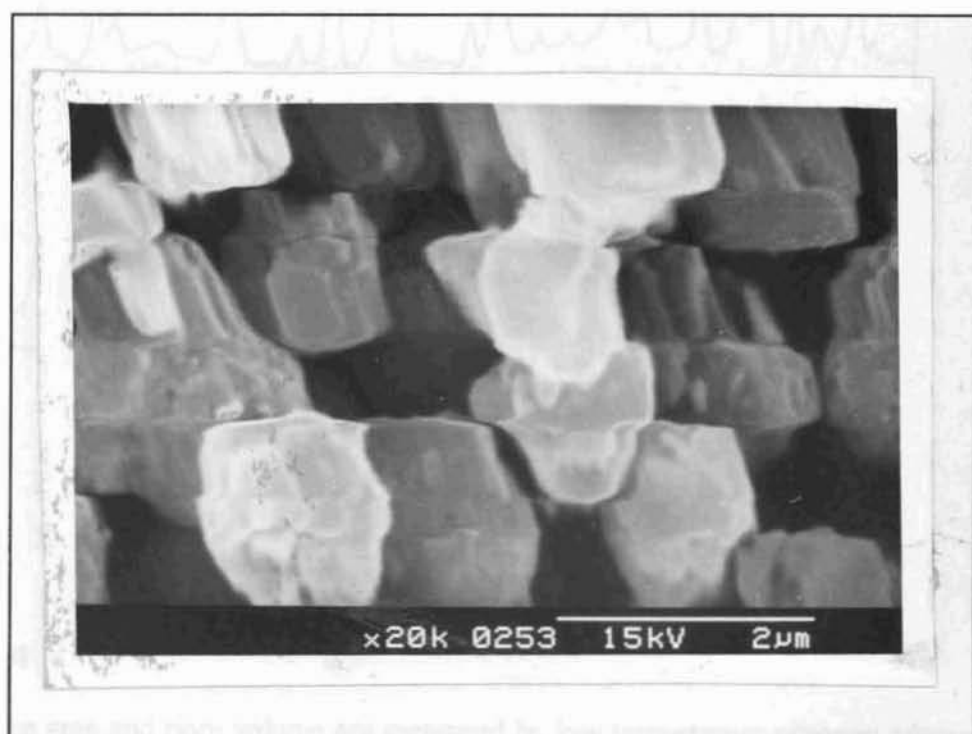


Figure III. 7

SE micrographs of YCo-dmg (x 20 k) (i). before and (ii). after soxhlet extraction

3.3.2.3 X-ray diffraction pattern

XRD patterns (Figure III. 8) recorded for YMn-dmg, YCo-dmg and YCu-dmg complexes are quite comparable to those of the corresponding metal exchanged zeolites and the parent zeolite. Therefore, the zeolite framework structure was not damaged by the synthesis of metal complexes in their cavities as has been reported in previous studies^{25, 26}.

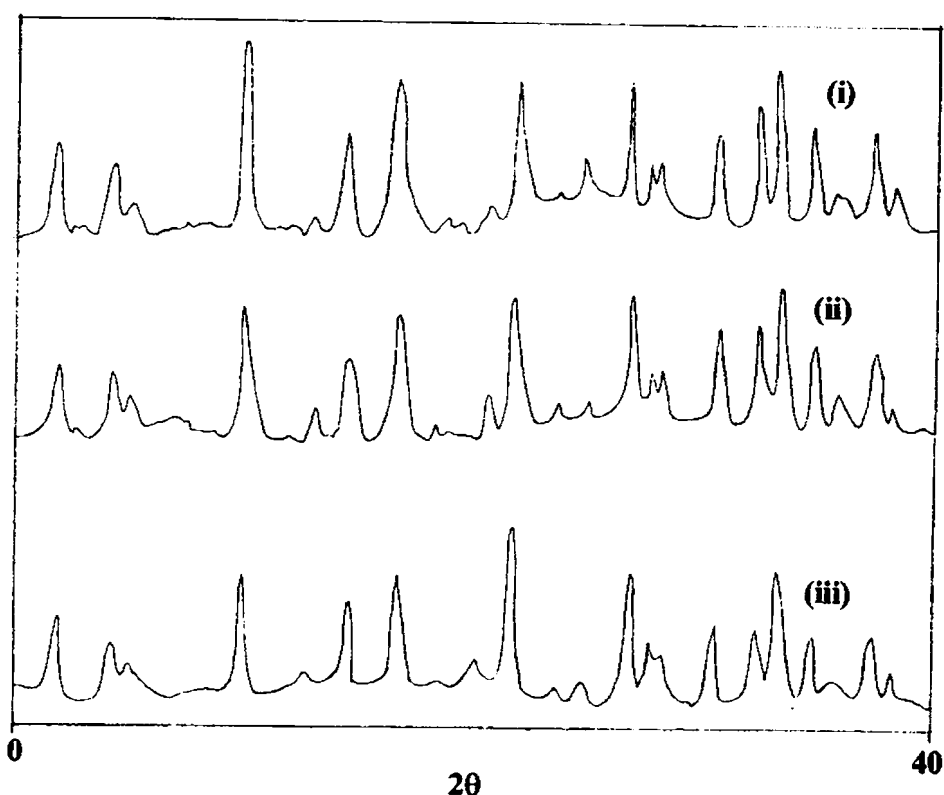


Figure III. 8

XRD patterns of (i). YMn-dmg, (ii). YCo-dmg and (iii). YCu-dmg

3.3.2.4 Surface area and pore volume

Surface area and pore volume are measured by low temperature nitrogen adsorption at relative pressures in the range 0.1 to 0.9. The adsorption isotherms of zeolite encapsulated dmg complexes are shown in Figure III. 9. Surface area and pore volume

values are given in Table III. 6. The data reveal that the values are lower in the case of zeolite complexes than those of corresponding metal exchanged zeolite. The loss in surface area and pore volume of metal exchanged zeolites on encapsulating dmg complexes is given in Table III. 6 and is shown graphically in Figure III. 10 and III. 11 respectively.

Since the zeolite framework structure is not affected by encapsulation as shown by the XRD patterns, the lowering of surface area and pore volume can be attributed to the filling of zeolite pores with metal complexes ²⁵. This observation provides strong evidence for the encapsulation of metal complexes in zeolite pores. Such pronounced lowering of surface area has been reported on encapsulating phthalocyanine and salen complexes ^{16,27}.

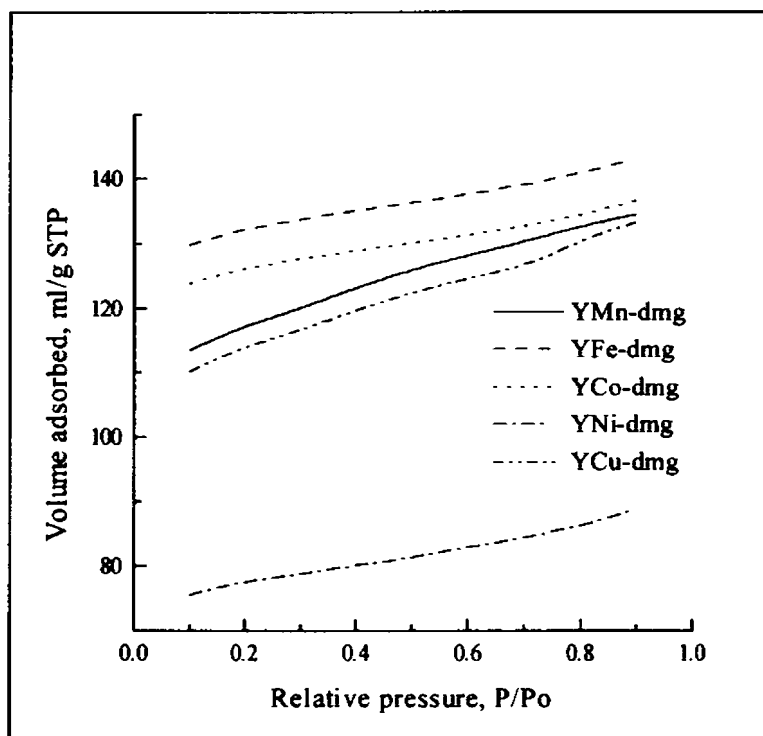


Figure III. 9
Nitrogen adsorption isotherms

Table III. 6

Surface area and pore volume data

Sample	Surface area (m^2/g)			Pore volume (ml/g)		
	MY	YM- dmg	% Loss	MY	YM- dmg	% Loss
YMn-dmg	531	354	33.3	0.2961	0.2292	22.6
YFe-dmg	540	393	27.2	0.3011	0.2436	19.1
YCo-dmg	532	375	29.5	0.2966	0.2321	21.7
YNi-dmg	528	232	56.1	0.2944	0.1436	51.2
YCu-dmg	534	344	35.6	0.2978	0.2235	24.9

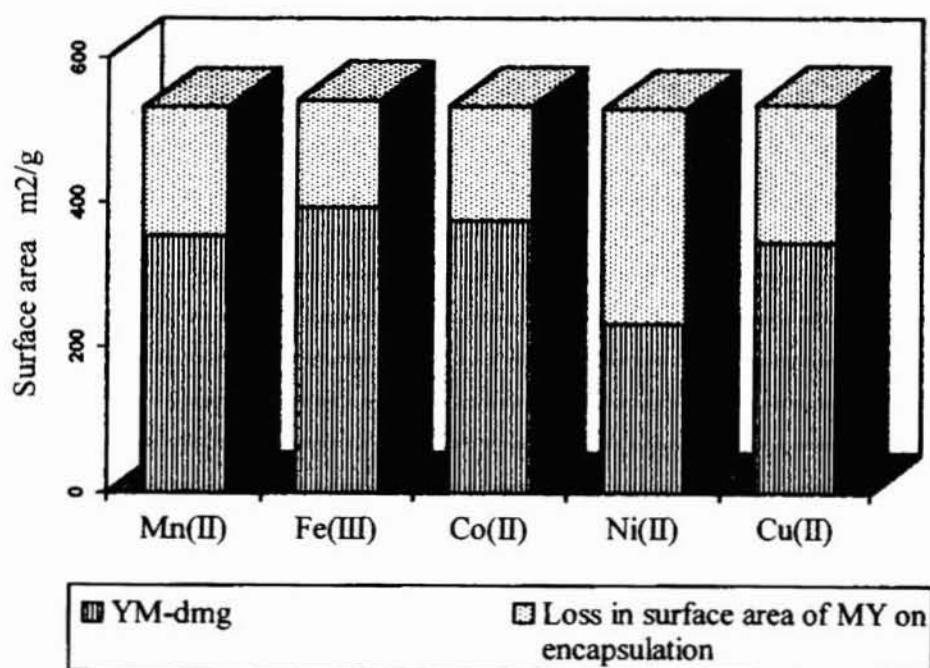


Figure III. 10

Decrease of surface area of metal exchanged zeolites on encapsulation

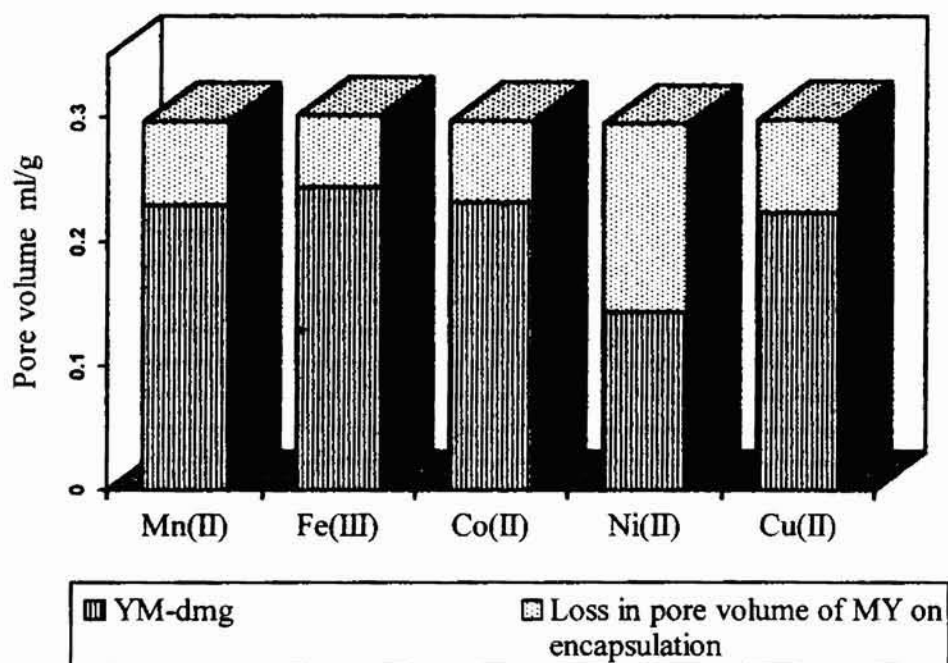


Figure III. 11

Decrease of pore volume of metal exchanged zeolites on encapsulation

3.3.2.5 Magnetic moment

The magnetic moments of zeolite complexes were measured using room temperature Guoy method. The determination of magnetic moment of encapsulated complexes is usually complicated by the high diamagnetic contribution of zeolite support and paramagnetic contribution from the traces of iron present in the zeolite lattice as impurity. However, the susceptibility of NaY zeolite was measured and its contribution for the magnetic moment of the encapsulated complex per mole of metal ion was calculated. The diamagnetic contribution of the ligand molecules present in the complex was also considered. This method is expected to give a qualitative idea about the magnetic behaviour of encapsulated complexes.

Room temperature magnetic moments of zeolite dmg complexes are given in Table III. 7. Magnetic moment of YMn-dmg is 5.82 BM which is very close to spin only value of 5.92 BM. High spin Mn(II) complexes are reported to exhibit magnetic moments

close to spin only value irrespective of their coordination in octahedral or tetrahedral fields, or geometries of lower symmetry. In the case of YFe-dmg, a magnetic moment of 5.92 BM was observed. Fe(III) complexes are known to possess magnetic moments in the range 5.7-6.0 BM irrespective of the coordination geometry^{28, 29}. Hence, it is difficult to assign geometries for Mn(II) or Fe(III) complexes on the basis of magnetic moment alone.

Table III. 7
Magnetic moment data

Sample	Magnetic moment (BM)
YMn-dmg	5.82
YFe-dmg	5.92
YCo-dmg	5.25
YNi-dmg	2.19
YCu-dmg	1.86

Usually, octahedral Co(II) complexes have magnetic moments in the range 4.8-5.2 BM which is higher than spin only value of 3.89 BM due to the large orbital contribution to magnetic moment^{28, 29}. Magnetic moment of 5.25 BM observed for YCo-dmg indicates the possibility of an octahedral symmetry for the encapsulated complex.

Ni(II) octahedral complexes have usually magnetic moments in the range 2.9-3.3 BM whereas higher magnetic moments in the range 3.2-4.1 BM are reported for tetrahedral complexes²⁹. A lower magnetic moment of encapsulated Ni-dmg complex i.e. 2.19 BM rejects the possibility of octahedral and tetrahedral coordination. In addition, this value is lower than that expected for two unpaired electrons in a high spin d^8 square planar complex. Furthermore, high spin square planar Ni(II) complexes are rarely found due to the large separation of $d_{x^2-y^2}$ and d_{xy} orbitals, which leads to spin pairing and consequent diamagnetism. But, the partial paramagnetism of encapsulated

Ni-dmg complex rejects the probability of a low spin square planar structure ²⁹. However, a decrease in the effective ligand field or a slight distortion from the strict square planar structure can reduce the energy difference between the singlet and triplet state, so that, ΔE will be comparable to thermal energy, kT ³⁰. The decreased singlet-triplet separation may give rise to partial paramagnetism for Ni(II) distorted square planar complexes ³¹. Therefore, a distorted square planar geometry could be assigned to encapsulated Ni-dmg complex to explain the observed magnetic moment. The structure of free Ni-dmg complex has been known to be strictly square planar. The distortion observed could be attributed to the interactions of zeolite framework on the encapsulated complex.

A magnetic moment of 1.86 BM was observed for YCu-dmg. Usually, magnetic moments of Cu complexes are in the range 1.75-2.2 BM ²⁹. It is not possible to assign stereochemical structures for Cu complexes on the basis of magnetic moment alone. However, square planar Cu complexes usually show magnetic moments near the lower limit, whereas the value increases with increase in distortion from planar structure. Therefore, a tetrahedrally distorted square planar geometry could be assigned to the encapsulated Cu(II) complex on the basis of its magnetic moment.

3.3.2.6 Electronic spectra

Electronic spectral measurement in the absorbance mode is not recommended for zeolite complexes as the radiations scattered by zeolite interfere with absorptions due to electronic transitions. Therefore, optical reflectance spectra of the complexes were recorded as a plot of percentage reflectance versus wavelength. Kubelka-Munk (KM) analysis ³² was performed on the reflectance data as explained in Chapter II. A plot of KM factor, $F(R)$, against wavelength is shown in Figure III. 12.

Generally, the intensity of absorption bands is low as a result of low metal ion concentration in zeolite. The ligand absorptions and charge transfer transitions may further complicate the interpretation of electronic spectra. The bands near 1950 nm

(5128 cm^{-1}) and 1450 nm (6896 cm^{-1}) were observed in the spectra of all zeolite samples. These bands can be attributed to overtones $2\nu_1$ and $2\nu_3$ and to the combinations $\nu_1 + \nu_2$ and $\nu_3 + \nu_2$ of the stretching and bending vibrations of water molecules³³. These vibrations have given broad bands at 3100-3500 cm^{-1} (ν_3 & ν_1) and near 1650 cm^{-1} (ν_2) in the IR spectra of all the zeolite samples.

The electronic spectral data of encapsulated complexes and their tentative assignments are given in Table III. 8. In the case of high spin complexes of Mn(II) ion (d^5 system), electronic transitions are both spin and orbitally forbidden as it involve pairing of electrons. Therefore, no characteristic d-d bands were observed in the electronic spectra. However, forbidden bands of much lower intensity may appear due to weak spin-orbit coupling. But, these bands were not observed in the case of YMn-dmg, probably due to interferences from charge transfer bands³⁴.

In the case of high spin Fe(III) complexes (d^5 system), all excited states have spin multiplicity different from that of the ground state and therefore no characteristic d-d bands were observed. Because of the greater oxidising power of Fe(III), the intense charge transfer transitions often appear in visible region and obscure very low intensity d-d forbidden bands^{29, 34}. The bands observed at 12410 cm^{-1} and 18250 cm^{-1} in the spectrum of YFe-dmg may be due to spin forbidden d-d transitions in high spin Fe(III) state.

Co(II) complexes (d^7 system) are expected to show three spin allowed transitions in octahedral symmetry. They are: $\nu_1 = {}^4T_{1g}(F) \rightarrow {}^4T_{2g}(F)$, $\nu_2 = {}^4T_{1g}(F) \rightarrow {}^4A_{2g}(F)$ and $\nu_3 = {}^4T_{1g}(F) \rightarrow {}^4T_{1g}(P)$. Usually the band ν_2 is very weak or not observed as it is a two electrons transfer from $t_{2g}^5 e_g^2$ to $t_{2g}^3 e_g^4$ ²⁹. In the case of YCo-dmg, the bands are in agreement with the absorptions reported for octahedral complexes of Co(II) ion. The absorptions at 11910 cm^{-1} and 22570 cm^{-1} may be assigned to the transitions ν_1 and ν_3 , whereas ν_2 is assumed to be too weak to give a band in the spectrum. Furthermore, the absence of a broad intense band in the visible region at $\sim 15000 \text{cm}^{-1}$ with fine splitting, a characteristic of Co(II) ions in tetrahedral geometry³⁴, rejects the possibility of

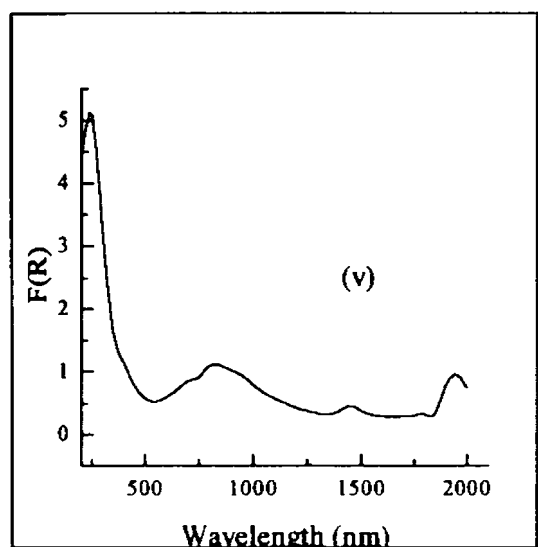
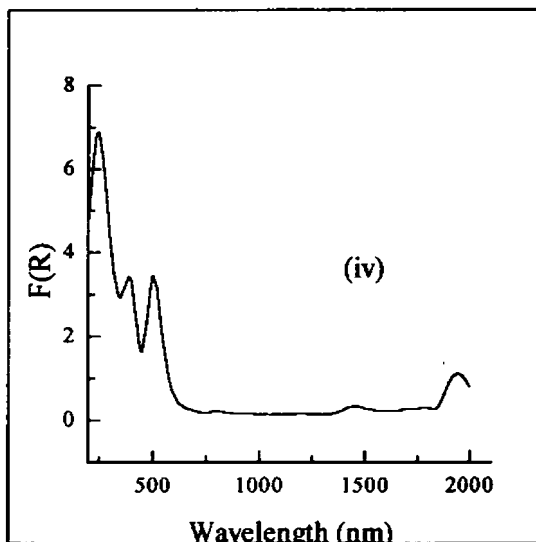
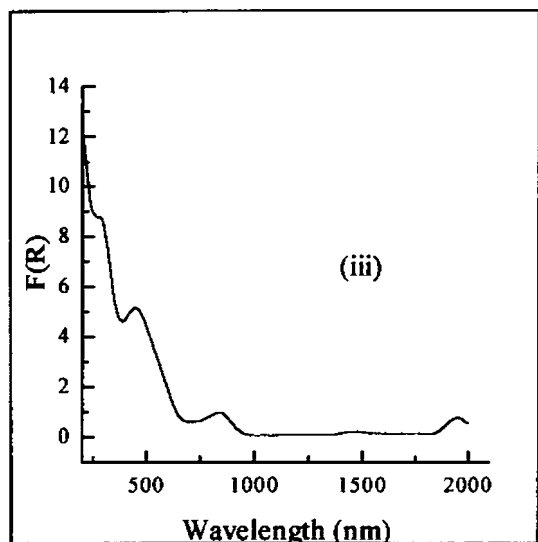
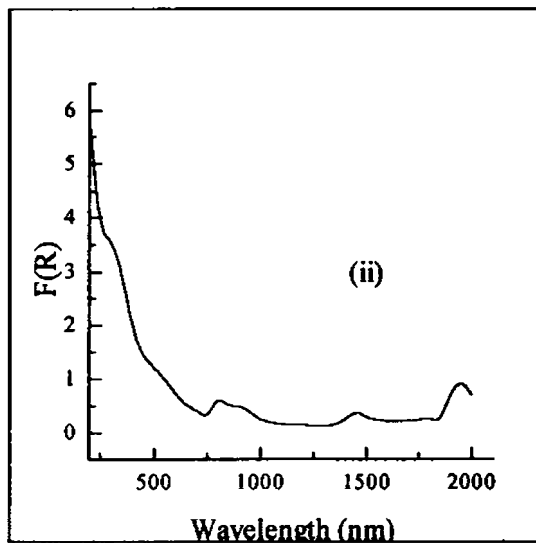
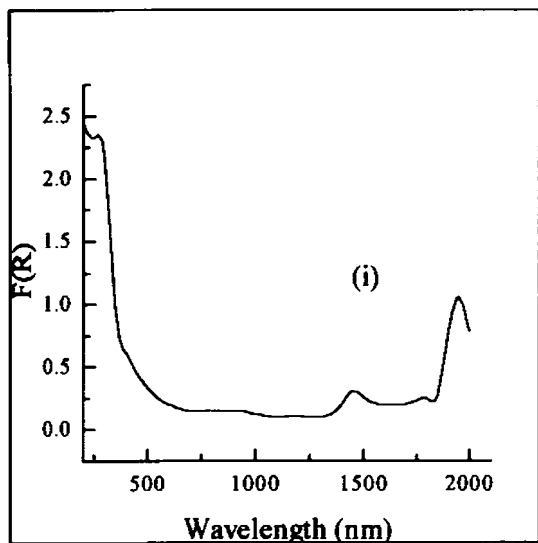


Figure III. 12

Electronic spectra of encapsulated dmg complexes

- (i) YMn-dmg
- (ii) YFe-dmg
- (iii) YCo-dmg
- (iv) YNi-dmg
- (v) YCu-dmg

tetrahedral geometry for the encapsulated complex. Room temperature magnetic moment of 5.25 BM for YCo-dmg also suggests octahedral coordination. The formation of a distorted octahedral complex, $\text{Co}(\text{dmg})_2(\text{O}_{\text{zeolite}})_2$, has been reported on treating Co exchanged X zeolite with dmg¹⁰. In addition, the participation of oxygen atoms at the walls of zeolite cage in coordination has been confirmed by EPR studies on Co-dmg encapsulated in X zeolite⁹. Therefore, in the case of YCo-dmg, zeolite oxygen atoms are likely to participate in the octahedral coordination of Co(II) ion. However, the involvement of water molecules in the coordination sphere of YCo-dmg cannot be fully rejected.

Table III. 8
Electronic spectral data

Sample	Abs. Max. (cm^{-1})	Tentative assignments
YMn-dmg	25250	Charge transfer transition
	37040	Intraligand transition
YFe-dmg	12410	d-d transition
	18250	d-d transition
	37740	Intraligand transition
YCo-dmg	11910	${}^4\text{T}_{1g}(\text{F}) \rightarrow {}^4\text{T}_{2g}(\text{F})$
	22570	${}^4\text{T}_{1g}(\text{F}) \rightarrow {}^4\text{T}_{1g}(\text{P})$
	37310	Intraligand transition
YNi-dmg	18660	d-d transition
	25840	Charge transfer transition
	40000	Intraligand transition
YCu-dmg	12550	d-d transition
	14470	d-d transition
	41320	Intraligand transition

Note: The bands at $\sim 6890 \text{ cm}^{-1}$ and $\sim 5150 \text{ cm}^{-1}$ in the spectra of all samples are characteristic of zeolite lattice and not included in this table

Ni(II) complexes (d^8 system) exhibit three spin allowed transitions in a cubic field. They also tend to form square planar complexes giving a single intense band in the range $18000-25000\text{ cm}^{-1}$ ³⁴. Ni-dmg encapsulated in Y zeolite shows an intense absorption at 18660 cm^{-1} , which is responsible for its reddish colour and indicates square planar geometry. One of the major differences of square planar complexes as compared to cubic geometry is the absence of absorptions below 10000 cm^{-1} ³⁴. Therefore, the possibility of tetrahedral or octahedral geometry for encapsulated Ni-dmg complex could be discarded as no absorption bands are seen below 10000 cm^{-1} . Considering the magnetic moment value of 2.19 BM also, a distorted structure close to square planar geometry may be assigned to encapsulated Ni-dmg complex.

Cu(II) complexes (d^9 system) usually experience large distortions from octahedral symmetry due to Jahn Teller effects giving rise to a number of bands. It is difficult to assign various bands because of the overlapping between them. Most of the Cu(II) complexes give a single broad absorption band in the region $11000-16000\text{ cm}^{-1}$ resulting blue or green colour ²⁹. In the case of encapsulated Cu-dmg, this band is observed at 12550 cm^{-1} with a shoulder at 14470 cm^{-1} . It is difficult to distinguish between a square planar and tetrahedral geometry for Cu(II) complex on the basis of electronic spectra alone. However, the presence of a band at 12550 cm^{-1} with a shoulder at higher energy side hints a square pyramidal configuration ³⁴.

The absorption bands at $\sim 25000\text{ cm}^{-1}$ in the spectra of YMn-dmg and YNi-dmg can be attributed to charge transfer transitions, whereas the bands at $37000 - 41400\text{ cm}^{-1}$ in the spectra of all zeolite complexes are due to intraligand transitions.

3.3.2.7 Infrared spectra

Infrared spectroscopy is a widely used technique to identify the formation of metal complexes in zeolite cavities. IR spectra of dmg and zeolite encapsulated dmg complexes are given in Figure III. 13. A comparison of IR spectral data of MY, dmg ligand and encapsulated metal complexes is presented in Table III. 9. Some of the bands

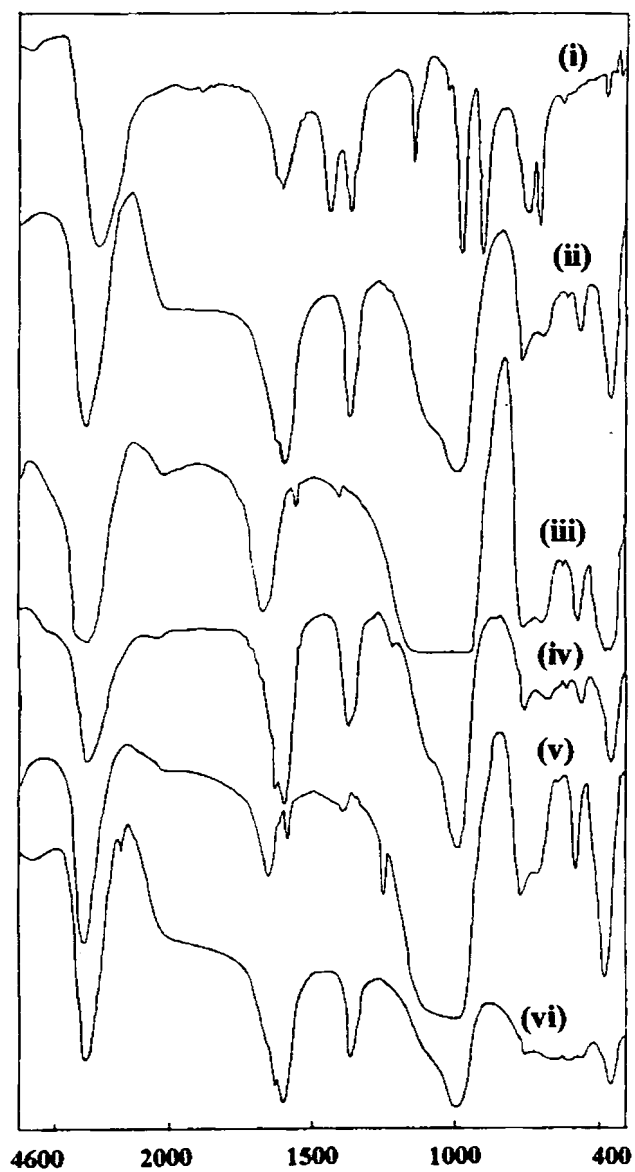


Figure III. 13

IR spectra-(i) dmg, (ii) YMn-dmg, (iii) YFe-dmg, (iv) YCo-dmg,
(v) YNi-dmg and (vi) YCu-dmg

of the coordinated ligand molecules are masked by the strong absorptions of the zeolite support.

From Table III. 9, it is possible to identify the bands due to ligand molecules, which are not interfered by zeolite bands. However, the coordination of metal atoms with dmg in zeolite cavity could be confirmed from the available bands of metal complexes.

Table III. 9

IR spectral data (cm^{-1}) of MY, dmg and zeolite complexes

MY	dmg	YMn-dmg	YFe-dmg	YCo-dmg	YNi-dmg	YCu-dmg
	427					
460	469	463	467	461	465	459
570		567	567	565	569	567
	627	624		619	636	611
680	710	689	691	681		654
750	748	768	758	762	760	764
1000	907	995	903	994		997
	987					
	1144			1221	1240	
	1364	1371	1398	1372	1389	1371
	1443					
	1620	1599	1547	1599	1572	1595
1654		1641	1641	1630	1638	1630
	2820	2832	2887	2816		2812
3453	3250	3570	3544	3554	3475	3551

IR spectra of dmg and its complexes have been studied extensively³⁵. Two bands each have been reported for C=N and N-O vibrations. The existence of two bands may be due to two unequal C=N and N-O linkages. It has also been attributed to the two types of infrared active vibrations of the skeleton of dmg complex with D_{2h} symmetry. In the case of free dmg ligand, the bands which occur at 1443 cm^{-1} and 1620 cm^{-1} are due

to C=N stretching vibrations and those appearing at 987 cm⁻¹ and 1144 cm⁻¹ are due to N-O stretching frequencies.

A new band can be observed at 1599 cm⁻¹ for YMn-dmg, 1547 cm⁻¹ for YFe-dmg, 1599 cm⁻¹ for YCo-dmg, 1572 cm⁻¹ for YNi-dmg and at 1595 cm⁻¹ for YCu-dmg. No band is present at 1550-1600 cm⁻¹ in the spectra of either the ligand or the metal exchanged zeolite. Therefore, this new band observed in the spectra of zeolite complexes at 1550 - 1600 cm⁻¹ can be assigned to C=N stretching vibration. It is clear that $\gamma_{C=N}$ of dmg ligand has shifted to lower frequencies in encapsulated complexes. The lowering of $\gamma_{C=N}$ suggests the coordination of nitrogen atom of dmg ligand to metal.

The N-O stretching vibration (γ_{N-O}) occurs at 1221 cm⁻¹ and 1240 cm⁻¹ in YCo-dmg and YNi-dmg respectively. The $\gamma_{C=N}$ and γ_{N-O} frequencies agree with those reported for its simple complexes³⁶. However, this band does not appear in the spectra of other complexes. The O-H stretching vibration is seen as a broad band at 3250 cm⁻¹ in free dmg ligand. Changes, if any, in this band due to complexation could not be distinguished as it overlaps with γ_{O-H} of water molecules present in zeolite lattice.

3.3.2.8 EPR spectra

EPR spectroscopy is a valuable technique for investigating the coordination environment in zeolite encapsulated transition metal complexes. In the present study, EPR parameters were determined without computer simulation and hence the values may not be accurate. However, these parameters provide a qualitative idea about the nature of coordination in the encapsulated complexes. EPR spectrum of YCu-dmg analysed at liquid nitrogen temperature is shown in Figure III. 14. The EPR parameters, unpaired electron density and magnetic moment were calculated from EPR spectral data as explained in Chapter II. These results are given in Table III. 10.

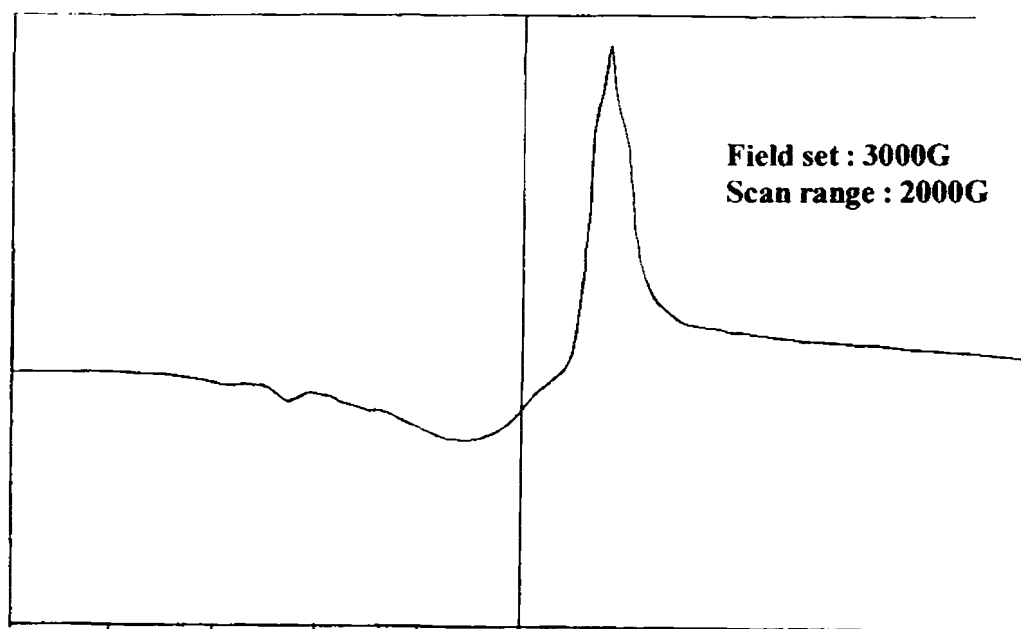


Figure III. 14
EPR spectrum of YCu-dmg

Table III. 10
EPR spectral data of zeolite complexes of dmg

EPR parameter	YCu-dmg
g_{\parallel}	2.32
A_{\parallel}	$157.8 \times 10^{-4} \text{ cm}^{-1}$
g_{\perp} / A_{\perp}	146.7 cm
g_{\perp}	2.04
A_{\perp}	$29.11 \times 10^{-4} \text{ cm}^{-1}$
α^2	0.812
μ_{eff}	1.85 BM

The g_{\parallel} value of YCu-dmg is 2.32, which is higher than that usually reported for Cu complexes. According to Sakaguchi and Addison³⁷, such high value of g_{\parallel} is obtained as result of tetrahedral distortion of square planar complexes. The ratio, $g_{\parallel} / A_{\parallel}$, is also taken as a convenient measure of tetrahedral distortion from square planar geometry. This ratio is reported to be in the range 105-135 cm for square planar complexes, whereas it increases as the distortion increases. A flattened tetrahedral structure is expected for $g_{\parallel} / A_{\parallel}$ values in the range 150-160 cm³⁸⁻⁴⁰. In the case of YCu-dmg, the $g_{\parallel} / A_{\parallel}$ ratio as found to be 146.7 cm which is close to the values for flattened tetrahedral structure. Based on these EPR parameters a tetrahedrally distorted square planar structure may be assigned for encapsulated Cu-dmg. The observed distortion may be due to the interactions of zeolite framework on encapsulated complex. This observation is in agreement with inferences from magnetic moment and electronic spectra of YCu-dmg.

The density of unpaired electrons at the metal atom and magnetic moment were computed from EPR parameters using expressions given in Chapter II. The α^2 value of YCu-dmg was computed as 0.81, which indicates an ionic environment for Cu²⁺ ions. μ_{eff} of YCu-dmg was found to be 1.85 BM which is in agreement with the value obtained from room temperature magnetic susceptibility measurement (1.86 BM) by Gouy method²⁹.

3. 3. 2. 9 Thermal analysis

Thermal analysis is useful for the decomposition studies of metal complexes. The stability of complexes is believed to be enhanced on heterogenizing them, especially by encapsulating in zeolite pores⁴¹. The decomposition pattern of zeolite complexes is influenced by many procedural variables such as the physical state and particle size of the sample, nature of static or dynamic atmosphere, heating rate etc. Therefore, the analysis of zeolite complexes and metal exchanged zeolites was performed at identical conditions. The TG/DTG data may provide the temperature range of stability, the

decomposition temperature range and the decomposition peak temperature. Changes in the TG pattern as compared to that of metal exchanged zeolite hint the encapsulation of complexes.

TG/DTG curves of zeolite complexes of dmg were recorded in an atmosphere of air from ambient to 550 °C at a heating rate of 10 °C/minute. These curves are shown in Figure III. 15. The curves show that most of the intrazeolite free water molecules are released in the temperature range 60 °C to 220-250 °C. The absence of well defined patterns for the removal of the ligand moisties is because of the low amount of metal complexes present in the lattice. Due to the same reason, a correlation of mass loss with expelled ligand moisties was not attempted in this study. However, an approximate temperature of decomposition could be ascertained from the curves, which provide a qualitative idea about the decomposition of complexes. The IR spectra of the residue obtained after analysis have indicated that the encapsulated complexes are completely decomposed.

Weight losses are observed in two stages except in the case of YCu-dmg and YFe-dmg. The single stage weight loss in these two samples can be attributed to the simultaneous removal of water and the decomposition of encapsulated complex. The temperature range for each stage and respective percentage weight loss are given in Table III. 11.

The TG/DTG data show that the dmg complexes decompose in the range 250-410 °C. The thermal stability of the complexes varies in the order YNi-dmg > YMn-dmg > YCo-dmg > YFe-dmg ~ YCu-dmg. The decomposition temperature of encapsulated Co-dmg is close to that reported for the simple complex⁴². Therefore, the thermal stability of Co-dmg is not increased on encapsulating in Y zeolite.

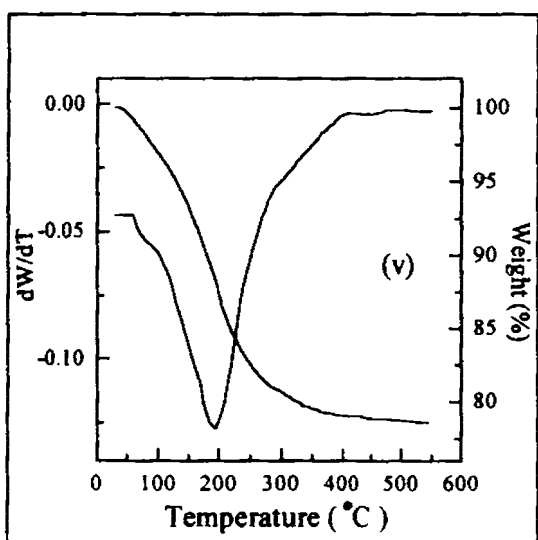
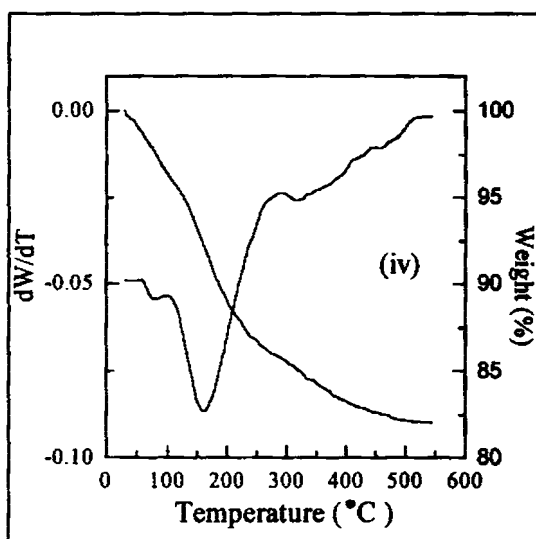
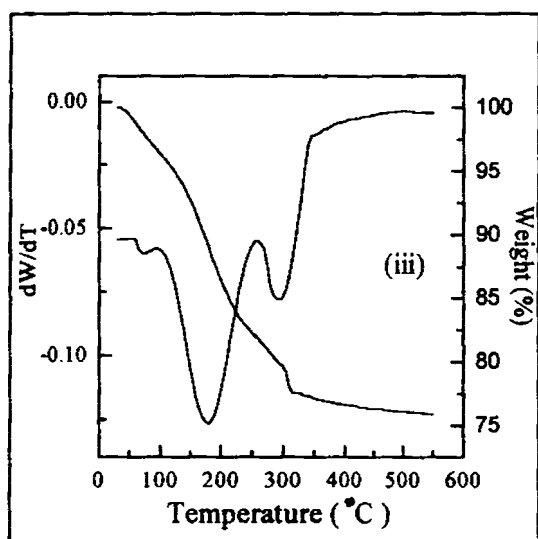
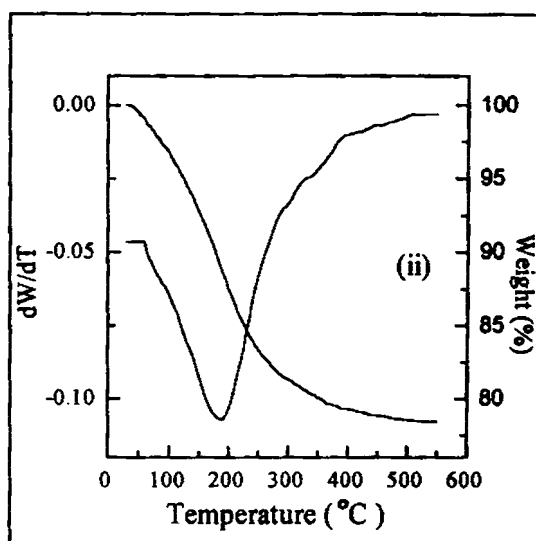
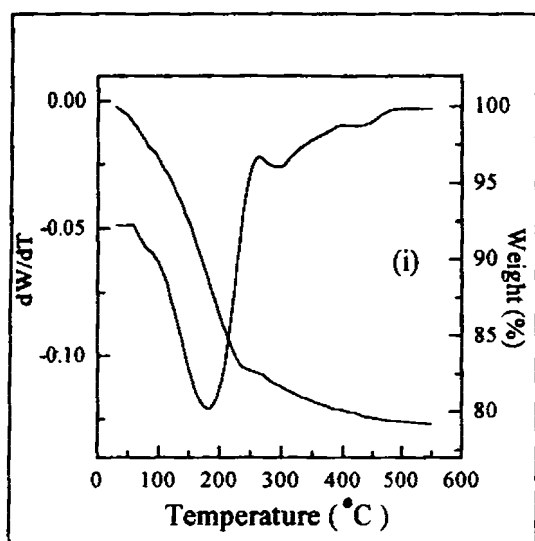


Figure III. 15

TG/DTG curves of encapsulated dmg complexes

- (i) YMn-dmg
- (ii) YFe-dmg
- (iii) YCo-dmg
- (iv) YNi-dmg
- (v) YCu-dmg

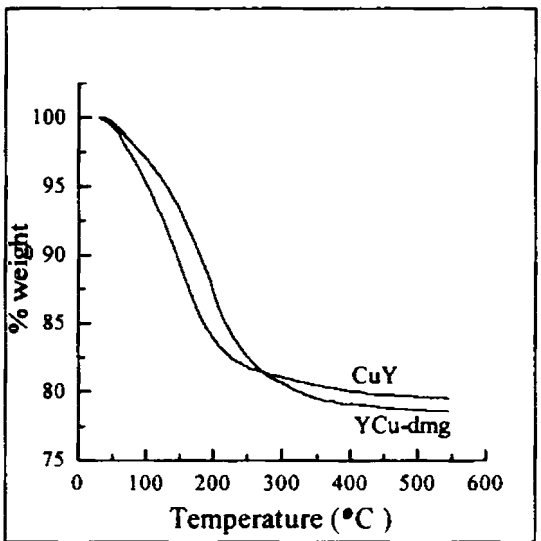
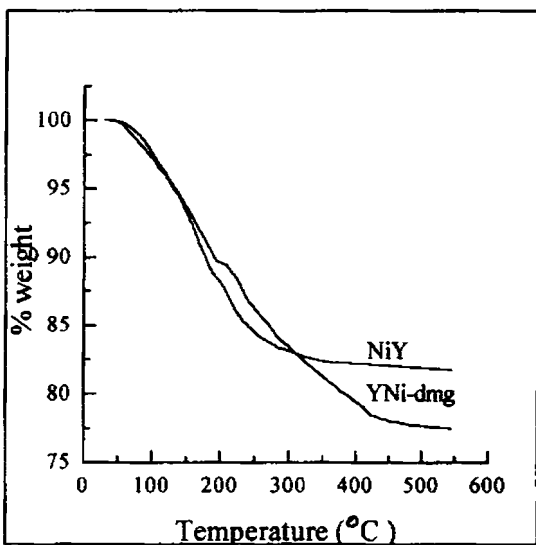
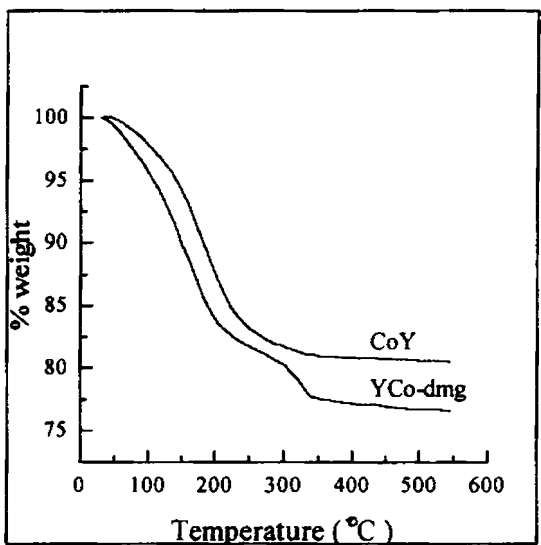
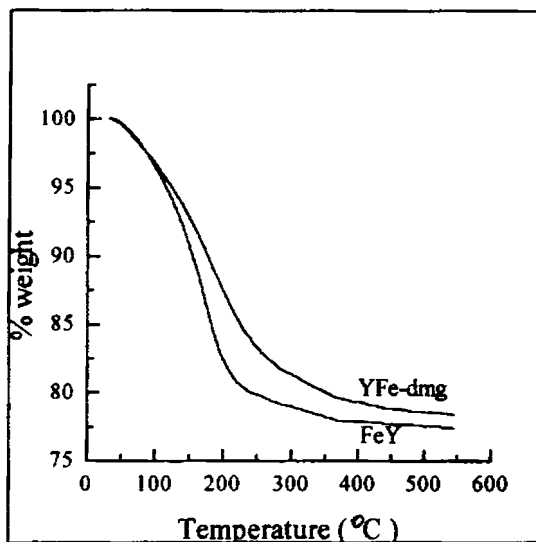
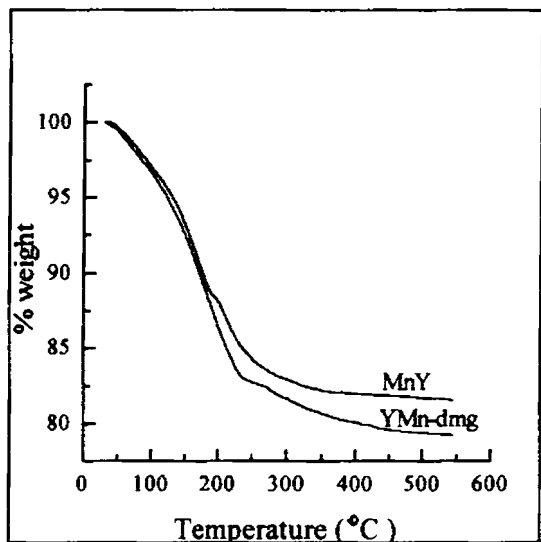


Figure III. 16

TG curves of zeolite complexes and metal exchanged zeolites



Table III. 11
TG/DTG data

Sample	Weight loss-Stage I			Weight loss-Stage II		
	Temp. range (°C)	Peak temp. (°C)	% Mass loss	Temp. range (°C)	Peak temp. (°C)	% Mass loss
YMn-dmg	60-240	185	16.2	265-350	300	1.9
YFe-dmg	60-250	190	15.5			
YCo-dmg	60-240	175	16.0	255-340	290	4.8
YNi-dmg	60-240	165	12.6	285-410	345	5.4
YCu-dmg	60-245	195	15.5			

A comparison of TG curves of zeolite dmg complexes with that of corresponding metal exchanged zeolite is shown in Figure III. 16. The difference in the pattern of TG curve of zeolite complexes as compared to metal exchanged zeolite indicates the decomposition of encapsulated dmg complexes. This observation could be considered as an evidence for the encapsulation of complexes

3. 4 SUMMARY AND CONCLUSION

Zeolite encapsulated Mn(II), Fe(III), Co(II), Ni(II) and Cu(II) complexes of dimethylglyoxime have been synthesized and characterized with a view to study the chemical and physical properties, the coordination geometry and thermal stability of the complexes. The unit cell formula of NaY zeolite used for the present study was found to be $Na_{56} [(AlO_2)_{56} (SiO_2)_{136}] xH_2O$. The crystalline structure of the parent HY zeolite could be almost retained on ion exchange by using a metal salt solution of low concentration and pH ~ 4.0-4.5. Retention of zeolite structure was also observed in the case of encapsulated complexes by XRD analysis. The complete removal of surface complexes as observed in the SEM could be achieved by the purification procedure employed in this study. The lower surface area and pore volume of zeolite complexes as compared to metal exchanged zeolites suggest encapsulation of

complexes. On the basis of magnetic moment, electronic spectra and EPR of Cu(II) complex, the following geometries were tentatively assigned for encapsulated complexes: octahedral for YCo-dmg, distorted square planar for YNi-dmg and tetrahedrally distorted square planar for YCu-dmg. However, the structure of Mn(II) and Fe(III) complexes could not be ascertained from the available data. The coordination of metal ions with dimethylglyoxime was clearly observed in the IR spectra. The thermal stability of the complexes varies more or less in the order YNi-dmg > YMn-dmg > YCo-dmg > YFe-dmg ~ YCu-dmg. TG patterns of zeolite complexes are quite different from those of metal exchanged zeolites indicating the encapsulation of complexes.

REFERENCES

1. G. N. Schrauzer, *Acc. Chem. Res.*, 97 (1968) 1
2. H. Eckert, G. N. Schrauzer and I Ugi, *Tetrahedron*, 31 (1975) 1399
3. G. N. Schnauzer and L. P. Lee, *J. Am. Chem. Soc.*, 92, 6 (1970) 1551
4. S. Nemeth, Z. Szeverenvi and L. I. Simandi, *Inorg. Chim. Acta.*, 44 (1980) L 107
5. S. Nemeth and L. I. Simandi, *J. Mol. Catal.*, 14 (1982) 87
6. R. F. Howe and J. H. Lunsford, *J. Am. Chem. Soc.*, 97 (1975) 5156
7. R. F. Howe and J. H. Lunsford, *J. Phys. Chem. Soc.*, 79 (1975) 1836
8. R. A. Schoonheydt and J. Pelgrims, *J. Chem. Soc., Dalton Trans.*, (1981) 914
9. C. J. Winscom and W. Lubitz, *Stud. Surf. Sci. and Catal.*, 12 (1982) 15
10. H. Diegruber and P. J. Plath, *Stud. Surf. Sci. and Catal.*, 12 (1982) 23
11. V. Yu Zakharov, O. M. Zakharova, B. V. Romanowski and R. E. Mardaleishvili, *React. Kinet. Catal. Lett.*, 6 (1977) 133
12. H. Diegruber, P. J. Plath and G. Schulz-Ekloff, *J. Mol. Catal.*, 24 (1984) 115
13. C. Tollman and H. Herron, *Symposium on Hydroc. Oxidation*, 194th National Meeting of the American Chemical Society, New Orleans, LA, Aug. 30 - Sept. 4 (1987)
14. P. G. Menon, " *Lectures on Catalysis* ", 41st Ann. Meeting, Ind. Acad. Sci., S. Ramasheshan (Ed.); 1975
15. N. Herron, G. D. Stucky and C. A. Tolman, *J. Chem. Soc., Chem. Commun.*, (1986) 1521
16. E. Paez-Mozo, N. Gabriunas, F. Lucaccioni, D. D. Acosta, P. Patrono, A. La Ginestra, P. Ruiz and B. Delmon, *J. Phys. Chem.*, 97 (1993) 12819
17. H. Van Koningsveld, J. C. Jansen and H. Van Bekkum, *Zeolites*, 10 (1990) 235
18. N. Herron, *J. Coord. Chem.*, 19 (1988) 25
19. Bindhu Jacob, " PhD Thesis ", Cochin University of Science and Technology, 1998
20. J. Strutz, H. Diegruber, N. I. Jaeger and R. Moseler, *Zeolites*, 3 (1983) 102
21. K. Mizuno and J. H. Lunsford, *Inorg. Chem.*, 22 (1983) 3483
22. S. Enrist, Y. Traa and O. Deeg, *Stud. Surf. Sci. and Catal.*, 84B (1994) 925
23. J. M. Thomas and C. R. A. Catlow, *Progr. Inorg. Chem.*, 35 (1988) 1
24. R. Raja and P. Ratnasamy, *J. Catal.*, 170 (1997) 244
25. K. J. Balkus Jr and A. G. Gabrielov, *J. Inclusion Phenom. Mol. Recogn. Chem.*, 21 (1995) 159
26. S. P. Varkey and C. R. Jacob, *Ind. J. Chem.*, 37A (1998) 407
27. A. K. Mukherjee and P. Ray, *J. Ind. Chem. Soc.*, 32 (1955) 581
28. A. Earnshaw, " *Introduction to Magnetochemistry* ", Academic Press, London, 1968

28. A. Earnshaw, " *Introduction to Magnetochemistry* ", Academic Press, London, 1968
29. N. N. Greenwood and A. Earnshaw, " *Chemistry of the Elements* ", Pergamon Press, 1984
30. G. Maki, *J. Chem. Phys.*, 28 (1958) 651
31. G. Maki, *J. Chem. Phys.*, 9 (1958) 169
32. S. K. Tiwary and S. Vasudevan, *Inorg. Chem.*, 37 (1998) 5239
33. K. Klier, R. Kellerman and P. J. Hutta, *J. Chem. Phys.*, 61 (1974) 4224
34. A. B. P. Lever , " *Inorganic Electronic Spectroscopy* ", Elsevier, Amsterdam, 1968
35. E. S. Shpiro, G. V. Antoshin, O. P. Tkachenko, S. V. Gudkov, B. V. Romanovsky and Kh. M. Minachev, *Stud. Surf. Sci. and Catal.*, 18 (1984) 31
36. P. S. E. Dai and J. H. Lunsford, *Inorg. Chem.*, 19 (1980) 262
37. U. Sakaguchi and A. W. Addison, *J. Chem. Soc., Dalton Trans.*, (1979) 600
38. R. A. Palmer, W. C. Tennant, M. F. Dix and A. D. Rae, *J. Chem. Soc., Dalton Trans.*, (1976) 2345
39. H. J. Stoklosa, G. L. Seebach and J. R. Wasson, *J. Phys. Chem.*, 78 (1974) 962
40. H. Yokoi, *Bull. Chem. Soc. Jpn.*, 47 (1974) 3037
41. H. Diegruber, P. J. Plath, G. Schulz-Ekloff, M. Mohl, *J. Mol. Catal.*, 24 (1984) 115
42. K. Brown, G. Jang, R. Segel and K. Rajeshwar, *Inorg. Chim. Acta.*, 128 (1987) 197

CHAPTER IV

STUDIES ON Y ZEOLITE ENCAPSULATED TRANSITION METAL COMPLEXES OF 3-FORMYLSALICYLIC ACID

Abstract

Y Zeolite encapsulated Mn(II), Fe(III), Co(II), Ni(II) and Cu(II) complexes of 3-formylsalicylic acid have been synthesized and characterized. Chemical analysis of the encapsulated complexes indicates a composition that almost corresponds to a binuclear structure. XRD pattern, surface area and pore volume data suggest the encapsulation of complexes without affecting the crystalline structure of the zeolite. Magnetic moments and electronic spectral data explain the geometry of complexes and also hint binuclear structure as reported for free complexes. EPR of Cu(II) complex provides an idea about the distortion of square planar geometry. The coordination of metal ion with ligands in zeolite pores was confirmed by IR spectra. Thermal stability of encapsulated complexes was studied by TG/DTG analysis.

4. 1 INTRODUCTION

The interest in the chemistry of binuclear metal complexes is due to their ability to model metalloenzymes containing two metal ions at their active sites¹. Binuclear Cu(II) and Ni(II) complexes of 3-formylsalicylic acid and its Schiff bases with diamines have been studied. Considering the analytical and spectral data, these complexes are believed to possess a structure (Figure IV. 1) involving an oxygen bridge to link the metal ions^{2,3}. Hetero-metal binuclear complexes of these ligands are also interesting as it can simulate the properties of enzymes like superoxide dismutase⁴ and cytochrome oxidase⁵ containing two types of metal ions.

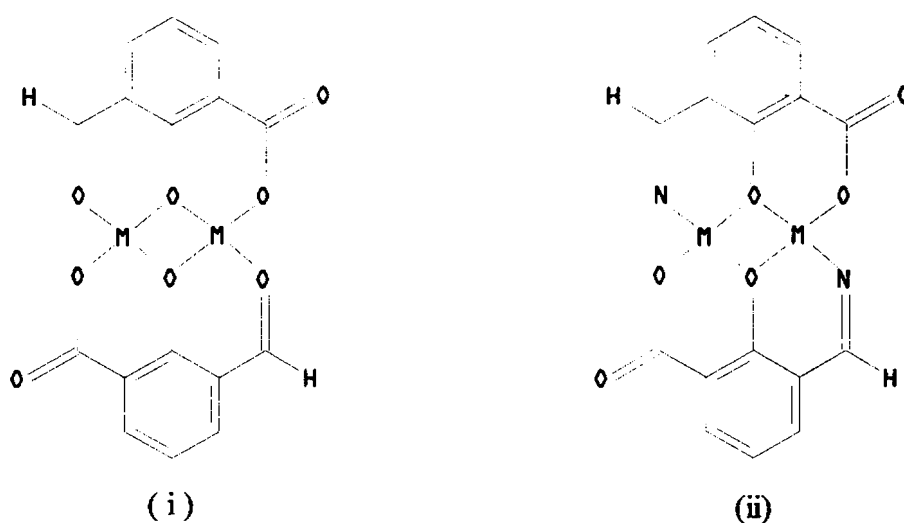


Figure IV. 1

Binuclear structure of complexes of 3-formylsalicylic acid (i) and its Schiff base (ii)

Several electrochemical studies have been carried out on Cu(II) complexes of 3-formylsalicylic acid to understand the redox behaviour of binuclear copper proteins^{6,7}. Electrochemical studies of hetero-metal complexes of 3-formylsalicylic acid have also been reported. However, such studies are only a few in numbers because of the difficulty in preparation and poor stability in solvents⁸.

The hetero-metal binuclear complexes are useful to study the interactions between different metal atoms. Such interactions are likely to occur in catalytic materials containing these metallic sites as reaction centers. For example, transition metal-lanthanide binuclear complex with Schiff base of 3-formylsalicylic acid has been studied with a view to augur the role of lanthanide in mixed oxide catalysts like perovskites⁹.

The complexes of 3-formylsalicylic acid are expected to mimic the catalysis of binuclear metalloenzymes. However, better models with respect to activity and stability can be obtained by encapsulating such complexes in zeolites¹⁰. This has prompted us to synthesize encapsulated complexes of 3-formylsalicylic acid (fsal) and evaluate their catalytic activity. In this chapter, details regarding the synthesis and characterization of Y zeolite encapsulated complexes of Mn(II), Fe(III), Co(II), Ni(II) and Cu(II) with 3-formylsalicylic acid are presented.

4. 2 EXPERIMENTAL

4. 2. 1 Materials

Details regarding the synthesis and purification of fsal are provided in Chapter II. Metal exchanged zeolites were also prepared according to the procedure given in Chapter II.

4. 2. 2 Synthesis of zeolite encapsulated fsal complexes

The general procedure employed for encapsulating metal complexes in Y zeolite is described in Chapter II. Metal exchanged zeolite (3.0 g) was treated with fsal (0.62 g for YMn, 0.28 g for YFe, 0.62 g for YCo, 0.64 g for YNi and 0.60 g for YCu) at 125°C for 16 hours. The ligand to metal mole ratio in the reaction mixture was around 2. The product was soxhlet extracted with methanol. The uncomplexed metal ions and protons released from ligand to zeolite during complexation were removed by ion exchange. The purification procedure followed here is similar to that employed in the case of dmg complexes (vide page 69). Zeolite complexes obtained were filtered,

washed to remove chloride ions, dried at 100 °C for 2 hours and stored in vacuum over anhydrous calcium chloride.

4. 2. 3 Analytical methods

Details regarding the analytical methods and other characterization techniques are given in Chapter II.

4. 3 RESULTS AND DISCUSSION

Zeolite Y encapsulated Mn(II), Fe(III), Co(II), Ni(II) and Cu(II) complexes with fsal were synthesized. The characterization techniques used were chemical analysis, XRD, surface area and pore volume, magnetic moment, electronic, FTIR and EPR spectroscopy and TG analysis.

4. 3. 1 Chemical analysis

The results of chemical analysis of zeolite fsal complexes are given in Table IV. 1. The Si/Al ratio of zeolite complexes (2.43) is same as that of metal exchanged zeolites as in the case of dmg complexes (vide page 70). About 40-80 % of metal initially present in metal exchanged zeolite was found to remain in zeolite after complexation and the rest was removed during the final ion exchange with NaCl solution.

Table IV. 1

Analytical data of encapsulated fsal complexes

Sample	% Metal	%Si	%Al	%Na	%C	%H
YMn-fsal	2.08	19.76	7.79	5.66	1.96	0.14
YFe-fsal	1.30	19.82	7.82	6.23	2.16	0.09
YCo-fsal	1.26	18.63	7.38	6.21	1.99	0.17
YNi-fsal	2.30	19.89	7.88	5.30	3.46	0.15
YCu-fsal	2.71	19.43	7.69	5.42	3.60	0.15

The ligand coordinated to metal can be quantified from the analytical data. The empirical formulae of encapsulated fsal complexes are $MnL_{0.94}$, $FeL_{0.97}$, $CoL_{0.97}$, $NiL_{0.92}$ and $CuL_{0.88}$ in YMn -fsal, YFe -fsal, YCo -fsal, YNi -fsal and YCu -fsal respectively. A ligand to metal mole ratio of 1:1 has been reported for unencapsulated complexes of fsal and its Schiff bases^{2,3}. The lower mole ratio in zeolite complexes may be because of the presence of unexchanged metal ions in the lattice. Therefore, a binuclear structure could be assumed for encapsulated fsal complexes on the basis of the analytical data. The oxide anions of zeolite framework might have induced charge neutralisation in the case of $Fe(III)$ complex.

4.3.2 X-ray diffraction pattern

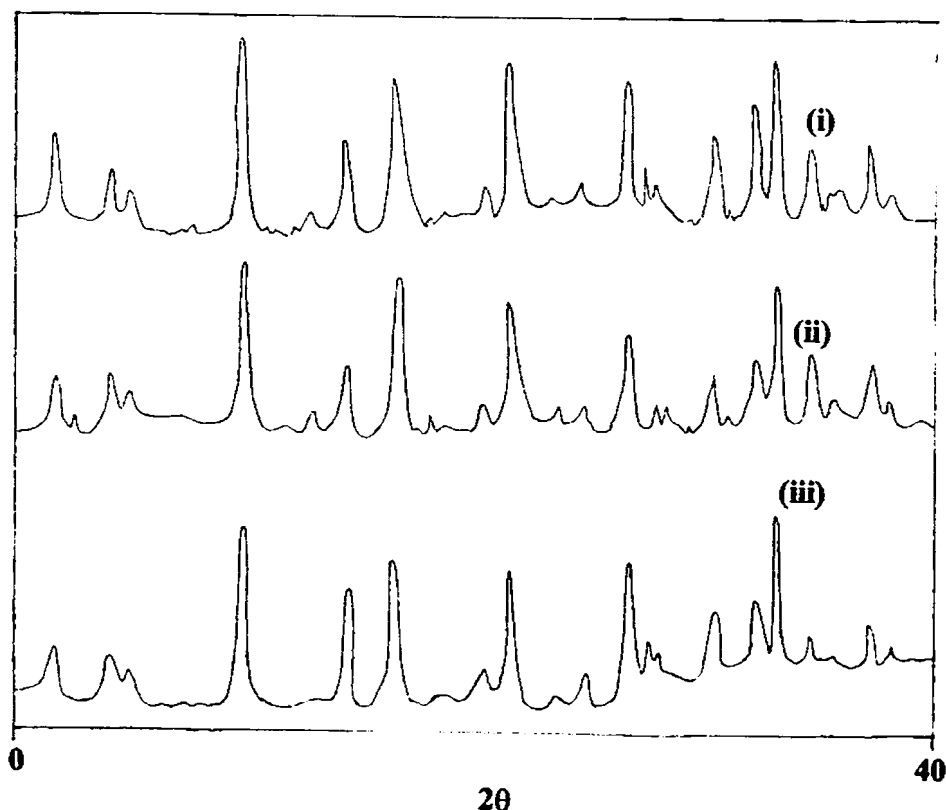


Figure IV. 2

XRD patterns of (i). YMn -fsal, (ii). YCo -fsal and (iii). YCu -fsal

Figure IV. 2 shows the XRD patterns of YMn-fsal and YCo-fsal and YCu-fsal. Crystalline patterns are similar to those shown by metal exchanged zeolites indicating the retention of zeolite structure (vide page 72).

4.3.3 Surface area and pore volume

Table IV. 2

Surface area and pore volume data

Sample	Surface area			Pore volume		
	MY	YM-fsal	% Loss	MY	YM-fsal	% Loss
YMn-fsal	531	415	21.8	0.2961	0.2339	21.0
YFe-fsal	540	367	32.0	0.3011	0.2068	31.3
YCo-fsal	532	320	39.8	0.2966	0.1985	33.1
YNi-fsal	528	273	48.3	0.2944	0.1694	42.5
YCu-fsal	534	313	41.4	0.2978	0.1942	34.8

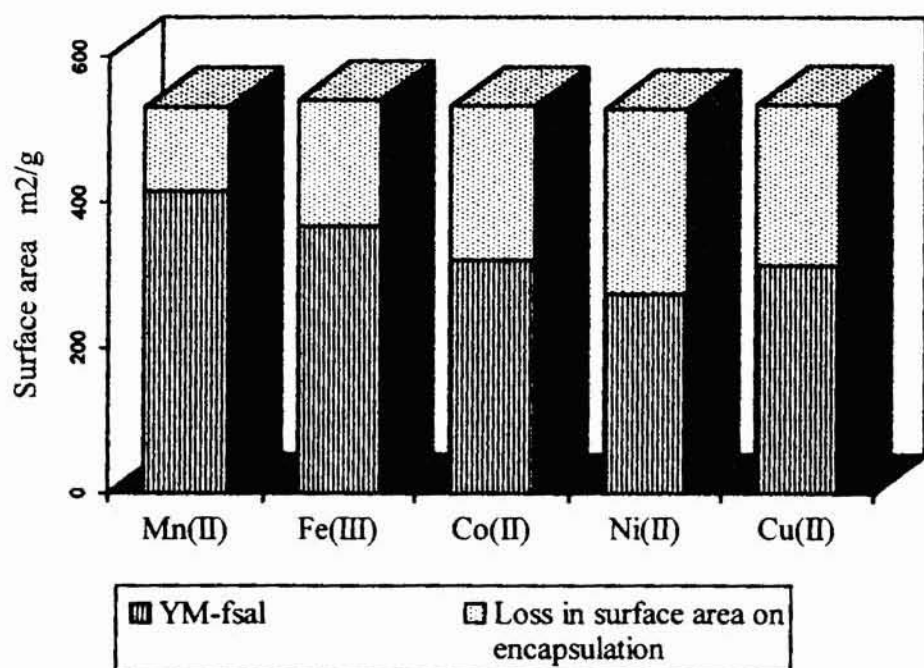


Figure IV. 3

Decrease of surface area of metal exchanged zeolites on encapsulation

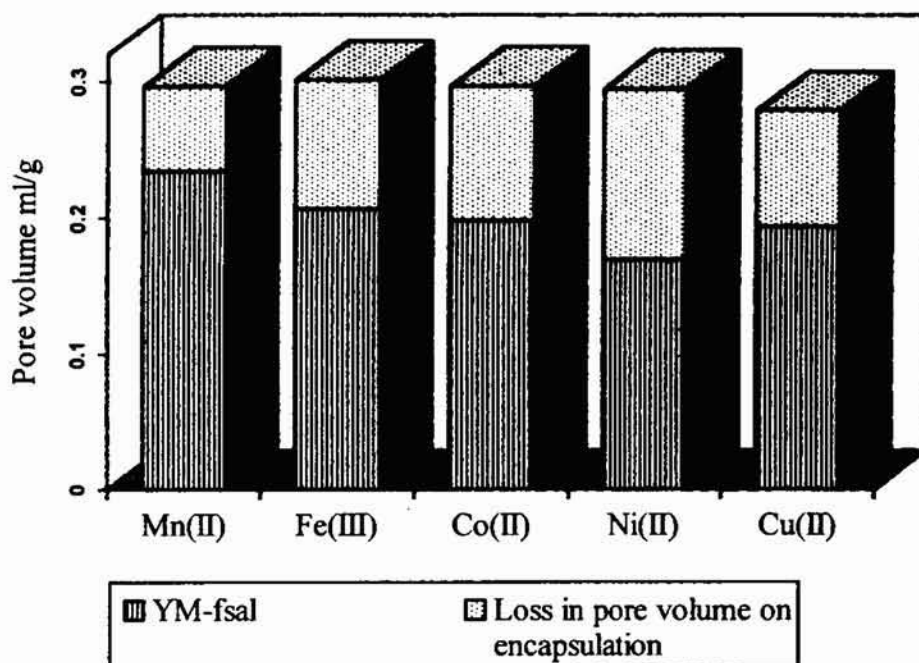


Figure IV. 4

Decrease of pore volume of metal exchanged zeolites on encapsulation

Surface area and pore volume data are given in Table IV. 2 and are also represented in Figure IV. 3 and IV. 4 respectively. The lower surface area and pore volume of zeolite complexes confirm the encapsulation of fsal complexes (vide page 82).

4. 3. 4 Magnetic moment

Table IV. 3

Magnetic moment data

Sample	Magnetic moment (BM)
YMn-fsal	6.00
YFe-fsal	5.78
YCo-fsal	4.60
YNi-fsal	3.40
YCu-fsal	1.82

Room temperature magnetic moments of fsal complexes are given in Table IV. 3. YMn-fsal and YFe-fsal have magnetic moments of 6.0 BM and 5.78 BM respectively. The interpretation of these values is difficult since Mn(II) and Fe(III) complexes exhibit such moments irrespective of their coordination geometry ¹¹. Magnetic moment of 4.6 BM observed for YCo-fsal suggests tetrahedral coordination for which it usually lies in the range 4.4-4.8 BM ¹². Ni(II) octahedral complexes often exhibit magnetic moments in the range 2.9-3.4 BM. Therefore, an octahedral symmetry can be assigned to the encapsulated Ni(II) complex to account for its magnetic moment 3.4 BM ¹². Magnetic moment of YCu-fsal was found to be 1.82 BM. The magnetic moment values of YNi-fsal and YCu-fsal are in accord with those reported for respective unencapsulated binuclear complexes ^{2,3}.

4. 3. 5. Electronic spectra

Kubelka-Munk (KM) factor, $F(R)$, obtained by applying KM analysis on reflectance data is plotted against wavelength as shown in Figure IV. 5. The electronic transitions and their tentative assignments are given in Table IV. 4.

In the case of high spin Mn(II) or Fe(III) complex, d-d transitions are forbidden and as a result , characteristic d-d bands are lacking in their spectra. However, the bands observed for YFe-fsal in the visible region at 12270 cm^{-1} and 19720 cm^{-1} are assignable to forbidden d-d transitions in high spin Fe(III) state ¹³.

Co(II) ions exhibit three d-d transitions in tetrahedral fields. The transition, $\nu_1 = {}^4A_2(F) \rightarrow {}^4T_2(F)$ normally lies below 5000 cm^{-1} and therefore could not be observed with the spectrophotometer used in the present study. The other transitions are $\nu_2 = {}^4A_2(F) \rightarrow {}^4T_1(F)$ and $\nu_3 = {}^4A_2(F) \rightarrow {}^4T_1(P)$, which appear as multiple absorptions in the near infra-red and visible region respectively ¹³. In the case of YCo-fsal, the bands at 15390 cm^{-1} and 19880 cm^{-1} can be assigned to ${}^4A_2(F) \rightarrow {}^4T_1(P)$ transition. This fine structure in the region $15000\text{-}20000\text{ cm}^{-1}$, a characteristic of tetrahedral complex, arises

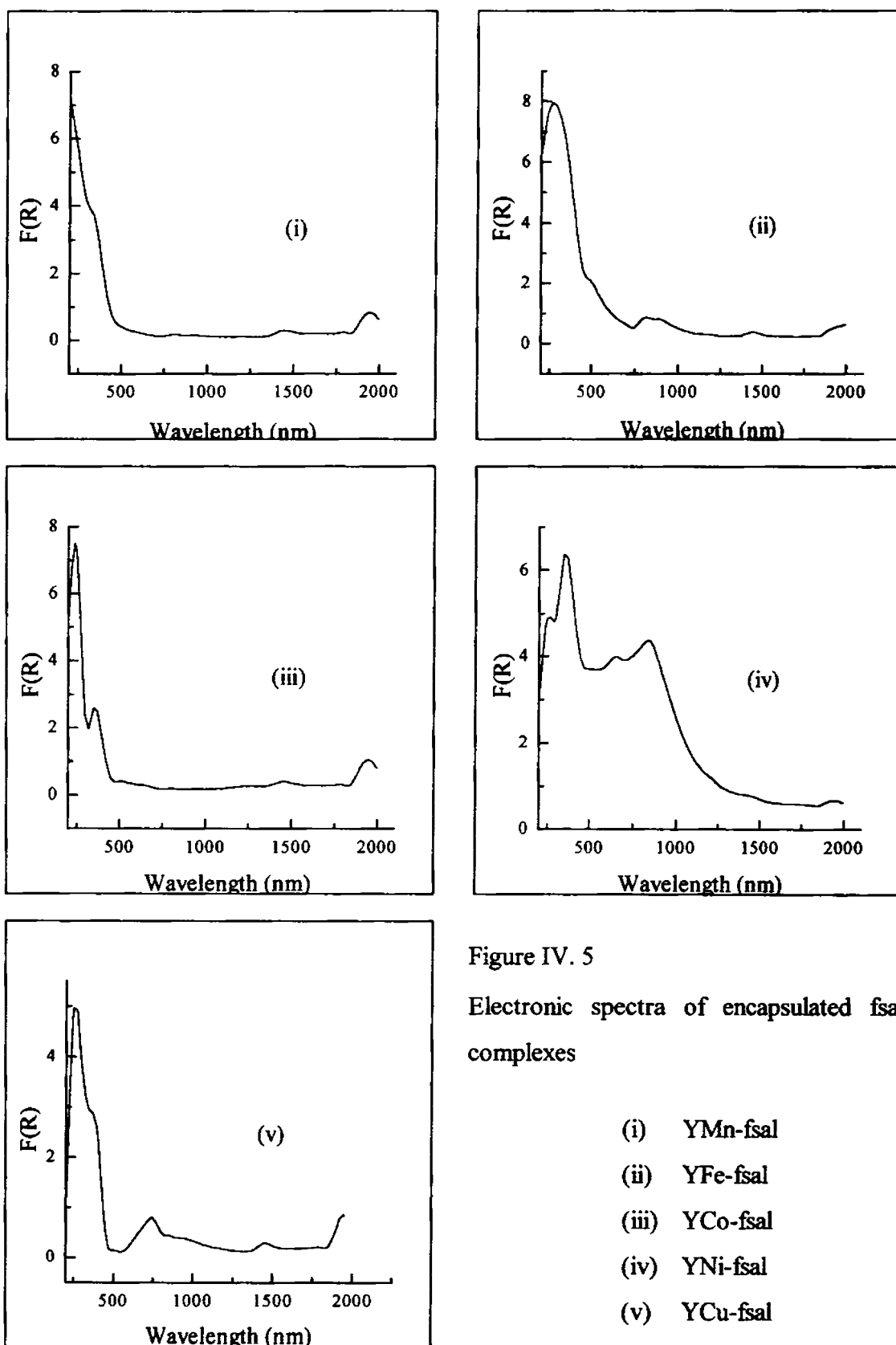


Figure IV. 5

Electronic spectra of encapsulated fsal complexes

- (i) YMn-fsal
- (ii) YFe-fsal
- (iii) YCo-fsal
- (iv) YNi-fsal
- (v) YCu-fsal

Table IV. 4

Electronic spectral data

Sample	Abs. Max. cm ⁻¹	Tentative assignments
YMn-fsal	29590	Charge transfer transition
YFe-fsal	12270	d-d transition
	19720	d-d transition
	37230	Intraligand transition
YCo-fsal	15390	${}^4A_2(F) \rightarrow {}^4T_1(F)$
	19880	
	28090	Charge transfer transition
	41490	Intraligand transition
YNi-fsal	11930	${}^3A_{2g}(F) \rightarrow {}^3T_{2g}(F)$
	15290	${}^3A_{2g}(F) \rightarrow {}^3T_{1g}(F)$
	28090	${}^3A_{2g}(F) \rightarrow {}^3T_{1g}(P)$
	38460	Intraligand transition
YCu-fsal	13510	d-d transition
	26950	Charge transfer transition
	38610	Intraligand transition

Note: The bands at $\sim 6890\text{ cm}^{-1}$ and $\sim 5150\text{ cm}^{-1}$ in the spectra of all samples are characteristic of zeolite lattice and not included in this table

due to spin-orbit coupling of the T-state¹⁴. Similar observation has been reported for other tetrahedral complexes of Co(II) ion¹⁵. The magnetic moment value of 4.6 BM also suggests a tetrahedral symmetry for YCo-dmg.

In the case of YNi-fsal, the d-d transitions at 11930 cm^{-1} , 15290 cm^{-1} and 28090 cm^{-1} agree with those reported for octahedral Ni(II) complexes¹⁴. Magnetic

moment of 3.4 BM observed for encapsulated Ni-fsal complex also hints an octahedral symmetry. Therefore, the bands can be assigned to ${}^3A_{2g}(F) \rightarrow {}^3T_{2g}(F)$, ${}^3A_{2g}(F) \rightarrow {}^3T_{1g}(F)$ and ${}^3A_{2g}(F) \rightarrow {}^3T_{1g}(P)$ transitions of octahedral Ni(II) complex. The axial positions in octahedral symmetry might have occupied by water molecules or oxide ions of zeolite lattice. The reflectance data of YNi-fsal complex are consistent with those reported for the binuclear simple complexes of fsal or its Schiff bases which also possess an octahedral geometry^{2,3}. The close resemblance of magnetic moment and reflectance data of YNi-fsal with those of simple Ni(II)fsal complex indicates the possibility of a binuclear structure for the encapsulated complex.

The electronic spectrum of YCu-fsal shows a broad absorption band at 13510 cm^{-1} due to d-d transition. This band, due to $[CuO_4]^-$ chromophore, lies very close to that of free binuclear Cu-fsal complex (14100 cm^{-1}) reported in earlier studies^{2,3}. This implies that the encapsulated Cu(II) complex exhibits a binuclear structure similar to that of free fsal complexes.

The charge transfer and intraligand transitions are responsible for the bands in the range $26900\text{-}29600\text{ cm}^{-1}$ and $37200\text{-}41500\text{ cm}^{-1}$ respectively.

4.3.6 Infrared spectra

Figure IV. 6 shows the IR spectra of fsal ligand and its complexes encapsulated in Y zeolite. IR bands of metal exchanged zeolite, fsal and encapsulated complexes are presented in Table IV. 5, so that, the ligand bands which are not masked by zeolite bands can be easily identified.

In the case of free fsal, asymmetric CO stretching vibration of carboxyl group occurs at 1609 cm^{-1} . This band is usually observed almost at the same position in the spectra of such ligands containing -COO group¹⁹. In encapsulated fsal complexes, this band disappears and a new band is observed at $1540\text{-}1550\text{ cm}^{-1}$. There are no bands at this position for the free ligand or zeolite. Usually, γ_{CO} mode of carboxyl groups shifts to lower frequency by coordination. Therefore, the band observed at $1540\text{-}1550\text{ cm}^{-1}$ in the

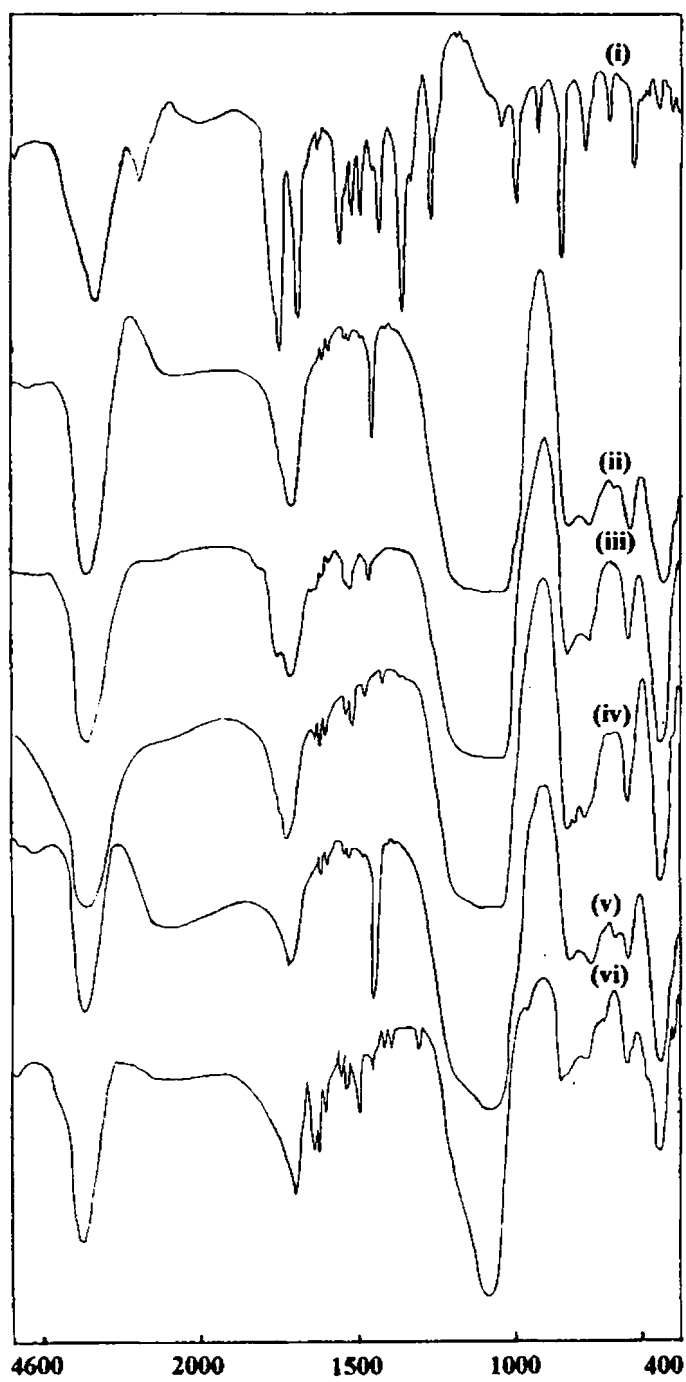


Figure IV. 6

IR spectra-(i) fsal, (ii) YMn-fsal, (iii) YFe-fsal, (iv) YCo-fsal,
(v) YNi-fsal and (vi) YCu-fsal

Table IV. 5

IR spectral data (cm^{-1}) of MY, fsal and zeolite complexes

MY	fsal	YMn-fsal	YFe-fsal	YCo-fsal	YNi-fsal	YCu-fsal
	427					420
460	460	461	461	461	457	461
	491					
570	538	567	567	565	567	567
	617	615			608	
680	695	691	687	700	687	688
750	770	758	760	756	758	774
1000	843	970	976	985	1001	999
	906					
	956					
	1183					
	1248					
	1279					
	1350			1339		1339
	1376	1385	1399	1399	1383	1397
	1408	1412		1437	1417	1418
	1435	1454	1456	1456	1456	1456
	1476	1479			1473	1473
	1541	1522		1522	1524	
				1541		
	1609	1549	1545	1558	1547	1543
1654	1668	1645	1645	1649	1649	1620
	2550					
	2855					
	3197					
3453	3389	3481	3453	3474	3485	3453

spectra of encapsulated fsal complexes can be attributed to coordinated carboxylate group. The unencapsulated binuclear complexes of fsal² and its Schiff bases³ have also showed γ_{CO} at around 1550 cm^{-1} ¹⁷. A binuclear structure could be assumed for zeolite fsal complexes as their γ_{CO} is close to that of binuclear unencapsulated complexes.

The band due to symmetric -COO stretching vibration is at 1406 cm^{-1} in the case of free fsal ligand. This frequency is also often lowered on coordinating the -COO group¹⁶. However, this shift is not clear in encapsulated fsal complexes. The band at 1277 cm^{-1} in observed for free fsal can be assigned to the $\gamma_{\text{C-O}}$ stretching vibration of the phenolic group. This band has been found to shift towards higher frequencies during complexation¹⁶. In the case of YCu-fsal, the band at 1290 cm^{-1} could be assigned to $\gamma_{\text{C-O}}$ of the phenolic group.

The broad band at $\sim 3500 \text{ cm}^{-1}$ is due to O-H stretching of the phenolic groups in fsal ligand. This band is expected to be absent in the spectra of complexes as OH groups are deprotonated for the oxygen atoms to link the metal ions. However, a band exists at this position for encapsulated complexes as a result of $\gamma_{\text{O-H}}$ of water molecules present in their lattice.

4.3.7 EPR spectra

EPR spectrum of YCu-fsal is shown in Figure IV. 7. Table IV. 6 gives EPR parameters and, unpaired electron density and magnetic moment calculated from EPR data. The g_{\parallel} value of YCu-fsal is 2.33 indicating the possibility of a tetrahedrally distorted square planar geometry¹⁸. The ratio, $g_{\parallel}/A_{\parallel}$, is greater than that reported for square planar geometry (105-135 cm) and less than that of flattened tetrahedral Cu(II) ion (150-160 cm). The α^2 value of 0.85 suggests an ionic environment for Cu^{2+} ions. Magnetic moment of YCu-fsal calculated from EPR data agrees with that obtained from magnetic susceptibility measurement (1.82 BM).

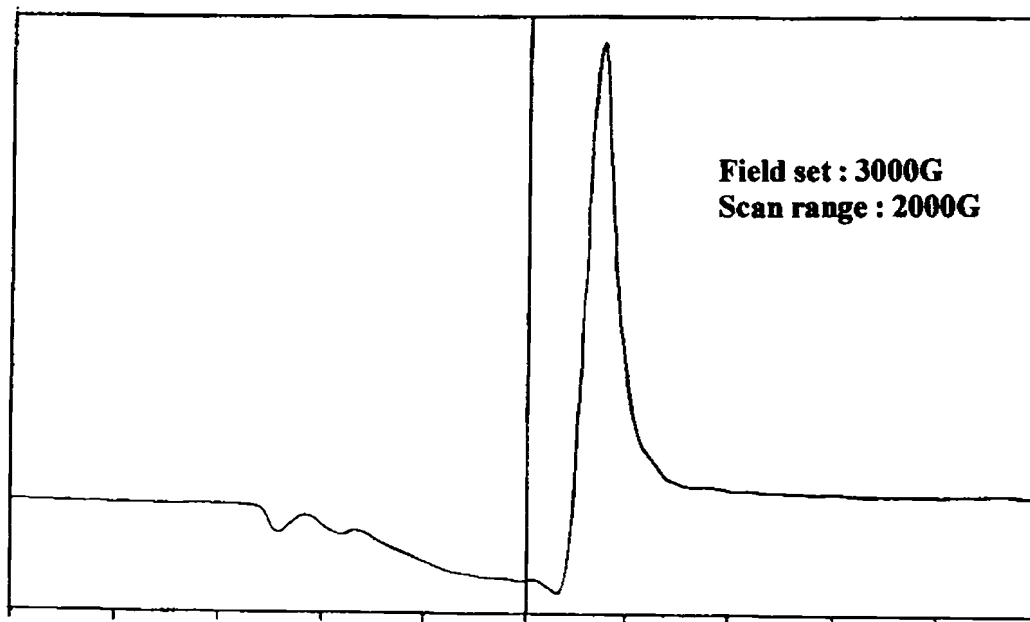


Figure IV.7
EPR spectrum of YCu-fsal

Table IV. 6
EPR spectral data of YCu-fsal

EPR parameter	YCu-fsal
$g_{ }$	2.33
$A_{ }$	$163.32 \times 10^4 \text{ cm}^{-1}$
$g_{ } / A_{ }$	142.8 cm
g_{\perp}	2.05
A_{\perp}	$31.85 \times 10^4 \text{ cm}^{-1}$
α^2	0.85
μ_{eff}	1.86 BM

3.3.8 Thermal analysis

TG/DTG curves recorded for encapsulated fsal complexes are shown in Figure IV. 8. It is generally observed that the major portion of intrazeolite water is removed in the temperature range of 60 °C to 220-250 °C. The weight loss due to the decomposition of encapsulated complex does not appear as a distinct stage in the case of YMn-fsal as it might have occurred simultaneously with the removal of water. In addition, well defined TG patterns are not obtained except for YCo-fsal and YCu-fsal (vide page 96). However, probable decomposition temperatures are identified in these cases. The sample taken out after the analysis in each case was found to be pure metal exchanged zeolite, showing that the encapsulated complex is completely decomposed. The temperature ranges for different stages and respective percentage weight losses are given in Table IV. 7. The thermal stability of the complexes can be approximately graded in the order YCo-fsal ~ YCu-fsal > YNi-fsal > YFe-fsal > YMn-dmg. TG curves of zeolite fsal complexes are compared with those of corresponding metal exchanged zeolite in Figure IV. 9. A difference in the pattern of curves is observed in almost all cases. The encapsulation of metal complexes in zeolite cavities may be a reason for the difference in the shape of TG curve of zeolite complex as compared to metal exchanged zeolite.

Table IV. 7
TG/DTG data

Sample	Weight loss-Stage I			Weight loss-Stage II		
	Temp. range (°C)	Peak temp. (°C)	% Mass loss	Temp. range (°C)	Peak temp. (°C)	% Mass loss
YMn-dmg	60-280	180	13.6			
YFe-dmg	60-220	140	13.8	260-370	310	1.5
YCo-dmg	60-275	150	12.3	350-505	415	6.4
YNi-dmg	60-245	195	14.7	325-390	335	1.2
YCu-dmg	60-240	145	16.1	350-500	410	1.4

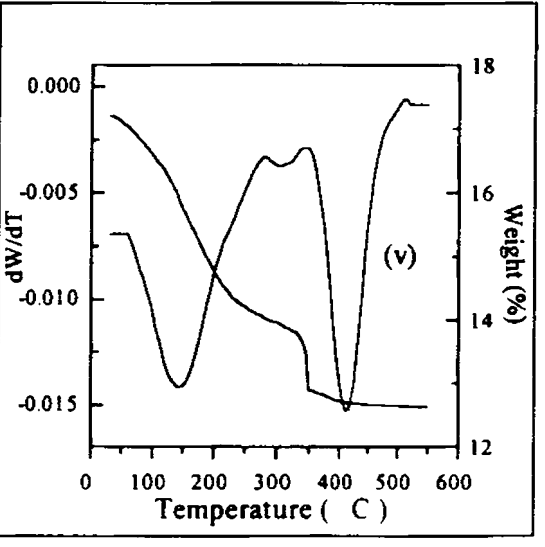
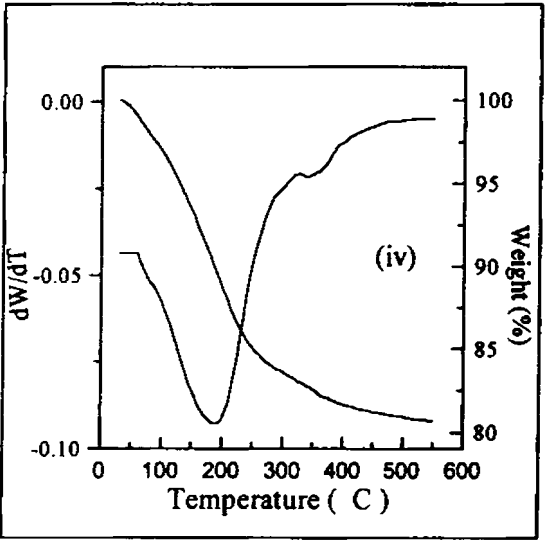
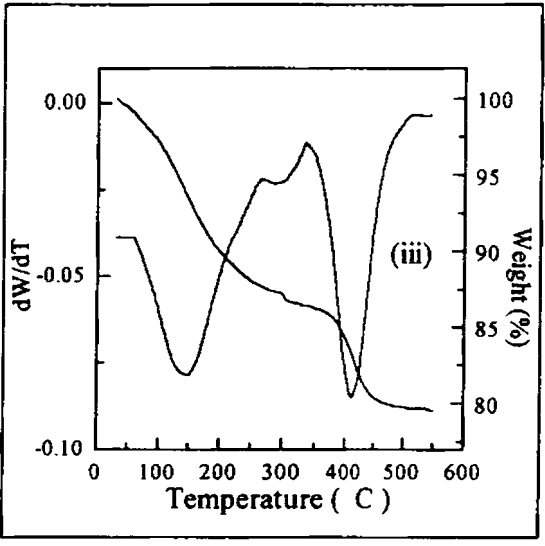
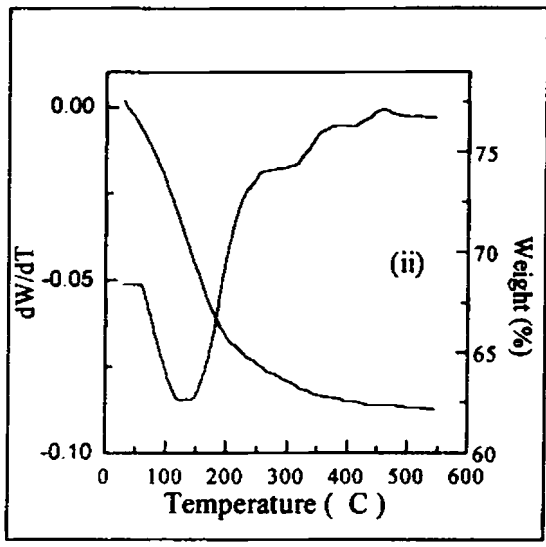
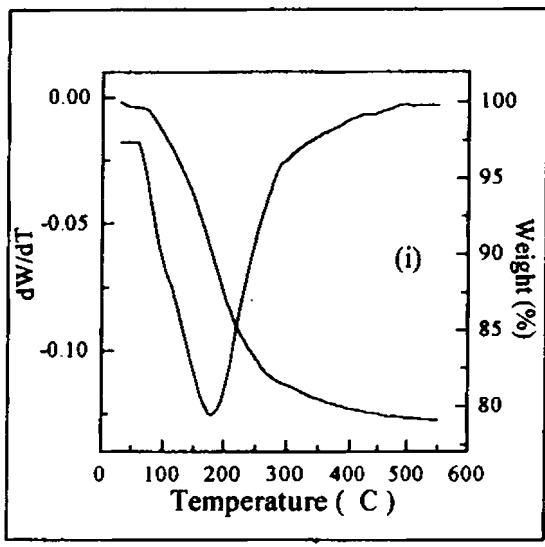


Figure IV. 8
TGDTG curves of encapsulated fsal
complexes

- (i) YMn-fsal
- (ii) YFe-fsal
- (iii) YCo-fsal
- (iv) YNi-fsal
- (v) YCu-fsal

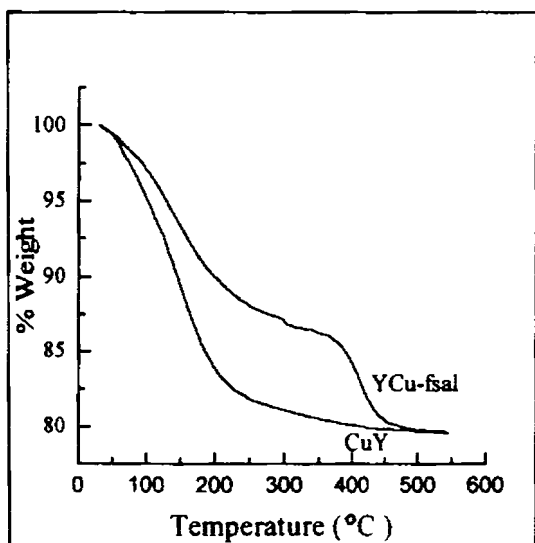
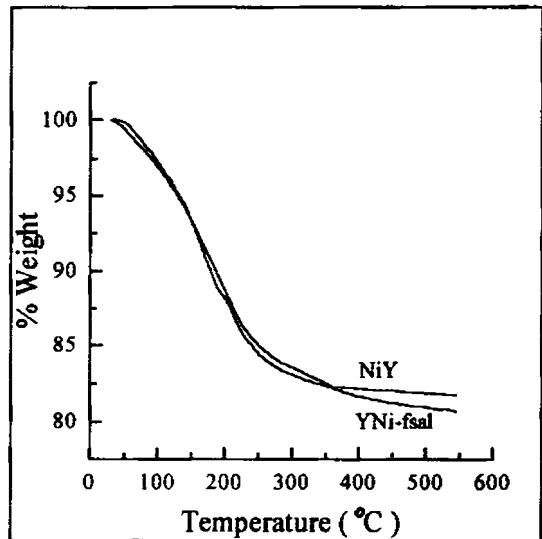
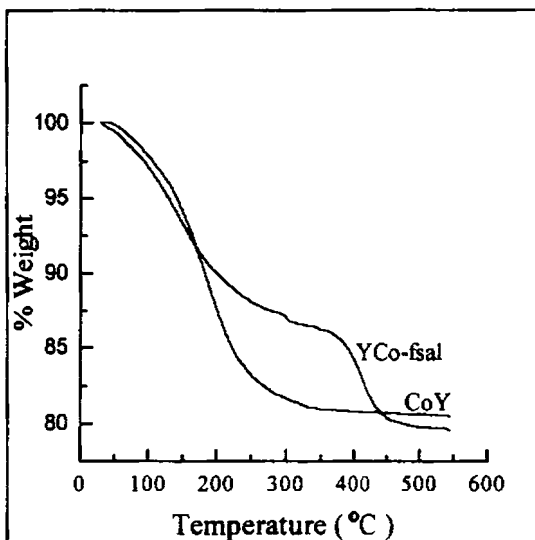
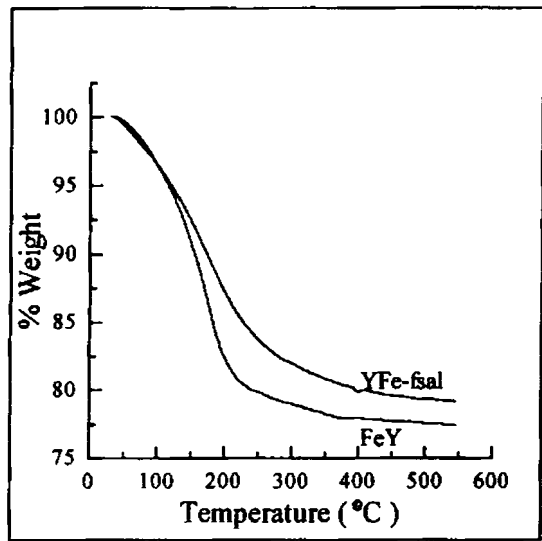
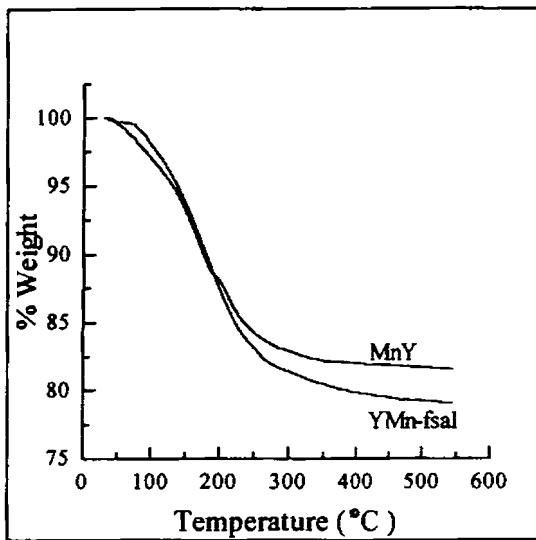


Figure IV. 9

TG curves of zeolite complexes and metal exchanged zeolites

4. 4 **SUMMARY AND CONCLUSION**

The analytical data indicate a binuclear structure for zeolite encapsulated fsal complexes. The resemblance of magnetic moment and reflectance data with those reported for simple complexes further support the binuclear structure. Crystalline structure of the zeolite support has undergone little changes on encapsulation. The lower surface area and pore volume of zeolite complexes as compared to zeolites indicate encapsulation of complexes. Considering magnetic moment, electronic and EPR spectral data, Co(II), Ni(II), and Cu(II) complexes are assumed to possess tetrahedral, octahedral and tetrahedrally distorted square planar geometry respectively in zeolite cavities. Structural elucidation, however, has not been possible in the case of Mn(II) and Fe(III) complexes from available data. The coordination of ligands with metal ion was ascertained in all cases by IR spectra. TG/DTG analysis distinctly shows the decomposition of ligands only in the case of Co(II) and Cu(II) complexes. However, difference in TG pattern as compared to that of metal exchanged zeolite hints at encapsulation of complexes.

REFERENCES

1. G. L. Eichhorn, " *Inorganic Biochemistry* ", Elsevier, New York (1973) Vols. 1 and 2.
2. M. Tanaka, H. Okawa, I. Hanaoka and S. Kida, *Chem. Lett.*, (1974) 71
3. M. Tanaka, H. Okawa, T. Tamura and S. Kida, *Bull. Chem. Soc. Jpn.*, 47, 7 (1974) 1669
4. J. S. Richardson, K. A. Thomas, B. H. Rubin and D. C. Richardson, *Proc. Natl. Acad. Sci. U.S.A.*, 72 (1975) 1349
5. G. Palmer, G. T. Babcoak and L. E. Vickery, *Proc. Natl. Acad. Sci. U.S.A.*, 73 (1977) 2206
6. D. E. Fenton, R. R. Schroeder and R. L. Lintvedt, *J. Am. Chem. Soc.*, 100 (1978) 1931
7. J. P. Gisselbrecht, M. Gross, A. H. Alberts and J. M. Lehn, *Inorg. Chem.*, 19 (1980) 1386
8. R. R. Gagne and C. L. Spiro, *J. Am. Chem. Soc.*, 102 (1980) 1443
9. M. Sakamoto, M. Takagi, T. Ishimori and H. Okawa, *Bull. Chem. Soc. Jpn.*, 61 (1988) 1613
10. N. Herron, *Chemtech*, Sept. (1989) 542
11. A. Earnshaw, " *Introduction to Magnetochemistry* ", Academic Press, London, 1968
12. N. N. Greenwood and A. Earnshaw, " *Chemistry of the Elements* ", Pergamon Press, 1984
13. F. L. Ulbach, R. D. Bereman, J. A. Topich, M. Hariharan and B. J. Kalbacher, *J. Am. Chem. Soc.*, 96 (1974) 5063
14. A. B. P. Lever , " *Inorganic Electronic Spectroscopy* ", Elsevier, Amsterdam, 1968
15. S. J. Gruber, C. M. Harris and E. Sinn, *J. Inorg. Nucl. Chem.*, 30 (1968) 1805
16. K. Nakamoto, " *Infrared Spectra of Inorganic and Coordination Compounds* ", 2 nd Ed., John-Wiley and Sons Inc. (1970) 232
17. M. Tanaka, M. Kitaoka, H. Okawa and S. Kida, *Bull. Chem. Soc. Jpn.*, 49 (1976) 2469
18. U. Sakaguchi and A. W. Addison, *J. Chem. Soc., Dalton Trans.*, (1979) 600
19. S. D. Robinson and M. F. Uttley, *J. Chem. Soc.*, 1912 (1973)

CHAPTER V

**STUDIES ON Y ZEOLITE ENCAPSULATED
TRANSITION METAL COMPLEXES OF
N, N'-ETHYLENEBIS(7-METHYLSALICYLIDENEAMINE)**

Abstract

Mn(II), Fe(III), Co(II), Ni(II) and Cu(II) complexes of N, N'-ethylenebis-(7-methylsalicylideneamine) have been synthesized in Y zeolite and characterized. The analytical, XRD, surface area and pore volume data suggest the encapsulation of these complexes without damaging the framework of the zeolite. Magnetic moment, electronic spectral and EPR data provide an idea about the geometry of the encapsulated complexes. IR spectra provide clue about the coordination of metal ion with ligands in zeolite pores. Thermal stability of encapsulated complexes was studied by TG/DTG analysis.

5. 1 INTRODUCTION

The coordination chemistry of Schiff base complexes has been an important focus in fundamental research, mainly because of the ease for designing and fabricating novel structures for them¹⁻³. Schiff base complexes can provide insight into the behaviour of metalloenzymes in biological systems by explaining the role of metallic site and its coordination environment, through model studies. The square planar tetradentate Schiff base complexes such as Co(salen) are known as model compounds for Vitamin B₁₂⁴. Cobalt(I)salen complex has been constructed in Y zeolite as a mimic of hemoglobin for studying the binding and transport of molecular oxygen^{5, 6}. In addition, zeolite encapsulated salen complexes have been received wide attention as catalysts for several chemical reactions⁷⁻¹².

The behaviour of encapsulated salen complexes is quite different from those of free salen complexes due to the interactions of zeolite framework on them¹³. The encapsulated complex distorts itself to fit into the cage altering its structural, electronic and hence catalytic properties. It is interesting to synthesize encapsulated complexes of bulkier substituted salen like ligands in view of increasing the distortion of the complex in zeolite cavities and thus to obtain a modified catalytic activity. The encapsulated complex of N,N'-ethylenebis(7-methylsalicylideneamine) (Mesalen) is an attractive system for catalytic studies in comparison with salen complexes. In this chapter, details regarding the synthesis and characterization of Y zeolite encapsulated Mn(II), Fe(III), Co(II), Ni(II) and Cu(II) complexes of Mesalen are presented.

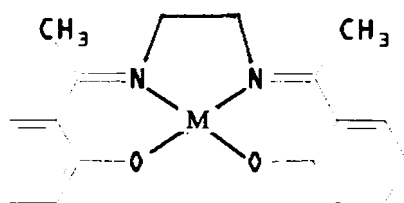


Figure V. 1

Structure of simple Mesalen complex

5. 2 EXPERIMENTAL

5. 2. 1 Materials

Details about the synthesis and purification of Mesalen ligand and the preparation of metal exchanged zeolites are given in Chapter II.

5. 2. 2 Synthesis of zeolite encapsulated Mesalen complexes

The general method used for encapsulating metal complexes in Y zeolite is explained in Chapter II. A mixture of metal exchanged zeolite (3.0 g) and Mesalen ligand (1.11 g for YMn, 0.49 g for YFe, 1.09 g for YCo, 1.12 g for YNi and 1.07 g for YCu) at a ligand to metal mole ratio of around 2 was heated at 150 °C for 16 hours in a sealed glass ampule. The procedure employed for the purification of the product was same as that described previously (vide page 106). The zeolite complex was stored in vacuum over anhydrous calcium chloride after drying at 100 °C for 2 hours.

5. 2. 3 Analytical methods

Details of the analytical methods and other characterization techniques are given in Chapter II.

5. 3 RESULTS AND DISCUSSION

Zeolite encapsulated Mesalen complexes of Mn(II), Fe(III), Co(II), Ni(II) and Cu(II) ions were synthesized and characterized using techniques like chemical analysis, XRD, surface area and pore volume, magnetic moment, electronic spectra, FTIR, EPR and TG analysis.

5. 3. 1 Chemical analysis

The analytical data of zeolite encapsulated Mesalen complexes are given in Table V. 1. The Si/Al ratio of these zeolite complexes was found to be 2.43 as in the case of

metal exchanged zeolites (vide page 70). The empirical formulae of encapsulated Mesalen complexes are $MnL_{0.85}$, $FeL_{0.93}$, $CoL_{0.89}$, $NiL_{0.82}$ and $CuL_{0.87}$ in YMn-Mesalen, YFe-Mesalen, YCo-Mesalen, YNi-Mesalen and YCu-Mesalen respectively. The ligand to metal mole ratio has been found to be 1 in free complexes of salen and salen like ligands ^{14, 15}. But, this mole ratio is slightly less than 1 in the case of encapsulated complexes indicating the presence of minute amount of uncomplexed metal ions in the lattice. The charge neutralization in the case of Fe(III) complex might have occurred by combining with negatively charged oxide ions of the zeolite lattice.

Table V. 1
Analytical data of Mesalen complexes

Sample	% Metal	%Si	%Al	%Na	%C	%H	%N
YMn-Mesalen	2.50	18.46	7.28	5.32	8.36	0.71	1.09
YFe-Mesalen	1.10	19.32	7.65	6.52	3.96	0.33	0.51
YCo-Mesalen	1.85	19.45	7.67	6.82	6.03	0.51	0.78
YNi-Mesalen	2.78	19.40	7.68	5.25	8.39	0.71	1.09
YCu-Mesalen	1.61	19.43	7.67	6.30	4.76	0.40	0.62

5. 3. 2 X-ray diffraction pattern

XRD patterns of YFe-Mesalen, YNi-Mesalen and YCu-Mesalen are given in Figure V. 2. Zeolite framework structure was found to remain unaffected during the synthesis of Mesalen complexes as indicated by similar XRD patterns of metal exchanged zeolites and corresponding zeolite complexes.

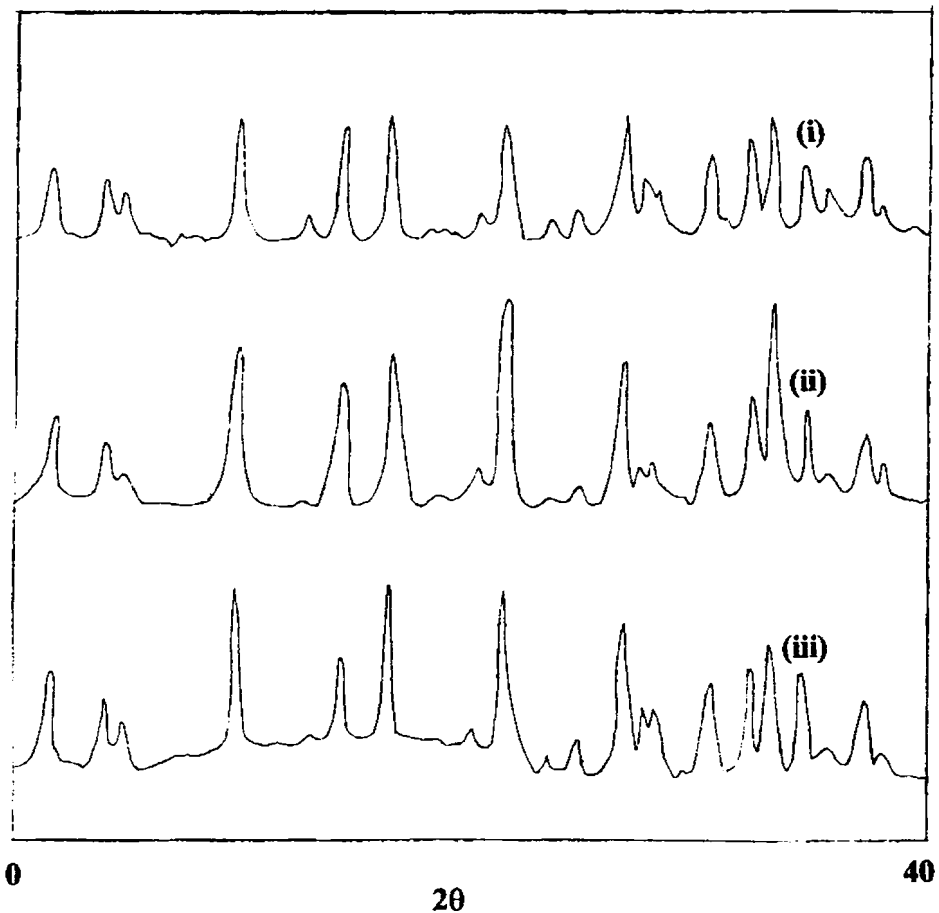


Figure V. 2

XRD patterns of (i). YFe-Mesalen, (ii). YNi-Mesalen and (iii). YCu-Mesalen

5. 3. 3 Surface area and pore volume

Surface area and pore volume data are given in Table V. 2. Surface area and pore volume of metal exchanged zeolite was found to be lowered on encapsulation indicating the formation of complexes in zeolite pores. The lowering of these values on encapsulation is represented in Figure V. 3 and V. 4 as bar charts.

Table V. 2

Surface area and pore volume data

Sample	Surface area (m ² /g)			Pore volume (ml/g)		
	MY	YM- Mesalen	% Loss	MY	YM- Mesalen	% Loss
YMn-Mesalen	531	388	26.9	0.2961	0.2457	17.0
YFe-Mesalen	540	372	31.1	0.3011	0.2388	20.7
YCo-Mesalen	532	269	49.4	0.2966	0.1669	43.7
YNi-Mesalen	528	260	50.8	0.2944	0.1713	41.8
YCu-Mesalen	534	389	27.2	0.2978	0.2403	19.3

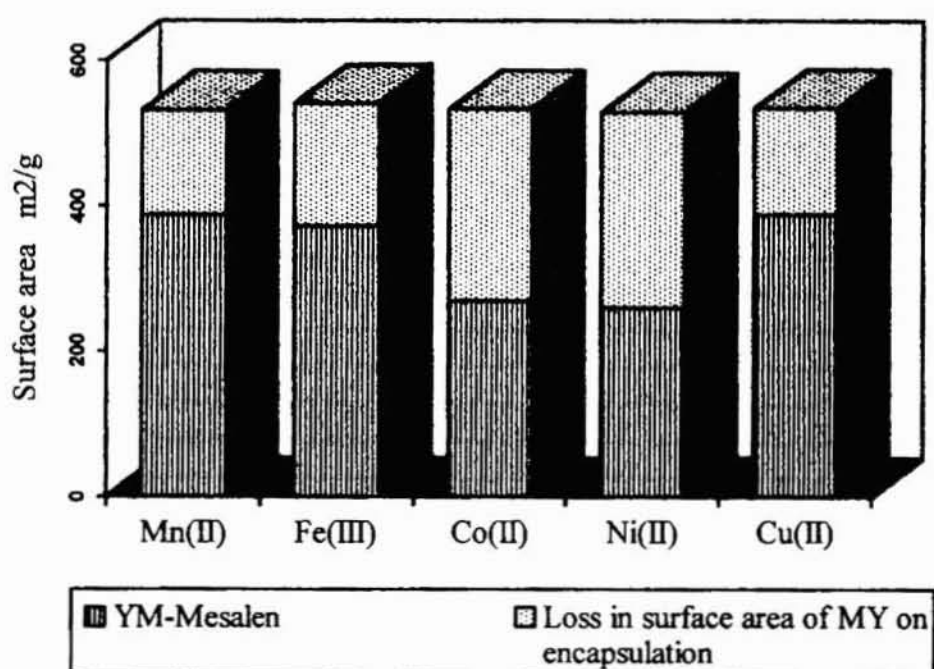


Figure V. 3

Decrease of surface area of metal exchanged zeolites on encapsulation

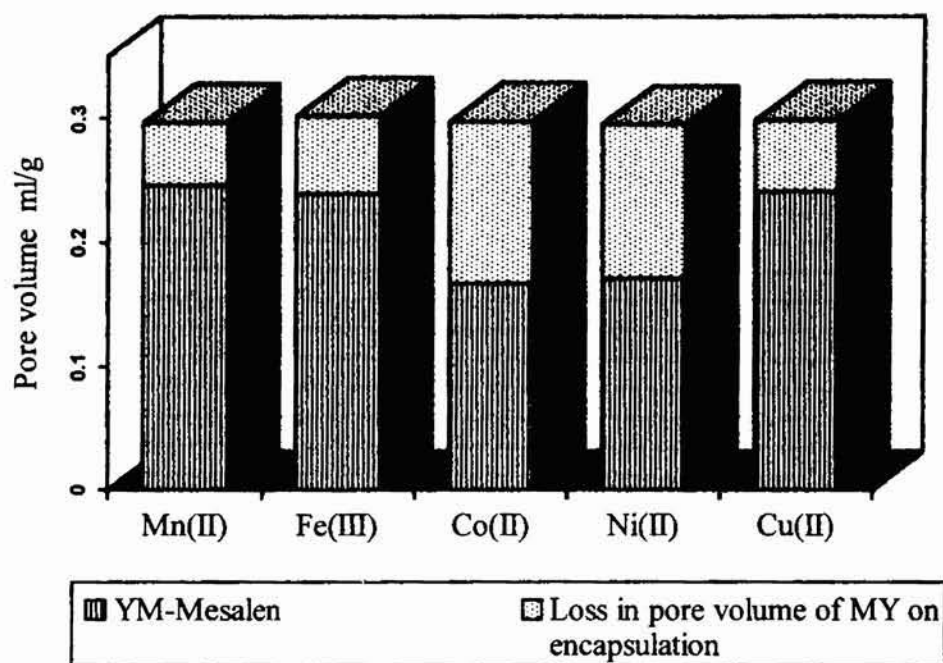


Figure V. 4

Decrease of pore volume of metal exchanged zeolites on encapsulation

5.3.4 Magnetic moment

Table V. 3

Magnetic moment data

Sample	Magnetic moment (BM)
YMn-Mesalen	6.12
YFe-Mesalen	5.87
YCo-Mesalen	4.93
YNi-Mesalen	3.21
YCu-Mesalen	1.80

Room temperature magnetic moments of Mesalen complexes are given in Table V. 3. Magnetic moment value of 6.12 BM for YMn-Mesalen or 5.87 BM for YFe-Mesalen is close to that often observed for high spin Mn(II) or Fe(III) complexes

irrespective of the coordination geometry. Magnetic moment of YCo-Mesalen, 4.93 BM, agrees with that of octahedral Co(II) complexes which is in the range 4.8-5.2 BM¹⁶. YNi-Mesalen has exhibited a magnetic moment of 3.21 BM indicating an octahedral symmetry for the encapsulated complex¹⁶. Magnetic moment of 1.85 BM was observed for YCu-Mesalen.

5.3.5 Electronic spectra

Optical reflectance data were analysed by Kubelka-Munk (KM) method. The plot of KM factor, F(R), obtained from reflectance data against wavelength is shown in Figure V. 5. The electronic transitions and their tentative assignments are given in Table V. 4.

Table V. 4
Electronic spectral data

Sample	Abs. Max. (cm ⁻¹)	Tentative assignments
YMn-Mesalen	26110	Charge transfer transition
YFe-Mesalen	12410	d-d transition
	28820	Charge transfer transition
	40000	Intraligand transition
YCo-Mesalen	13330	d-d transition
	25450	Charge transfer transition
	31750	Intraligand transition
YNi-Mesalen	13410	³ A _{2g} (F) → ³ T _{2g} (F)
	16080	³ A _{2g} (F) → ³ T _{1g} (F)
	26740	³ A _{2g} (F) → ³ T _{1g} (P)
	39220	Intraligand transition
YCu-Mesalen	12480	d-d transition
	32260	Intraligand transition

Note: The bands at ~ 6890 cm⁻¹ and ~ 5150 cm⁻¹ in the spectra of all samples are characteristic of zeolite lattice and not included in this table

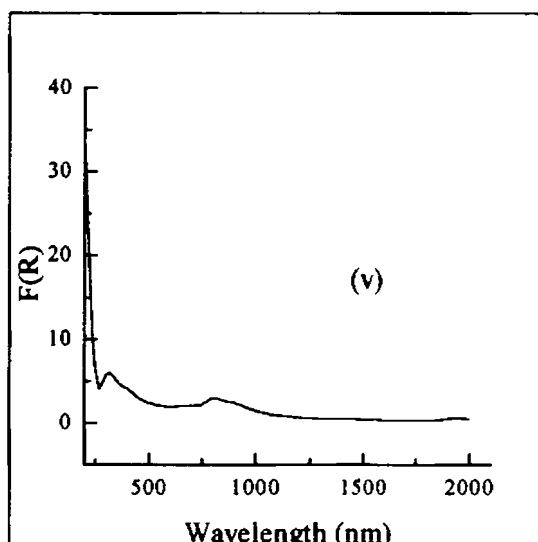
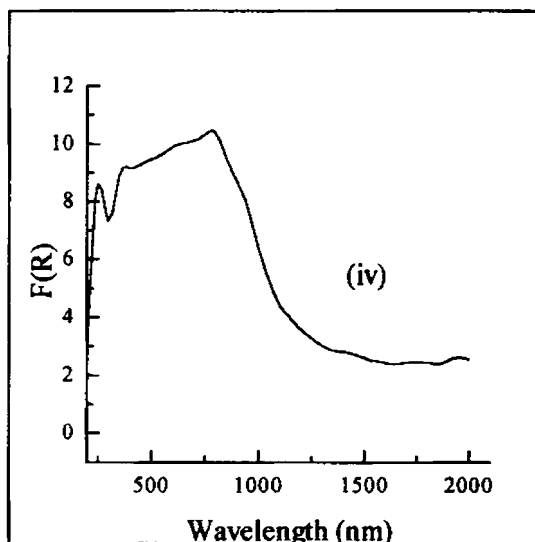
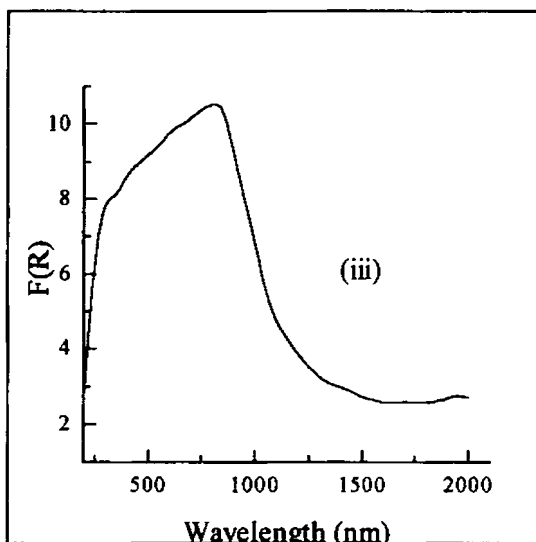
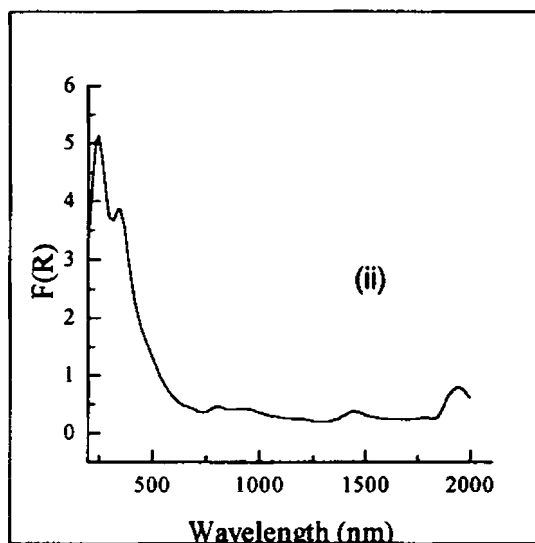
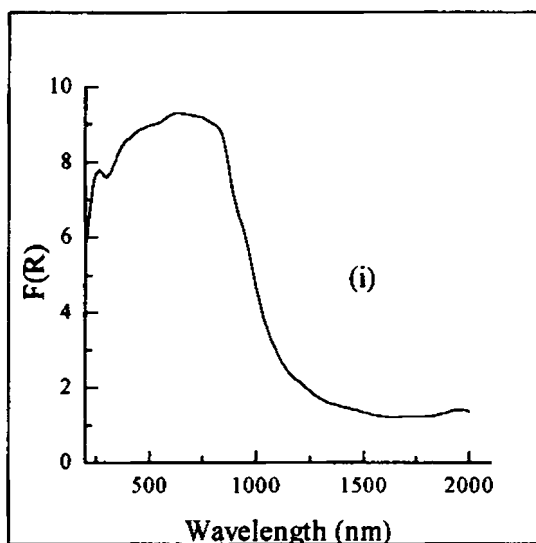


Figure V. 5
Electronic spectra of encapsulated
Mesalen complexes

- (i) YMn-Mesalen
- (ii) YFe-Mesalen
- (iii) YCo-Mesalen
- (iv) YNi-Mesalen
- (v) YCu-Mesalen

In the case of YMn-Mesalen, the broad charge transfer band at 26110 cm^{-1} extends to the visible region with a maximum at 13740 cm^{-1} . YFe-Mesalen exhibits spin forbidden d-d band at 12410 cm^{-1} . YCo-Mesalen shows a very broad band in the UV region tailing to visible region with a maximum at 13330 cm^{-1} which could be considered as a d-d band.

In the case of YNi-Mesalen, d-d bands are masked by a very broad absorption with peak maxima at 13410 cm^{-1} , 16080 cm^{-1} and 26740 cm^{-1} . Unambiguous interpretation of the data is difficult in this case. However, the magnetic moment value of 3.21 BM hint at an octahedral coordination for the Ni(II) complex¹⁷. Assuming an octahedral symmetry, the bands observed can be attributed to the following transitions: ${}^3A_{2g}(F) \rightarrow {}^3T_{2g}(F)$, ${}^3A_{2g}(F) \rightarrow {}^3T_{1g}(F)$ and ${}^3A_{2g}(F) \rightarrow {}^3T_{1g}(P)$. The axial positions in the octahedral symmetry might have occupied by either water molecules or oxide ions of zeolite lattice. The electronic spectrum of YCu-Mesalen shows a d-d band at 12480 cm^{-1} .

5.3.6 Infrared spectra

IR spectra of Mesalen and zeolite encapsulated Mesalen complexes are shown in Figure V. 6. IR spectral bands of MY, Mesalen ligand and encapsulated metal complexes are presented in Table V. 5.

In the spectra of free Mesalen ligand, C=N stretching frequency is observed at 1611 cm^{-1} . This band has been shifted to 1600 cm^{-1} in unencapsulated Mesalen complexes¹⁸. Similar lowering of $\gamma_{C=N}$ is expected in encapsulated complexes also. But, the new band is not observed in the spectra of zeolite complexes as it might have masked by δ_{H-O-H} band of water molecules in zeolite lattice. The γ_{O-H} band at 3055 cm^{-1} in the ligand is expected to disappear in complexes as deprotonation occurs prior to the coordination of phenolic oxygens. This change could not be distinguished due to the presence of γ_{O-H} of water molecules almost at same position in the spectra. In the spectra of free ligand, there are bands at 1294 cm^{-1} for γ_{C-O} of phenolic group and at 1163 cm^{-1} for γ_{C-N} . These bands are not observed in the case of zeolite complexes as they might

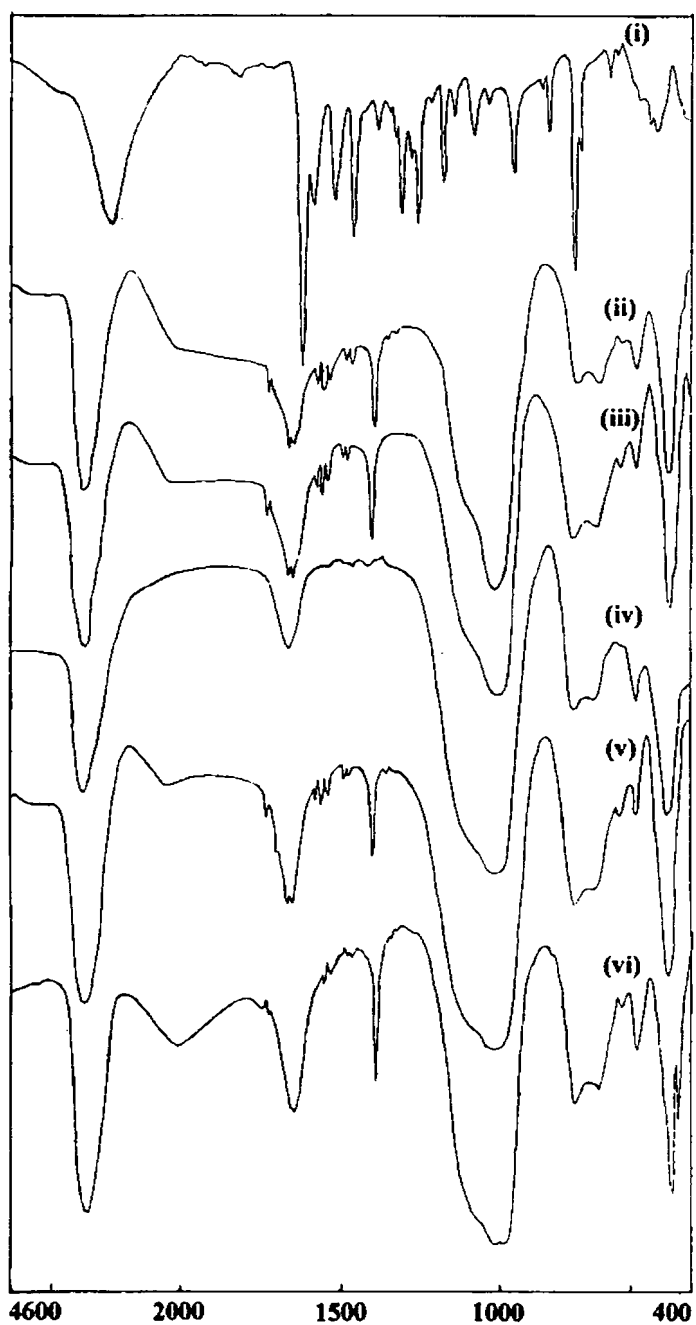


Figure V. 6
IR spectra-(i) Mesalen, (ii) YMn-Mesalen, (iii) YFe-Mesalen,
(iv) YCo-Mesalen,(v) YNi-Mesalen and (vi) YCu-Mesalen

Table V. 5

IR spectral data (cm^{-1}) of MY, Mesalen and zeolite complexes

MY	Mesalen	YMn- Mesalen	YFe- Mesalen	YCo- Mesalen	YNi- Mesalen	YCu- Mesalen
460		465	461	465	457	459
	505					
570		567	567	565	565	565
680	650	685	687	689	700	688
750	758	758	758	756	758	756
1000	837	997	996	998	997	1001
	949					
	1026					
	1067					
	1130					
	1163					
	1242					
	1294					
	1367	1385	1385	1397	1385	1385
	1447		1455	1442		1455
			1470			1480
	1508	1543	1520	1517	1520	1525
	1576	1549	1545		1545	1548
			1562		1555	
1650	1611	1651	1650	1642	1650	1650
	1812	1719	1721		1719	1719
	2899	2885	2874	2872		2871
	2910	2918	2920	2928		2925
3453	3056	3480	3445	3505	3450	3485

have masked by the broad zeolite band at around 1000 cm^{-1} . However, the bands due to C-C stretching vibrations of benzene rings are visible at $1500\text{-}1600\text{ cm}^{-1}$ in the spectra of all zeolite complexes. Since there are no zeolite bands at this position, $\nu_{\text{C-C}}$ of benzene rings indicates encapsulation of complexes.

5.3.7 EPR spectra

Table V. 6
EPR spectral data

EPR parameter	YCu-Mesalen (BM)
g_{\parallel}	2.31
A_{\parallel}	$139.4 \times 10^{-4}\text{ cm}^{-1}$
$g_{\parallel} / A_{\parallel}$	165.7 cm
g_{\perp}	2.01
A_{\perp}	$47.2 \times 10^{-4}\text{ cm}^{-1}$
α^2	0.74
μ_{eff}	1.83 BM

EPR spectrum of YCu-Mesalen is shown in Figure V. 7 and the EPR parameters, unpaired electron density and magnetic moment are given in Table V. 6. A high g_{\parallel} value of 2.31 is seen for encapsulated Cu-Mesalen complex as a result of tetrahedral distortion of square planar complexes. The ratio, $g_{\parallel} / A_{\parallel}$ is 165.7 showing a high degree of distortion. A flattened tetrahedral structure is reported for $g_{\parallel} / A_{\parallel}$ values of around 150-160 cm. Metal complexes of salen and salen like ligands have been reported to exhibit square planar complexes ¹⁵. The observed distortion in YCu-Mesalen may be considered as a consequence of the interactions of zeolite framework on encapsulated complex. The steric effects of methyl groups at the α position may cause a high degree of distortion for encapsulated Cu-Mesalen complex. The α^2 value of YCu-Mesalen is found to be 0.74 indicating an ionic environment for Cu^{2+} ions.

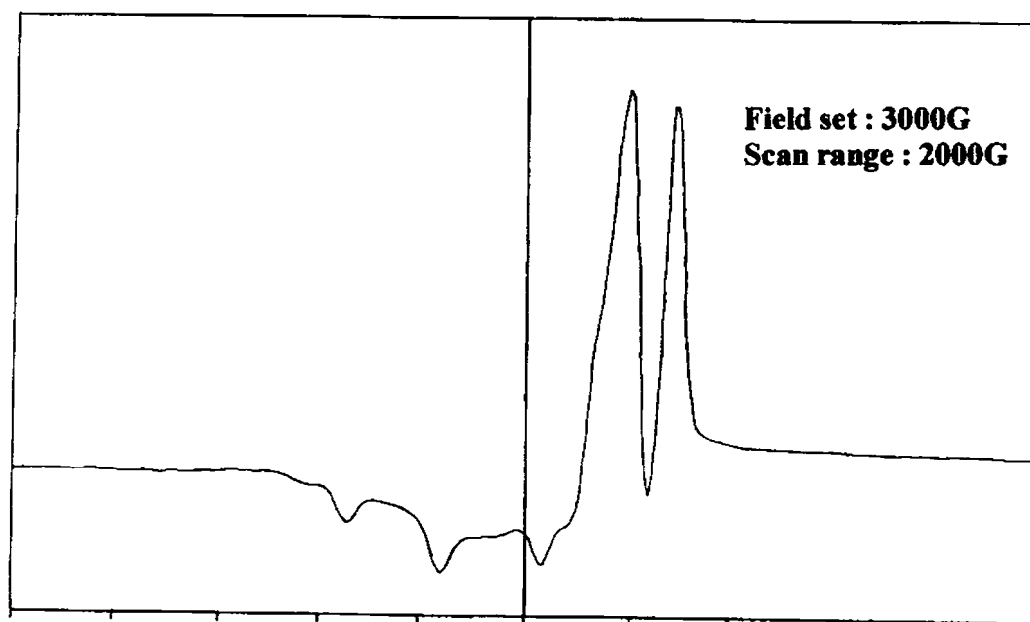


Figure V. 7
EPR spectrum of YCu-Mesalen

μ_{eff} of YCu-Mesalen, 1.83 BM, agrees with the value obtained from room temperature magnetic susceptibility measurement (1.8 BM).

5. 3. 8 Thermal analysis

TG/DTG curves recorded for zeolite Mesalen complexes are shown in Figure IV. 8. The weight loss observed in the temperature range of 60 °C to 220-250 °C is due to deaquation of the samples. The weight loss due to the expulsion of ligand moisties is not clearly visible in the patterns (vide page 96). The single stage observed in the case of YMn-fsal may be due to simultaneous removal of water and decomposition of the complex. However, the probable temperatures of decomposition were identified in other cases (Table V. 7) for qualitatively evaluating the thermal stability of zeolite complexes. The thermal stability of encapsulated complexes was found to vary approximately in the order of metal ions as Ni(II) > Co(II) > Cu(II) > Fe(III) > Mn(II).

The residue obtained after the analysis was analysed for IR spectra to ensure the complete decomposition of the encapsulated complex.

Table V. 7
TG/DTG data

Sample	Weight loss-Stage I			Weight loss-Stage II		
	Temp. range (°C)	Peak temp. (°C)	% Mass loss	Temp. range (°C)	Peak temp. (°C)	% Mass loss
YMn-Mesalen	60-310	200	18.4			
YFe-Mesalen	60-220	140	11.6	260-370	310	3.0
YCo-Mesalen	110-275	180	10.2	345-480	360	3.9
YNi-Mesalen	100-260	160	9.2	360-450	390	1.4
YCu-Mesalen	80-280	160	16.0	340-390	350	1.0

TG curves of Mesalen complexes are compared with those of corresponding metal exchanged zeolites in Figure V. 9. The difference in the pattern of curves implies the presence of metal complexes in zeolite cavities.

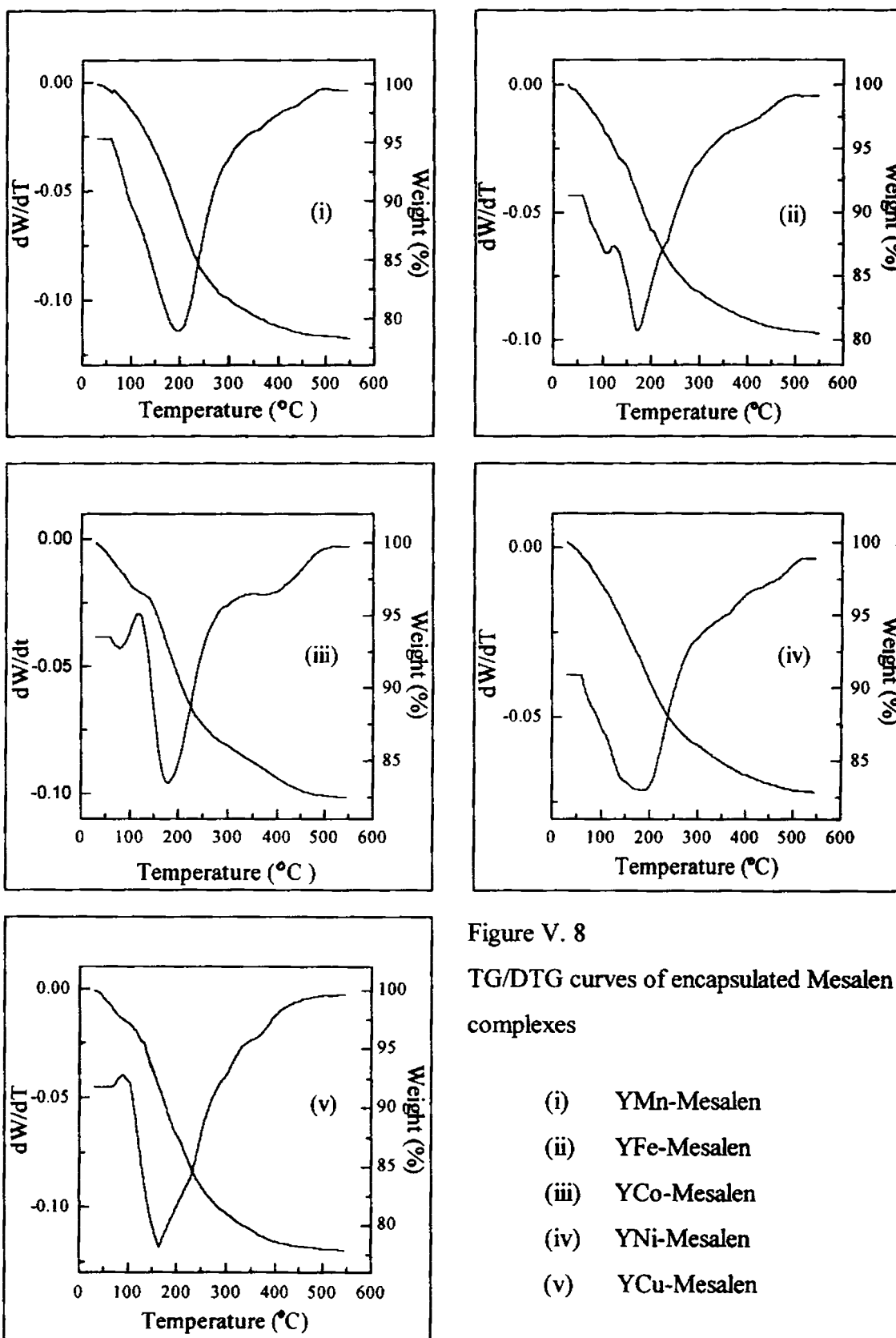


Figure V. 8

TG/DTG curves of encapsulated Mesalen complexes

- (i) YMn-Mesalen
- (ii) YFe-Mesalen
- (iii) YCo-Mesalen
- (iv) YNi-Mesalen
- (v) YCu-Mesalen

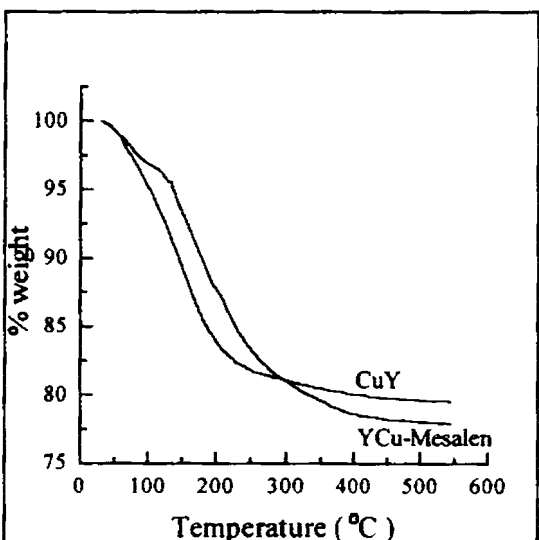
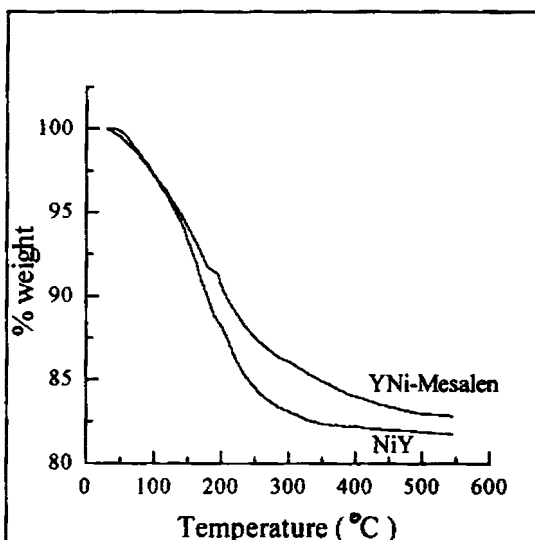
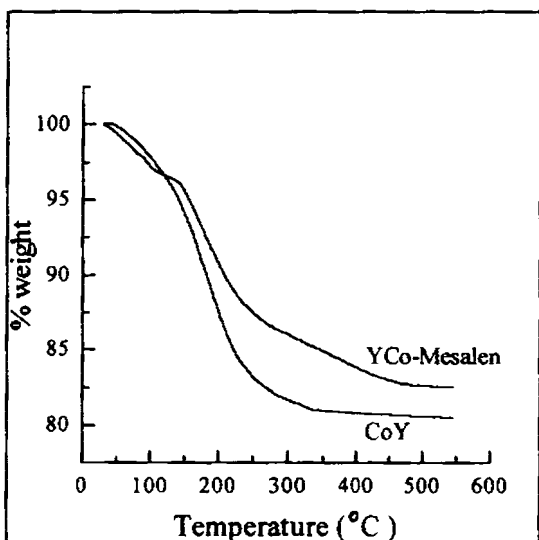
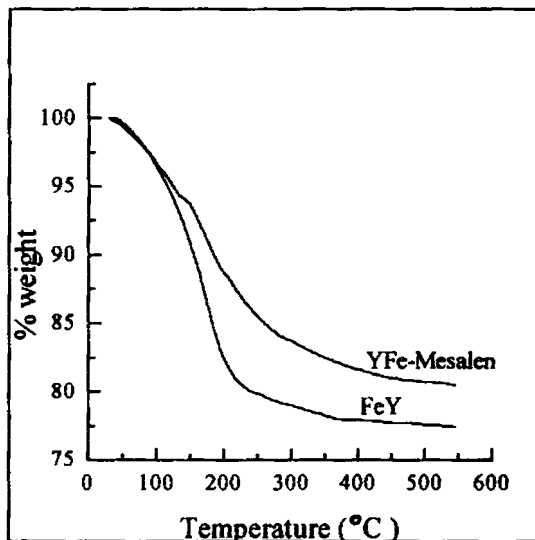
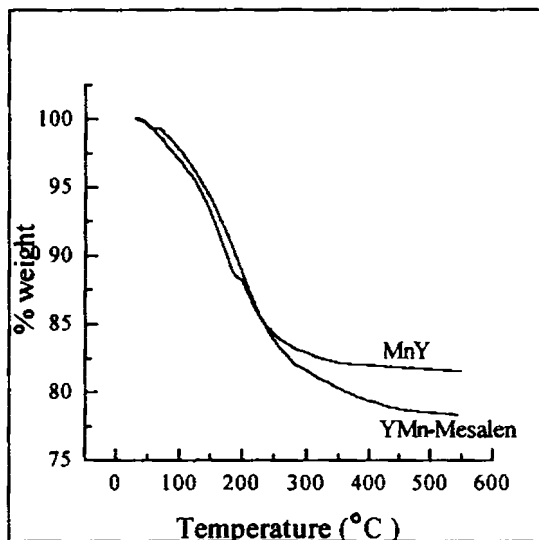


Figure V. 9
 TG curves of metal exchanged zeolites
 and zeolite complexes

5.4 SUMMARY AND CONCLUSION

The analytical data indicate the formation of monomeric complexes of Mesalen in zeolite cavities. The Si/Al ratio and XRD patterns show that the crystalline structure of zeolites has remained intact during encapsulation. The lower surface area and pore volume of zeolite complexes as compared to zeolites is an evidence for the encapsulation of complexes. The geometries assumed for the encapsulated complexes on the basis of magnetic moment, electronic and EPR data are octahedral for both Co(II) and Ni(II) complexes and tetrahedrally distorted square planar for Cu(II) complex. However, the interpretation of these data is difficult in the case of Mn(II) and Fe(III) complexes. EPR data also suggest a high degree of distortion in the encapsulated Cu(II) complex. IR spectra also indicate the encapsulation of complexes. From TG/DTG data, the complexes can be graded with respect to thermal stability in the order of metal ions as Ni(II) > Co(II) > Cu(II) > Fe(III) > Mn(II). The distinctly different TG patterns of zeolite complexes as compared to those of corresponding metal exchanged zeolites is because of the decomposition of encapsulated complexes, which can be considered as an evidence for encapsulation.

REFERENCES

1. R. M. Countryman, W. T. Robinson and E. Sinn, *Inorg. Chem.*, 13 (1974) 2003
2. A. P. Summerton, A. A. Diamantis and M. R. Snow, *Inorg. Chim. Acta*, 27 (1978) 123
3. J. C. Stevens and D. H. Busch, *J. Am. Chem. Soc.*, 102 (1980) 3285
4. G. N. Schrauzer, *J. Am. Chem. Soc.*, 92 (1970) 7078
5. A. D. Gupta, D. Bhuniya and V. K. Singh, *J. Indian Inst. Sci.*, 74 (1994) 71
6. F. Aoi, M. Ishimori, S. Yoshikawa and T. Tsuruta, *J. Organomet. Chem.*, 85 (1975) 241
7. J. P. Collman, X. Zhang, V. J. Lee, V. S. Uffelman and J. I. Brauman, *Science*, 261 (1993) 1404
8. N. Herron, *Chemtech*, Sept. (1989) 542
9. S. P. Varkey and C. R. Jacob, *Ind. J. Chem.*, 37A (1998) 407
10. N. Ulagappan, *Proceedings of The 31st annual convention of chemists, Varanasi*, (1994) F1
11. R. Chandra, M. Anupa and P. Subhash, *Ind. J. Chem.*, 35A (1996) 1
12. T. Yamamoto, T. Shido, S. Inagaki, Y. Fukushima and M. Ichikawa, *J. Am. Chem. Soc.*, 118 (1996) 5810
13. N. Herron, *Inorg. Chem.*, 25 (1986) 4714
14. Y. Fujii, T. Isago, M. Sano, N. Yanagibashi, S. Hinasalva and S. Takahashi, *Bull. Chem. Soc. Jpn.*, 49 (1976) 3509
15. Y. Fujii, Y. Kuwana, S. Takahashi, K. Shimizu and K. Hiroi, *Bull. Chem. Soc. Jpn.*, 55 (1982) 2598
16. N. N. Greenwood and A. Earnshaw, " *Chemistry of the Elements* ", Pergamon Press, 1984
17. A. B. P. Lever, " *Inorganic Electronic Spectroscopy* ", Elsevier, Amsterdam, 1968
18. R. S. Downing and F. L. Urbach, *J. Am. Chem. Soc.*, 91 (1969) 5977

CHAPTER VI

STUDIES ON Y ZEOLITE ENCAPSULATED

TRANSITION METAL COMPLEXES OF

N, N'-ETHYLENEBIS(5,6-BENZOSALICYLIDENEAMINE)

Abstract

Y Zeolite encapsulated Mn(II), Fe(III), Ni(II) and Cu(II) complexes of N,N'-ethylenebis(5,6-benzosalicylideneamine) have been synthesized and characterized. The analytical, XRD, surface area and pore volume data provide evidence for the formation of complexes in the zeolite cavities and the retention of zeolite crystallinity. Magnetic moments, electronic spectral data and EPR of Cu(II) complex enable the assignment of geometry of the encapsulated complexes. IR spectra indicate the coordination in encapsulated complexes. TG/DTG analysis has been carried out to study the thermal stability of encapsulated complexes.

6. 1 INTRODUCTION

Zeolite encapsulated salen complex is considered to be an efficient catalyst for a variety of hydrogenation and dehydrogenation reactions ¹⁻³. There have been attempts to improve the catalytic activity and selectivity of intrazeolite salen complex ⁴. The performance of such systems in chemical reactions depends, to a large extent, on the stereochemical arrangement of the encapsulated complex ⁵. Therefore, one approach for improving the catalytic activity of zeolite complexes would be to fulfil the steric requirements for the desired chemical reaction.

The use of bulky salen like ligands may result in a different stereochemistry for the encapsulated complex and would make it more strained in zeolite cavities. It is interesting to investigate the effect of such substituted salen ligands on catalytic activity of zeolite complexes. With this interest, the synthesis and characterisation of Y zeolite encapsulated complexes of methyl substituted salen ligand have been undertaken in the previous chapter. N,N'-ethylenebis(5,6-benzosalicylideneamine) (Benzosalen) is also likely to form an intrazeolite structure entirely different from that of encapsulated salen complex which might work as a more efficient catalyst. We have synthesized and characterized Y zeolite encapsulated Mn(II), Fe(III), Ni(II) and Cu(II) complexes with Benzosalen ligand. These studies are presented in this chapter.

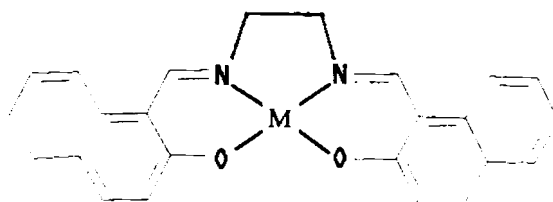


Figure VI. 1

Structure of simple Benzosalen complex

6. 2 EXPERIMENTAL

6. 2. 1 Materials

Details regarding the synthesis of Benzosalen ligand and metal exchanged zeolite supports are given in Chapter II.

6. 2. 2 Synthesis of zeolite encapsulated Benzosalen complexes

The general method used for synthesising zeolite encapsulated complexes is given in Chapter II. A mixture of metal exchanged zeolite (3.0 g) and Benzosalen ligand (0.69 g for YMn, 0.31 g for YFe, 0.68 g for YCo, 0.70 g for YNi and 0.67 g for YCu) with ligand to metal mole ratio of around 2 was heated at 225 °C for 16 hours. The product was soxhlet-extracted with chloroform and then ion-exchanged using sodium chloride solution as explained previously (vide page 70). The zeolite complex obtained was filtered, washed free of chloride ions, dried at 100 °C for 2 hours and stored in vacuum over anhydrous calcium chloride.

6. 2. 3 Analytical methods

Details regarding the analytical methods and other characterization techniques are given in Chapter II.

6. 3 RESULTS AND DISCUSSION

Zeolite encapsulated Benzosalen complexes of Mn(II), Fe(III), Ni(II) and Cu(II) ions were synthesised. Our attempts to synthesize YCo-Benzosalen were unsuccessful. The red mass formed on heating a mixture of CoY and Benzosalen at 225 °C was seen to have been leached out from the zeolite, while soxhlet-extracting with chloroform. Probably, the larger hydrated Co(II) complexes which are likely to present in CoY might have prevented the entry of bulky Benzosalen ligand.

The various characterisation techniques used in this study were chemical analysis, XRD, surface area and pore volume, magnetic moment, electronic, FTIR and EPR spectroscopy and TG analysis.

6.3.1 Chemical analysis

The analytical data of zeolite encapsulated Benzosalen complexes are presented in Table VI. 1. The data reveal that Si/Al ratio of metal exchanged zeolites (2.43) remains unchanged in zeolite complexes indicating the capability of zeolite structure to withstand encapsulation conditions.

Table VI. 1

Analytical data of Benzosalen complexes

Sample	% Metal	% Si	% Al	% Na	% C	% H	% N
YMn-Benzosalen	2.62	18.40	7.28	5.21	11.40	0.72	1.11
YFe-Benzosalen	1.39	18.70	7.37	6.30	6.81	0.43	0.67
YNi-Benzosalen	1.41	18.70	7.41	6.29	6.37	0.40	0.62
YCu-Benzosalen	2.49	18.28	7.22	5.40	9.25	0.58	0.90

The empirical formulae of encapsulated Benzosalen complexes are $MnL_{0.83}$, $FeL_{0.95}$, $NiL_{0.92}$ and $CuL_{0.82}$ in YMn-Benzosalen, YFe-Benzosalen, YNi-Benzosalen and YCu-Benzosalen respectively. Ligand to metal mole ratio of 1 is expected in free complexes of Benzosalen⁶. The lower fraction of ligand in zeolite complexes could be attributed to the presence of traces of free metal ions in the lattice. The complexes may be expected to form monomeric species as there is no room for dimerisation in cavities. In the case of Fe(III) complex, the charge neutralization might have occurred by combining with negatively charged oxide ions of the zeolite structure.

6.3.2 X-ray diffraction pattern

XRD patterns of YMn-Benzosalen, YFe-Benzosalen and YCu-Benzosalen are given in Figure VI. 2. These patterns are very much identical to those of metal

exchanged zeolites which implies that the framework structure remains uncollapsed during the synthesis.

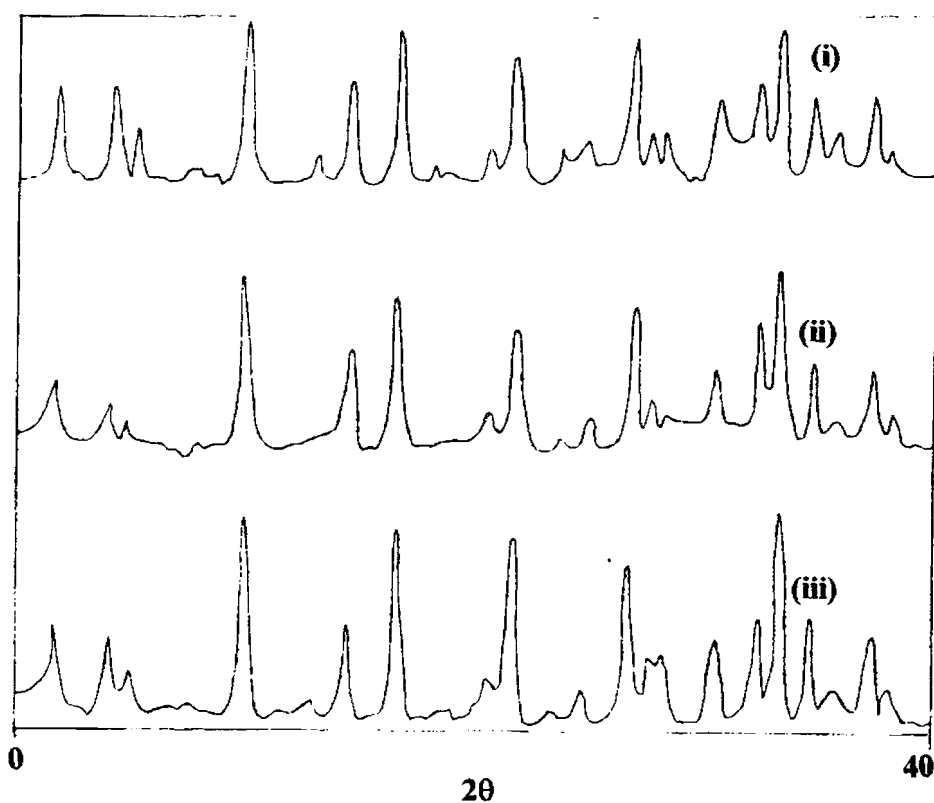


Figure VI. 2

XRD patterns of **i** . YMn-Benzosalen, **ii** . YFe-Benzosalen and **iii** . YCu-Benzosalen

6. 3. 3 Surface area and pore volume

Surface area and pore volume data are given in Table VI. 2. These values are lower than those of the corresponding metal zeolites due to the encapsulation of complexes in the pores. The lowering of surface area and pore volume is shown graphically in Figure VI. 3 and VI. 4 respectively.

Table VI. 2

Surface area and pore volume data

Sample	Surface area (m^2/g)			Pore volume (ml/g)		
	MY	YM- Benzo- salen	% Loss	MY	YM- Benzo- salen	% Loss
YMn-Benzosalen	531	332	37.5	0.2961	0.2060	30.4
YFe-Benzosalen	540	341	36.9	0.3011	0.2160	28.3
YNi-Benzosalen	528	412	22.0	0.2944	0.2575	12.5
YCu-Benzosalen	534	282	47.2	0.2978	0.1869	37.2

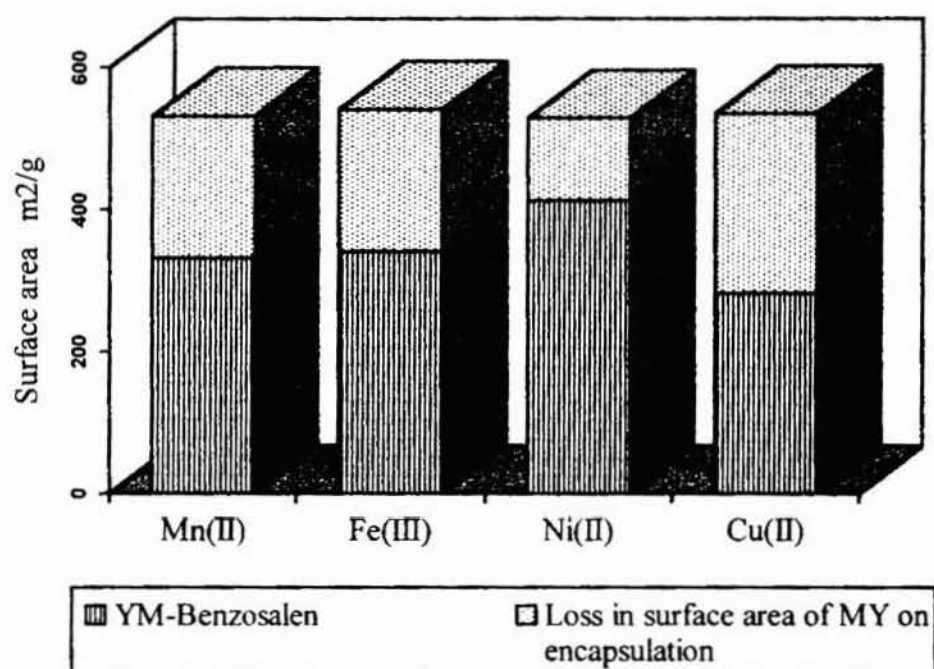


Figure VI. 3

Decrease of surface area of metal exchanged zeolites on encapsulation

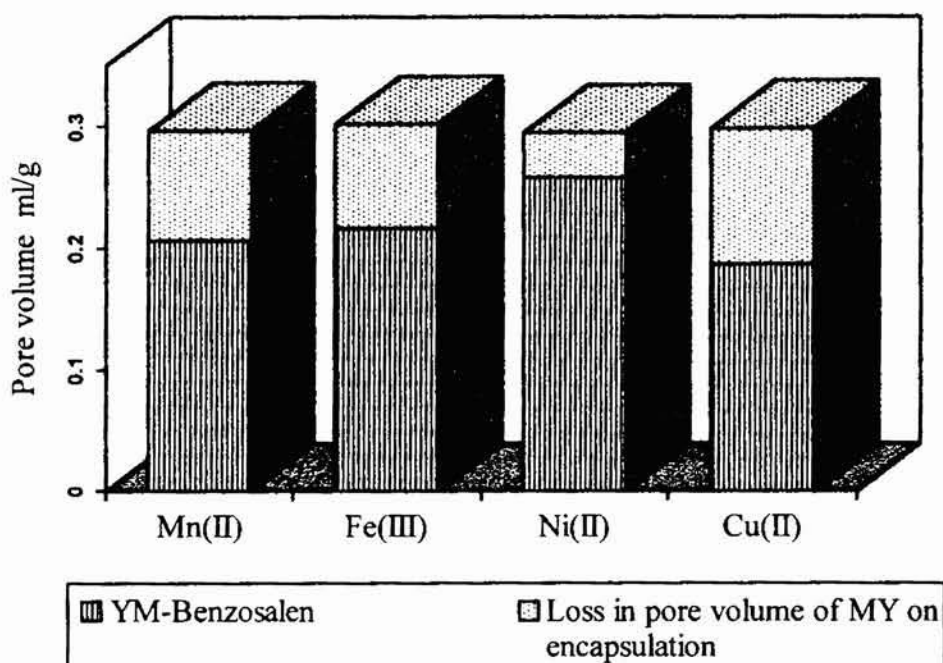


Figure VI. 4

Decrease of pore volume of metal exchanged zeolites on encapsulation

6. 3. 4 Magnetic moment

Table VI. 3

Magnetic moment data

Sample	Magnetic moment (BM)
YMn-Benzosalen	5.90
YFe-Benzosalen	5.81
YNi-Benzosalen	2.92
YCu-Benzosalen	1.80

Room temperature magnetic moments of Benzosalen complexes are given in Table VI. 3. Magnetic moments of 5.90 BM and 5.81 BM are observed for encapsulated Mn(II) and Fe(III) complexes respectively. These complexes can exhibit such values irrespective of the coordination environment⁸. Ni(II) octahedral complexes usually show

magnetic moments in the range 2.9-3.3 BM⁷. A magnetic moment of 2.92 BM observed for YNi-Benzosalen could therefore be attributed to an octahedral symmetry. YCu-Benzosalen complex exhibits a magnetic moment of 1.80 BM which might be due to a tetrahedrally distorted square planar structure⁷.

6. 3. 5 Electronic spectra

Kubelka-Munk (KM) analysis was performed on the reflectance data and KM factor, F(R), is plotted against wavelength as shown in Figure VI. 5. The electronic transitions and their tentative assignments are given in Table VI. 4.

Table VI. 4

Electronic spectral data

Sample	Abs. Max. (cm ⁻¹)	Tentative assignments
YMn-Benzosalen	25190	Charge transfer transition
	33220	Intraligand transition
YFe-Benzosalen	25190	Charge transfer transition
	33220	Intraligand transition
YNi-Benzosalen	12410	³ A _{2g} (F) → ³ T _{2g} (F)
	18080	³ A _{2g} (F) → ³ T _{1g} (F)
	23310	³ A _{2g} (F) → ³ T _{1g} (P)
	27400	Charge transfer transition
	40000	Intraligand transition
YCu-Benzosalen	12480	d-d transition
	33780	Intraligand transition

Note: The bands at ~ 6890 cm⁻¹ and ~ 5150 cm⁻¹ in the spectra of all samples are characteristic of zeolite lattice and not included in this table

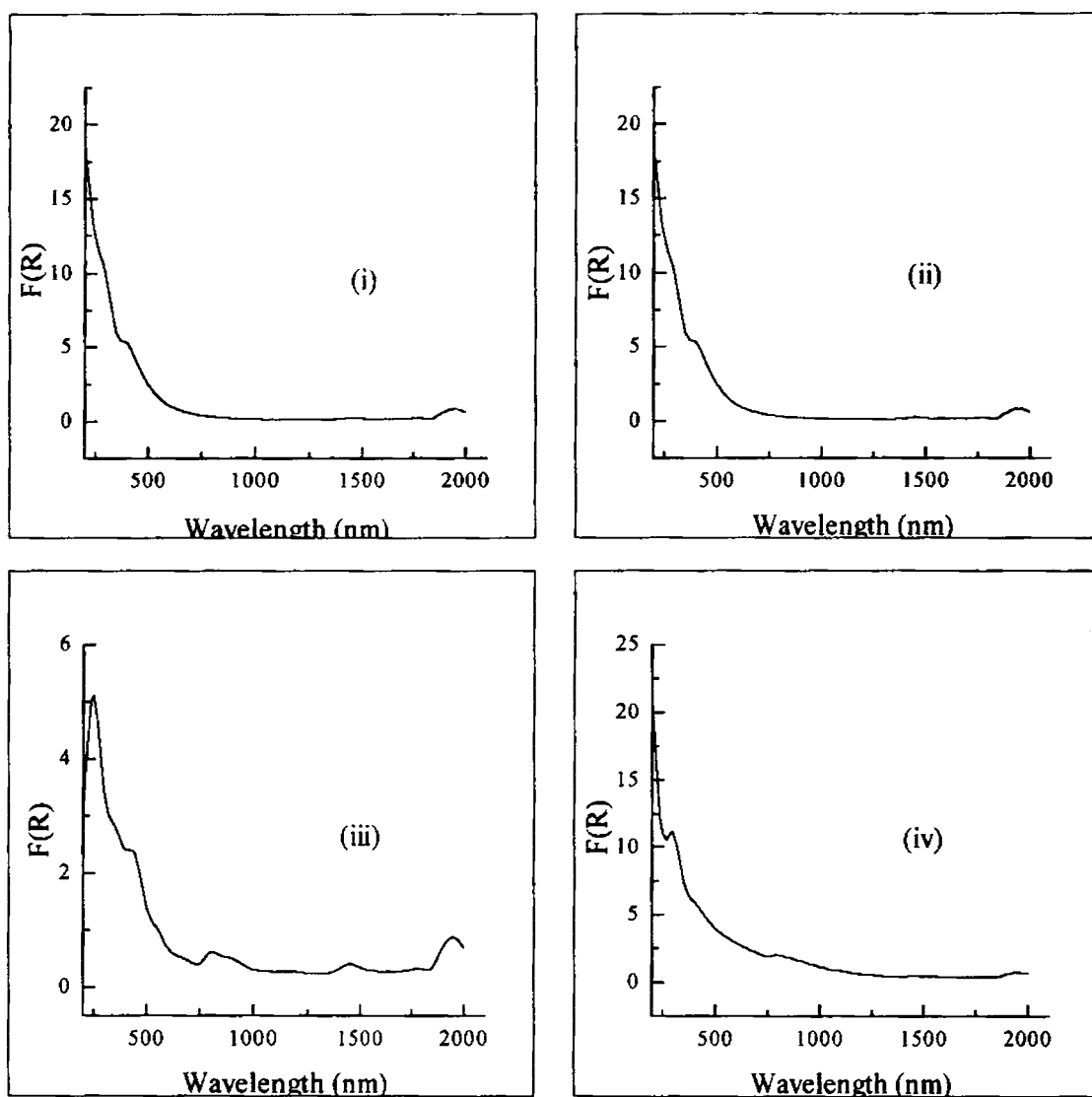


Figure VI. 5

Electronic spectra of encapsulated Benzosalen complexes

- (i) YMn-Benzosalen
- (ii) YFe-Benzosalen
- (iii) YNi-Benzosalen
- (iv) YCu-Benzosalen

The d-d transitions are not observed in the case of encapsulated Mn(II) or Fe(III) complexes as they are spin forbidden. The spectrum of YNi-Benzosalen shows d-d bands at 12410 cm^{-1} , 18080 cm^{-1} and 23310 cm^{-1} . These absorption bands agree with those reported for octahedral complexes of Ni(II) ion⁹. Therefore these bands could be attributed to ${}^3A_{2g}(F) \rightarrow {}^3T_{2g}(F)$, ${}^3A_{2g}(F) \rightarrow {}^3T_{1g}(F)$ and ${}^3A_{2g}(F) \rightarrow {}^3T_{1g}(P)$ transitions in octahedral Ni(II) complex. The magnetic moment value of 2.92 BM observed for encapsulated Ni(II) complex also suggests an octahedral symmetry. The water molecules in zeolite lattice or oxide ions of the framework are likely to involve in the octahedral symmetry of Ni(II) ion. YCu-Benzosalen shows d-d band at 12480 cm^{-1} .

6. 3. 6 FTIR spectra

IR spectra of Benzosalen and zeolite encapsulated complexes of Benzosalen are shown in Figure VI. 6. IR spectral bands of MY, Benzosalen ligand and zeolite complexes are listed in Table VI. 5.

The band at 1640 cm^{-1} in the spectrum of free ligand is due to the stretching vibration of C=N group. Usually, $\gamma_{C=N}$ shifts to lower frequency upon coordination¹⁰. This shift in frequency could not be clearly seen in the spectra of zeolite complexes as this band is masked by δ_{H-O-H} band of water molecules in zeolite. The participation of phenolic oxygen atoms in coordination could not be distinguished due to the presence of a broad γ_{O-H} band of water molecules at $3000\text{-}3500\text{ cm}^{-1}$.

In the spectra of the free ligand, the bands at 1140 cm^{-1} and 1295 cm^{-1} can be attributed to γ_{C-N} and γ_{C-O} vibrations respectively. These bands are not visible in the spectra of encapsulated Benzosalen complexes as they are obscured by the broad zeolite band at around 1000 cm^{-1} .

The bands observed for all zeolite complexes in the range $1500\text{-}1600\text{ cm}^{-1}$ are due to C-C stretching vibrations in benzene rings of the ligand. There are no zeolite bands present in the spectra at this position. Therefore, the aromatic bands in the spectra of

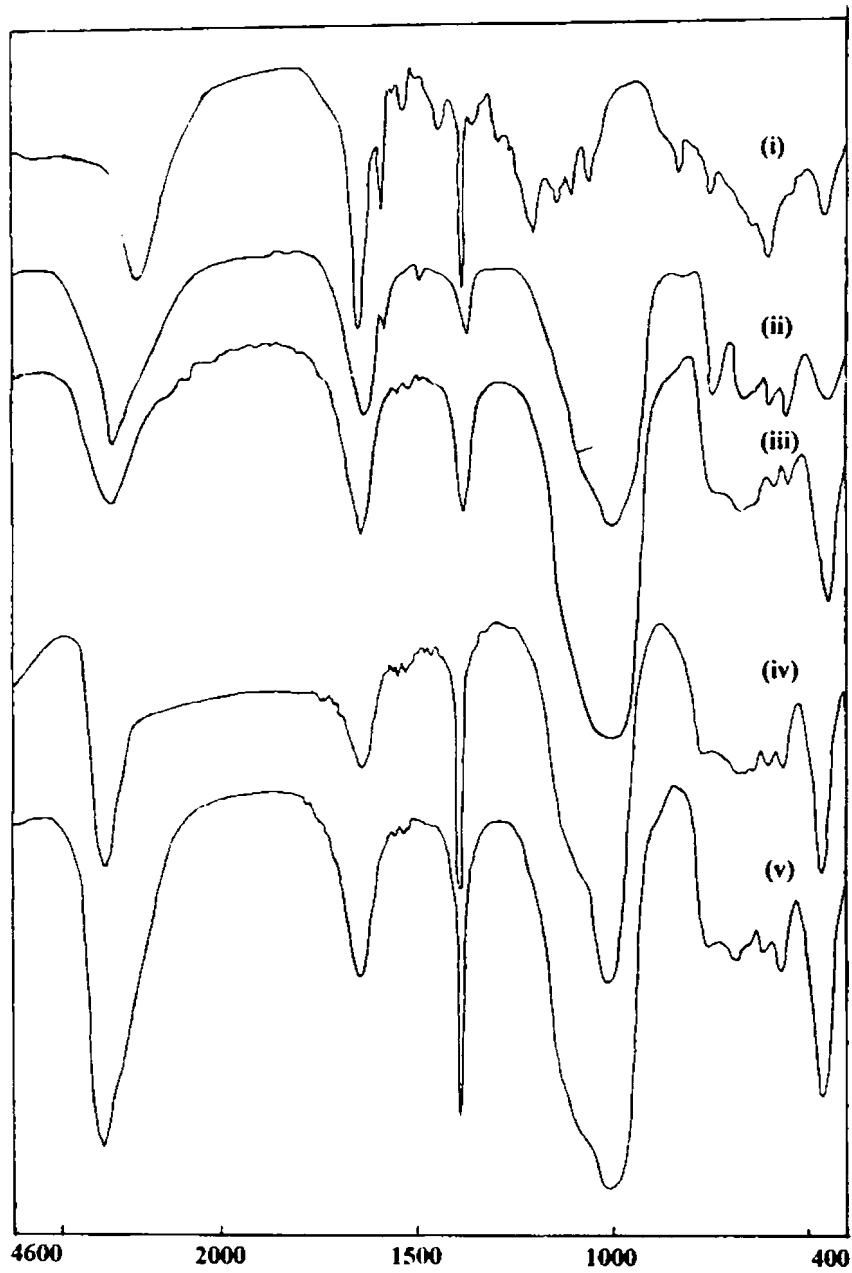


Figure VI. 6

IR spectra-(i) Benzosalen, (ii) YMn-Benzosalen, (iii) YFe-Benzosalen,
(iv) YCo-Benzosalen,(v) YNi-Benzosalen and (vi) YCu-Benzosalen

zeolite complexes confirms encapsulation. However, the coordination in encapsulated complexes could not be explained using IR spectra due to interferences of zeolite bands.

Table VI. 5

IR spectral data (cm^{-1}) of MY, Benzosalen and zeolite complexes

MY	Benzosalen	YMn- Benzosalen	YFe- Benzosalen	YNi- Benzosalen	YCu- Benzosalen
460	459	466	460	459	459
570	599	575	564	565	565
	648		613	612	615
680		680	680	700	680
750	751	759	752	730	754
				775	
1000	831	1006	1000	1007	1005
	1055				
	1100				
	1140				
	1200				
	1295				
	1351	1340			
	1383	1403	1380	1383	1385
	1438	1435		1455	
				1480	
		1500			1500
	1522		1520	1520	1525
	1550		1545	1545	1550
	1576	1586			
1650	1640	1639	1645	1648	1647
				1750	
	3039	3445	3475	3570	3480

6. 3. 7 EPR spectra

Figure VI. 7 shows the EPR spectrum of zeolite encapsulated Cu-Benzosalen complex. The EPR parameters, unpaired electron density and magnetic moment are given in Table VI. 6.

Table VI. 6
EPR spectral data

EPR parameter	YCu-Benzosalen
$g_{ }$	2.33
$A_{ }$	$151.9 \times 10^{-4} \text{ cm}^{-1}$
$g_{ } / A_{ }$	153.4 cm
g_{\perp}	2.02
A_{\perp}	$45.2 \times 10^{-4} \text{ cm}^{-1}$
α^2	0.80
μ_{eff}	1.84 BM

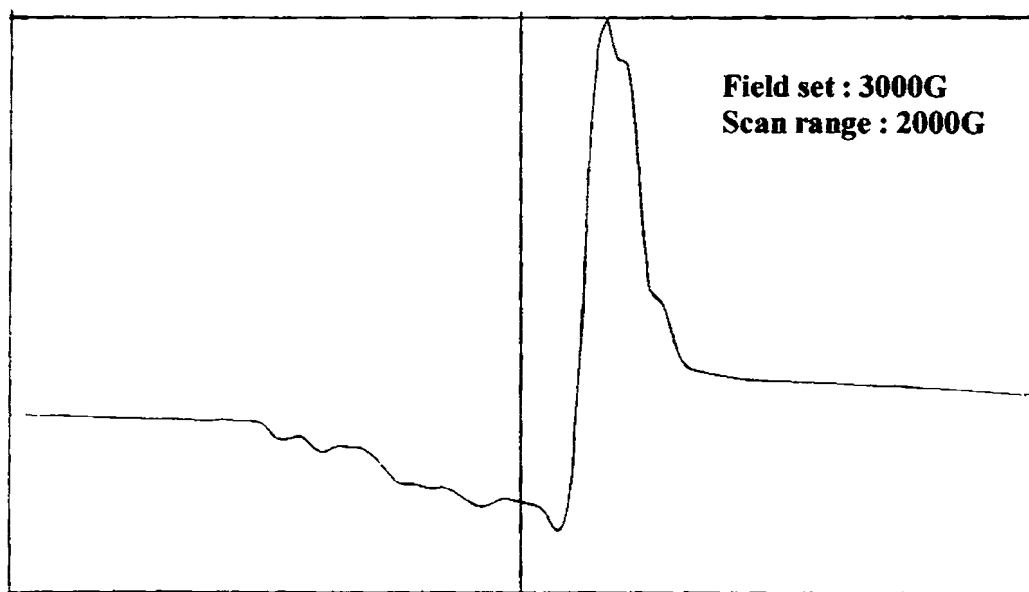


Figure VI. 7
EPR spectrum of YCu-Benzosalen

The g_{II} value, 2.33, corresponds to tetrahedrally distorted square planar complex¹¹. The ratio of g_{II} to A_{II} is 153.4 cm for YCu-Benzosalen. This value has been reported to be in the range 150-160 cm for flattened tetrahedral structure of Cu(II) complexes¹¹. Magnetic moment of 1.84 BM obtained from EPR parameters also hint tetrahedrally distorted square planar geometry⁷. The α^2 value of 0.80 indicates ionic environment for Cu^{2+} ions of encapsulated complex.

6.3.8 Thermal analysis

TG/DTG curves of zeolite encapsulated Benzosalen complexes are shown in Figure VI. 8. The removal of free moisture from zeolite samples was seen as the first stage in TG curves. The decomposition of encapsulated complexes is clearly visible as another stage in the case of Fe(III) and Cu(II) complexes. However, this weight loss is not well defined in other cases. The complete decomposition of encapsulated complexes was confirmed by analysing the residue obtained after the run for IR spectrum. The TG data is tabulated in Table VI. 7. The thermal stability of the complexes was found to vary in the order of metal ions as Mn(II) > Fe(III) > Cu(II) > Ni(II).

Table VI. 7

TG/DTG data

Sample	Weight loss-Stage I			Weight loss-Stage II		
	Temp. range (°C)	Peak temp. (°C)	% Mass loss	Temp. range (°C)	Peak temp. (°C)	% Mass loss
YMn-Benzosalen	60-275	170	13.4	450-520	505	2.4
YFe-Benzosalen	60-250	150	6.3	320-510	440	9.9
YNi-Benzosalen	60-310	170	19.8			
YCu-Benzosalen	70-250	155	12.7	350-475	430	3.7

TG curves of Benzosalen complexes are compared with those of corresponding metal exchanged zeolites in Figure VI. 9. The difference in the pattern of the curves could be taken as a clue for the encapsulation of Benzosalen complexes in zeolite cavities.

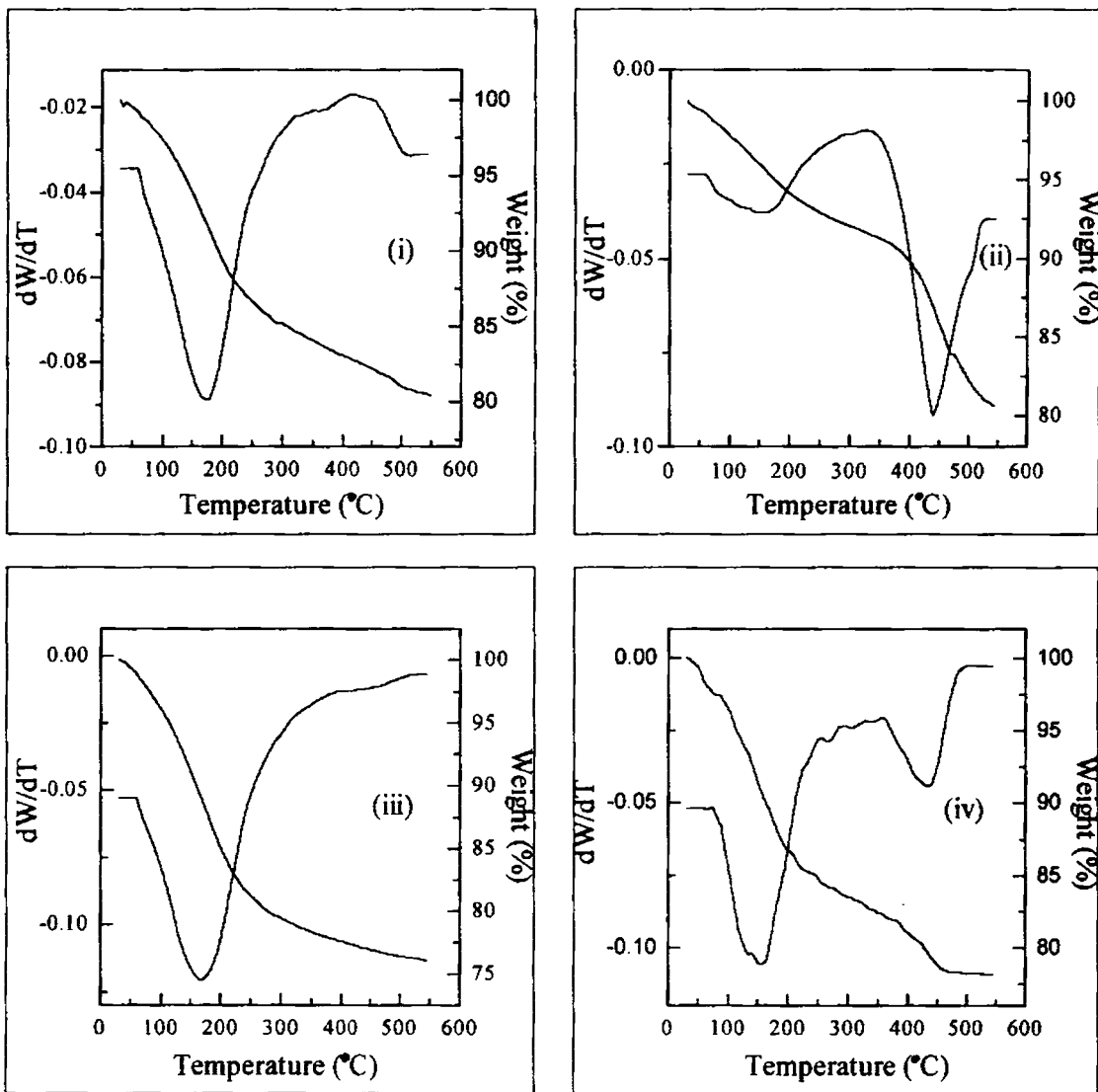


Figure VI. 8

TG/DTG curves of encapsulated Benzosalen complexes

- (i) YMn-Benzosalen
- (ii) YFe-Benzosalen
- (iii) YNi-Benzosalen
- (iv) YCu-Benzosalen

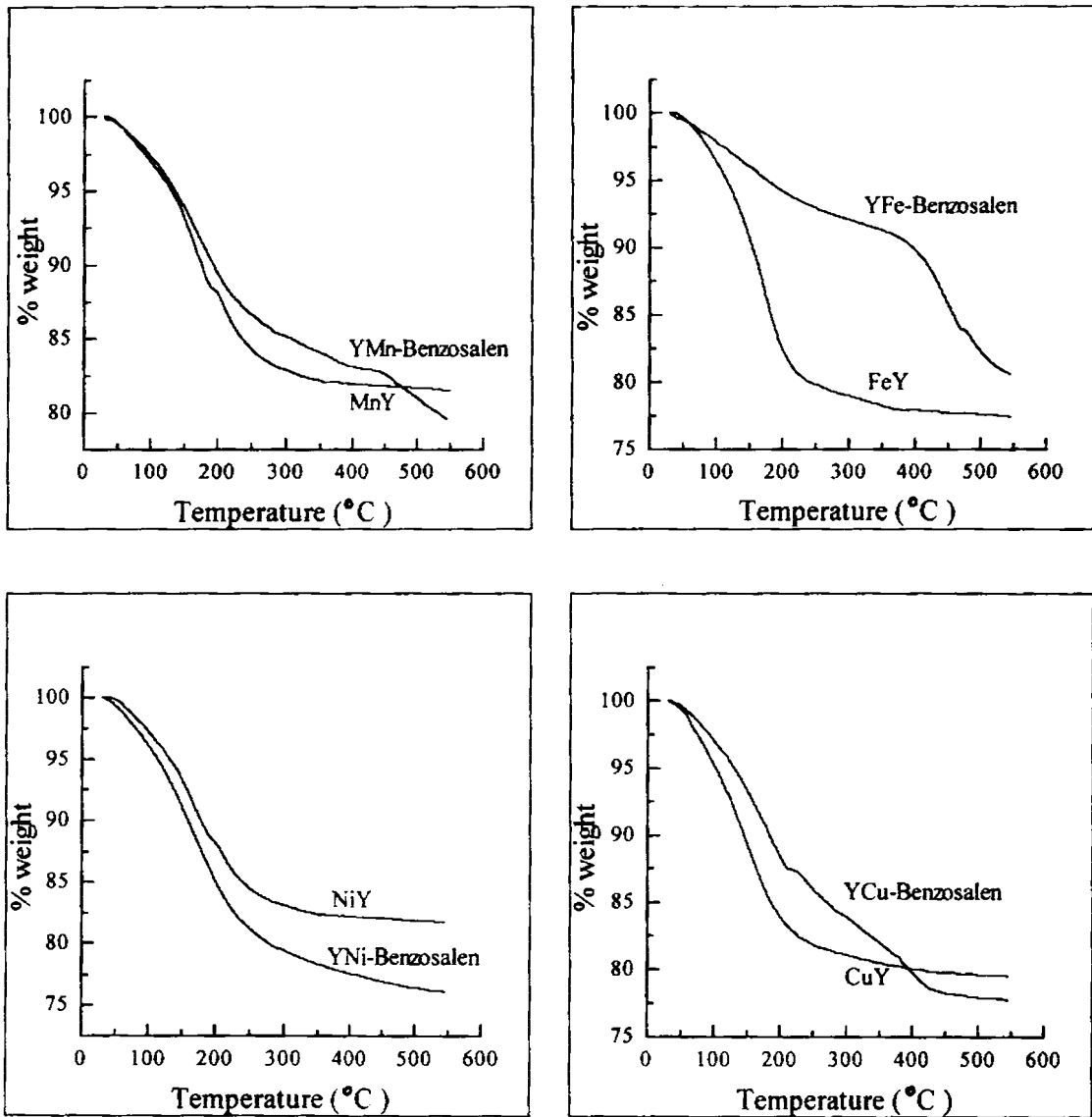


Figure VI. 9

TG curves of metal exchanged zeolites and zeolite complexes

6. 4 **SUMMARY AND CONCLUSION**

Chemical analysis reveals the formation of monomeric complexes of Mn(II), Fe(III), Ni(II) and Cu(II) with Benzosalen in the zeolite cavities. The lowering of surface area and pore volume of metal exchanged zeolites on encapsulation strongly support the occupancy of zeolite pores with metal complexes. Zeolite crystalline structure was found to remain unchanged on encapsulation as shown by XRD patterns. The encapsulated complexes of Ni(II) and Cu(II) ions are found to exhibit octahedral and tetrahedrally distorted square planar symmetry respectively. IR spectra also suggest the encapsulation of complexes. TG/DTG analysis ranks the complexes with respect to thermal stability in the order of metal ions as Mn(II) > Fe(III) > Cu(II) > Ni(II). The encapsulation of complexes accounts for the difference in the TG patterns of metal exchanged zeolites and zeolite complexes.

6.4 REFERENCES

1. S. P. Varkey and C. R. Jacob, *Ind. J. Chem.*, 37A (1998) 407
2. N. Ulagappan, *Proceedings of The 31st annual convention of chemists, Varanasi*, (1994) F1
3. R. Chandra, M. Anupa and P. Subhash, *Ind. J. Chem.*, 35A (1996) 1
4. T. Yamamoto, T. Shido, S. Inagaki, Y. Fukushima and M. Ichikawa, *J. Am. Chem. Soc.*, 118 (1996) 5810
5. P. C. H. Mitchell, *Chem. Ind.*, 6 May (1991) 308
6. Y. Fujii, Y. Kuwana, S. Takahashi, K. Shimizu and K. Hiroi, *Bull. Chem. Soc. Jpn.*, 55 (1982) 2598
7. N. N. Greenwood and A. Earnshaw, " *Chemistry of the Elements* ", Pergamon Press, 1984
8. A. Earnshaw, " *Introduction to Magnetochemistry* ", Academic Press, London, 1968
9. A. B. P. Lever, " *Inorganic Electronic Spectroscopy* ", Elsevier, Amsterdam, 1968
10. K. Nakamoto, " *Infrared Spectra of Inorganic and Coordination Compounds* ", 2 nd Ed., John-Wiley and Sons Inc. (1970) 232
11. U. Sakaguchi and A. W. Addison, *J. Chem. Soc., Dalton Trans.*, (1976) 600

CHAPTER VII

CATALYTIC STUDIES ON

ZEOLITE ENCAPSULATED COMPLEXES

Abstract

The catalytic activity of zeolite encapsulated complexes for hydrogen peroxide decomposition and the oxidation of benzyl alcohol or ethylbenzene with hydrogen peroxide has been investigated. The activity for the aerobic oxidation of organic substrates has also been studied. Zeolite complexes are suitable for the partial oxidation of organic compounds. Cu(II) complexes, especially that with 3-formyl salicylic acid have exhibited maximum activity. The recycling ability of this zeolite complex has also been tested. The poison resistance of the zeolite complexes has also been investigated. The encapsulated complexes of substituted salen ligands were evaluated for activity and poison resistance in comparison with that of salen. The bulkier salen like ligands reduce activity, but exhibit good poison resistance

7.1 INTRODUCTION

Zeolite encapsulated complexes are known to exhibit catalytic behaviour similar to the corresponding homogeneous complex catalysts. The reactivity of such systems is considered to be bio-mimetic due to their structural similarity with natural enzymes. The special interest on these catalytic materials is due to their ability to possess the advantages of both homogeneous and heterogeneous catalysis. Of late, intensive research efforts have been initiated to investigate the utility of zeolite complexes as catalysts for oxidation reactions¹⁻⁴. The efficiency of such systems depends, to a large extent, on the structural and electronic properties of encapsulated complexes. Therefore, the design and synthesis of novel zeolite complexes with improved characteristics and evaluation their catalytic activity are the main tasks in this area of investigation.

In this study, the following reactions were carried out on zeolite encapsulated complexes:

- a) Decomposition of hydrogen peroxide
- b) Oxidation of benzyl alcohol
- c) Oxidation of ethylbenzene
- d) Oxidation of 4-methoxybenzaldehyde

a) Decomposition of hydrogen peroxide

The catalytic decomposition of hydrogen peroxide has found wide application in the oxidation of organic substrates⁵. This process has attracted considerable attention in the development of an oxygen electrode for electrochemical fuel cells⁶. This reaction is also a convenient alternative to the electrolysis of water for the production of oxygen⁷. Furthermore, this reaction has been employed as a convenient and reliable test for the determination of catalytic activity⁸.

The decomposition of hydrogen peroxide has been studied homogeneously using transition metal ions and their complexes as catalysts⁹. Transition metal oxide or noble metal catalysts have been used for carrying out this reaction heterogeneously¹⁰.

Supported transition metal complexes have also received wide attention as catalysts for this application^{8, 11}. Zeolite encapsulated metal complexes are expected to be active for the decomposition of hydrogen peroxide.

b) Oxidation of benzyl alcohol/ethyl benzene

The complete oxidation of organic substrates over various catalysts has been studied at length, especially with respect to pollution control. However, studies on catalytic partial oxidation of hydrocarbons and oxygenated compounds are relatively scanty. But, the partial oxidation is an attractive method for the production of aldehydes and ketones from primary and secondary alcohols respectively. The production benzaldehyde from benzyl alcohol over perovskite catalysts is an excellent example for such partial oxidation¹². Catalytic oxidative dehydrogenation of ethylbenzene to acetophenone is also important in fine chemical industry¹³. This reaction could be taken as a model for the oxyfunctionalisation of hydrocarbons in catalytic studies.

c) Oxidation of 4-methoxybenzaldehyde

The Baeyer-Villiger oxidation or Dakin reaction for the synthesis of phenols from aldehydes using peracids or hydrogen peroxide is an important reaction in organic chemistry¹⁴. Methyltrioxorhenium (MTOR) has been reported to be an effective homogeneous catalyst for this oxidation with hydrogen peroxide¹⁵. A variety of phenols have been synthesized using this catalyst. However, the operational difficulty of this homogeneous catalyst was the major problem encountered in MTOR based process. Zeolite encapsulated transition metal complexes are generally considered to avoid operational inconvenience associated with homogeneous catalysis. It was therefore thought interesting to study the catalytic activity of zeolite complexes for the Baeyer-Villiger oxidation of 4-methoxybenzaldehyde.

In this study, zeolite encapsulated Mn(II), Fe(III), Co(II), Ni(II) and Cu(II) complexes of dmg, fsal, Mesalen and Benzosalen were screened with respect to the

efficiency for H_2O_2 decomposition and oxidation of benzyl alcohol or ethylbenzene. H_2O_2 and molecular oxygen are the oxidants used in this study. These oxidants are expected to be very effective due to their high mobility in zeolite cavities. The effect of oxidant/substrate mole ratio and reaction temperature on activity was studied. The recycling ability and the poison resistance properties of the catalysts were evaluated. The effect of using substituted ligands instead of salen in zeolite systems was investigated. The suitability of zeolite complex as catalyst for the oxidation of 4-methoxybenzaldehyde was studied using the most promising catalyst. The details of these studies are presented in this chapter.

7. 2 EXPERIMENTAL

7. 2. 1 Materials

Zeolite encapsulated complexes of dmg, fsal, Mesalen and Benzosalen were used for catalytic studies. The various reagents used for the experiments are mentioned in Chapter II.

7. 2. 2 Determination of Catalytic activity

a) Decomposition of hydrogen peroxide

The experimental set up used for the decomposition of hydrogen peroxide is shown in Figure VII. 1. The decomposition efficiency was evaluated by monitoring the volume of oxygen evolved using a gas burette attached to the reaction flask. The procedure of this test is as follows:

Hydrogen peroxide solution (30 ml, 10 % H_2O_2 (wt/v)) was taken in a reaction flask of 100 ml capacity containing a magnetic paddle for stirring. A plastic float containing catalyst sample (50 mg) was placed over the solution in the reaction flask.

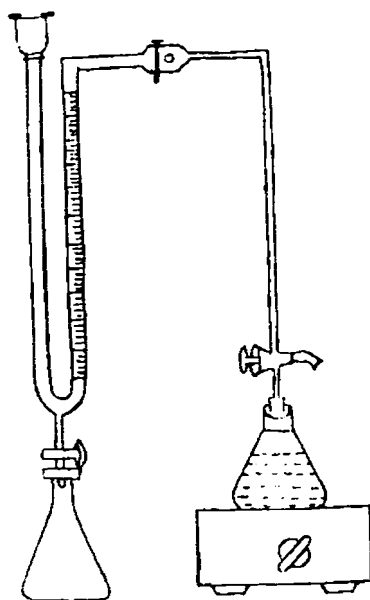


Figure VII. 1

Experimental set up for the decomposition of hydrogen peroxide

Gas burette was filled with ~ 20 % NaCl solution acidified with dil. HCl and coloured using methyl orange. The solution levels in both arms of gas burette were equalized at ' zero ' before connecting to reaction flask. The three-way valve connecting reaction flask and gas burette can be adjusted to maintain atmospheric pressure in the system before starting the reaction. The catalyst was dispersed in the H_2O_2 solution by magnetic stirring. As the reaction proceeds, oxygen liberated was collected in the right arm of gas burette. The volume of oxygen liberated was noted after equalizing the solution levels in both arms at intervals of 5 minutes. The experiment was continued until 10 ml (total capacity of gas burette) of oxygen was liberated or for 90 minutes.

b) Oxidation of benzyl alcohol/ethylbenzene

The experimental set up used for performing oxidation reactions is shown in Figure VII. 2. An oil bath with a temperature controller was used for maintaining the reaction temperature with an accuracy of ± 2 °C.

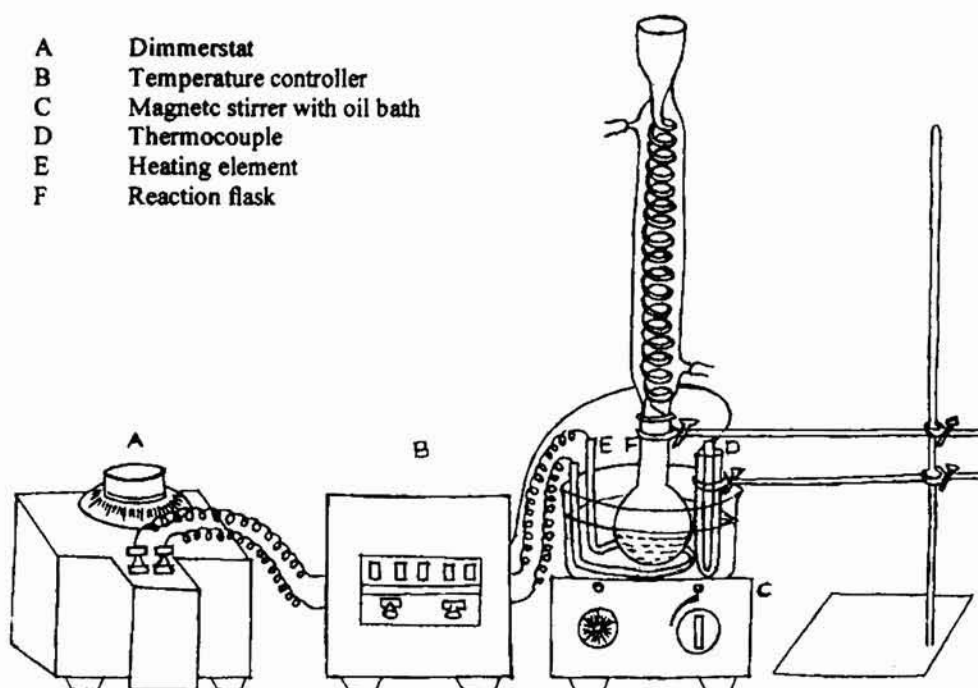


Figure VII. 2
Experimental set up for oxidation reaction

The procedure of the experiment is as follows: The catalyst sample (50 mg) was taken in the reaction flask containing a magnetic paddle. It was immersed in the oil bath whose temperature was previously adjusted to that specified for the test. The required amount of the substrate, benzyl alcohol or ethylbenzene and benzene (10 ml) was taken in the reaction flask. Hydrogen peroxide required for keeping the specified oxidant/substrate mole ratio was also added. The reaction mixture was stirred magnetically for 8 hours. After the experiment, the flask was cooled and the organic layer was separated. The aqueous layer was extracted several times with diethyl ether to collect the traces of substrate and product, dissolved in the aqueous solution. After evaporating ether, this extract was mixed with the organic layer collected previously. The product and unreacted substrate were analysed using gas chromatograph.

Molecular oxygen was also used as oxidant. A flow of dry air at 10 ml/minute was scrubbed in the substrate-solvent mixture in the reaction flask under atmospheric

pressure. Tertiary butyl hydrogen peroxide (0.25 ml) was added as an initiator for the reaction.

The reaction conditions specific to each test are given along with the results in section 7. 3. The oxidation activity of the catalyst was represented as the percentage conversion of the substrate.

c) *Oxidation of 4-methoxybenzaldehyde*

The experimental set up shown in Figure VII. 2 was used for the oxidation of 4-methoxybenzaldehyde. The procedure of the experiment is as follows: 4-methoxybenzaldehyde (1.57 g, 11.5 mmol) was mixed with hydrogen peroxide (30 % H_2O_2 (wt/v); 3.3 ml) and 10 ml methanol in the reaction flask. The oxidant/substrate mole ratio in this mixture was ~ 2.5 . 50 mg of the catalyst was added and the mixture was then stirred at 50 °C for 24 hours. Then, the reaction mixture was extracted with diethyl ether and the unreacted substrate was separated by silica gel column chromatography using a mixture of hexane and dichloromethane (7:3) as eluent.

7. 2. 3 Recycling test

After the initial activity measurement for the oxidation of benzyl alcohol, the catalyst in the aqueous layer of the reaction mixture was filtered, washed with acetone and again tested for activity at identical conditions. After the test, the catalyst was filtered and analysed for IR spectrum.

7. 2. 4 Poison resistance test

The poison resistance of encapsulated complexes was studied by determining the activity using a substrate containing traces of pyridine. The percentage loss in activity indicates the extent of deactivation by poisoning.

7.2.5 Catalytic studies on salen type complexes

The activity and poison resistance properties of the encapsulated Cu(II) complexes of substituted salens, Mesalen and Benzosalen were studied in comparison with those of zeolite Cu(II)salen complex. Zeolite encapsulated Cu(II)salen was synthesized for this purpose as per the method given in the literature¹⁶.

7.3 RESULTS

(a) Decomposition of hydrogen peroxide

The H₂O₂ decomposition data are given in Table VII. 1. The catalysts can be graded with respect to the decomposition activity on the basis of volume of oxygen evolved and time taken for this evolution. Figure VII. 3, a plot of volume of oxygen liberated against time, provides a comparison of the rate of decomposition of hydrogen peroxide over encapsulated complexes of each ligand.

Table VII. 1

Hydrogen peroxide decomposition data

	dmg		fsal		Mesalen		Benzosalen	
	Duration (min.)	V _{O2} (ml)						
YMn(II)	90	1.92	90	2.78	90	3.75	90	3.88
YFe(III)	90	5.45	90	3.20	90	3.70	90	3.42
YCo(II)	90	7.18	65	9.47	90	8.31	*	*
YNi(II)	90	6.44	90	4.56	90	2.44	90	2.40
YCu(II)	35	9.59	15	8.9	55	9.56	45	9.45

* Co-Benzosalen could not be encapsulated (vide page 145)

Reaction conditions

Catalyst weight	50 mg	Temperature	30 °C
H ₂ O ₂ (10 %)	30 ml	Duration	90 min.

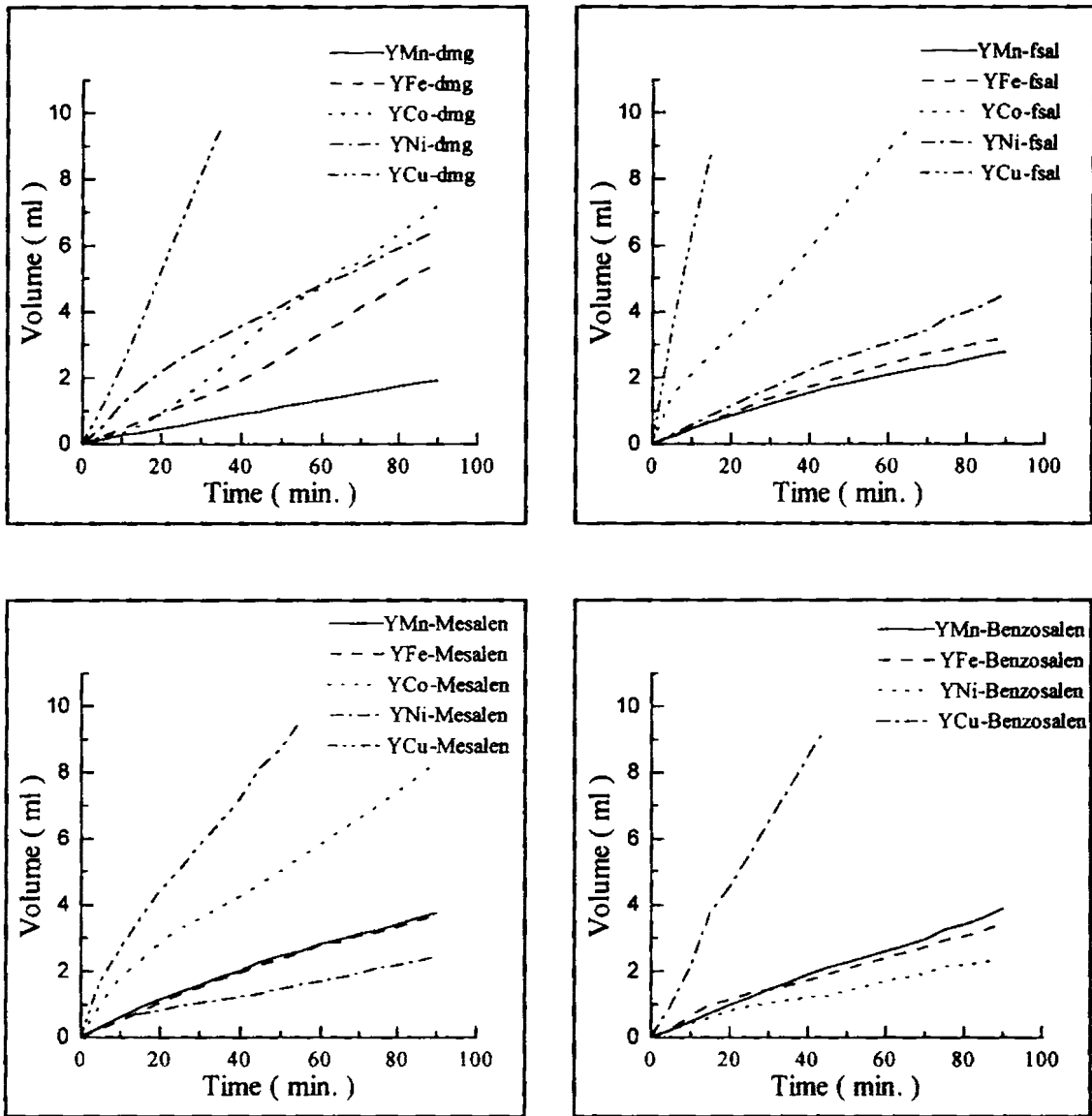


Figure VII. 3

H_2O_2 decomposition - Volume of oxygen liberated versus time

Since hydrogen peroxide itself decomposes in alkaline medium, a solution of pH ~ 6 was used for determining the activity of the catalyst. A blank experiment was carried out at identical test conditions using NaY zeolite. Only a negligible decomposition, which might be due to impurities, was observed over NaY zeolite. The decomposition data reveal that the catalytic activity of Cu(II) complexes is higher than that of complexes of

other metal ions. Co(II) complexes are found to be moderately active as compared to others. The complexes of Mn(II), Fe(III) and Ni(II) ions are weakly active. In general, the decomposition efficiency of zeolite encapsulated complexes of each ligand varies in the order of metal ions as Cu(II) > Co(II) > Ni(II) ~ Mn(II) ~ Fe(III).

The decomposition data of Cu(II) complexes are represented in Figure VII. 4. Among them, fsal complex shows distinctly better activity than others. The activity of Cu(II) complexes varies in the order YCu-fsal > YCu-dmg > YCu- Mesalen ~ YCu-Benzosalen. There is only a minor difference in activity between YCu-Mesalen and YCu-Benzosalen.

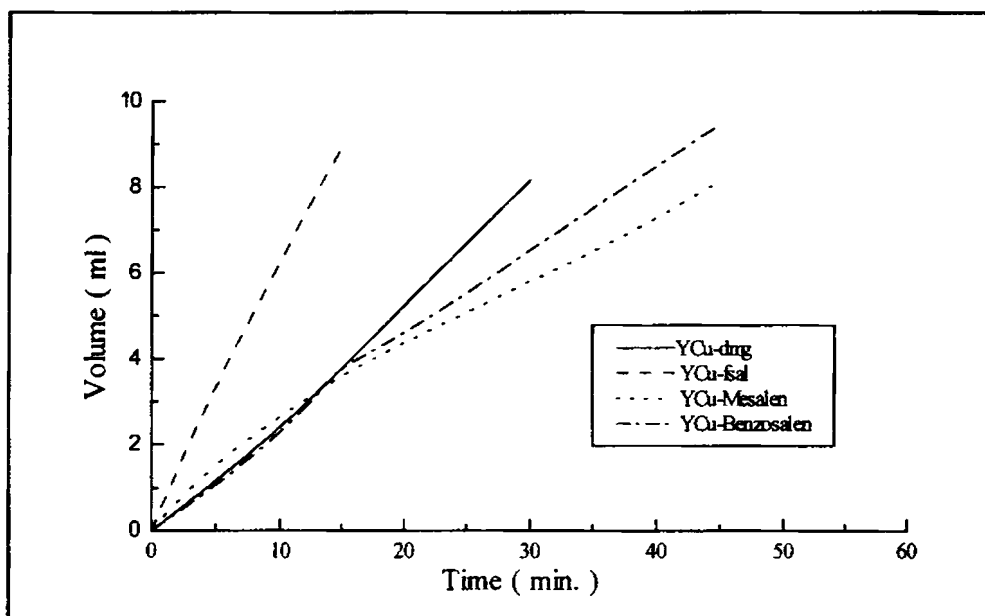


Figure VII. 4

H₂O₂ decomposition data of encapsulated Cu(II) complexes

b) Oxidation of benzyl alcohol/ethyl benzene

The oxidation of benzyl alcohol or ethylbenzene was performed over the zeolite complexes using H₂O₂ or molecular oxygen as the oxidant. The extent of oxidation of organic substrates usually depends on the relative concentration of oxidant in the reaction mixture. Therefore, oxidant/substrate mole ratio was optimized for the

oxidation of benzyl alcohol with hydrogen peroxide. YCu-fsal, the most active catalyst for H₂O₂ decomposition was used for this optimization study. The oxidant/substrate mole ratio was varied in the range 0.5-2.5. The effect of mole ratio on activity is represented as a plot of % conversion of benzyl alcohol against the oxidant/substrate mole ratio in Figure VII. 5. The oxidation efficiency was found to be enhanced on increasing the mole ratio upto 2 and then almost stabilised in the range 2.0-2.5. Therefore, the optimum mole ratio can be fixed as 2.0-2.5. In this study, the oxidant/substrate mole ratio was kept at 2.5 for carrying out the oxidation reactions.

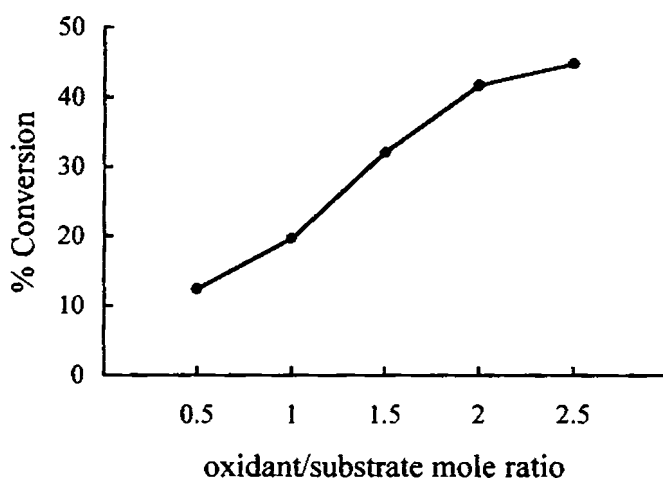


Figure VII. 5

% Conversion of benzyl alcohol versus oxidant/substrate mole ratio

Reaction conditions

Catalyst weight	50 mg	Temperature	50 °C
Benzyl alcohol	5 ml	Duration	8 hours
Solvent (benzene)	10 ml		

The catalytic activity for the oxidation of benzyl alcohol was determined with a view to screen the zeolite encapsulated complexes. These results are given in Table VII. 2 and are represented as bar chart in Figure VII. 6. A blank reaction was carried out on zeolite NaY under the same reaction conditions. There was only negligible reaction over Zeolite NaY indicating that it is inactive for the oxidation reaction.

Table VII. 2

Activity for benzyl alcohol oxidation

	dmg	fsal	Mesalen	Benzosalen
YMn(II)	11.6	7.4	6.9	9.3
YFe(III)	13.5	6.9	8.3	8.9
YCo(II)	18.7	23.5	12.1	
YNi(II)	12.9	7.1	8.1	12.1
YCu(II)	30.0	44.7	28.3	32.7

Reaction conditions

Catalyst weight	50 mg	Temperature	50 °C
Benzyl alcohol	5 ml	Duration	8 hours
Oxidant/substrate	2.5		
Solvent (benzene)	10 ml		

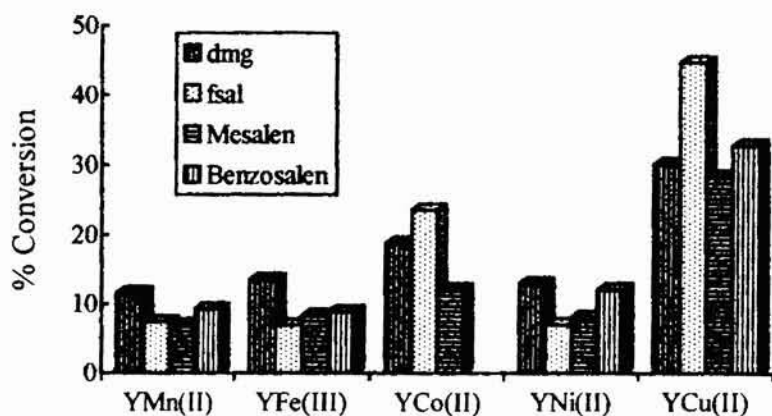


Figure VII. 6

% Conversion of benzyl alcohol over zeolite complexes

The oxidation efficiency of zeolite Cu(II) complexes is much greater than that of corresponding complexes of other metal ions. The Co(II) complexes of dmg and fsal are also active, but not to the extent of respective Cu(II) complex. However, the activity of YCo-Mesalen is not promising. Among Cu(II) complexes, YCu-fsal is distinctly better as compared to others. However, the activity of other Cu(II) complexes, YCu-dmg,

YCu-Mesalen and YCu-Benzosalen are comparable to each other and about 30% lower than that of YCu-fsal. From the above results, it was understood that zeolite encapsulated Cu(II) complexes exhibit maximum activity and, therefore, further catalytic studies were confined to only Cu(II) complexes.

Table VII. 3

Effect of reaction temperature on benzyl alcohol oxidation

Reaction temp. (°C)	YCu-dmg	YCu-fsal	YCu-Mesalen	YCu-Benzosalen
50	30.0	44.7	28.3	32.7
60	40.8	61.6	36.8	44.2
70	52.6	76.7	47.7	56.1

Reaction conditions

Catalyst weight	50 mg	Temperature	50/60/70°C
Benzyl alcohol	5 ml	Duration	8 hours
Oxidant/substrate	2.5		
Solvent (benzene)	10 ml		

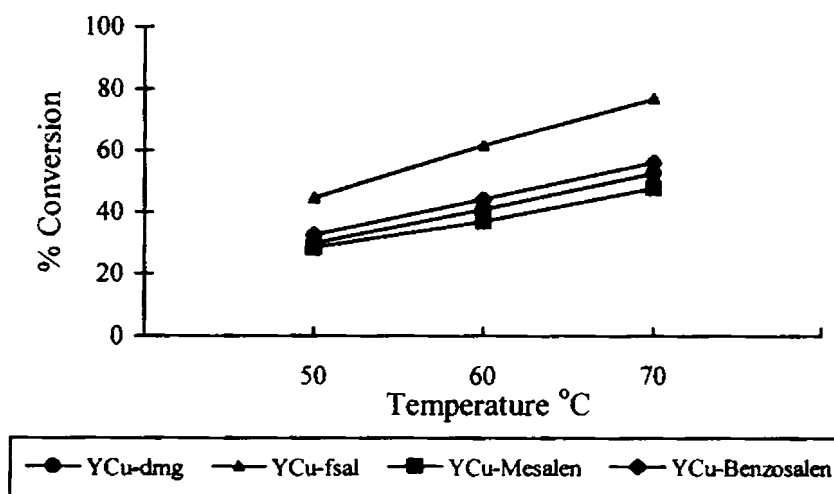


Figure VII. 7

% Conversion of benzyl alcohol versus reaction temperature

The oxidation of benzyl alcohol was carried out at temperatures 50 °C, 60 °C and 70 °C with a view to evaluate the influence of reaction temperature on oxidation activity. These activity results are given in Table VII. 3. The variation of activity on increasing the temperature is shown in Figure VII. 7. Generally, the activity is found to increase on increasing the reaction temperature. From the plot, it is clear that the extent of elevation of activity with temperature is higher for YCu-fsal.

Table VII. 4
Effect of reaction temperature on ethylbenzene oxidation

Reaction temp. (°C)	YCu-dmg	YCu-fsal	YCu-Mesalen	YCu-Benzosalen
50	24.0	37.8	23.1	25.9
60	33.6	51.2	29.4	33.7
70	46.3	65.6	39.2	43.8

Reaction conditions

Catalyst weight	50 mg	Temperature	50/60/70 °C
Ethylbenzene	5 ml	Duration	8 hours
Oxidant/substrate	2.5		
Solvent (benzene)	10 ml		

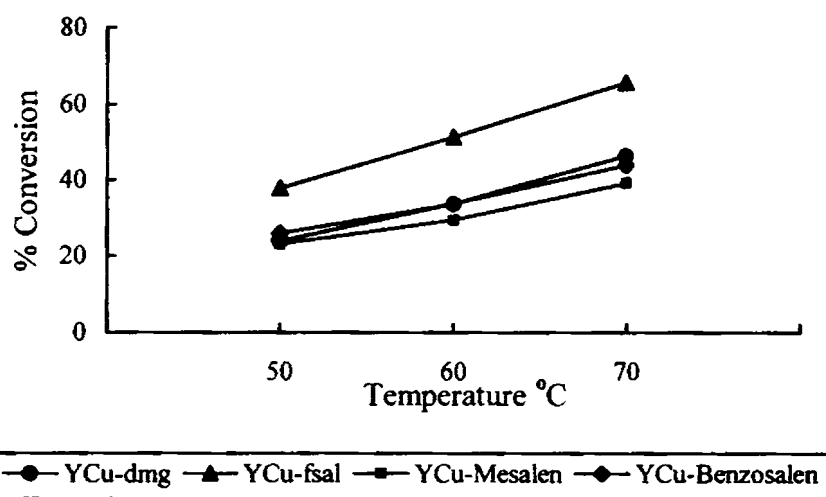


Figure VII. 8

% Conversion of ethylbenzene versus reaction temperature

The results of ethylbenzene oxidation are given in Table VII. 4. The % conversion of ethylbenzene is higher for YCu-fsal as in the case of benzyl alcohol oxidation. Figure VII. 8 indicates that the activity for ethylbenzene oxidation also increases on increasing the reaction temperature. However, the activity values are lesser in this case as compared to those for benzyl alcohol oxidation. YCu-fsal showed 90 % conversion for the oxidation of 4-methoxybenzaldehyde.

The oxidation reactions were also carried out using molecular oxygen. The efficiency of encapsulated Cu(II) complexes for the aerobic oxidation is lower than that obtained when hydrogen peroxide is used as the oxidant. However, YCu-fsal is much better than others for aerobic oxidation as well. During benzyl alcohol oxidation, the formation of traces of benzoic acid is quite possible by the oxidation of benzaldehyde on contacting with air. However, it would not affect the comparative evaluation of zeolite complexes.

Table VII. 5

Activity results of benzyl alcohol / ethylbenzene oxidation with oxygen

	YCu-dmg	YCu-fsal	YCu-Mesalen	YCu-Benzosalen
<u>Benzyl alcohol oxidation</u>				
% Conversion	18.6	28.1	16.8	19.8
<u>Ethylbenzene oxidation</u>				
% Conversion	16.8	24.1	11.1	12.9

Reaction conditions

Catalyst weight	50 mg	Temperature	50 °C
Substrate	5 ml	Duration	12 hours
TBHP	0.25 ml	Air flow	10ml/min.
Solvent (benzene)	10 ml	Pressure	atmospheric

The ability of YCu-fsal to recycle for the oxidation of benzyl alcohol was evaluated. The initial conversion of 44.7% is reduced to 42.3% indicating a marginal loss in activity

on recycling the catalyst. The IR spectrum of the reused sample is quite similar to that of fresh sample.

Table VII. 6
Poison resistance of Cu(II) complexes

%Conversion	YCu-dmg	YCu-fsal	YCu-Mesalen	YCu-Benzosalen
without poisoning	30.0	44.7	28.3	32.7
with poisoning	14.2	27.1	20.5	20.9
% Loss in conversion	52.7	39.4	27.6	36.1

Reaction conditions

Catalyst weight	50 mg	Temperature	50 °C
Benzyl alcohol with traces of pyridine	5 ml	Duration	8 hours
Solvent (benzene)	10 ml		

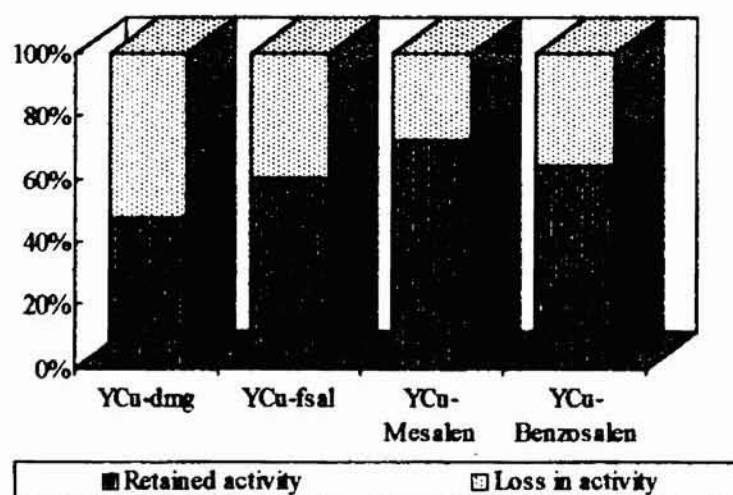


Figure VII. 9
Poison resistance of encapsulated Cu(II) complexes

The poison resistance of Cu(II) complexes was evaluated using benzyl alcohol poisoned with pyridine as substrate. The activity results of this test along with those of

corresponding fresh catalysts are presented in Table VII. 6. Figure VII. 9 provides an idea about the rate deactivation of different Cu(II) complexes on poisoning. The encapsulated Cu(II) complexes can be graded with respect to poison resistance as YCu-Mesalen > YCu-Benzosalen ~ YCu-fsal > YCu-dmg.

Table VII. 7

Activity of Cu(II) complexes of salen and substituted salens

% Conversion	YCu-salen	YCu-Mesalen	YCu-Benzosalen
Without poisoning	37.8	28.3	32.7
With poisoning	20.3	20.5	20.9
% Loss in conversion	46.3	27.6	36.1

Reaction conditions

Catalyst weight	50 mg	Temperature	50 °C
Benzyl alcohol with traces of pyridine	5 ml	Duration	8 hours
Solvent (benzene)	10 ml		

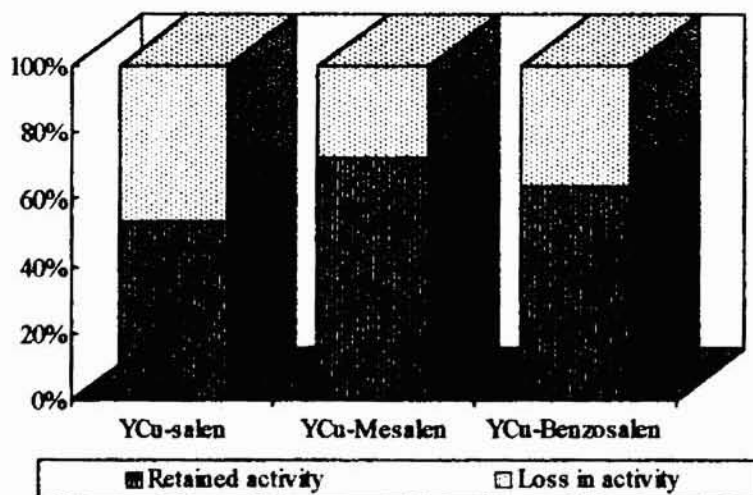


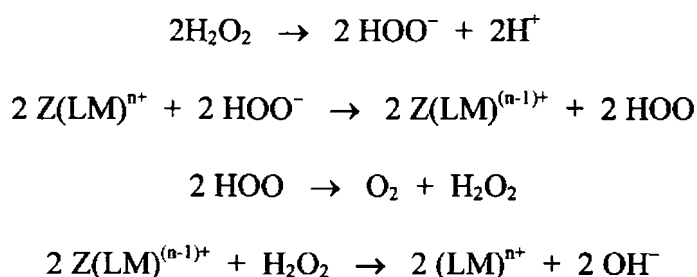
Figure VII. 10

Poison resistance of salen and substituted salen complexes

The oxidation activity and poison resistance of zeolite encapsulated Cu(II) complexes of salen and substituted salens are presented in Table VII. 7. The poison resistance of these catalysts is represented in Figure VII. 10. From these results, the effect of using bulkier salen like ligands on catalytic activity can be assessed in comparison with salen ligand. The oxidation activity of YCu-salen is better than that of encapsulated complex of Mesalen or Benzosalen. However, YCu-salen was undergone severe deactivation on poisoning, whereas YCu-Mesalen and YCu-Benzosalen are more resistant to poisoning. The poison resistance of these complexes varies in the order YCu-Mesalen > YCu-Benzosalen > YCu-salen.

7.4 DISCUSSION

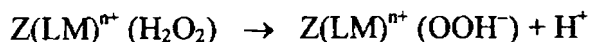
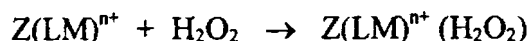
The decomposition of hydrogen peroxide is usually catalysed by transition metal ions or their complexes. In order to explain this reaction, a radical chain mechanism has been proposed in which the catalyst increases the rate of initiation reaction for the formation of HOO radical¹⁶. In the case of zeolite encapsulated complexes, this mechanism can be represented as follows:



As per this reaction scheme, the redox potential of active metal ion plays a vital role in the decomposition of hydrogen peroxide. The coordination of metal ion with ligand may slightly alter the redox potential and as a result of this, a modified catalytic activity might have obtained

In another mechanism proposed, the decomposition reaction occurs in the coordination sphere of the metal ion with the formation of intermediate peroxo species, $(\text{LM}^{n+})(\text{OOH})$ ^{9, 11}.

The following reaction scheme may be suggested for this mechanism:



This peroxo intermediate can also be formed by the action of OOH^- generated from free H_2O_2 molecules in solution.

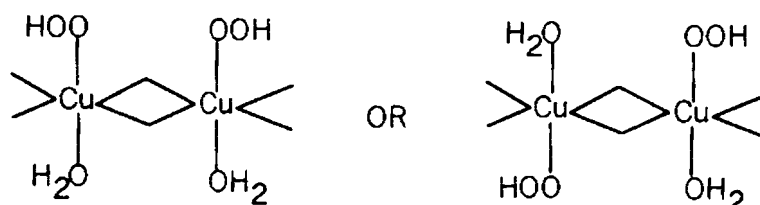


The accessibility of the coordination sphere for H_2O_2 or OOH^- and the availability of vacant coordination sites at the metal ion are the main requirements for the decomposition to proceed via this mechanism. Sigel has found that the vacant coordination site in copper polyamine chelate leads to high decomposition rate whereas fully coordinated Cu(II) complexes are inactive¹⁷. Mn(II) and Fe(III) chelates of diethyltriammine have also been found to be active as two metal sites are available for coordination with peroxo anions¹⁸.

In the case of zeolite encapsulated complexes, the mechanism involving peroxo intermediates is more probable at the available coordination sites of metal ion. A colour change was observed for the complexes on contacting with H_2O_2 which is an indicative of the formation of intermediate peroxo species. Similar colour change has been found in the case of supported Cu(II) complex by previous workers¹¹.

The decomposition data show that zeolite encapsulated Cu(II) complexes are more active than other metal complexes. The characterization data of these complexes indicate the possibility of a tetrahedrally distorted square planar geometry for Cu(II) complexes. This geometry may facilitate the formation of peroxo intermediates in the coordination sphere leading to enhanced decomposition activity. The distinctly better activity of YCu-fsal among encapsulated Cu(II) complexes may be due to the formation of an intermediate in which two peroxo groups are coordinated in the binuclear structure

as shown below. The formation of such active peroxy intermediates in binuclear complexes has been proposed in earlier studies¹⁹.

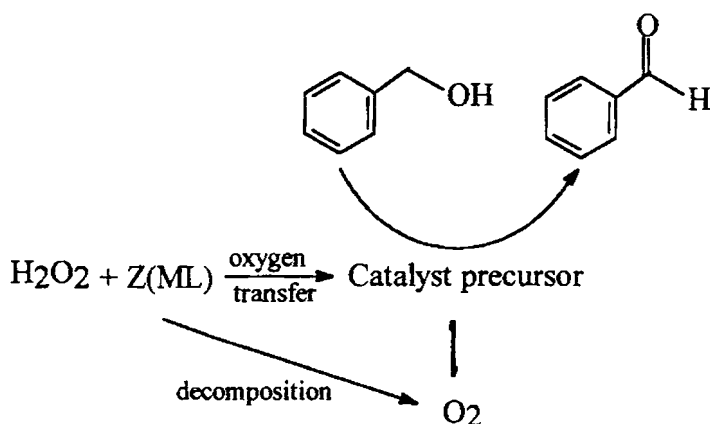


Although Co(II) complexes possess octahedral or tetrahedral symmetry with no vacant sites, they are moderately active indicating the formation of peroxy intermediates on them. The peroxy species can be formed in octahedral Co(II) complexes only by the replacement of coordinated water molecules or oxide ions of zeolite framework, whereas in tetrahedral symmetry, a rearrangement of coordination sphere is essential for the reaction to proceed. The process of ligand replacement or rearrangement of coordination sphere restricts the rate of formation of peroxy intermediate which leads to a lower activity for Co(II) complex as compared to Cu(II) complex. YNi-dmg is also moderately active, may be because of the slightly distorted square planar symmetry observed for it. The other Ni(II) complexes are comparatively inactive as they possess an octahedral symmetry. All the Mn(II) and Fe(III) complexes are weak for H₂O₂ decomposition. The fine-tuning of redox potentials of metal ions by ligation also might have played a major role in the decomposition of H₂O₂.

Zeolite encapsulated complexes can be screened with respect to the catalytic activity for the oxidation of benzyl alcohol. The oxidation of benzyl alcohol is negligible over NaY zeolite under the same experimental conditions employed for screening zeolite complexes. This indicates that zeolite support is inactive for the oxidation reaction. Furthermore, hydrogen peroxide only slightly oxidises these substrates in the absence of a catalyst. Therefore, the catalysis by encapsulated complex is the sole reason for the oxidation reaction. The percentage conversion of benzyl alcohol varies depending on the nature of encapsulated complex. This observation also suggests that the reaction is

catalytic in nature i.e. it proceeds by the catalysis of metal complexes encapsulated in zeolite.

The optimum oxidant/substrate mole ratio was found to be 2.5 for the oxidation of benzyl alcohol over YCu-fsal. An excess of hydrogen peroxide is required because of its parallel decomposition which is independent of the oxidation of organic substrate. The oxygen gas liberated may partially involve in the oxidation reaction by interacting with the active sites of the catalyst²⁰. The catalytic oxidation of benzyl alcohol to benzaldehyde can be represented as given below:



The above mechanism involves the interaction of the encapsulated complex with hydrogen peroxide. The oxidant donates an oxygen atom to coordinate at the vacant metal site in the complex forming the catalyst precursor. This oxygen atom is transferred to benzyl alcohol molecule approaching the metal complex to form benzaldehyde. The interaction of the substrate with the catalyst precursor is considered to be weak as per this mechanism. The ability of transition metal complexes to oxidise non-interacting type compounds like saturated hydrocarbons may hint the lack of interactions between the metallic site and substrate²¹. The oxidation of ethylbenzene is also expected to follow a similar mechanism.

Zeolite encapsulated Cu(II) complexes are found to be more active than others for the oxidation of benzyl alcohol. The tetrahedrally distorted square planar structure of these complexes may account for their higher activity. High activity is also expected for Co(II) complexes as they are usually very efficient for the reversible adsorption of

oxygen. But, YCo-dmg and YCo-fsal are only moderately active as compared to Cu(II) complexes, whereas YCo-Mesalen is weakly active. The octahedral symmetry of YCo-dmg and YCo-Mesalen and tetrahedral symmetry of YCo-fsal may restrict them to effectively catalyse oxidation reactions. The structure necessitates the replacement of coordinated water molecules in octahedral case and the rearrangement of coordination sphere in tetrahedral case for the catalysis to occur. In spite of having distorted square planar geometry, YNi-dmg is weakly active, may be because of the poor affinity of Ni sites for oxygen atoms to form the intermediate complex. The poor activity of other Ni(II) complexes can be attributed to their octahedral geometries in zeolite pores. The encapsulated Fe(III) and Ni(II) complexes are generally inactive. However, the oxidation activity of all zeolite complexes increases on increasing the reaction temperature.

The structure of encapsulated Mn(II) and Fe(III) complexes could not be recognized from their magnetic moment and electronic spectral data. However, the lower catalytic activity of these complexes hints the absence of vacant coordination sites. Therefore, an octahedral symmetry can be assumed for encapsulated Mn(II) and Fe(III) complexes.

YCu-fsal is superior to other Cu(II) complexes with respect to oxidation activity. The binuclear structure of Cu-fsal is expected to have facilitated the reaction by forming an intermediate precursor complex, which is entirely different from that formed on mononuclear complexes. However, further studies are necessary to confirm the effect of binuclear structure. The oxidation activity of other Cu(II) complexes is comparable to each other and less than that of YCu-fsal by around 30 %. Similar trend could be observed in the efficiency of Cu(II) catalysts for the oxidation of ethylbenzene also. However, these values are slightly lower than corresponding values for benzyl alcohol oxidation showing the difficulty in oxidising hydrocarbons YCu-fsal is also active for the oxidation 4-methoxybenzaldehyde.

Zeolite encapsulated complexes have been found to be active for the aerobic oxidation of organic substrates⁴. The ability of zeolite complexes for the oxidation of

benzyl alcohol and ethylbenzene with molecular oxygen was evaluated. The activity observed in these cases is lower than that obtained on using hydrogen peroxide as oxidant. The ability of H_2O_2 to donate active oxygen atoms to metallic site might be the reason for the higher reactivity.

The oxidation of benzyl alcohol with hydrogen peroxide over zeolite complexes gives benzaldehyde as the exclusive product. In contrast to conventional metal oxides, the formation of benzoic acid by the further oxidation of benzaldehyde or other side products is not observed in the present cases. This shows that zeolite encapsulated complexes can act as catalysts for partial oxidation. Similar behaviour of zeolite encapsulated iron phthalocyanine complex for the partial oxidation of hydrocarbons has been reported²².

One of the attractive features of zeolite encapsulated complexes is the ability to be recycled without much deterioration. The recycling test was performed on YCu-fsal. The retention of catalytic activity indicates the ability of this system to be used for longer periods and to be recycled in oxidation reactions. The IR spectrum recorded for the catalyst collected after recycling test is quite comparable to that of fresh sample showing little changes in the coordination of the ligand. The zeolite framework is expected to prevent the deactivation of encapsulated complexes by processes like dimerisation. Furthermore, there is no scope for the leaching of metal complexes as observed in polymer supported systems due to their exclusive immobilization in zeolite cavities.

Poison resistance properties of encapsulated Cu(II) complexes were studied by using a substrate poisoned with traces of pyridine. The extent of poison resistance was found to vary as YCu-Mesalen > YCu-Benzosalen ~ YCu-fsal > YCu-dmg. In the case of YCu-Mesalen, the steric effects of methyl group may prevent the approach of pyridine molecules to the vacant coordination sites. Relatively, a high degree of tetrahedral distortion was observed for YCu-Mesalen by EPR studies (vide page 136). This distortion may also induce poison resistance for this complex. YCu-fsal and YCu-

Benzosalen exhibit relatively moderate poison resistance whereas YCu-dmg is severely affected.

The activity and poison resistance of encapsulated Cu(II) complexes of substituted salen ligands are compared with those of zeolite salen complex. Zeolite Cu(II)salen is more active than substituted salen complexes. The lower activity of substituted salen complexes could be explained in terms of the lower mobility of reactant molecules in zeolite cavities. A high degree of distortion, which is likely in the case of zeolite encapsulated complexes of bulkier substituted salens is expected to lower the mobility of reactant molecules in the cage. The steric effects of methyl groups in YCu-Mesalen may further reduce the mobility of reactants and therefore exhibit lower activity. These aspects may also account for the enhanced poison resistance properties of substituted salen complexes in comparison to salen complex. However, molecular modeling studies with a simulation for these oxidation reactions are necessary to confirm the steric effects on activity and poison resistance.

7. 5 **SUMMARY AND CONCLUSION**

Zeolite encapsulated complexes can act as catalysts for hydrogen peroxide decomposition and the partial oxidation of organic substrates like benzyl alcohol and ethylbenzene with hydrogen peroxide. The oxidant/substrate mole ratio has been optimised as 2.0-2.5. These systems are also suitable for aerobic oxidation of organic compounds. Generally, encapsulated Cu(II) complexes are more active than complexes of other metal ions. Co(II) complexes are moderately active as compared to Cu(II) complexes. YCu-fsal is the most promising catalyst with respect to activity among various complexes studied. The geometries of the encapsulated complexes may account for their catalytic behaviour. The activity of YCu-fsal is almost sustained on recycling indicating little deactivation for the encapsulated complex. However, poison resistance of this complex is slightly lower than that of complexes of substituted salens. The use of bulkier substituted salens as ligand reduces the catalytic activity as compared to salen complex, but imparts poison resistance. The lower activity and enhanced poison resistance of these bulkier complexes could be attributed to the reduced mobility of molecules in the cage.

REFERENCES

1. N. Herron, *Chemtech*, Sept. (1989) 542
2. S. P. Varkey and C. R. Jacob, *Ind. J. Chem.*, 37A (1998) 407
3. N. Ulagappan, *Proceedings of The 31st annual convention of chemists, Varanasi, (1994)* F1
4. N. Herron, *Inorg. Chem.*, 25 (1986) 4714
5. R. A. Sheldon and J. K. Kochi, " *Metal-Catalysed oxidations of organic compounds* ", (Academic Press, New York) 1981
6. T. Katan, M. Chin and F. J. Schoenweis, *Nature*, Sept. 19 (1964) 1281
7. S. K. Sengupta and L Preeti, *Ind. J. Tech.*, 30 (1992) 172
8. R. Sreekala and K. K. Mohammed Yusuff, *Ind. J. Chem.*, 34A (1995) 994
9. V. S. Sharma and J. Schubert, *J. Am. Chem. Soc.*, 91 (1969) 6291
10. J. R. Goldstein and A. C. C. Tseung, *J. Catal.*, 32 (1974) 452
11. R. V. Prasad and N. V. Thakkar, *Ind. J. Chem.*, 33A (1994) 861
12. R. Sumathi, K. Johnson, B. Viswanathan and T. K. Varadarajan, *Ind. J. Chem.*, 38A (1999) 40
13. C. Ratnasamy, A. Murugkar, S. Padhye and S. A. Pardhy, *Ind. J. Chem.*, 35A (1996) 1
14. G. R. Krow, *Organic reactions*, Wiley, New York, 43 (1993) 251
15. S. Yamazaki, *Chem. Lett.*, (1995) 127
16. I. Mochida and K. Takeshita, *J. Phys. Chem.*, 78, 16 (1974) 1655
17. H. Sigel, *Angew. Chem. Internat. Edu.*, 8 (1969) 167
18. R. C. Jarinagin and J. H. Wang, *J. Am. Chem. Soc.*, 80 (1958) 6477
19. N. Mala, Kamaluddin and C. Jasleen, *Ind. J. Chem.*, 32A (1993) 108
20. A. Puzari, L. Nath and J. B. Baruah, *Ind. J. Chem.*, 37A (1998) 723
21. M. Moiseev and M. N. Vargaftik, *Russ. Chem. Rev.*, 59, 12 (1990) 1133
22. N. Herron, G. D. Stucky and C. A. Tolman, *J. Chem. Soc., Chem. Commun.*, 25 (1986) 1521

CHAPTER VIII

CATALYTIC ACTIVITY OF

Cu-Cr/Al₂O₃ CATALYSTS FOR CO OXIDATION

Abstract

Cu and Cu-Cr based catalysts were prepared on γ -Al₂O₃ support to study the carbon monoxide oxidation activity and the resistance to severe thermal and hydrothermal deactivation. The effect of modification of alumina by the addition of CeO₂ or TiO₂ on the overall performance of the catalyst was also studied. In general, all Cu catalysts are more active than corresponding Cu-Cr catalysts. The activity and stability of the catalyst vary with respect to support as Al₂O₃-CeO₂ > Al₂O₃-TiO₂ > Al₂O₃. The promoting effect of these dopants could be explained in terms of the metal-dopant interactions.

8.1 INTRODUCTION

Supported noble metal catalysts form an important class of heterogeneous catalysts as they are extensively used for a variety of industrially applied reactions including petroleum reforming¹, organic hydrogenation and dehydrogenation reactions², deoxygenation reaction³ etc. High specific activity and the ability to work at milder conditions are the main attractions in using these catalyst systems in chemical industry. Major application of noble metal based catalysts is for the control of automobile emissions^{4, 5}. A combination of Pt, Pd and Rh is used as the active component in three-way automobile catalyst for the simultaneous reduction of NO and oxidation of CO and hydrocarbons. Nowadays, noble metals are dispersed on monolith support for critical applications like automobile exhaust control⁶, catalytic combustion⁷ etc where the catalyst is subjected to (i) high temperature, (ii) numerous poisons and (iii) fluctuating gas compositions.

Noble metal catalysts have also found application for the oxidation of carbon monoxide⁸. The oxidation activity has been found to vary with respect to the active metal as Pd>Pt>Rh⁷. However, a strict control of air/fuel ratio is required for such catalysts to function effectively. Furthermore, these catalysts are highly sensitive to impurities since only a low amount of metal is present in them. Besides, the factors like high cost, noble metal scarcity, low recycling rates and increased diversified usage of noble metals restrict the use of these catalysts. Mainly because of these disadvantages, attention has focused on the development of cheaper non-noble metal alternatives for the oxidation of carbon monoxide in the past few years⁹.

Mehandjeev, Piperov and Bliznakov examined the possibility of replacement of noble metals with mixed oxides of Cu and Co and observed high oxidation activity at Cu/Co atomic ratio of 0.5, but poor poison resistance at lower Cu loading on the catalyst¹⁰. Interestingly, copper chromite catalyst was claimed as an efficient non-noble metal catalyst for automobile exhaust control¹¹. This catalyst was also applied for CO oxidation¹², water gas shift reaction¹³, selective oxidation of propylene¹⁴, hydrogenation of carbonyl compounds and olefins¹⁵ and decomposition of alcohols¹⁶.

From an industrial point of view, supported metal oxides are superior to unsupported systems on account of their improved stability and longer life. Alumina supported Cu-Cr catalyst was found to be as efficient as their unsupported counterparts for CO oxidation¹⁷. In addition, the use of monolith supported Cu-Cr catalysts for the simultaneous NO_x reduction and oxidation of carbon monoxide and hydrocarbons in catalytic converter was addressed in the literature¹⁸. Efficient functioning of these catalytic systems depends, to a great extent, on the activity and stability of reaction sites on the surface. In Cu-Cr catalysts, Cu has been proposed as the main active species and Cr as a promoter, which reduces deactivation rates. However, some contradictions still exist about the nature of active sites in Cu-Cr based catalysts^{19,20}.

Although Cu-Cr catalysts have been studied extensively, only scant information is available on the suitability of such systems for the oxidation of carbon monoxide at lower temperatures. This study aims at the development of alumina supported Cu-Cr catalysts with improved low temperature oxidation efficiency by incorporating additives like CeO₂ and TiO₂. Besides, special attention has been given to evaluate the effect of these dopants on the resistance against particle growth in severe thermal and hydrothermal conditions. The role of active metals in imparting activity and stability to the catalyst was investigated. Attempts have also been made to correlate the catalytic activity and stability with active metal dispersion and different crystalline phases present in the lattice.

8. 2 EXPERIMENTAL

8. 2. 1 Materials

Details regarding various chemicals and other materials used in the present study are given in Chapter II.

8. 2. 2 Catalyst preparation

A brief account of the impregnation technique employed for the catalyst preparation is provided in Chapter II. Gamma alumina extrusions (3 mm dia. & 10 mm height, Surface area = 245 m²/g) were modified with CeO₂ or TiO₂ by impregnating with an aqueous solution of cerous nitrate or ammonium titanyloxalate respectively. They were dried at 120 °C for 6 hours and then calcined at 540 °C for 1 hour. Both Cu and Cu-Cr catalysts were prepared on γ -Al₂O₃, γ -Al₂O₃-CeO₂ and γ -Al₂O₃-TiO₂ supports keeping copper concentration at 10 % and Cr/Cu mole ratio at around 2. Copper and chromium were incorporated from aqueous solutions of their nitrates by incipient wetness impregnation method. The wet extrusions were dried at 120 °C for 6 hours and then calcined at 500 °C for 2 hours.

8. 2. 3 Analytical Methods

Details of analytical methods and other characterization techniques are given in Chapter II.

8. 2. 4 Catalytic studies

The catalytic behaviour of the catalysts was studied by evaluating metal dispersion by O₂ or CO chemisorption, CO oxidation activity and stability in thermal and hydrothermal conditions. These experiments are carried out at identical conditions so as to compare the results of various catalysts. The procedures employed for these measurements are as follows:

a) Oxygen chemisorption

Oxygen chemisorption was performed in a pulse microcatalytic reactor attached to thermal conductivity detector. A schematic representation of the apparatus is given in Figure VIII. 1 The samples were reduced at 300 °C for 30 minutes, switched over to helium and the temperature raised to and maintained at 310 °C for 10 minutes. The reactor was cooled to room temperature and then pulsed with oxygen. From the amount

of oxygen consumed, % metal dispersion was calculated assuming a stoichiometry of 1:1.

b) CO Chemisorption

CO chemisorption was carried out in the same pulse injection system used for oxygen chemisorption. The samples were reduced with hydrogen at 300 °C for 30 minutes and cooled to room temperature before injecting pulses of carbon monoxide. A stoichiometry of 1:1 was taken for evaluating the metal dispersion from the amount of CO adsorbed.

c) CO oxidation activity

CO oxidation was performed in a continuous flow test unit as represented in Figure VIII. 2. The oxidation activity of the catalysts was evaluated in the temperature range 150 °C-250 °C in a tubular reactor loaded with 3 cc of the catalyst. The reactant flow used was a mixture of 130 ml/minute dry air and 20 ml/minute carbon monoxide. The inlet and outlet concentrations of carbon monoxide and carbon dioxide formed during reaction were analysed in a GC with FID detector. Carbon monoxide and carbon dioxide were converted to methane before entering the detector using a microcatalytic methanator connected after Poropak Q column in Gas Chromatograph.

d) Thermal and hydrothermal deactivation

Catalyst samples were subjected to high temperature treatments at 700 °C and 800 °C for one hour and were evaluated for CO oxidation activity at 200 °C.

For hydrothermal deactivation, catalyst samples were kept at 300 °C in a nitrogen stream containing steam for 48 hours and then dried at 120 °C for one hour. The CO oxidation activity of these samples was measured at 200 °C. The continuous test facility shown in Figure VIII. 2 was used for the hydrothermal treatment of the catalysts.

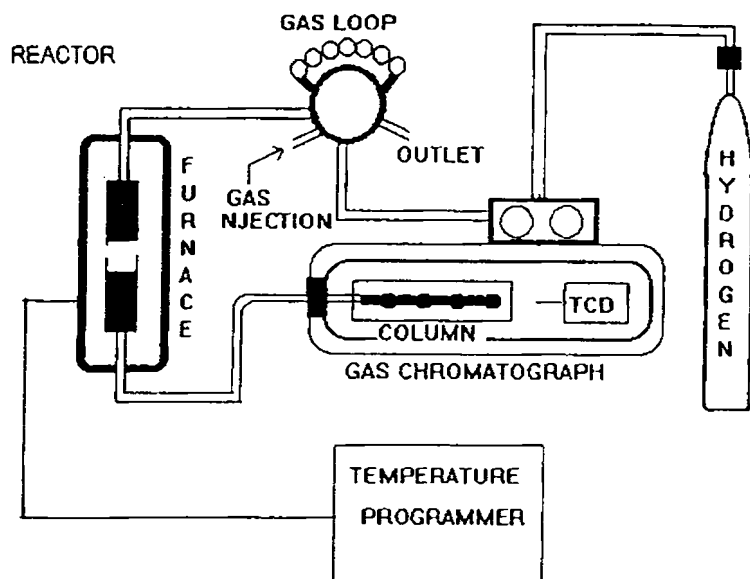


Figure VIII. 1
Pulse microcatalytic reactor for chemisorption

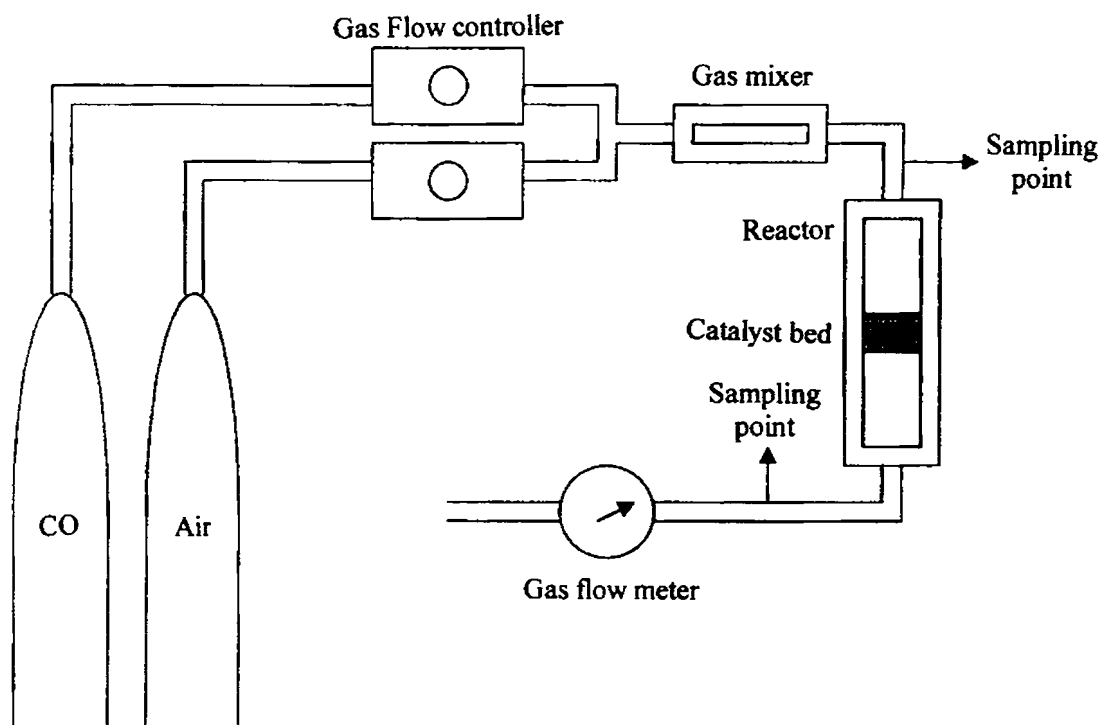


Figure VIII. 2
Continuous flow test unit for CO oxidation

8.3 RESULTS

Chemical analysis of $\text{Al}_2\text{O}_3\text{-CeO}_2$ and $\text{Al}_2\text{O}_3\text{-TiO}_2$ supports showed dopant concentrations of 6.2% CeO_2 and 4.8% TiO_2 respectively. Surface area of the alumina extrusions used for the catalyst preparation is $245 \text{ m}^2/\text{g}$ and that of CeO_2 and TiO_2 modified alumina was found to be $226 \text{ m}^2/\text{g}$ and $232 \text{ m}^2/\text{g}$ respectively. Cu and Cr contents, BET surface area and pore volume of all the catalyst samples are given in Table VIII. 1.

Table VIII. 1
Analytical, surface area and pore volume data

	Cu/ Al_2O_3	Cu-Cr/ Al_2O_3	Cu/ $\text{Al}_2\text{O}_3\text{-CeO}_2$	Cu-Cr/ $\text{Al}_2\text{O}_3\text{-CeO}_2$	Cu/ $\text{Al}_2\text{O}_3\text{-TiO}_2$	Cu-Cr/ $\text{Al}_2\text{O}_3\text{-TiO}_2$
Cu (wt %)	9.85	9.66	10.02	9.91	9.88	9.98
Cr (wt%)		15.80		16.21		16.15
Surface area (m^2/g)	170	105	153	95	160	99
Pore volume (ml/g)	0.48	0.34	0.45	0.32	0.46	0.32

Analytical results indicate that Cu and Cr contents are quite close to the values targeted during preparation of the catalysts. The required quantities of metal salts were taken in the impregnating solution of volume just enough to fill the pores of the support so as to incorporate the components completely into it. In this way, % Cu in all the catalysts could be controlled at around 10 and Cr/Cu mole ratio at around 2. Surface area was found to reduce on incorporating the active ingredients into the support. In addition, surface area and pore volume of the catalysts containing Cr are lower than those of non-chrome catalysts.

Figure VIII. 3 shows the XRD patterns of Cu-Cr catalysts. The patterns indicate the presence of a number of crystalline phases including CuO , CuAl_2O_4 , CuCr_2O_4 and

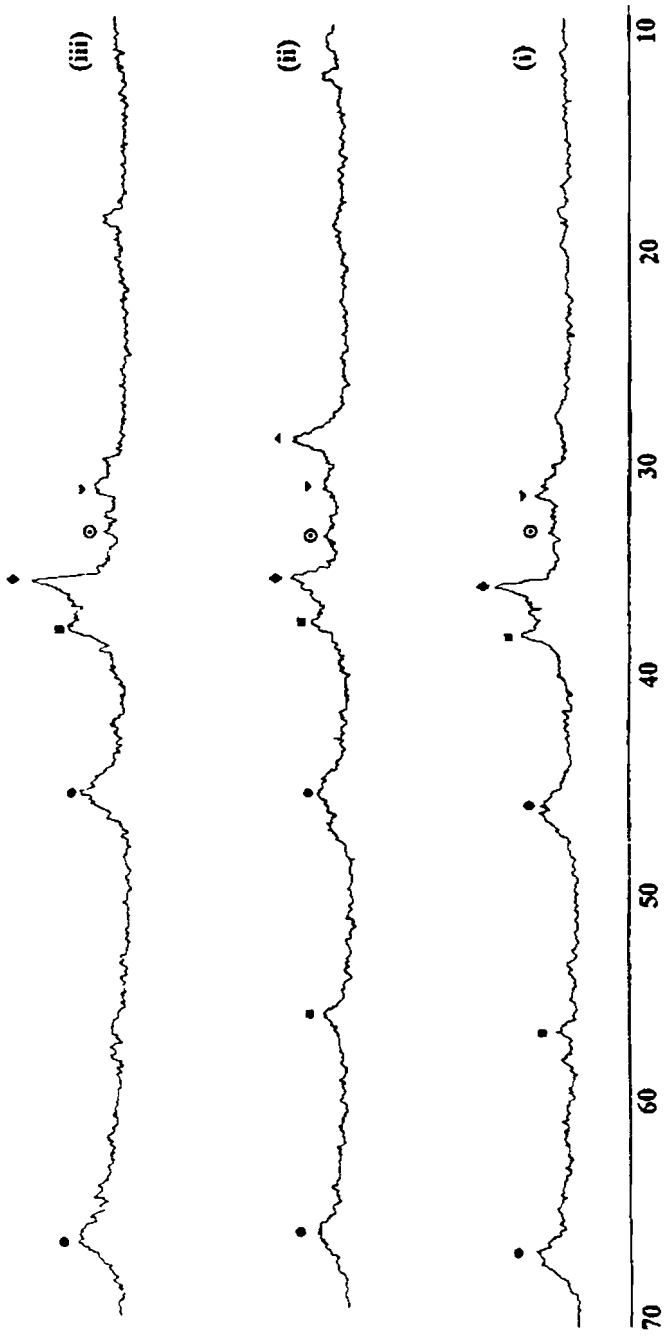


Figure VIII. 3

XRD spectra of Cu-Cr catalysts supported on (i) Al_2O_3 , (ii) $\text{Al}_2\text{O}_3\text{-CeO}_2$, and (iii) $\text{Al}_2\text{O}_3\text{-TiO}_2$
 (●) $\gamma\text{-Al}_2\text{O}_3$, (■) CuO , (◆) CuCr_2O_4 , (○) Cr_2O_3 , (▼) CuAl_2O_4 , (▲) CeO_2 , (◻) TiO_2

Cr₂O₃. The formation of such crystalline phases in Cu-Cr/Al₂O₃ catalyst was observed by previous workers also¹⁷.

The oxidation activity is represented as the percentage conversion of carbon monoxide to carbon dioxide. These values at different temperatures are given in Table VIII. 2. Figure VIII. 4, a plot of % conversion against temperature, indicates the effect of temperature on the efficiency of the catalysts for carbon monoxide oxidation. Cu based catalysts are more active than those containing Cu and Cr as active components. Similar observation has been reported previously at low metal concentrations²¹.

Cu and Cu-Cr catalysts on Al₂O₃-CeO₂ support showed substantial increase in activity than those supported on Al₂O₃ and Al₂O₃-TiO₂. For Cu/Al₂O₃-CeO₂, 100 % conversion was achieved at 210 °C whereas in the case of Cu-Cr/Al₂O₃-CeO₂, a temperature of 220 °C was required to get full conversion. TiO₂ incorporated catalysts also showed better performance than those prepared on alumina support, but not to the extent of those prepared on Al₂O₃-CeO₂. For Cu and Cu-Cr catalysts on Al₂O₃-TiO₂

Table VIII. 2

Carbon monoxide oxidation data

Catalyst	% Conversion of CO to CO ₂				
	150 °C	175 °C	200 °C	225 °C	250 °C
Cu/Al ₂ O ₃	9.0	23.4	59.3	84.8	95.2
Cu-Cr/Al ₂ O ₃	6.9	18.6	49.7	75.2	88.3
Cu/Al ₂ O ₃ -CeO ₂	60.7	88.3	95.9		
Cu-Cr/Al ₂ O ₃ -CeO ₂	48.3	64.1	85.5	97.9	
Cu/Al ₂ O ₃ -TiO ₂	32.4	62.8	78.6	99.3	
Cu-Cr/Al ₂ O ₃ -TiO ₂	23.4	48.3	71.7	89.7	

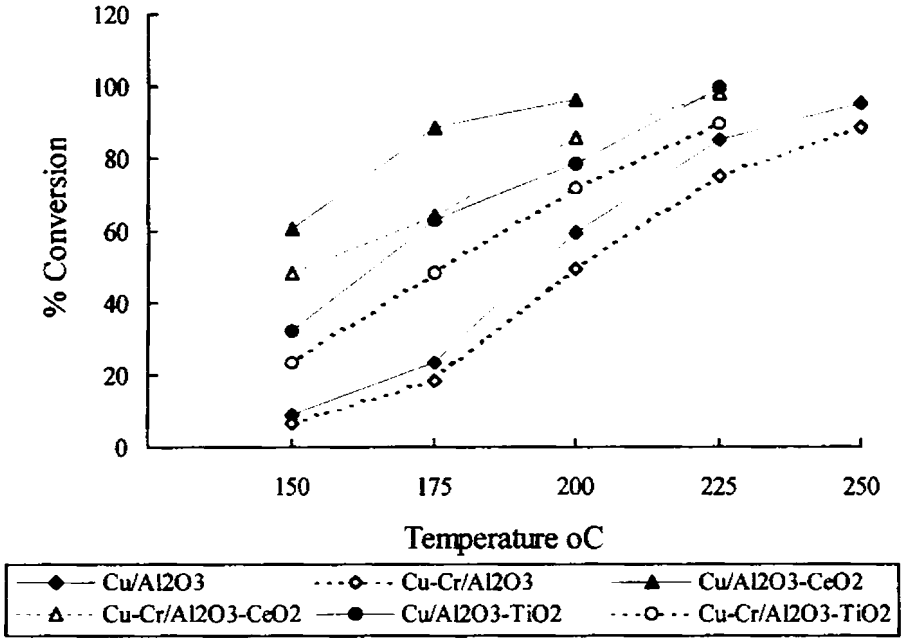


Figure VIII. 4
Activity versus temperature

support, the conversion of carbon monoxide to carbon dioxide was 100 % at 225 °C and 240 °C respectively whereas those on undoped support showed full conversion only at temperatures above 250 °C. Thus the incorporation of additives like CeO₂ or TiO₂ reduces the reaction temperature. It is also evident that the activity of various catalysts increases with respect to support in the order Al₂O₃ < Al₂O₃-TiO₂ < Al₂O₃-CeO₂.

Metal dispersions obtained from oxygen and carbon monoxide chemisorption are given in Table VIII. 3 and the values are represented as bar chart in Figure VIII. 5. The data reveal that adsorption sites are more dispersed in Cu catalysts than in Cu-Cr catalysts and vary with respect to support as Al₂O₃ < Al₂O₃-TiO₂ < Al₂O₃-CeO₂. Metal dispersions with respect to CO chemisorption is much lower than those obtained by oxygen chemisorption, indicating poor affinity of the catalyst for CO.

Table VIII. 3

Cu dispersion data from oxygen and carbon monoxide chemisorption

Catalyst	% Cu dispersion	
	from O ₂ chemisorption	from CO chemisorption
Cu/Al ₂ O ₃	37.5	3.6
Cu-Cr/Al ₂ O ₃	30.1	3.0
Cu/Al ₂ O ₃ -CeO ₂	44.7	7.8
Cu-Cr/Al ₂ O ₃ -CeO ₂	38.3	7.1
Cu/Al ₂ O ₃ -TiO ₂	41.6	7.3
Cu-Cr/Al ₂ O ₃ -TiO ₂	35.6	6.7

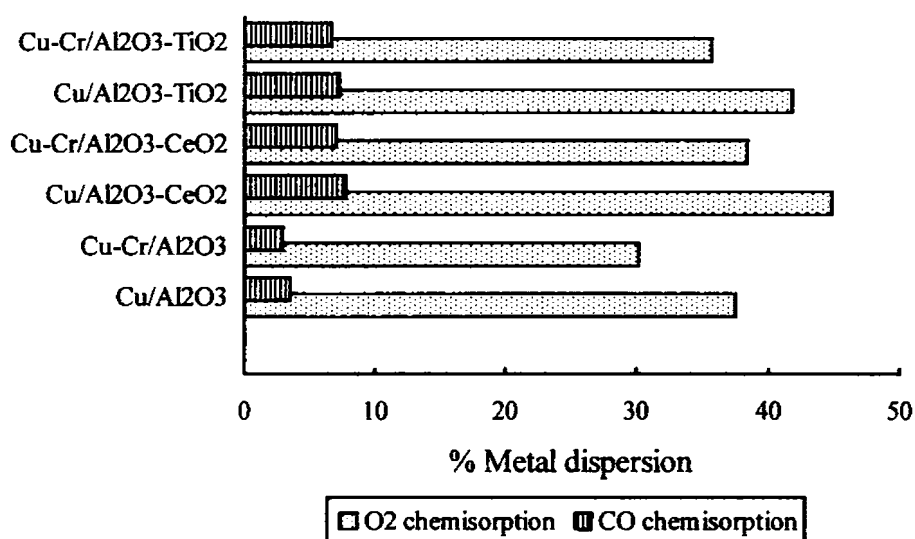


Figure VIII. 5

Cu dispersion from oxygen and carbon monoxide chemisorption

The activity results of thermally and hydrothermally deactivated samples are given in Table VIII. 4. These results are represented in Figure VIII. 6 and VIII. 7 respectively. It is evident that the extent of deactivation on high temperature treatment is more for Cu based catalysts. Similarly, Cu catalysts have experienced severe deactivation than Cu-Cr

catalysts on hydrothermal treatment also. This observation indicates that the addition of chromium, despite reducing the activity, improves stability against particle growth, which is likely to occur at severe operating conditions.

Table VIII. 4

Activity of thermally and hydrothermally treated catalyst samples

Catalyst	% Conversion after TT				% Conversion after HTT	
	700 °C	% Loss	800 °C	% Loss	300°C/ 48 hours	% Loss
Cu/Al ₂ O ₃	40.6	31.5	33.3	43.8	33.3	43.8
Cu-Cr/Al ₂ O ₃	37.2	25.2	34.0	31.6	34.0	31.6
Cu/Al ₂ O ₃ -CeO ₂	86.7	9.6	83.5	12.9	83.5	12.9
Cu-Cr/Al ₂ O ₃ -CeO ₂	80.2	6.2	78.7	8.0	78.7	8.0
Cu/Al ₂ O ₃ -TiO ₂	61.5	21.8	56.0	28.8	56.0	28.8
Cu-Cr/Al ₂ O ₃ -TiO ₂	59.8	16.6	57.4	19.9	57.4	19.9

TT = thermally treated HTT = hydrothermally treated

Figures VIII. 6 and VIII. 7 afford a comparison of various Cu and Cu-Cr catalysts with respect to the support vis-a-vis resistance against thermal and hydrothermal deactivation. It can be observed that among various catalyst samples, deactivation rate is much less for that prepared on Al₂O₃-CeO₂. The resistance to thermal and hydrothermal sintering varies with respect to support as Al₂O₃ < Al₂O₃-TiO₂ < Al₂O₃-CeO₂. On the basis of above observation, it should be expected that CeO₂ and to a certain extent TiO₂ play an important role as structural promoter to minimise deactivation on severe thermal and hydrothermal treatments.

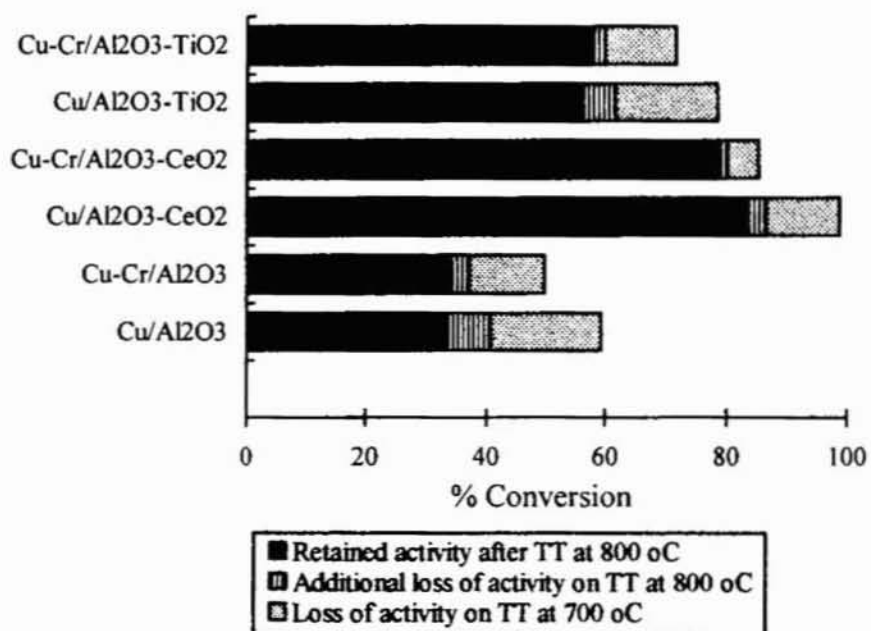


Figure VIII. 6

Effect of thermal deactivation on activity

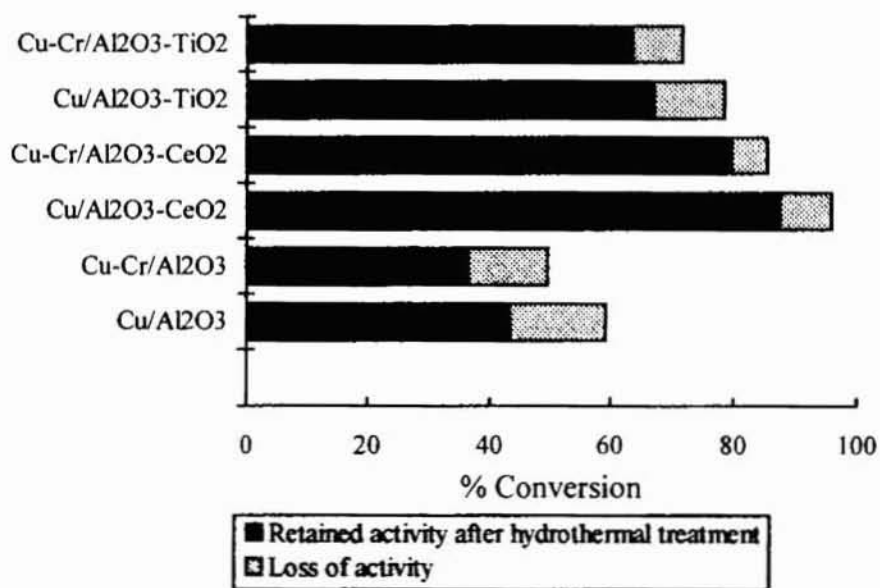


Figure VIII. 7

Effect of hydrothermal deactivation on activity

8.4 DISCUSSION

Supported Cu based catalysts are generally more active for the oxidation of carbon monoxide than Cu-Cr catalysts. This observation is in agreement with previous reports on Cu-Cr catalysts²¹. Lower activity exhibited by Cu-Cr catalysts can be attributed to its lower surface area and pore volume than those of Cu based catalysts. The lowering of surface area and pore volume could be due to the dilution of support and the filling of pores on introducing active components into the support. Furthermore, high Cu dispersion in Cu catalysts may also be a reason for their enhanced activity as Cu sites provide the main reaction centers for the oxidation of carbon monoxide.

CuO and CuAl₂O₄ are the possible phases in Cu based catalysts, whereas CuCr₂O₄ and Cr₂O₃ are also identified in the XRD patterns of Cu-Cr catalysts. CuO and CuAl₂O₄ phases have been reported to be present predominantly on the surface of Cu-Cr catalysts with Cu concentration less than 12%. These phases are more active for the oxidation of carbon monoxide as they are more reducible than CuCr₂O₄¹⁷. However, in the case of Cu-Cr catalysts with high Cu concentration, weakly active CuCr₂O₄ phase plays a major role in CO oxidation, as most of the Cu on the surface is available as CuCr₂O₄¹⁷. Therefore, the higher activity of Cu catalysts used in the present study is due to the well dispersed Cu sites formed by the reduction of easily reducible CuO and CuAl₂O₄ phases on the surface of alumina. But, only a low concentration of these phases are present in Cu-Cr catalysts due to the partial formation of inactive CuCr₂O₄²².

Additionally, the chromium introduced may not enter fully into the alumina lattice, but stays on the surface as small crystallites of Cr₂O₃²⁴. XRD patterns show the presence of surface Cr₂O₃ in Cu-Cr catalysts. This inactive surface species can cover the Cu sites so as to lower metal dispersion, adsorption capacity and hence activity.

It is obvious from the deactivation studies that Cu catalysts experience significant loss in activity than Cu-Cr catalysts on thermal treatment. Cu sites can be stabilized in the spinel structure of either CuAl₂O₄ in Cu catalysts or CuCr₂O₄ in Cu-Cr catalysts²⁵.

CuAl_2O_4 is a partially inverse spinel with about 40% Cu ions in octahedral sites, whereas CuCr_2O_4 is a normal spinel with copper ions in tetrahedral sites²⁶. It appears that Cu ions are stabilized more in tetrahedral sites than in octahedral sites. Therefore, on high temperature treatment, CuAl_2O_4 in Cu catalysts may undergo drastic sintering while the formation of stable CuCr_2O_4 spinels in Cu-Cr catalysts reduces particle growth¹⁷.

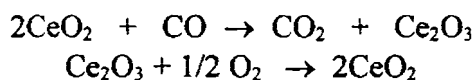
Water has been found to be not only an inhibitor for carbon monoxide oxidation with either oxygen or nitrogen oxides on Cu based catalysts but also a medium which facilitates particle growth²⁷. Cu catalysts are significantly affected on hydrothermal treatment than are Cu-Cr catalysts. This observation further shows the promoting effect of chromium in imparting stability for Cu sites via stable CuCr_2O_4 formation.

The CO oxidation activity of both Cu and Cu-Cr catalysts could be improved by the addition of dopants such as CeO_2 or TiO_2 . However, CeO_2 is superior to TiO_2 in its ability to enhance the oxidation efficiency at lower temperatures. The promoting effect of dopants could be attributed to higher metal dispersion in the modified catalysts. Catalysts modified with CeO_2 have showed considerable improvement in dispersion as compared to that of catalysts containing TiO_2 . It is interesting that similar trend is observed for activity or Cu dispersion on comparing promoted and unpromoted catalysts. Furthermore, these additives impart stability to resist particle growth in severe thermal and hydrothermal deactivation processes. The stability of both Cu and Cu-Cr catalysts varies with respect to support as $\text{Al}_2\text{O}_3 < \text{Al}_2\text{O}_3\text{-TiO}_2 < \text{Al}_2\text{O}_3\text{-CeO}_2$. The ability of CeO_2 and TiO_2 to enhance metal dispersion, catalytic activity and stability has been seen previously in supported noble metal catalysts^{28, 29}.

The promoting effect of CeO_2 or TiO_2 could be interpreted in terms of the interactions between these additives and metal ions. The interaction between Group VIII metals and support has been of scientific and industrial interest^{30, 31}. The unusual effect observed in a series of metal/oxide support systems is called " strong metal-support interaction " (SMSI). The SMSI in supported noble metal catalysts results in high metal dispersion, small crystallite size, high sorption and high relative activity^{32, 33}.

Similar effects are also expected in the case of alumina supported Cu or Cu-Cr oxides. Several mechanisms and models have been proposed in the case of noble metal catalysts to explain the role of CeO₂ and TiO₂ in metal support interactions leading to enhanced activity and stability of the catalyst.

Earlier studies have provided some insight into the role of cerium oxide in increasing the catalytic activity³⁵. Non-stoichiometry sets in rare earth oxides under reducing conditions leading to n-type semiconductivity. The activation energy for semiconductivity, which reflects the ease with which oxygen atoms can be removed from the lattice, has found to be very low for CeO₂. The formation of CeO_{1.945} by evacuation followed by hydrogen treatment of CeO₂ at 450 °C has been reported³⁶. A phase change has also been detected using X-ray diffraction patterns on the partial reduction of CeO₂. The reduced species can be oxidised back to CeO₂ with oxidising reactants. This redox property of CeO₂ plays a major role in enhancing the oxidation activity by providing parallel working sites³⁷ as given below

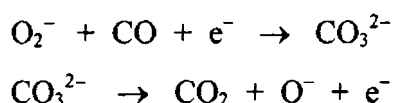


In a series of lanthanide oxides, CeO₂ is particularly active for both oxidation³⁸ and hydrogenation³⁵ reactions. The high activity has been attributed to the relative ease of oxygen vacancy formation and their involvement in the reaction mechanism. This redox behavior has also shown by TiO₂^{34,39}.

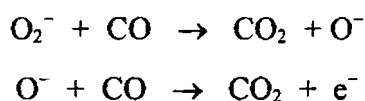
The electronic effects have also been considered to rationalize SMSI. As per this, the electronic interactions between the active metal atoms and reduced dopant ions at the dopant-metal interface account for the sorptive and catalytic changes observed^{34,40}. The role of CeO₂ in the phenomenon of increase of CO oxidation activity of alumina supported noble metal⁴¹ and Cu catalysts⁴² has been studied by EPR spectra. The enhanced CO oxidation activity observed for CeO₂ doped catalysts is due to the increased reactivity of O₂⁻ radicals adsorbed in the coordination sphere of Ce⁴⁺ ions. The

reactivity of these O_2^- radicals can be explained in terms of the metal-dopant electronic interactions.

The work function of reduced CeO_2 is much lower than that of Cu metal and therefore electrons are transported to metal from the conduction zone of CeO_2 adjacent to it until the Fermi levels of both the solids are equalised. The interaction of CO with O^{2-} radicals leads to the formation unstable carbonate like anion intermediates on the catalyst. The high electron density on the metal enhances the rate of formation of this intermediate at the expense of transfer of electrons from the metal to the intermediate. The reaction scheme can be represented as given below



The reactivity of O^{2-} radicals lying deeper relative to the Fermi level i.e. located away from metal-dopant interface is low and the reaction with CO can occur as per the following reactions:



This mechanism explains that the higher reactivity of O_2^- radicals at the metal-dopant interface leads to the enhancement of CO oxidation activity.

The migration of dopants onto the surface of active metal has also been suggested for explaining metal-dopant interactions^{34,43}. Partially reduced species of both CeO_2 and TiO_2 are able to migrate through or across the metal particles to cover some of their surface. In extreme cases metal particles can be totally immersed in the oxide support, which is termed as 'encapsulation'. As per this concept, the dopant not only shields the surface of active metal but also enters into electronic interaction with it, thus causing alterations in its catalytic properties.

A tentative model, called as "Vacancy interaction model", which involves the occupancy of oxygen ion vacancies in the oxide support by noble metal atoms has been proposed to account for the metal support interactions⁴⁵. The vacancies are called as nests and the process is called nesting. The same phenomenon may be applicable for Al₂O₃-CeO₂ or Al₂O₃-TiO₂ supported Cu atoms obtained on reducing the catalyst. In the case of metal atoms located on an ideal surface i.e. without oxygen vacancies, only a weak interaction exists between the metal atom and the surface. In such cases the atoms will easily migrate on the surface until they coalesce to form large crystallites. This results in the loss of metal dispersion, adsorption capacity and hence catalytic activity. In contrast to the above case, the metal atoms supported on reducible oxides like CeO₂ and TiO₂ can occupy the oxygen vacancies formed on the surface during reduction. This phenomenon increases active metal dispersion and surface area, maintains high sorptive capacity and hence results in high catalytic activity. In addition, the metal atoms are expected to be stabilized more when occupied in these vacancies as compared to those on the ideal surface.

Ceria appears to enhance the noble metal dispersion, thermal stability and activity in automotive catalysts²⁸. However, the important feature of ceria in oxidation reaction is the ability to store oxygen, which in turn helps to maintain required oxygen stoichiometry during lean operating conditions^{3,4}. Furthermore, the migration of oxygen molecules weakly adsorbed on ceria to the metallic site has been reported to facilitate CO oxidation on Rh/Ceria catalyst⁴⁵. However, further work will be needed to find the role of this spill over process in oxidation reactions over ceria promoted Cu-Cr catalysts.

8. 4 SUMMARY AND CONCLUSION

The overall performance of alumina supported Cu-Cr catalysts shows its suitability for use as an effective non-noble metal system for the oxidation of carbon monoxide. The role of chromium is to stabilise the Cu sites against thermal and hydrothermal deactivation, but it marginally reduces the carbon monoxide oxidation activity as compared to that of non-chrome catalyst. The stability imparted by Cr is particularly important for high temperature operation

of such catalysts. The additives like CeO₂ or TiO₂ can enhance not only the ability of the catalyst to withstand severe thermal and hydrothermal conditions but also the low temperature oxidation efficiency. These dopants not only improve Cu dispersion and facilitate reaction on it but also provide parallel reaction sites, and thus render the catalyst to be effective even at low temperatures. In all respects, CeO₂ is much superior to TiO₂ as a promoter in Cu-Cr catalysts for CO oxidation. The exact nature of Cu-CeO₂ interactions and how these interactions influence catalyst performance are aspects that need to be the foci of future investigations.

REFERENCES

1. G. M. Bickle, J. N. Beltramini and D. D. Do, *Ind. Eng. Chem. Res.*, 29 (1990) 1801
2. J. Cunningham, S. O'Brian, J. M. Rojo, J. A. Soria and J. L. G. Fierro, *J. Mol. Catal.*, 57 (1990) 379
3. M. G. Jones and T. G. Nevell, *J. Catal.*, 122 (1990) 219
4. H. C. Yao and Y. F. Yu-Yao, *J. Catal.*, 86 (1984) 254
5. H. C. Yao, H. S. Gandhi and M. Shelef, " *Metal-Support and Metal-Additive Effects in Catalysis* " (Imelik B, Ed.), Elsevier, Amsterdam, 1982
6. E. C. Su, C. N. Montreuil and W. G. Rothschild, *Appl. Catal.*, 17 (1985) 75
7. M. F. M. Zwinkels, S. G. Jaras and P. G. Menon, *Catal. Rev.- Sci. & Eng.* 35, 3 (1993) 319
8. B. N. Racine and R. K. Herz, *J. Catal.* 137 (1992) 158
9. J. Ghose, K. S. R. C. Murthy, *J. Catal.*, 162 (1996) 359
10. Mehandeej, Piperov and Bliznakov, *British Patent* 153 4047 (1979)
11. F. G. Dwyer, *Catal. Rev.* 6, 261 (1972)
12. Y. F. Yu Yao and J. T. Kummer, *J. Catal.* 46 (1977) 388
13. T. M. Yureva, G. K. Boreskov and V. S. Gruver, *Kinet. Katal.*, 10 (1969) 294
14. S. H. Inami and H. Wise, *J. Catal.*, 18 (1970) 343
15. H. Adkins, *J. Am. Chem. Soc.*, 72 (1950) 2626
16. A. Iimura, Y. Inoue and I. Yasumori, *Bull. Chem. Soc. Jpn.*, 56 (1983) 2203
17. F. Severino, J. Brito, O. Carias and Laine, *J. Catal.*, 102 (1986) 172
18. S. Stegenga, N. Dekker, J. Bijsterbosch, F. Kapteijin, J. Moulijn, G. Belot G and R. Roche, " *Catalysis and Automotive Pollution Control II* " (Crucq A, Ed.), Elsevier Science Publishers B. V., Amsterdam (1991) 353
19. E. D. Pierron, J. A. Rashkin and J. F. Roth , *J. Catal.*, 9 (1967) 38
20. J. Mooi and P. W. Selwood, *J. Am. Chem. Soc.*, 74 (1952) 2461
21. J. Laine and F. Severino, *Appl. Catal.*, 65 (1990) 253
22. R. M. Friedman, J. J. Freeman and F. W. Lytle, *J. Catal.*, 55 (1978) 10
23. K. Jagannathan, A. Srinivasan and C. N. R Rao, *J. Catal.*, 69 (1981) 418
24. C. P. Poole and D. S. MacIver, " *Advances in Catalysis* ", Vol. 17, p 223, Academic Press, New York, 1967
25. A. F. Wells, " *Structural Inorganic Chemistry* ", 3rd Ed., pp. 457, 487, Oxford Univ. Press, London, 1962
26. A. d' Huysser, G. Wrobel and J. P. Bonnelle, *Nouv. J. Chim.*, 6 (1982) 437
27. S. Stegenga, A. J. C. Milrop, C. de Vaies, F. Kapteijin and J. A. Moulijn, *19th Biennial Conf. Of Carbon*, Penn. State Univ., 1989, p 74
28. J. E Kubsh, J. S. Rieck and N. D. Spencer, " *Catalysis and Automotive Pollution Control II* " (Crucq A, Ed.), Elsevier Science Publishers B. V., Amsterdam (1991) 125
29. C. Kuei, J. Lee and M. Lee, *J. Mol. Catal.*, 59 (1990) 333

30. S. J. Tauster, S. C. Fung and R. L. Garten, *J. Am. Chem. Soc.*, 100 (1978) 170
31. S. J. Tauster and S. C. Fung, *J. Catal.*, 55 (1978) 29
32. R. T. K. Baker, E. B. Prestridge and R. L. Garten, *J. Catal.*, 56 (1979) 390
33. R. T. K. Baker, E. B. Prestridge and R. L. Garten, *J. Catal.*, 59 (1979) 293
34. L. V. Ermolov and A. A. Slinkin, *Russ. Chem. Rev.*, 60,4 (1991) 331
35. J. C. Summers and S. A. Ausen, *J. Catal.*, 58 (1979) 131
36. T. Yamaguchi, N. Ikeda, H. Hattori and K. Tanabe, *J. Catal.*, 67 (1981) 324
37. A. F. Diwell, R. R. Rajaram, H. A. Shaw and T. J. Truex " *Catalysis and Automotive Pollution Control II* " (Crucq A, Ed.), Elsevier Science Publishers B. V., Amsterdam (1991) 139
38. T. Hattori, J. Inoko and Y. Murakami, *J. Catal.*, 42 (1976) 60
39. J. Sanz, J. M. Rojo, P. Malet, G. Munuera, M. T. Blasco, J. C. Conesa and J. Soria, *J. Phys. Chem.* 89 (1985) 5427
40. J. A. Horsley, *J. Am. Chem. Soc.* 101 (1979) 2870
41. A. S. Sass, V. A. Shavets and G. A. Sevel'eva, *Kinet. Katal.*, 27, 4 (1986) 894
42. A. L. Tarasov, L. K. Przheval' skaya, V. A. Shvets and Kazanskii, *Kinetika i Kataliz*, 29, 5 (1987) 1181
43. D. E. Resasco and G. L. Haller, *J. Catal.*, 82 (1983) 279
44. M. G. Sanchez and J. L. Gazquez, *J. Catal.*, 104 (1987) 120
45. G. S. Zafiris and R. J. Gorte, *J. Catal.*, 139 (1993) 561

SUMMARY AND CONCLUSIONS

The theme of the present investigation is mainly centered around the synthesis, characterization and catalytic studies on zeolite encapsulated transition metal complexes and metal oxide catalysts. Characterization data of zeolite complexes point out the encapsulation of complexes and their composition, structure and thermal stability. The catalytic behaviour of these complexes with respect to oxidation activity, recycling ability and poison resistance has been investigated. Studies carried out on Cu-Cr/Al₂O₃ catalyst to recognize the role of the active metal atoms and investigate the effect of additives like CeO₂ or TiO₂ on CO oxidation activity and stability are also reported in this thesis.

Chapter I of the thesis reviews the role of some important proven catalysts. The recent trends in the development of catalyst-technology and the scope of using heterogenized catalysts, especially zeolite encapsulated complexes, for achieving the desired targets are described. This chapter provides a brief account of various methodologies used for the synthesis and characterization of zeolite complexes. The catalytic studies conducted on this system are described.

Chapter II gives a brief account of various reagents and materials used in the present study. The techniques employed for the synthesis, characterization and catalytic studies of zeolite complexes and metal oxide catalysts are described. These techniques include: chemical analysis, CHN analysis, atomic absorption spectrophotometer, XRD, SEM, BET surface area and pore volume, mercury porosimetry, magnetic moment by Gouy method, reflectance spectra, FTIR spectra, EPR, TG analysis, chemisorption studies using microcatalytic reactor and gas chromatograph

Chapter III reports on studies on the synthesis and characterization of Y zeolite encapsulated Mn(II), Fe(III), Co(II), Ni(II) and Cu(II) complexes of dimethylglyoxime. The zeolite NaY used for supporting the complexes was found to possess a unit cell

formula of $\text{Na}_{56} [(\text{AlO}_2)_{56} (\text{SiO}_2)_{136}] \cdot x\text{H}_2\text{O}$. The unit cell formulae of metal exchanged zeolites were also derived from the analytical data. The Si/Al ratio of metal exchanged zeolites is the same as that of the parent zeolite indicating that the collapse of zeolite framework by dealumination during ion exchange could be prevented in the present study by using very dilute metal salt solutions. Surface area, pore volume, XRD and FTIR data of metal exchanged zeolites also reveal the retention of zeolite framework.

The empirical formulae of encapsulated dmg complexes were calculated from the analytical results. Minute traces of uncomplexed metal ions were found to remain in the lattice of zeolite complexes which are unlikely to interfere in the behaviour of encapsulated complexes. SE micrographs of encapsulated Co(II) complex before and after soxhlet extraction indicate that the surface complexes are completely removed. XRD patterns and Si/Al ratio indicate the retention of zeolite framework on encapsulation. The lower surface area and pore volume of zeolite complexes as compared to those of corresponding metal exchanged zeolites is attributed to the encapsulation of complexes in zeolite pores.

The geometries of Mn(II) and Fe(III) complexes could not be inferred from the magnetic moment and electronic spectral data. However, a tentative assignment of an octahedral, distorted square planar and tetrahedrally distorted square planar symmetry for encapsulated Co(II), Ni(II) and Cu(II) complexes respectively has been proposed. The EPR data also support the distorted square planar structure of Cu(II) complex and provide evidence for ionic environment around the metal ion. Furthermore, $g_{\parallel}/A_{\parallel}$ ratio hints at the degree of distortion of the complexes. The formation of the complexes in the zeolite pores was also confirmed from the IR data. The thermal degradation patterns have not provided confirmable results due to the interferences from the deauration of the sample and the lack of appreciable weight losses for the decomposition of encapsulated complexes which are present only in low amounts in the zeolite. However, approximate stability could be ascertained in most of the cases. The encapsulation of the

complexes accounts for the difference in the TG patterns of metal exchanged zeolites and zeolite complexes.

Chapter IV deals with the encapsulation of transition metal complexes of 3-formyl salicylic acid. The complexes were characterized as described previously. The composition hints at a binuclear structure for the encapsulated complexes. Furthermore, magnetic moment and reflectance data are close to those reported for their simple binuclear complexes. Surface area, pore volume and XRD data are presented as an evidence for the encapsulation of complexes without the destruction of zeolite crystallinity. On the basis of magnetic moment, electronic and EPR spectral data, the encapsulated Co(II), Ni(II) and Cu(II) complexes are expected to possess tetrahedral, octahedral and tetrahedrally distorted square planar symmetry respectively. IR spectra confirm the formation of complexes in the cavities and explain the coordination in them. TG patterns also indicate the encapsulation of complexes.

Chapter V provides details regarding the encapsulation of complexes of the substituted salen like ligand, N, N'-ethylene(7-methylsalicylideneamine). The analytical, XRD, surface area and pore volume data are presented to explain the composition and encapsulation of these complexes. Magnetic moment and electronic spectral data could assign geometries only in the case of Ni(II) and Cu(II) complexes. The encapsulated Ni(II) complex exhibits an octahedral geometry whereas a tetrahedrally distorted square planar symmetry is observed for the Cu(II) complex. The higher $g_{||}/A_{||}$ ratio of Cu(II) complex indicates a high degree of distortion in this case, probably due to the steric effects of methyl groups of the ligand. IR spectral and TG data indicate the formation of complexes in zeolites

Chapter VI deals with the encapsulation of complexes of another bulkier substituted salen like ligand, N,N'-ethylene(5,6-benzosalicylideneamine). Our attempts to synthesize encapsulated Co(II) complex was unsuccessful. Characterization data indicate the formation of monomeric complexes in Y zeolite. An octahedral and

tetrahedrally distorted square planar structure are assigned for the encapsulated Ni(II) and Cu(II) complexes respectively. IR and TG data also suggest the encapsulation of the complexes.

Chapter VII discusses the catalytic properties of zeolite encapsulated complexes. Zeolite complexes were found to be active for the decomposition of hydrogen peroxide and the oxidation of benzyl alcohol or ethylbenzene. These systems can also catalyse the aerobic oxidation of organic compounds. The ability for the partial oxidation of organic compounds is the main attraction of catalysis of zeolite complexes. Encapsulated Cu(II) complexes, especially that with 3-formylsalicylic acid were found to be more active than others. The recycling ability of zeolite complexes was tested in the case of the most promising catalyst, which showed only little deactivation on reusing. Poison resistance of bulkier encapsulated complexes is higher than that of others even though they possess only a lower activity. The substitution in salen ligand reduces activity but enhances poison resistance as compared to zeolite salen complex. The geometry of various zeolite complexes accounts for the variation in the catalytic activity. The expected steric effects in bulkier zeolite complexes reduce the mobility of molecules leading to reduced activity and increased poison resistance.

Chapter VIII describes the preparation of Cu or Cu-Cr catalysts on Al_2O_3 , Al_2O_3 - CeO_2 and Al_2O_3 - TiO_2 supports. The catalytic activity of these catalysts for the oxidation of carbon monoxide was determined. Cu based catalysts are more active than Cu-Cr catalysts, probably because of the enhanced metal dispersion in them. However, the addition of Cr improves the stability of the catalyst by forming stable CuCr_2O_4 phases in the catalyst lattice. The additives, CeO_2 and TiO_2 , also enhance the activity and stability of the catalyst to perform effectively in hostile thermal and hydrothermal conditions. However, CeO_2 is much superior to TiO_2 as a dopant with respect to the ability to enhance activity and stability. The promoting action of these dopants is explained in terms of the increased metal dispersion, the redox properties and the metal-dopant interactions which are most likely in modified catalysts.

The general conclusions drawn from our studies are :

1. Well defined encapsulation of transition metal complexes in Y zeolite is possible by carefully synthesizing the metal exchanged zeolite and zeolite complex at optimised conditions.
2. The use of zeolite encapsulated complexes as catalysts avoids the practical difficulties associated with homogeneous catalysis. The encapsulated complexes exhibit the ability to be recycled in reactions by retarding the deactivation processes.
3. Zeolite encapsulated complexes are suitable as catalysts for the partial oxidation organic compounds with hydrogen peroxide and molecular oxygen. Cu(II) complexes, especially binuclear complex of 3-formylsalicylic acid, are more active catalysts than the complexes of other metal ions.
4. The geometry of the encapsulated complexes plays a vital role in regulating the functioning of the catalyst by providing vacant reaction sites. Encapsulated complexes interact with the zeolite framework to slightly distort the geometry which might lead to a modified catalytic activity. Therefore, the activity and poison resistance can be optimised by varying the stereochemistry of the encapsulated complexes by using bulkier ligands
5. The CO oxidation activity of Cu-Cr/Al₂O₃ catalysts is dependent on the dispersion of Cu sites indicating the structure sensitive nature of this reaction on metal oxide systems.
6. The dopants, CeO₂ or TiO₂, enhance the activity and stability of the catalyst. CeO₂ possess excellent features as an additive, which could be exploited in oxidation reactions.